
THE UNIVERSITY
*of* EDINBURGH

# SCHOOL OF CHEMISTRY

# THE UNIVERSITY OF EDINBURGH



# Novel microporous polymers for gas separation membranes

Thesis submitted for the degree of Doctor of Philosophy by:


**Sarah Abdulhalim Felemban**


Supervisor: Neil B. McKeown

2018

## Declaration

This work has not been submitted in substance for any other degree or award at this or any other university or place of learning, nor is it being submitted concurrently in candidature for any degree or other award .

Signed …… (candidate)

Date .23/08/2019……

**Statement 1**

This thesis is being submitted in partial fulfilment of the requirements for the degree of Doctor of Philosophy .

Signed …… (candidate)

Date .23/08/2019……

**Statement 2**

This thesis is the result of my own independent work/investigation, except where otherwise stated. Other sources are acknowledged by explicit references. Any views expressed are my own .

Signed …… (candidate)

Date .23/08/2019……

**Statement 3**

I hereby give consent for my thesis, if accepted, to be available for photocopying and for inter-library loan, and for the title and summary to be made available to outside organisations .

Signed …… (candidate)

Date .23/08/2019……

## Acknowledgments

First and foremost I owe my thanks to Allah for enabling me to take this thesis that was undertaken at the Chemistry school, Edinburgh University, under the supervision of Professor Neil McKeown.

I would like to thank my Professor Neil McKeown, for giving me this opportunity and for his supervision throughout my PhD. I'd also like to give special thanks to Grazia and Lino for their timely help whenever needed; it is really my good fortune to do this research under their guidance. I will be forever grateful.

I would like to thank Kadhum, Richard and Bibiana for the valued support and expertise they have shared with me over the last four years

I would like to thank the Saudi Ministry of Higher Education and Umm Al-Qura University for their encouragement and financial support.

I would like to express my thanks to everyone else who has worked with me in lab during this time: Ian, Rhodri, Sadiq, Ali, Luck, Rich II, Ariana, Angelos, Jie, Hannah and Chun chun for making it such a friendly place to work.

I would also like to show my appreciation for all of the technical staff at the School of Chemistry in Edinburgh for their expertise. A special mention should also go to everyone at ITM for all of the gas permeability data.

Last but not least, this work would not have been possible without the love, encouragement, patience and support from my parents, my sisters, my brother and my dear friends.


## Abstract

Polymers of intrinsic microporosity (PIMs) owe their microporosity to their rigid and contorted structure which prevents efficient space packing. Their microporosity and processability make them attractive for many industrial applications, such as heterogeneous catalysis, gas separation membranes, hydrogen storage and adsorbents for organic compounds. Our goal in this project is to broaden the spectrum of PIM structures by preparing novel PIMs with potential for different industrial applications but focusing on gas separation membranes. Characterisation of the novel polymers was achieved to establish their chemical and physical properties including solubility, surface area, thermal stability and their molecular weight. In some cases, casting the resulting PIMs from solution enabled the formation of self-standing films which could then be analysed for their ability to separate different gas mixtures. Three different types of PIM were targeted during the PhD programme. Firstly, the preparation of Tröger's base (TB) containing hypercrosslinked polystyrene was attempted. The first step was the nitration of polystyrene by using different reaction conditions, with the aim to introduce the highest possible number of nitro groups, followed by the reduction of nitropolystyrene to the aminated polystyrene. Finally, hyper-crosslinking of the amino-polystyrene was attempted by formation of TB units between polymer chains. Secondly, new ladder and network PIMs derived from different catechols monomers with 2,3,7,8-tetrafluoro-5,5',10,10'-tetraoxidethianthrene were synthesised. This thiathrene-based rigid monomer increases the distances between two consecutive "sites of contortion" within the polymer chains and provides sulfonyl functional groups, which may influence the adsorption and gas separation properties of the resulting polymers. Thirdly, a series of novel microporous polyimides (PIM-PIs) were prepared using different diamine monomers and thiathrene-based dianhydride monomers. All polymers were characterized by using NMR, IR spectrometers and their chemical and physical properties were measured using a variety of techniques. In addition, for some polymers successful film formation via casting from solution allowed the measurement of their gas

permeability to assess their ability to separate gas mixture. All chemical procedures for the synthesis of monomers and polymers, properties of the resulting polymers and comparisons with existing polymers are described in this thesis.

## Abbreviations

| Abbreviation | Definition |
|---|---|
| **3MPDA** | 2,4,6-trimethyl-1,3-phenylenediamine |
| **4MPDA** | 2,3,4,5-tetramethyl1,4-phenylenediamine |
| **APCI** | Atmospheric pressure chemical ionisation |
| **BAPF** | 9,9′-Bis(4-aminophenyl) fluorene |
| **$BBr_3$** | Boron tribromide |
| **BET** | Brunauer, Emmett and Teller |
| **$CHCl_3$** | Chloroform |
| **CMDP** | 1,4-bis-chloromethyldiphenyl |
| **CMM** | 2,4,6-trischloromethylmesitylene |
| **COF** | Covalent Organic Framework |
| **DMF** | N,N-Dimethylformamide |
| **DMFL** | Dimethylformal |
| **DMN** | 3,3’-dimethylnaphthidine |
| **DMSO** | Dimethylsulfoxide |
| **DPB** | p,p'-bis-chloromethyl-1,4-diphenylbutane. |
| **DVB** | Divinylbenzene |
| **DCM** | Dichloromethane |
| **DMF** | N,N-Dimethylformamide |
| **DMM** | Dimethoxymethane |
| **DMFL** | Dimethylformal |
| **DMN** | 3,3’-dimethylnaphthidine |
| **DMSO** | Dimethylsulfoxide |
| **DAPI** | Diaminophenylindane |
| **DCM** | Dichloromethane |
| **DMM** | Dimethoxymethane |
| **GPC** | Gel Permeation Chromatography |

| | |
|---|---|
| ***h*** | Hour(s) |
| **HCl** | Hydrochloric acid |
| **HCP** | Hypercrosslinked polymers |
| **HPB** | Hexaphenylbenzene |
| **HRMS** | High Resolution Mass Spectrometry |
| **IR** | Infrared spectroscopy |
| **IUPAC** | International Union of Pure and Applied Chemistry |
| **KAUST** | King Abdullah University of Science and Technology |
| **LRMS** | Low Resolution Mass Spectrometry |
| **MCDE** | Monochlorodimethylether |
| **NMP** | N-methyl pyrrolidone |
| **NMR** | Nuclear Magnetic Resonance |
| **PAA** | polyamic acid |
| **PI** | Polyimide |
| **PIM** | Polymer of Intrinsic Microporosity |
| **SBF** | Spirobifluorene |
| **SBI** | Spirobisindane |
| **SET** | Single electron transfer |
| **SNAr** | Nucleophilic aromatic substitution |
| **STI** | Stilbite |
| **Styrosorbs** | Hypercrosslinked polystyrene |
| **TADA** | Thianthrene-2,3,7,8-tetracarboxylicdianhydride |
| **TADATO** | Thianthrene-2,3,7,8-tetracarboxylicdianhydride-5,5,10,10- tetraoxide |
| **TB** | Tröger's base |
| **$T_d$** | Decomposition temperature |
| **TFA** | Trifluoroacetic acid |
| **TFAA** | Trifluoroacetic anhydride |
| **TFTPN** | 2,3,5,6-tetrafluoroterephthalonitrile |

| | |
|---|---|
| **$T_g$** | Glass transition temperature |
| **TGA** | Thermal gravimetric Analysis |
| **TLC** | Thin Layer Chromatography |
| **THF** | Tetrahydrofuran |
| **TOT** | 2,3,7,8-tetrafluoro-5,5’,10,10’-tetraoxidethianthrene |
| **Trip** | Triptycene |
| **TTSBI** | 5,5',6,6'-tetrahydroxy-3,3,3',3'-tetramethylspirobisindane |

## Table of molecules

| Chemical name and number | Chemical structure |
|---|---|
| Poly(4-nitrostyrene) **(1a-1e)** | 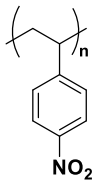 |
| Poly(4-aminostyrene) **(2a-2e)** | 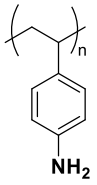 |
| 2,3,7,8-tetrafluorothianthrene **(3)** | 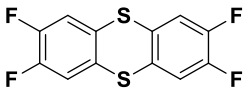 |
| 2,3,7,8-tetrafluoro-5,5',10,10'-tetraoxidethianthrene **(4)** | 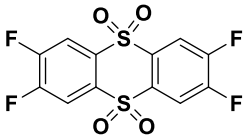 |
| Synthesis of 2,5-dichloro-2,5-dimethylhexane **(5)** | 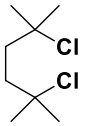 |
| Synthesis of 6,7-dimethoxy-1,1,4,4-tetramethyl-1,2,3,4-tetrahydronaphthalene **(6)** | 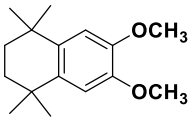 |
| 5,5,8,8-tetramethyl-5,6,7,8-tetrahydronaphthalene-2,3-diol **(7)** | 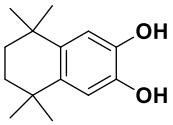 |
| Model compound **(8a-8b)** | 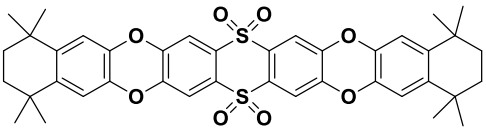 |
| 9,10-dimethyl-9,10-ethano-9,10-dihydro-2,3,6,7-tetrahydroxyanthracene **(9)** | 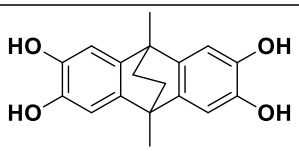 |

| | |
|---|---|
| 9,9-bis (3,4-dihydroxyphenyl) fluorene **(10)** | 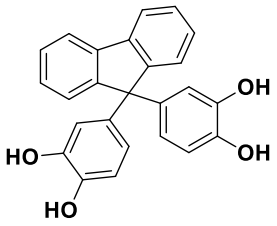  |
| 3,3-dimethoxybiphenyl **(11)** | 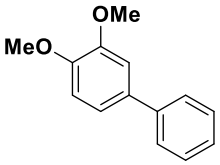  |
| 2-bromo-4,5-dimethoxy-biphenyl **(12)** | 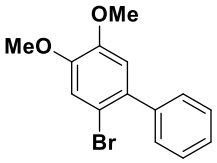  |
| 4,5-dimethoxy-2-phenylbenzoic acid **(13)** | 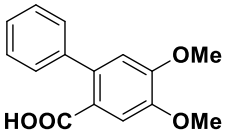  |
| 2,3-dimethoxy-9H-fluoren-9-one **(14)** | 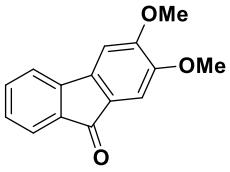  |
| 2,2',3,3''-tetramethoxy-9,9'-spirobifluorene **(15)** | 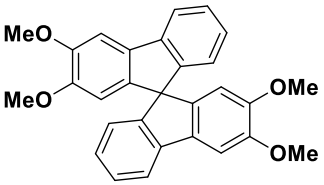  |
| 2,2',3,3'-tetrahydroxy-9,9'-spirobifluorene **(16)** | 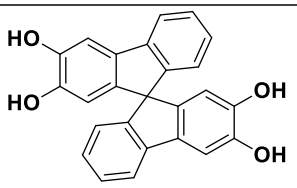  |
| 3,4-dimethoxy-4'-methyl-1,1'-biphenyl **(17)** | 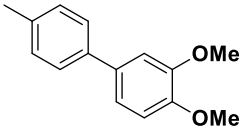  |

| | |
|---|---|
| 1-bromo-3,4-dimethoxy-4'-methyl-1,1'-biphenyl **(18)** | 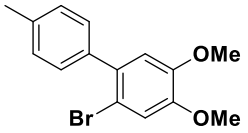  |
| 4,5-dimethoxy-2-(4-methylphenyl)benzoic acid **(19)** | 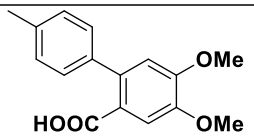  |
| 2,3-dimethoxy-7-methyl-9H-fluoren-9-one **(20)** | 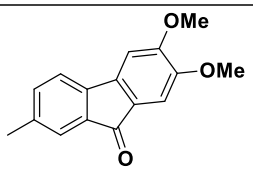  |
| 2,2',3,3'-tetramethoxy-6,6'-dimethyl-9,9'-spirobifluorene **(21)** | 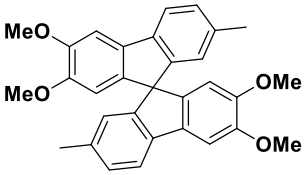  |
| 2,2',3,3'- tetrahydroxy -6,6'-dimethyl-9,9'-spirobifluorene **(22)** | 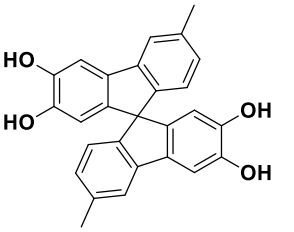  |
| 3,4-dimethoxy-4'-*t*-butyl-1,1'-biphenyl **(23)** | 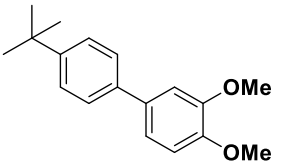  |
| 1-bromo-3,4-dimethoxy-4'-*t*-butyl-1,1'-biphenyl **(24)** | 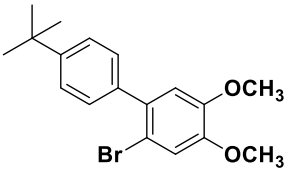  |
| 2-(4-*t*-butylphenyl)-4,5-dimethoxybenzoic acid **(25)** | 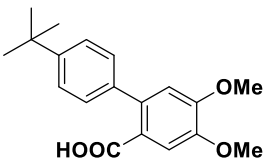  |

| | |
|---|---|
| 2,3-dimethoxy-7-t-butyl-9H-fluoren-9-one **(26)** | 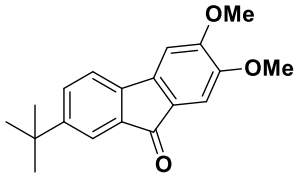 |
| 2,2',3,3'-tetramethoxy-6,6'-*t*-butyl-9,9'-spirobifluorene **(27)** | 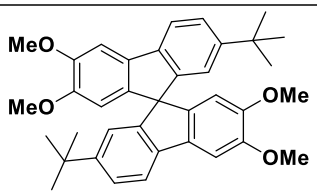 |
| 2,2',3,3'- tetrahydroxy-6,6'-*t*-butyl-9,9'-spirobifluorene **(28)** | 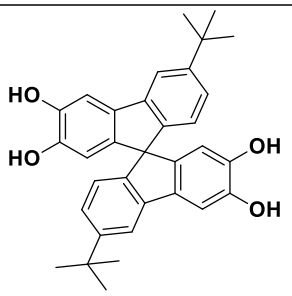 |
| 1,3-bis(3,4-dimethoxyphenyl)propan-2-one **(29)** | 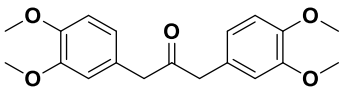 |
| 2,5-bis(3,4-dimethoxyphenyl)-3,4-diphenylcyclopenta-2,4-dien-1-one **(30)** | 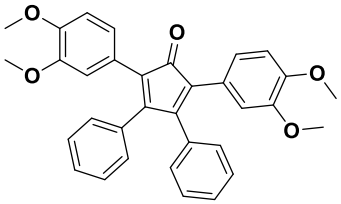 |
| 1,4-di(3',4'-dimethoxyphenyl)-2,3,5,6-tetraphenylbenzene **(31)** | 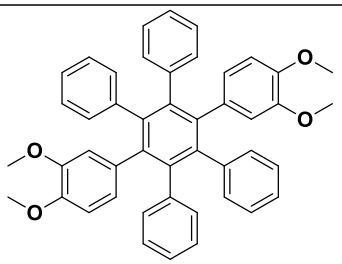 |
| 1,4-di(3',4'-dihydroxyphenyl)-2,3,5,6-tetraphenylbenzene **(32)** | 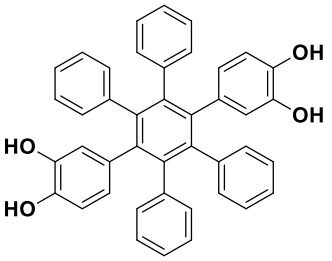 |

| | |
|---|---|
| 1,1,4,4-tetramethyl-1,2,3,4-tetrahydronaphthalene **(33)** | 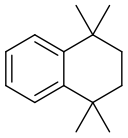 |
| 6,7-dibromo-1,1,4,4-tetramethyl-1,2,3,4-tetrahydronaphthalene **(34)** | 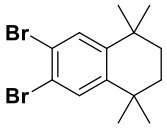 |
| 5,5,8,8-tetramethyl-1,4,5,6,7,8-hexahydro-1,4-epoxyanthracene **(35)** | 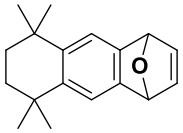 |
| 2,3,6,7-tetramethoxy-9,10-dimethylanthracene **(36)** | 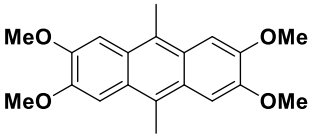 |
| (5*s*,14*s*)-2,3,18,19-tetramethoxy-5,8,8,11,11,14-hexamethyl-5,5a,6,8,9,10,11,13,13a,14-decahydro-5,14-[1,2]benzeno-6,13-epoxypentacene **(37)** | 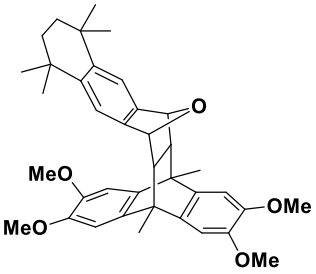 |
| 2,3,18,19-tetramethoxy-5,8,8,11,11,14-hexamethyl-5,8,9,10,11,14-hexahydro-5,14-[1,2]benzenopentacene **(38)** | 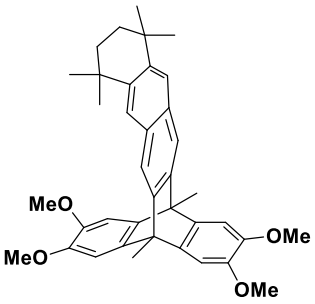 |

| | |
|---|---|
| 5,8,8,11,11,14-hexamethyl-5,8,9,10,11,14-hexahydro-5,14-[1,2]benzenopentacene-2,3,18,19-tetraol **(39)** | 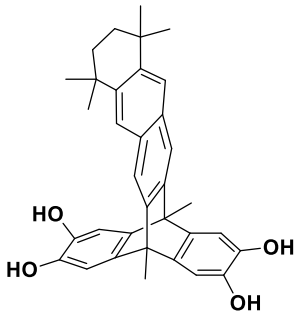 |
| 2,3,6,7,12,13-hexabromotriptycene **(40)** | 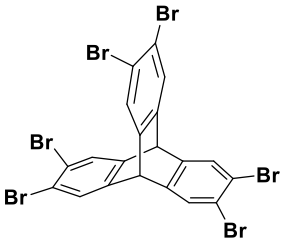 |
| 2,3,6,7,12,13-hexamethoxytriptycene **(41)** | 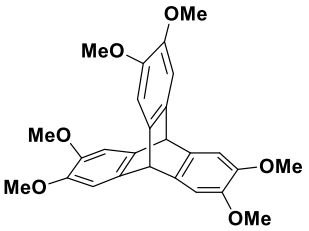 |
| 2,3,6,7,12,13-hexahydroxytriptycene **(42)** | 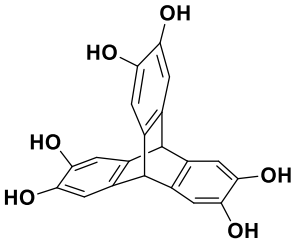 |
| 4,5-dichlorophthalic acid anhydride **(43)** | 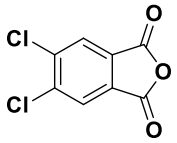 |
| N-phenyl-4,5-dichlorophthalimide **(44)** | 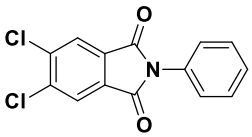 |
| *N,N'*-diphenyl thianthrene-2,3,7,8-tetracarboxyl bisimide **(45)** | 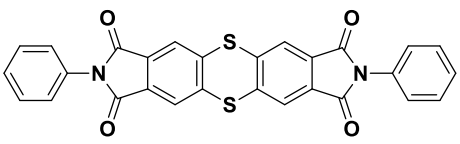 |

| | |
|---|---|
| Thianthrene-2,3,7,8-tetracarboxylic acid **(46)** | 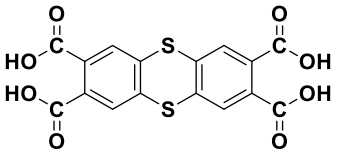 |
| Thianthrene-2,3,7,8-tetracarboxylic acid anhydride **(47)** | 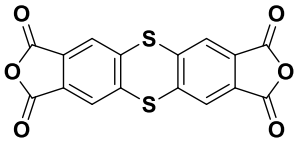 |
| Thianthrene-2,3,7,8-tetracarboxylic acid anhydride-5,5,10,10-tetraoxide **(48)** | 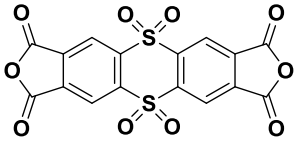 |
| 2,5-diphenylhexane-2,5-diol **(49)** | 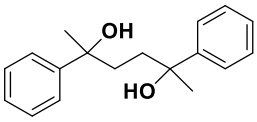 |
| 9,10-dimethyl-9,10-dihydro-9,10-ethanoanthracene **(50)** | 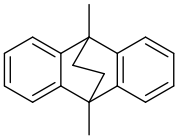 |
| 9,10-dimethyl-9,10-dihydro-2,6(7)-dinitro-9,10-ethanoanthracene **(51)** | 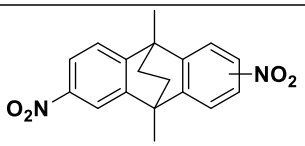 |
| 9,10-dihydro-2,6(7)-diamino-9,10-ethanoanthracene **(52)** | 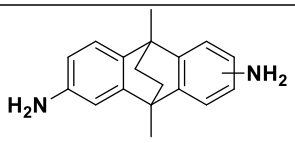 |
| 9,9′-bis(4-aminophenyl) fluorene (BAPF) **(53)** | 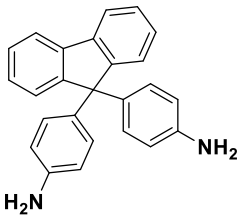 |
| 1,3,3-trimethyl-1-phenylindane **(54)** | 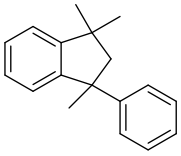 |

6,(7)-nitro-1,3,3-trimethyl-1-(4-nitrophenyl)indane **(55)**

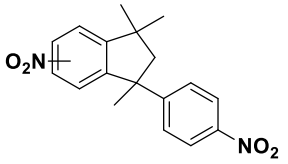

6,(7)-amino-1,3,3-trimethyl-1-(4-aminophenyl)indane **(56)**

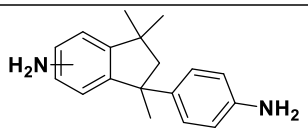

TB-polystyrene polymers **(TB-PS-57)**

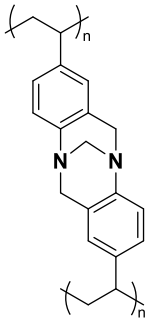

**TOT-TTSBI-58**

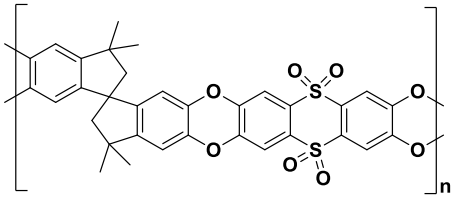

**TOT-SBC-59**

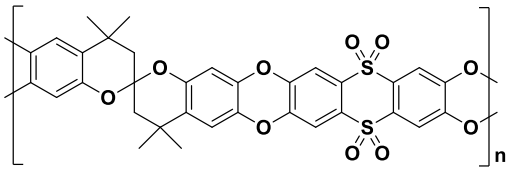

**TOT-EA-60**

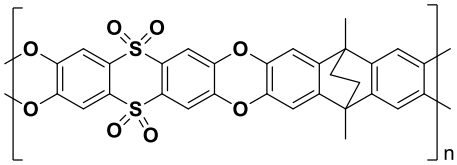

**TOT-Cardo-61**

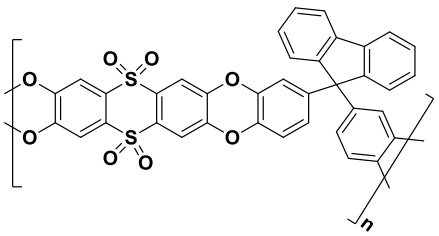

**TOT-SBF-62**

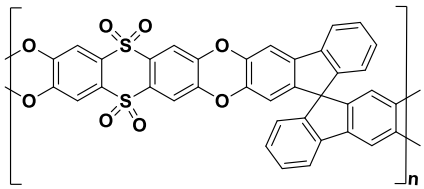

**TOT-SBF-63**

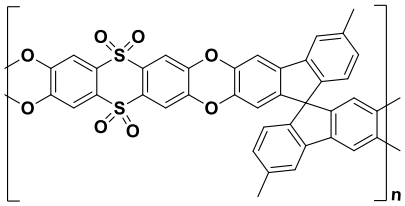

**TOT-SBF-64**

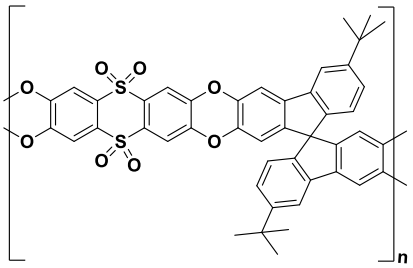

**TOT-HPB-65**

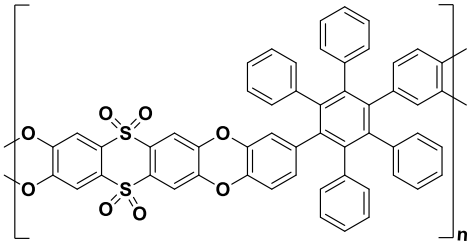

**TOT-TMN-Trip-66**

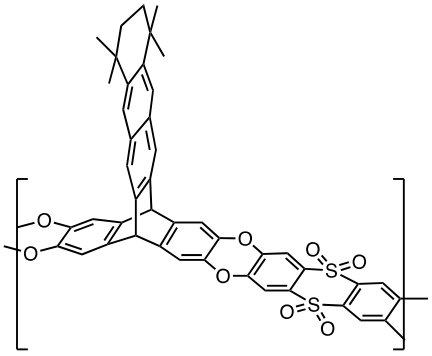

**TOT-Trip-67**

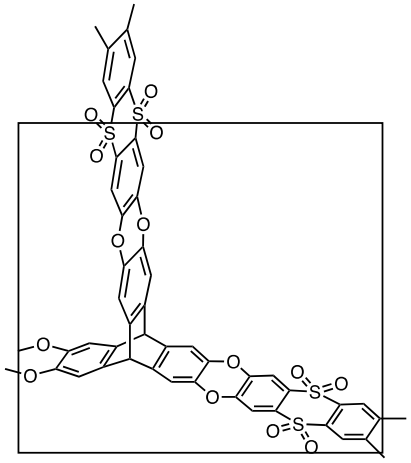

**TOT-PDA-68**

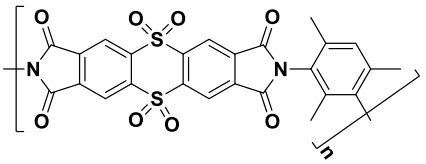

**TOT-PDA-69**

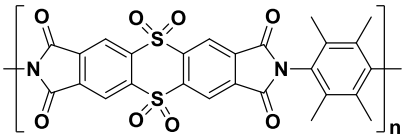

**TOT-DMN-70**

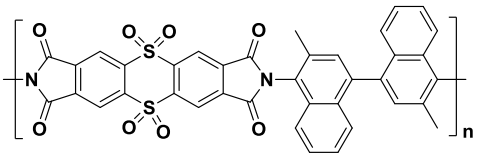

**TOT-EA-71**

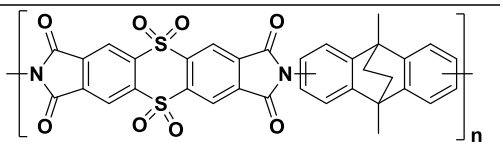

**TOT-BAPF-72**

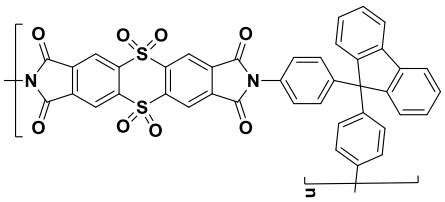

**TOT-TMPI-73**

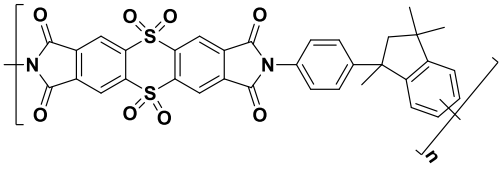

**TOT-PDA-74**

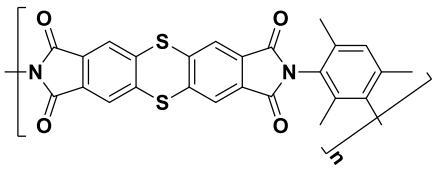

**TOT-PDA-75**

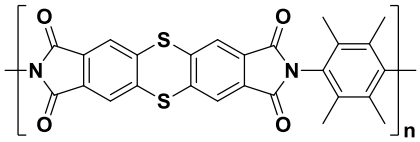

# Contents

# Chapter 1 Introduction

## 1.1 Porous materials

Porous materials can be defined as solids with pores, such as cavities or channels, which are deeper than they are wide. Whether prepared from organic or inorganic building blocks, porous materials have become of increasing importance for many areas of technological interest including heterogeneous catalysis, molecular separation and gas storage.[1] Three types of pores are classified according to their sizes by the International Union of Pure and Applied Chemistry (IUPAC). Firstly, macroporous materials which have pores of internal width greater than 50 nm. Secondly, mesoporous materials which have pores of internal width between 2 and 50 nm and finally, microporous materials which have pores of internal width are less than 2 nm.[2] Moreover, pores can be classified according to their shapes and accessibility as closed pores, open pores and roughness pores. These different types of pores are shown in **Figure 1**.

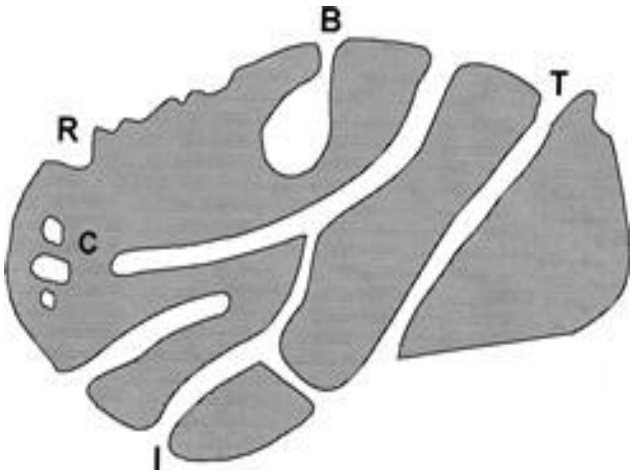


**Figure 1** Cross-section of a porous material showing various types of pores[2]

Firstly, closed pores can be defined as cavities not connected to the surface. Secondly, open pores are cavities or channels with access to the surface. Open pores exist in many types, blind pores (or dead-end pores) (B) which have pores with a single connection to the surface, interconnected pores (I) which communicate with other pores, through pores (T) which are open at both sides of the porous material. Finally, roughness pores(R) are regarded as external surface areas. Roughness pores must be deeper than they are

wide to be described as pores.[2] Furthermore, pores can also be classified by their shapes, for example, cylindrical shaped (I), ink bottle shaped (B) and funnel shaped (T).

## 1.2 Surface area measurement

Surface area is the extent of available (i.e. accessible) surface as determined by a given method under stated conditions. Surface area is a parameter used to measure the porosity of porous materials. There are many techniques available to determine surface area such as optical methods[3], porosimetry methods using a non-wetting liquid such as mercury[4] and computational methods.[5] However, the most often applied methods to determine the surface area of porous materials involves the measurement of gas sorption. Gas sorption involves enrichment at the interface between two bulk phases (i.e. solid and gas). Two types of forces can be involved; physisorption or chemisorption forces. Physisorption forces involve weak van der Waals forces between the gas molecules and solid, leading to a reversible process, which is well-suited for the determination of surface area. The gas sorption experiment starts with heating and degassing the sample of porous material in order to remove any adsorbed molecules. This is followed by the injection of controlled doses of inert gas, such as nitrogen gas, into the clean surface of the porous material. By measuring the amount of gas taken up by the sample, either by changes in sample weight (gravimetric analysis) or by change in the volume of the probe gas (volumetric analysis), it is possible to determine the number of gas molecules adsorbed to the surface, and hence estimate the surface area. In 1916-1918, Iriving Langmuir developed an adsorption model which considered the equilibrium between a gas molecule ($\mathrm{A}$), a free surface site ($\mathrm{S}$) and an adsorbed molecule ($\mathrm{AS}$).[6]

$$\mathrm{A} + \mathrm{S} \rightleftharpoons \mathrm{AS}$$

$$\mathrm{K} = \frac{[\mathrm{AS}]}{[\mathrm{A}][\mathrm{S}]}$$

In a dynamic equilibrium, the rate of adsorption is the same as the rate of desorption. The equilibrium constant $K$, can therefore also be defined in terms of the fraction of occupied sites ($\theta$) and the concentration of available sites, ($1 - \theta$):

$$K = \frac{K_{ads}}{k_{des}} = \frac{\theta}{(1-\theta)P}$$

where $P$ = partial pressure of the sorbing gas. By rearranging for $\theta$, the final form of the Langmuir adsorption isotherm is obtained which gives the volume of gas adsorbed ($V_A$) in relation to the total volume of the monolayer region ($V_M$):

$$\theta = \frac{KP}{1+KP} = \frac{V_A}{V_M}$$

This is often presented in the y = mx + c form in order to extrapolate values for $V_M$ from measurable data:

$$\frac{1}{V_A} = \frac{1}{KV_M}\left[\frac{1}{P}\right] + \frac{1}{V_M}$$

However, Langmuir's analysis is based on the assumptions that adsorption cannot proceed beyond monolayer coverage. The first significant attempt to overcome this weakness was in 1938 by Brunauer, Emmett and Teller (BET).[7] The BET method involves two stages. Firstly, construction of the BET plot to derive the value of the monolayer capacity, $V_M$. The Langmuir equation was modified by Brunauer, Emmett and Teller to give the following BET equation:

$$\frac{P}{V_A(P-P^o)} = \frac{C-1}{CV_M}\left[\frac{P}{P^o}\right] + \frac{1}{CV_M}$$

where $P$ is a partial pressure of the adsorbate gas in equilibrium with the sample surface ($Pa$), $P^o$ is a saturation pressure ($Pa$), $V_M$ is a monolayer volume (ml), $V_A$ is the volume of gas adsorbed (ml), and $C$ is a dimensionless BET constant. A plot of the gas adsorbed ($P/V_A(P\text{-}P^o)$) against the relative partial pressure ($P/P^o$) results in an adsorption isotherm, which by IUPAC definition can be categorized into six main types **Figure 2**. The isotherm most characteristic of a typical microporous material is represented by Type I, which demonstrates a large uptake of adsorbate at very low relative pressure ($P/P^o < 0.05$).

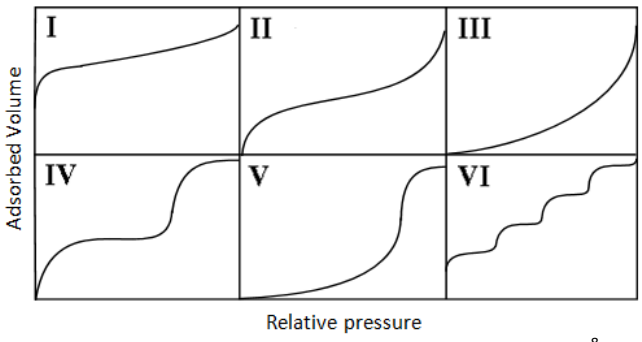


**Figure 2** IUPAC classification of adsorption isotherms[8]

At these very low pressures, the adsorbate gas molecules access the micropores and proceed in covering the surface of the solid. The curve then tends to flatten giving a linear plot over the range $0.05 \leq P/P^o \leq 0.35$, as adsorption of the first monolayer is completed. From this plot, the intercept ($I$) and gradient ($A$) can then be calculated and after rearrangement of the equation, the monolayer volume ($V_M$) is given as follows:

$$V_M = \frac{1}{A + I}$$

Secondly, calculation of the specific area by using the value of the monolayer capacity and the average area occupied by each molecule in the completed monolayer can be achieved during the measurement of the isotherm, the material is subjected to a range of pressures whilst the sample tube is immersed in liquid nitrogen (77 K). Hence, if the effective area occupied by one gas molecule is known and the monolayer volume ($V_M$) has been

calculated, the specific surface area ($S_{BET}$ ($m^2$ $g^{-1}$)) can then be determined using the following equation:

$$S_{BET} = \frac{N_A V_m \sigma}{W_S M_V}$$

where $N_A$ = Avogadro's number ($6.022 \times 10^{23}$ $mol^{-1}$), $\sigma$ = effective cross-sectional area of the probe molecule (e.g. 16.2 $Å^2$ for nitrogen),[9] $W_S$ = weight of sample (g) and $M_V$ = molar volume occupied by a gas at STP (22414 ml).

## 1.3 Introduction to Microporous Materials

Microporous materials have been at the centre of increasing interest over the past few decades. They owe their properties to their microporosity which make them attractive for many industrial applications, such as heterogeneous catalysis[10,11], gas separation membranes[12,13], hydrogen storage[14,15] and adsorbents for organic compounds. This section aims to provide an overview of some the most significant microporous materials.

### 3.3.1 Zeolites

A zeolite is a crystalline aluminosilicate with a three-dimensional framework structure that forms uniformly sized pores of molecular dimensions. It consists of robust crystalline silica ($SiO_2$) frameworks. At some places in the framework $Al^{3+}$ has replaced $Si^{4+}$ and the framework carries a negative charge. Loosely held cations that sit within the cavities preserve the electroneutrality of the zeolite.[16] These guest cations can be readily exchanged with other species in the contact solution without changing the crystal structure. The first recognised natural zeolite was stilbite (STI) which was discovered in 1756 by Cronstedt.[17] He discovered that when heated the mineral fused readily in a blowpipe flame with obvious loss of water. Despite occurring in nature, many attempts were made in order to develop and synthesise zeolites. In 1845, one of the earliest attempts to synthesise silicates was carried out by Schafhautle. He prepared quartz by heating a silicate with water in an autoclave. In the early 1940s, the pioneering work in

the synthesis of zeolites was carried out by Barrer.[18] He investigated the conversion of known mineral phases in strong salt solutions at fairly high temperatures (170-270 °C). In 1948, he successfully synthesised the first zeolite with no natural counterpart, ZK-5[19] **Figure 3**.

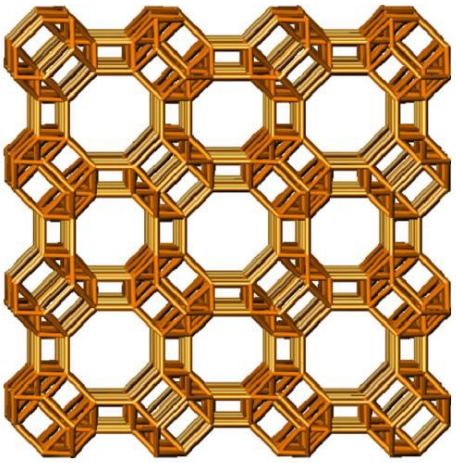

**Figure 3** Framework structures of ZK-5 first prepared by Barrer[20]

In the late 1940s, A(LTA), X(FAU) and P(GIS) zeolites were synthesised by Milton and co-workers by hydrothermal crystallization of reactive alkali metal aluminosilicate gels at lower temperatures (100 °C) under alkaline condition.[21] Subsequently, many zeolites were prepared. In 1982, a new family of aluminophosphate molecular sieves was synthesised by Wilson *et al*. (2007) The basic route of zeolite synthesis is the hydrothermal technique, which refers to reactions conducted under high temperature and high pressure (>100 °C, > 1 bar) in aqueous solutions in a closed system.[17,22] Zeolites play a significant role in many industrial applications. For example, their excellent ion exchange properties in the hydrated state allows use in applications such as water softening in the detergent industry.[23,24] In dehydrated zeolites, the uniform pore size becomes an important factor for their application as “molecular sieves”. The relative size of the pores dictates that only molecules smaller than the pore diameter may be adsorbed, whilst larger molecules are excluded.[25] This creates a sieve-like property which has been utilized in applications such as the purification of gaseous hydrocarbons and the preparation of catalysts for petroleum refining.[26]

### 3.3.2 Activated carbons

Activated carbons are a group of materials with highly developed internal surface area and porosity, leading to a large capacity for adsorbing chemicals from gases or liquids. It consists of a non-organized phase of randomly connected graphite-like sheets[27] **Figure 4**.

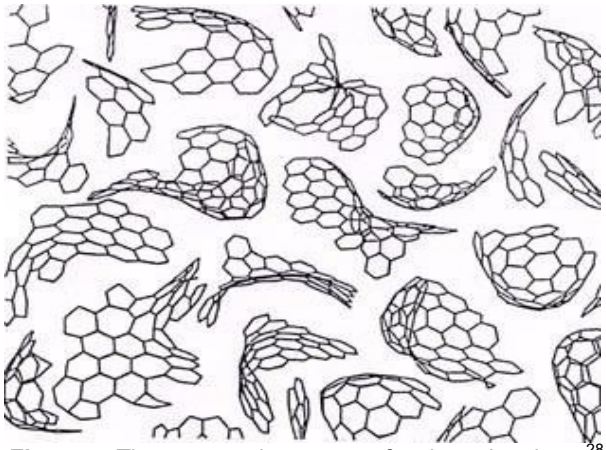

**Figure 4** The proposed structure of activated carbons[28]

Activated carbons are prepared via pyrolysis of a highly carbonaceous species which can then be activated by either thermal or chemical treatment. Source of a highly carbonaceous species could be natural, such as, wool, coal, peat, fruit stones and shells or synthetic precursors, such as viscose rayon and phenolic resins. The pyrolysis step involves decomposition of organic molecules and evolution of gaseous products. After that, carbonized materials are activated by physical or chemical procedures[29]. Thermal treatment is performed by treating the material at 700 – 1000 °C in the presence of oxidising gases, such as steam and carbon dioxide. Chemical treatment is performed by treating the material at 500 – 800 °C in the presence of a dehydrating species, such as potassium hydroxide or phosphoric acid. Activated carbons are used in many industrial applications due to their unique structure, high surface area and reactivity.[30] For example, they are used to remove undesired species by adsorption from gases or liquids. In addition, they used as catalysts or catalyst supports, purification and separation process. Moreover, they are using in medicine to combat certain types of bacteria.[29] Furthermore, activated carbon can be also

modified, for example, with nitric acid which makes its surface more hydrophilic[29] which affects their adsorption properties.

### 3.3.3 Metal Organic Frameworks (MOFs)

Metal Organic Frameworks (MOFs) are a class of crystalline materials, consisting of metal ions linked together by organic bridging ligands. In comparison to the conventionally used inorganic microporous materials such as zeolites and activated carbons, MOFs can show greater porosity. In addition, MOFs offer the ability to synthetically tailor the microporous structure based on the diversity of metals and organic bridging ligands.[31] MOF-5 is one of the successful designs of rigid frameworks.[32] MOF-5 structure is showing four $ZnO_4$ tetrahedral with six carboxylate carbon atoms which are joined together by benzene links **Scheme 1**.[31] It shows high thermal stability coupled with high surface area of 3000 $m^2/g$.

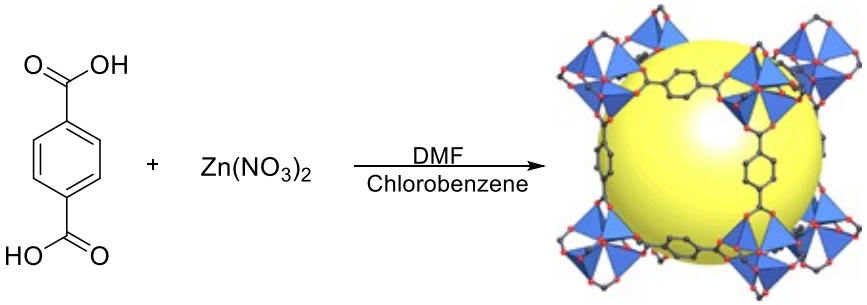


**Scheme 1** Synthesis of MOF-5 with structure showing ZnO4 tetrahedral and benzene dicarboxylate linkers giving an extended 3D cubic framework with interconnected pores[31]

HKUST-1 is another metal framework that involve benzene-1,3,5-tricarboxylate (TMA) which links with dimeric copper units.[33] It exhibits high thermal stability up to 240 °C. MOFs are widely regarded as promising materials for many applications. For example, gas storage is one potential application. For example, MOF-210 uptakes 17.6 wt% of $H_2$ gas at 77 K and 60 bar. Moreover, carbon dioxide capture is another application of MOFs. MOF-210 can adsorb 2.4 times its own weight of $CO_2$ at 50 bar and 298 K **Scheme 2**.[34]

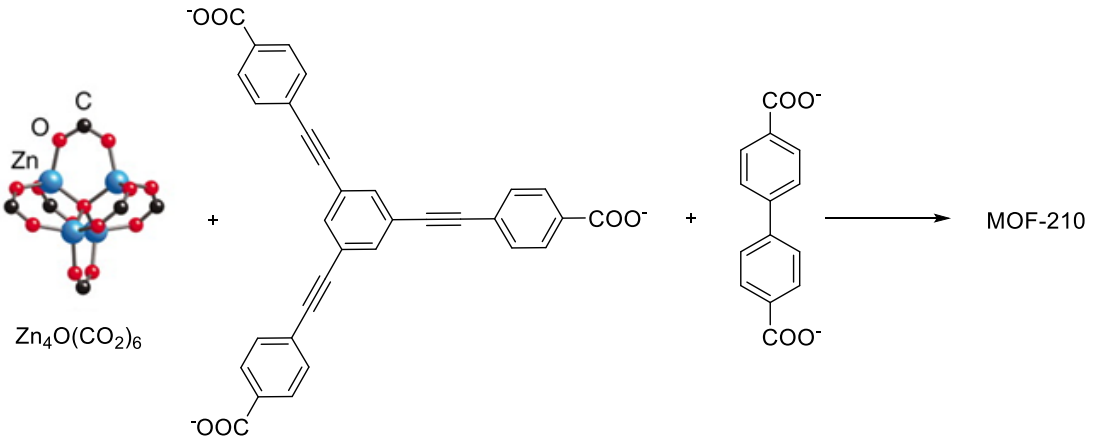


**Scheme 2** Synthesis of MOF-210

### 3.3.4 Covalent Organic Frameworks (COFs)

Covalent Organic frameworks (COFs) are crystalline materials prepared from linking organic monomers together via covalent bonds[35] and are made entirely from light elements (H, B, C, N and O). Hence, COFs have lower skeletal mass density than MOFs. In addition, COFs have synthetic flexibility, which enables structural diversity. COF-1 was prepared via the self-condensation of benzene-1,4-diboronic acid **Scheme 4**.[36] It is a hexagonal array of benzene rings connected by $B_3O_3$. The crystallinity of COFs is attributed to the reversible nature of the boroxine ring formation. COF-1 demonstrated a surface area of 711$m^2$/g. In 2007, a significant advance was achieved by preparing COFs-102-108.[37] Self-condensation reactions of tetra(4-dihydroxyborylphenyl) methane (TBPM) or tetra(4-dihydroxyborylphenyl)silane (TBPS) provided crystalline 3D COFs. Co-condensation reactions of TBPM or TBPS with triangular 2,3,6,7,10,11-hexahydroxytriphenylene (HHTP) produced crystalline solids of COF-105 and COF-108, respectively **Scheme 3**.[38] All of these materials were found to be crystalline with high surface areas up to 4210 $m^2$/g. Owing to their structural characteristics, they are very promising in many applications, such as adsorption, separation, catalysis and sensors. For example, COF-102 showed high capacity for gas storage, 7.24 wt. % for hydrogen at 77 K and 40 bars, and 187 mg/g for methane at 298 K and 35 bars.

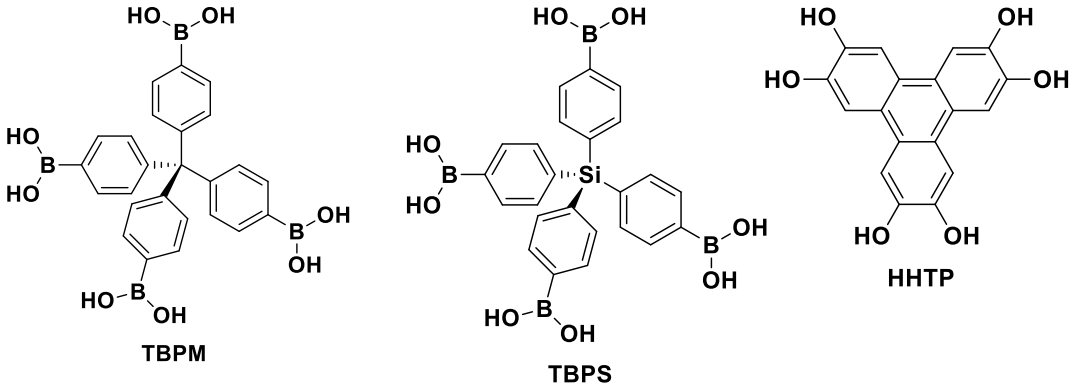


**Scheme 3** The chemical structure of TBPM, TBPS and HHTP

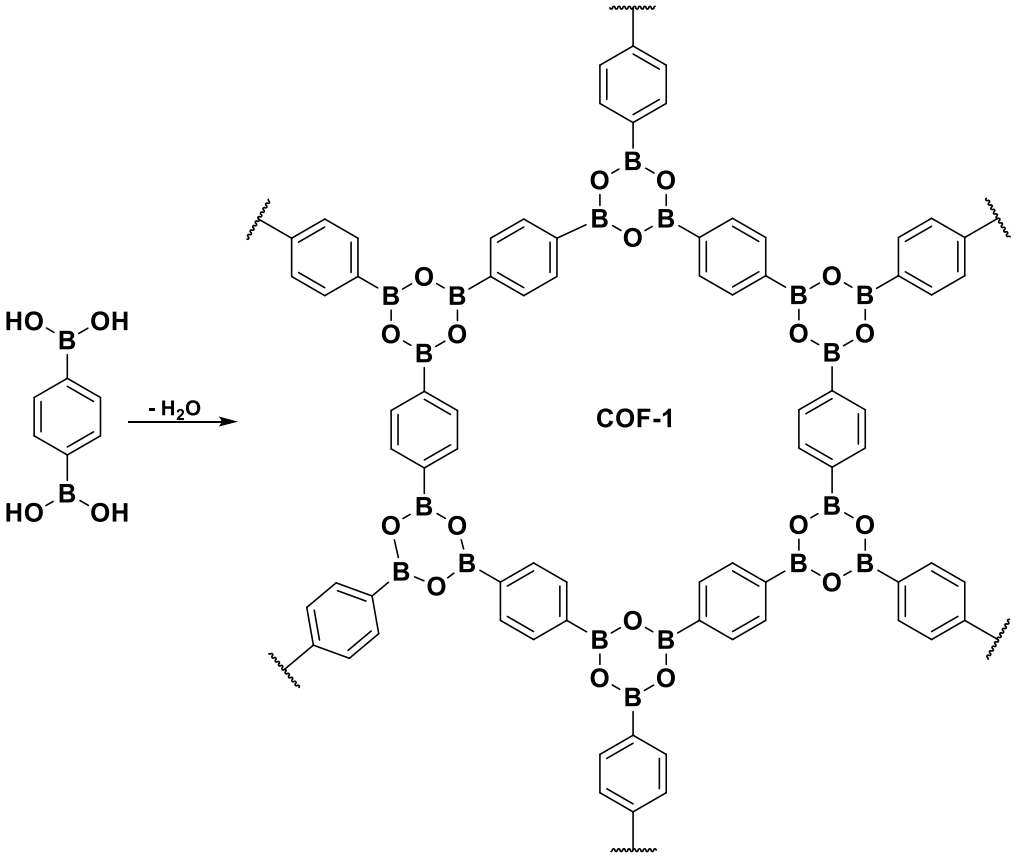


**Scheme 4** Synthesis of COF-1

### 3.3.5 Hypercrosslinked polymers (HCPs)

Hypercrosslinked polymers are a broad group of materials which are made from crosslinked polymer chains composed of light elements (C, H, N, and O). They possess very high surface areas and rigid structures which makes them attractive for many applications in modern technology, such as gas storage[39], solid phase extraction[40], treatment of waste water[40], chromatographic analysis[41] and sorption of organic compounds.[42,43] Various HCPs have been prepared by using different precursors, such as crosslinked polystyrene, EOF-1, EOF-2[44], polyanilines[45] and polypyrrole.[46] In the following section, hypercrosslinked polymers will be discussed in more detail due to their relevance to some of the work described in this thesis. Crosslinked polystyrene networks are commonly used sorbents because of their availability, simplicity of synthesis and their various pore structures which provides polymeric sorbents with a wide range of physical properties.[47,48] Styrene-divinylbenzene (DVB) copolymers are subdivided into two types according to the use of diluents during their preparation. The first type are conventional networks or homogeneous gel-type polymers, produced by the radical copolymerization of styrene with DVB monomers in the absence of any diluent.[49] The second type are macroporous (macroreticular) adsorbents which are heterogeneous networks and are produced by the copolymerization of styrene with a relatively large amount of DVB in the presence of solvent which precipitates the growing polystyrene chains. These adsorbents have relative high surface area. For example, the Amberlite XAD-4 polymeric resin, a macroporous styrene-divinylbenzene copolymer, has surface area up to 880 $m^2/g$.[50] Hypercrosslinked polystyrene (styrosorbs), first prepared in the early 1970s by Davankov, provided a new class of polystyrene sorbents. These sorbents have different chemical structures, therefore different properties of sorption.[48] The basic principle of styrosorb synthesis is to introduce a high number of rigid bridges between the polystyrene chains. These materials are prepared in two steps. Firstly, vinyl benzene chloride is crosslinked with a small amount of divinylbenzene (DVB) in order to obtain a lightly crosslinked polymer. In the following step

the swollen crosslinked polystyrene is hypercrosslinked by Friedel-Craft alkylation reaction, using a Lewis acid such as iron (III) chloride **Scheme 5** .[51]

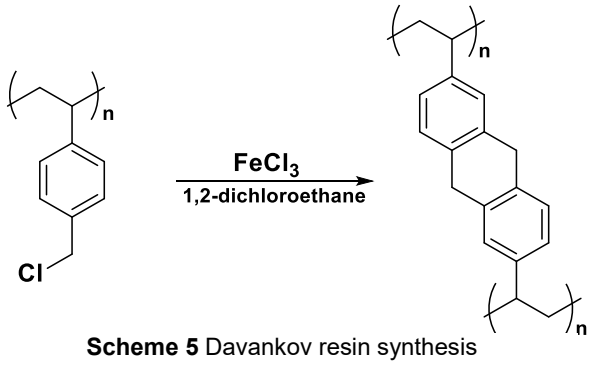


**Scheme 5** Davankov resin synthesis

Hypercrosslinked polystyrene has also been obtained without the need to form a precursor crosslinked polymer.[39] This procedure uses bifunctional compounds such as 1,4-bis-chloromethylbiphenyl and p-xylene dichloride, which crosslink linear polystyrene chains via Friedel-Crafts alkylation reaction to produce hypercrosslinked polystyrene **Scheme 6**.

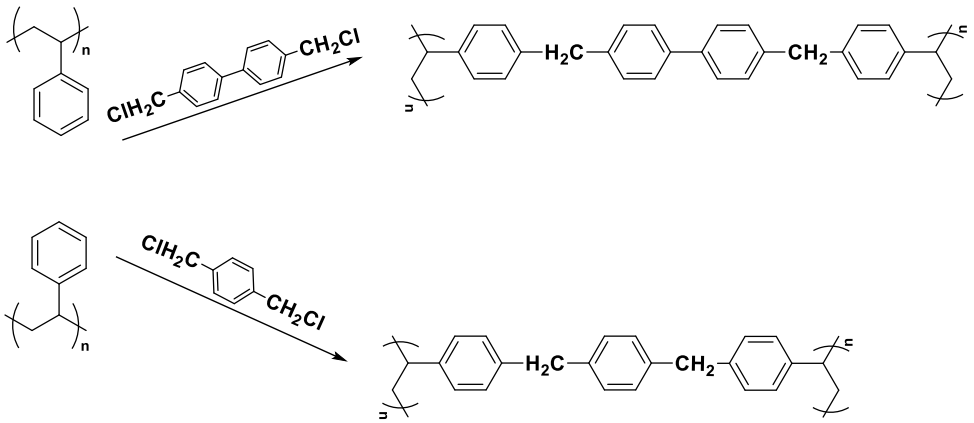


**Scheme 6** Synthesis of hypercrosslinked polystyrene

The obtained styrosorbs are homogeneous resins that have a greater sorption capacity for organic compounds than other organic and organo-mineral sorbents.[52] This is due to some unique properties that distinguish them from other sorbents.[53,54] For example, they possess high porosity and a high inner surface area, reaching 1000-1300 $m^2/g$ due to a high number of rigid bridging groups between the polystyrene chains. For instance, the sorption capacity of naphthalene derivatives by two hypercrosslinked resins CHA-101 and CHA-111, which were prepared from styrene-divinylbenzene

monomers, is higher than other classical adsorbents such as silica gel, alumina and activated carbons. This is due to their high surface areas, 898 and 736 $m^2/g$, respectively, homogeneous structure of pores and appropriate pore diameter and presence of polar segments.[43] Another advantage of styrosorb is their ease of swelling with any liquids or gases even those with negligible affinity towards polystyrene. This happens because of the highly stressed state of styrosorbs in their dry state, which is relaxed on swelling. In addition, styrosorbs can be regenerated by either vacuum or heating the sorbent to 80 °C, therefore using much less energy than for activated charcoal or Zeolites, for which regeneration typically occurs at 200-250 °C and at 300-350°C, respectively. The amount of adsorbed vapour of organic compounds by styrosorbs is considerably higher than that of inorganic sorbents with that of styrosorb reaching 1.2 $cm^3/g$ for small alkanes.[54] In particular, the amount of sorbed n-hexane by styrosorbs (0.8 $m^3/g$) is much greater than that of Zeolite NaX (0.2 $m^3/g$), activated charcoal AR-3 (0.15 $m^3/g$), or polysorb-1 (0.22 $m^3/g$). Similarly, styrosorbs adsorb greater amount of many organic substances in polar solutions. For example, the amount of lecitine which can be absorbed by styrosorb from isopropanol is 0.7g per 1g of the sorbent which is considerably greater than those of macroporous polystyrene adsorbent Amberlyte XAD-4 (0.35 g per 1 g of the sorbent).[53] A further advantage of these materials is their potential for scale-up so that the adsorption process is appropriate to industrial use.[55] Consequently, they can be used in a wide range of applications in many large-scale adsorption technologies and in analytical chemistry and offer various solutions to obstacles in modern technology. For example, styrosorbs have been successfully used as a stationary phase in the separation of N-containing compounds found in petroleum.[56] Furthermore hypercrosslinked polystyrene could be used to separate mineral salts, acids and bases via a size exclusion mechanism.[41] Moreover, hypercrosslinked polystyrene could be used for adsorption of organic compounds (lipids, phenols, chlorophenols, dyes and fatty acids) dissolved in water.[55] Interestingly, chemical modification of hypercrosslinked polystyrene can be achieved to modify adsorption

properties. The possibility of hypercrosslinked polystyrene to be modified is due to the existence of some residual unreacted chloromethyl groups in the polymer network. These groups can be replaced by a wide range of other functional groups to enhance the sorption ability of hypercrosslinked polystyrene.[42]

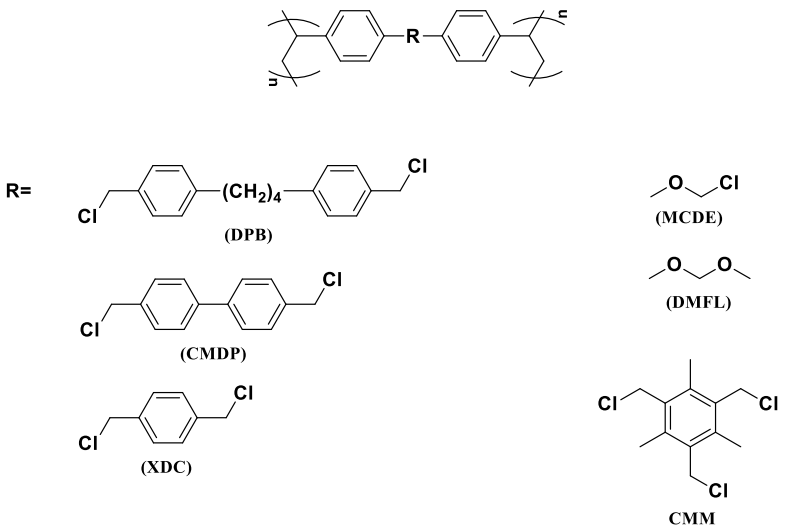


**(DPB):** p,p'-bis-chloromethyl-1,4-diphenylbutane. **(DMFL):** dimethylformal.
**(CMDP):** 1,4-bis-chloromethyldiphenyl. **(MCDE):** monochlorodimethylether.
**(XDC):** p-xylylenedichloride. **(CMM):** 2,4,6-trischloromethylmesitylene

**Scheme 7** Chemical structures of different hypercrosslinked polystyrene

Linear atactic polystyrene was hyper-crosslinked with different crosslinking agents[57,58,59] **Scheme 7**. The hyper crosslinking reaction was achieved via the Friedel-Crafts reaction by using stannic chloride as a catalyst and by using dichloroethane as a solvent. The resulting hyper-crosslinked styrene polymers are porous with surface areas reaches 1000 $m^2/g$. High surface area values of resulted hyper-crosslinked polymers are due to their rigidity which has influence on their adsorption properties. Adsorption performance was improved with increasing the rigidity of the polymers. For example, in the most rigid structures crosslinked by 2,4,6-trichloromethylmesitylene, the apparent surface area reaches 700 $m^2\ g^{-1}$ at only 25% degree of crosslinking, whereas for other rigid networks this value of the surface area is reached after the formation of a much larger number of linkages.

### 3.3.6 Polymers of intrinsic microporosity (PIMs)

In recent years, porous polymer based organic materials were developed by using the concept of "*intrinsic microporosity",* which is defined as *"a continuous network of interconnected intermolecular voids that forms as a direct consequence of the shape and rigidity of the component macromolecules".*[60] In general, polymers are not usually microporous and tend to pack space efficiently in order to maximize intermolecular interactions. Polymers are able to do this due to their conformational flexibility. Consequently, no microporosity will be produced. In contrast, the concept of PIMs aims to maximize intrinsic microporosity by minimizing the efficient pack space of polymers. Highly rigid and contorted polymer chains are required to achieve this goal. Rigid and contorted structures restrict the conformational flexibility of polymers, leading to less efficient space packing of the chains. This goal was achieved by using three different kinds of polymerization reactions: dibenzodioxin formation, imide formation and Tröger's base formation.

#### 3.3.6.1 Polymers of intrinsic microporosity using dibenzodioxin linkages

PIMs can be formed by a double nucleophilic aromatic substitution reaction between a tetrahydroxylated monomer and a tetrafluorinated monomer, resulting in the formation of dioxin links between monomer units **Scheme 8**. It is essential for the production of a microporous PIM for one of the monomers to have a highly rigid and contorted structure; if this is not the case then the resulting polymer will not be microporous.

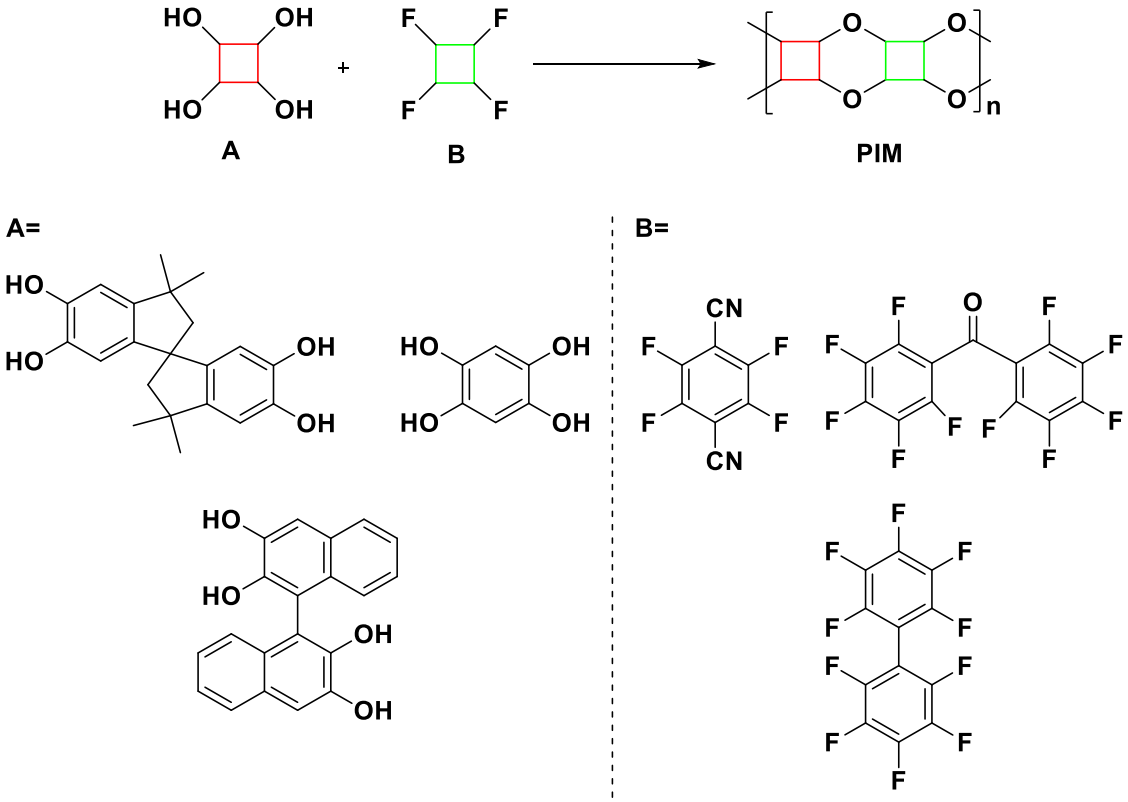


**Scheme 8** General synthesis of PIMs

In the late 1990s, McKeown and co-workers designed phthalocyanine network polymers by incorporation spirocyclic groups with phthalocyanines **Scheme 9**. This polymer was prepared by the reaction of spirocyclic bisphthalonitrile with metal ion. Bisphthalonitrile precursor was prepared by the reaction between 5,5',6,6'-tetrahydroxy-3,3,3',3'-tetramethyl-1,1'-spirobisindane and 4,5-dichlorophthalonitrile[61]. The resulting network polymer proved to be highly porous with a surface area over 750 $m^2$ $g^{-1}$. These materials were found to have useful catalytic activity in oxidations reactions.[62,63] After that, many highly porous network polymers were prepared by using the same strategy of reacting appropriate fluorinated or chlorinated monomers with complementary monomers that contain multiple catechol units.[64,65]

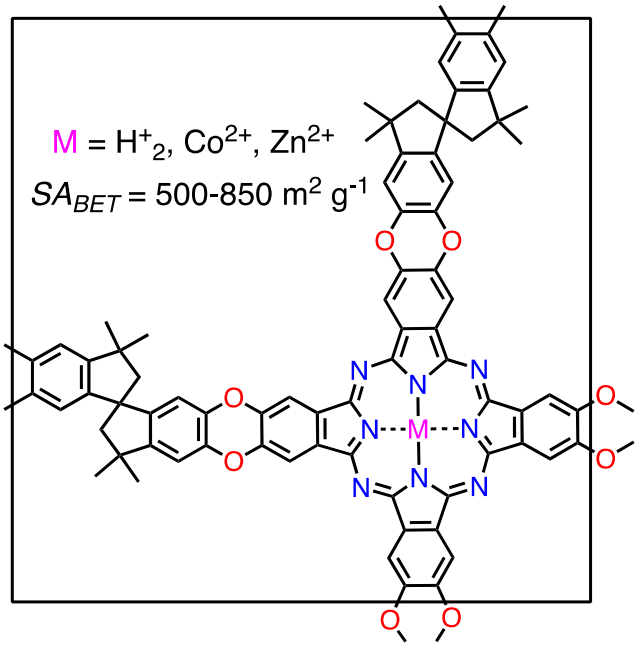


**Scheme 9** The phthalocyanine-based microporous polymer network

In 2004, the significant advance in this field was achieved by McKeown, Budd and co-workers.[66] They successfully prepared non-network polymers of intrinsic microporosity derived from a purely organic monomer. For example, PIM-1 was prepared via the aromatic nucleophilic substitution reaction between 5,5',6,6'-tetrahydroxy-3,3,3',3'-tetramethylspirobisindane TTSBI and 2,3,5,6-tetrafluoroterephthalonitrile TFTPN **Scheme 10**. PIM-1 showed high surface area (860 $m^2/g$) due to its rigid structure arising from its spirocyclic sites of contortions. In addition, it was fully soluble in polar solvents such as chloroform and tetrahydrofuran which enabled the polymer to form self-standing films. In tests to investigate their potential for use in gas separations, PIM-1 films exhibit high permeability and good selectivity for some important commercial gas pairs such as $O_2/N_2$, $CO_2/CH_4$, $H_2/N_2$ with overall gas performance over the 1991 Robeson upper bound.

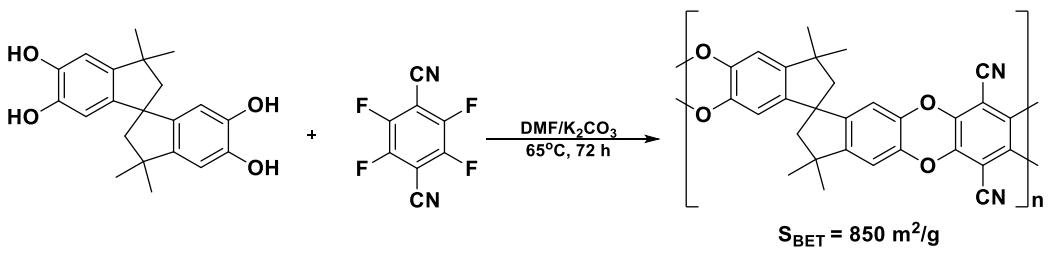


**Scheme 10** Synthesis of PIM-1

Since the synthesis of PIM-1 numerous soluble PIMs with similar or enhanced properties for gas separation have been obtained.[67-68] A soluble ladder polymer TPIM-1 was prepared by self-polymerisation of an A-B monomer containing 9,10-diisopropyl-o-quinone **Scheme 11**.[69] TPIM-1 was found to be highly porous, with a BET surface area of 862 $m^2$ $g^{-1}$. It showed high permeability to $H_2$ and $CO_2$, 2666 and 1549 Barrer, respectively, coupled with selectivity of 50 and 31 for gas pairs $H_2/N_2$ and $CO_2/CH_4$, respectively. Its overall gas separation performance was located close to the 2015 Robeson upper bound.

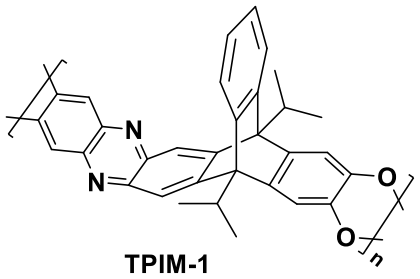


TPIM-1

**Scheme 11** The chemical structure of TPIM-1

Many PIM-1-based copolymers were prepared in order to enhance the gas separation properties. For example, PHPIM-061 was introduced by Yuan *et al*. (2017) **Scheme 12**. A rigid and twisty monomer, tetrahydroxyl-phthalazinone TPHPZ was polymerised with TTSBI and TFTPN[70]. The resulting co-polymer PHPIM-061 showed a high BET surface area of 812 $m^2$ $g^{-1}$. The gas separation performance surpassed the 2008 Robeson plot for $CO_2/CH_4$ and approached the 2008 upper bound for $H_2/N_2$, $O_2/N_2$ and $CO_2/N_2$.

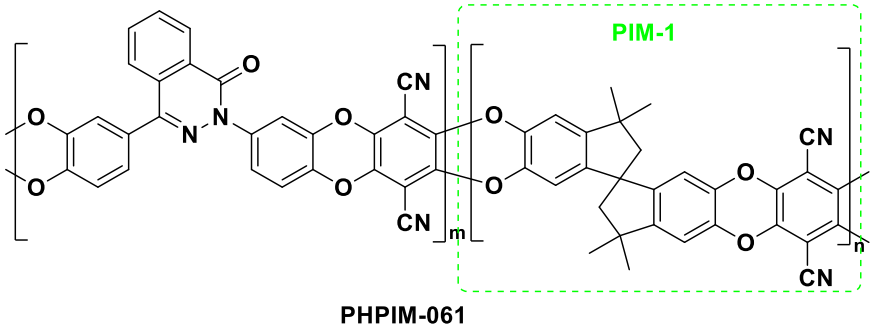


PHPIM-061

**Scheme 12** The chemical structure of PHPIM-061

In addition, PIM-1 was modified by alkaline hydrolysis with an extended reaction time of 360h to produce highly carboxylate-functionalised PIMs HCPIMs[71] **Scheme 13**. The resulting PIM was found to show higher $CO_2$ affinity than PIM-1, with a selectivity of 53.6 for $CO_2/N_2$ separation.[71]

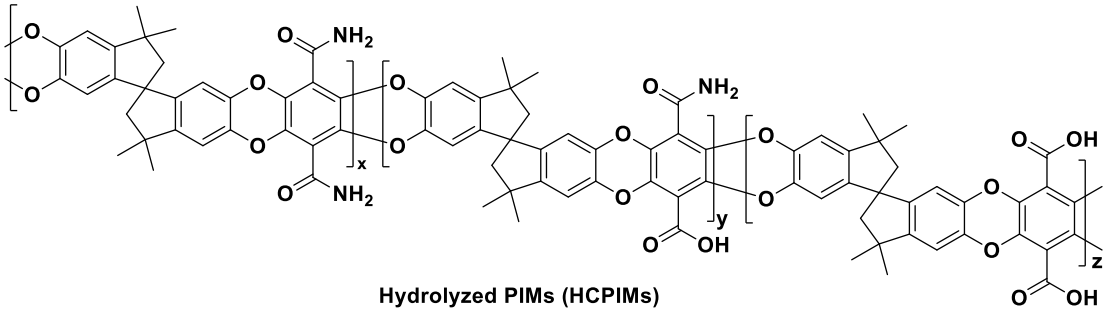


**Scheme 13** The chemical structure of HCPIMs

A cardo adamantane bis catechol monomer, 4,4'-((1r,3r)-adamantane-2,2'-diyl)bis(benzene-1,2-diol) THADM was polymerised with TFTPN to produce ADM-PIM **Scheme 14**. The resulting polymer (ADM-PIM) demonstrated high BET surface area, 703 $m^2$ $g^{-1}$. It showed excellent gas separation properties with performance surpassing the 2008 Robeson upper bound for the gas pair $O_2/N_2$.[72]

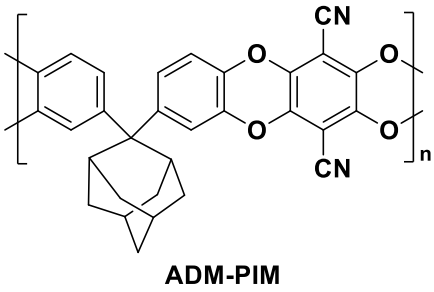


**Scheme 14** The chemical structure of ADM-PIM

### 3.3.6.2 Polymers of intrinsic microporosity for the formation of Tröger's base linkage (PIM-TBs)

Tröger's base is a bridged bicyclic molecule, which was first isolated as a reaction by-product by Julius Tröger in 1887. TB synthesis was achieved via condensation reaction of formaldehyde and aromatic amine (*p*-toluidine) in acid solution (hydrochloric acid) **Scheme 15**.[73]

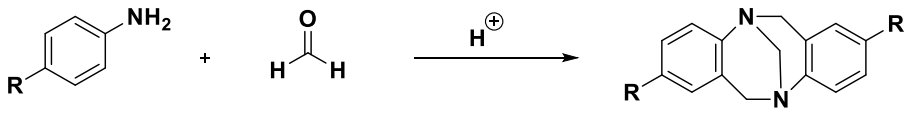


**Scheme 15** The synthesis of Tröger's base

The chemical structure of TB had puzzled chemists until 1935 when Spielman succeeded in assigning the correct structure of TB.[74] The correct chemical structure of Troger's base is (±)-2,8-dimethyl-6H,12H-5,11-mathanodibenzo[bf][1,5]diazocine **Scheme 16**, featuring central bridgehead nitrogen atoms and two benzene rings. Having such bridges lead to high rigidity in the TB structure.

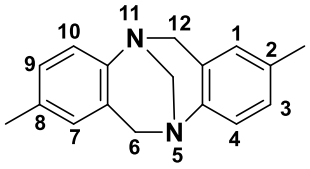


**Scheme 16** The structural formula of Troger's base

Enantiomers of Tröger's base were successfully separated in 1944 by using column chromatography on lactose.[75] Due to the presence of the bridged nitrogen atoms TB is a strong base. This property enables TB to be effective in many applications, for example, as a catalyst. In this context, mesoporous organosilica incorporating different amounts of TB showed considerable basic catalytic activity and high stability during recycling process in the Knoevenagel reaction **Scheme 17**.[76]

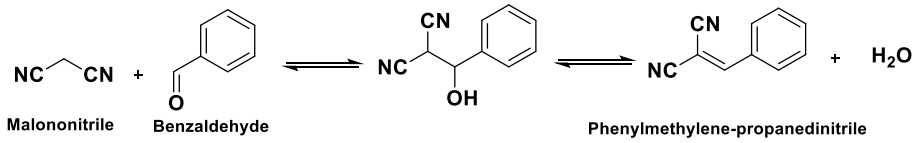


**Scheme 17** The Knoevenagel reaction

The catalytic activity in the presence of TB units is significant compared to that without TB units, the malononitrile conversion is about 100 % in the first case, while it is about 10 % without TB content. Due to its high structural rigidity, TB has been successfully used for the synthesis of microporous network polymers and Polymers of Intrinsic Microporosity. For example, tetra-anilyl-adamantane was reacted with dimethoxymethane to produce (TB-COP-1) **Scheme 18**, which showed a surface area of 1340 $m^2g^{-1}$ and

significant $CO_2$ uptake capacities 5.19 and 3.16 mmol $g^{-1}$ at 273 and 298k, respectively under ambient pressure.[77] For soluble PIMs the incorporation of TB was anticipated to increase the $CO_2$ uptake capacity to provide an improvement in their gas separation properties. For example, TB units were incorporated into the copolymer formed from 2,3,8,9-tetrahydroxy-6H,12H-5,11-methanodibenzo[bf][1,5]diazocine (THTB) and 5,5',6,6'-tetrahydroxy-3,3',3',3-tetramethylspirobisindane (TTSBI) and 2, 3, 5, 6-tetrafluoroterephthalonitrile (TFTPN) **Scheme 19**.

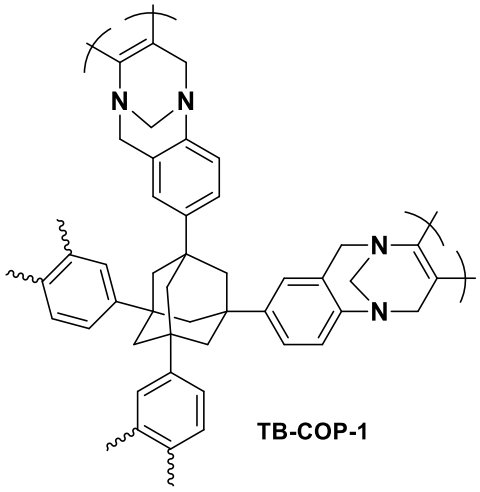


**Scheme 18** The chemical structure of TB-COP-1

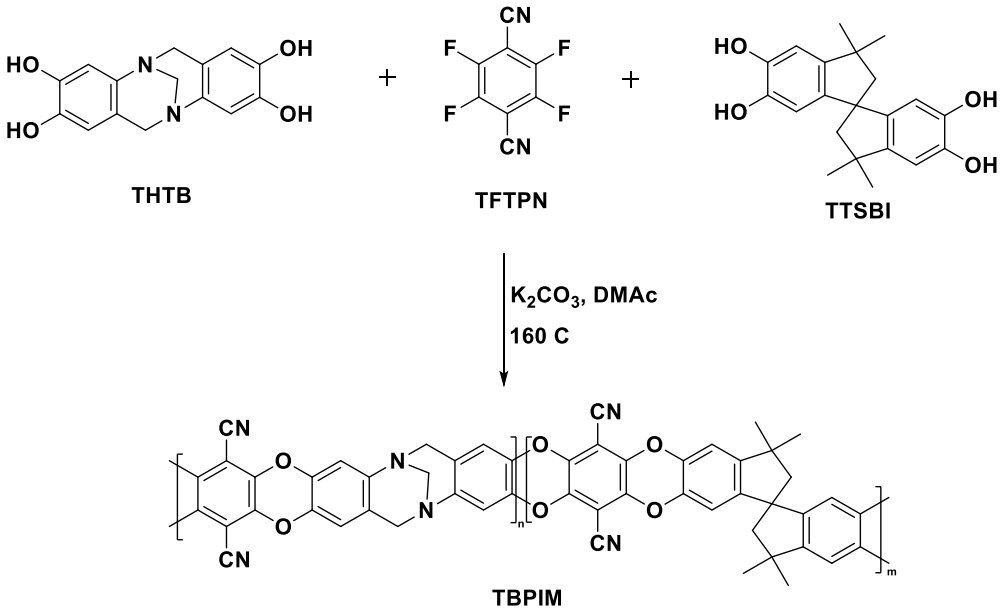


**Scheme 19** The synthetic route of TBPIM

When analysed for gas separation performance, the results showed a small improvement in selectivity for the $CO_2/N_2$ and $CO_2/CH_4$ gas pairs due to the increase in solubility of $CO_2$ which was attributed to the presence of nitrogen atoms in the TB structure.[78] Tröger's base forming reaction was used as a new polymerisation route to form novel PIMs such as PIM-EA-TB and PIM-SBI-TB **Scheme 20** which showed intrinsic microporosity and large apparent BET surface areas of 1028, 745 $m^2/g$, respectively. These are solution processable polymers which can be cast into films which showed high gas permeabilities and good selectivities for smaller gas molecules such as $H_2$ and $O_2$ over large ones such as $N_2$ and $CH_4$. Another example of this kind of polymer is PIM-Trip-TB **Scheme 20** with demonstrates enhanced performance for some important gas pairs and its data lie on the revised 2015 Robeson upper bounds for $O_2/N_2$, $H_2/CH_4$, $H_2/N_2$.[79]

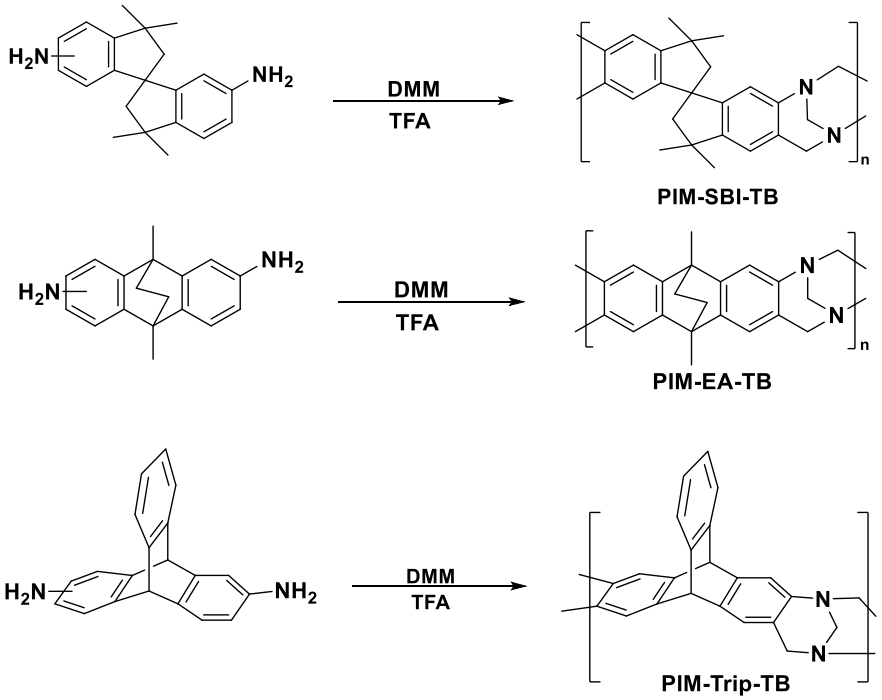


**Scheme 20** The synthesis and molecular structures of PIM-EA-TB, PIM-SBI-TB and PIM-Trip-TB

A polymer of intrinsic microporosity PIM-BTrip-TB was successfully synthesised by Rose *et al*. (2015) from 2,6-diaminobenzotriptycene based on Tröger's base formation reaction **Scheme 21**. It was shown to be highly microporous with an apparent BET surface area of 870 $m^2\ g^{-1}$ . The resulting

polymer showed exceptional oxygen permeability of 3290 Barrer and good selectivity of 3.6 for an $O_2/N_2$ gas pair with overall gas separation performance located over the 2008 Robeson upper bound[80]. Therefore, it was proved to be potentially useful material for oxygen enrichment from air. Another polymer of intrinsic microporosity PIM-MP-TB demonstrating a high selectivity of gas separation was prepared by Williams *et al*. (2018). The polymer PIM-MP-TB was prepared by the polymerisation reaction of 2,9-(10)-diamino-6,13-methanopentacene, involving Tröger's base formation **Scheme 21**. It showed high microporosity with a BET surface area of 743 $m^2$ $g^{-1}$ and high selectivity for several important gas pairs such as $O_2/N_2$, $H_2/N_2$ and $H_2/CH_4$, with gas separation performance over the 2008 Robeson upper bound[81].

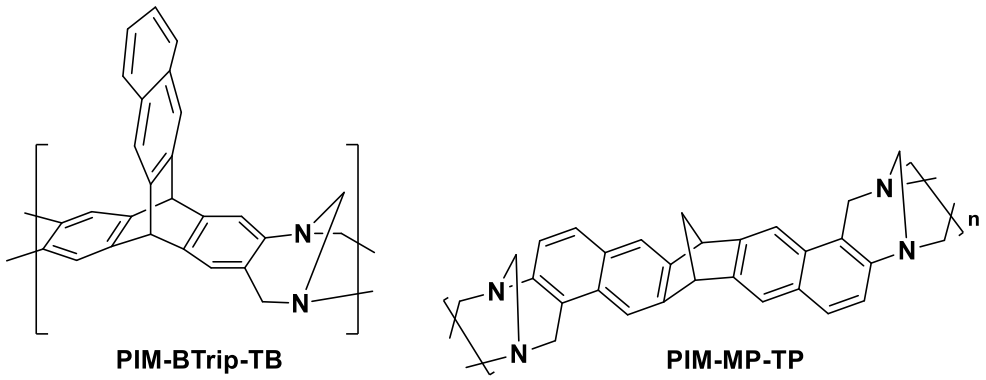


**Scheme 21** The chemical structure of PIM-BTTrip-TB and PIM-MP-TP

### 3.3.6.3 Polymers of intrinsic microporosity formed by using imide linkages (PIM-PIs)

During the 1950s and 1960s, the development of a unique class of material in the form of aromatic polyimides was achieved by DuPont.[82] It was discovered that the production of polyimides involves a two-step process **Scheme 22**: **(i)** condensation reaction of an aromatic bisaniline **(1)** and dianhydride **(2)** to generate the corresponding poly(amic acid) **(3)**, **(ii)** cyclodehydration of **(3)** to yield the polyimide **(4)**.

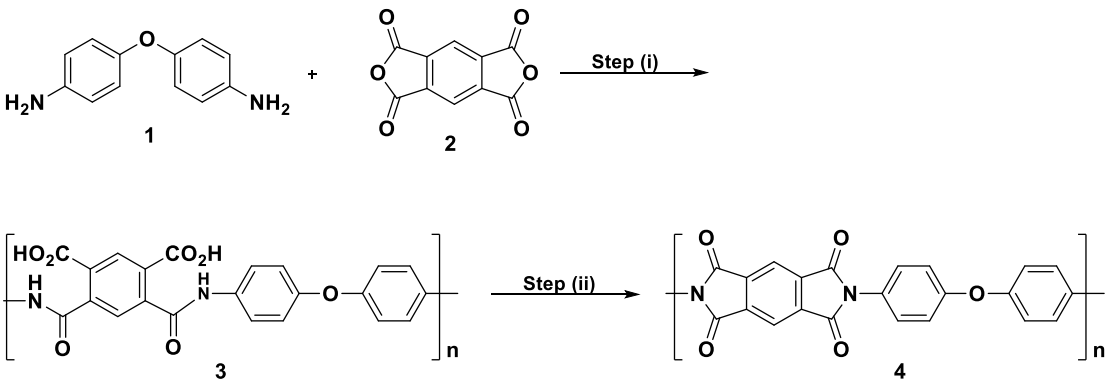


**Scheme 22** Two-step condensation polyimide synthesis of Kapton®

Since then, there has been increasing interest in this class of polymer due to their excellent combination of mechanical and thermal properties, which include thermoxidative stability, electrical properties, chemical resistance, mechanical robustness and structural diversity.[83,84,85] This has led to them being widely used in a variety of different applications.[86] Gas separation was one of polyimides applications that attracted attention. For example, Matrimid® is used commercially for a number of gas separations due to its high gas selectivity, but often at the cost of low permeability.[87] In order to improve the gas permeability of polyimides, more rigid polymer structures were designed by the incorporation of monomers which have rigid structures and sites of contortion. Resulting polymers prepared by McKeown and co-workers proved to be another class of polymers of intrinsic micrporosity (PIM-PIs) with good gas separation properties. The resulting PIM-PI-1 and PIM-PI-8 both exhibit remarkably enhanced permeability with high surface areas, 682 $m^2$ $g^{-1}$ and 683 $m^2$ g, respectively, and show modest gas selectivites[88] **Scheme 23**. Since the synthesis of this new class of polyimide, numerous investigations have been carried out with the aim to improve gas separation performance. Many PIM-PIs were synthesised by using different rigid structures based dianhydride. For example, SBFDA-DMN is a microporous polyimide which was prepared by Pinnau's group at the King Abdullah University of Science and Technology (KAUST), Saudi Arabia. It was synthesised via the cycloimidization condensation reaction of 9,9'-spirobifluorene-2,2',3,3'-dianhydride (SBFDA) with 3,3′-dimethylnaphthidine **Scheme 23**. SBFDA-DMN showed significant microporosity with high BET

surface area of 686 $m^2$ $g^{-1}$ and very high gas permeability with moderate selectivity for $O_2/N_2$[89]. KAUST-PI-1 was also introduced by the same group at KAUST. KAUST-PI-1 was synthesised by the condensation reaction of 9,10-di-iso-propyltriptycene-based dianhydride with 2,3,5,6-tetramethyl-1,4-phenylene diamine (TMPD) **Scheme 23**. It exhibited high microporosity with BET surface areas of 752 $m^2$ $g^{-1}$. This polymer was found to exhibit high gas permeability and good selectivity, surpassing the performance of many of the polymers in the literature.[90,91]

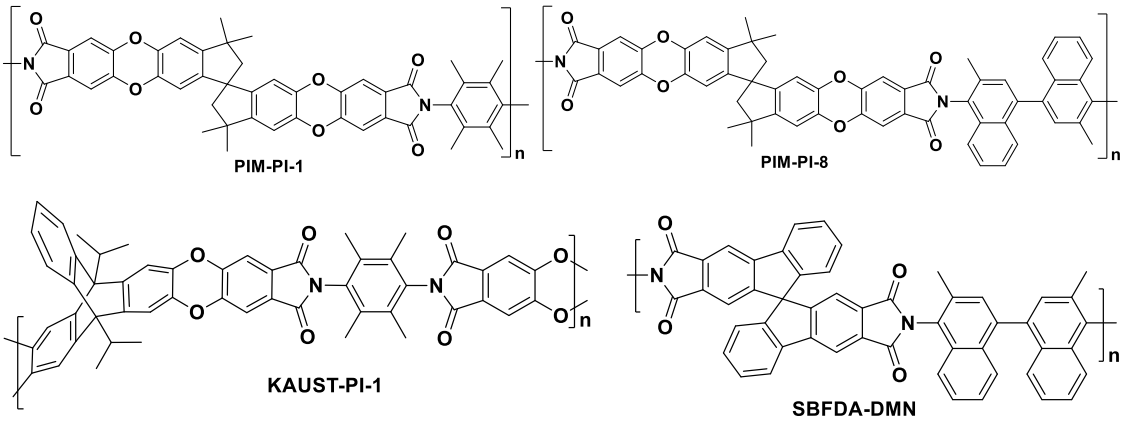


**Scheme 23** The chemical structure of PIM-PI-1, PIM-PI-8, KAUST-PI-1 and SBFFDA-DMN

Pinnau's group continued to introduce polyimides based on triptycene dianhydride. For example, in 2016, the polymer TDA1-DMN **Scheme 24** was prepared by the reaction of 9,10-dimethyl-triptycene tetracarboxylicdianhydride, with a commercially available highly sterically hindered 3,3'-dimethylnaphthisine (DMN) via a condensation reaction.[92] It showed ultramicroporosity with a BET surface area of 760 $m^2$ $g^{-1}$. It was found to show a combination of high gas permeability and moderate selectivity which was above the 2008 upper bounds for $O_2/N_2$ and $H_2/N_2$.

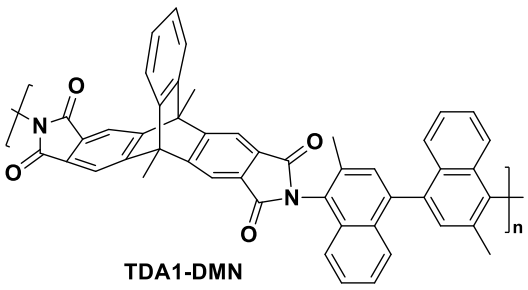


**Scheme 24** The chemical structure of TDA1-DMN

In addition, the polymer TPDA-TMDAT is another example of a triptycene-based polyimide which was produced by the same group. It was formed by the reaction of 1,3,6,8-tetramethyl-2,7-diaminotriptycene (TMDAT) and 9,10-di-iso-propyltriptycene-based dianhydride **Scheme 25**[93].It showed gas permeability/selectivity performance located between the 2008 and 2015 Robeson upper bounds for $H_2/N_2$ and $O_2/N_2$.

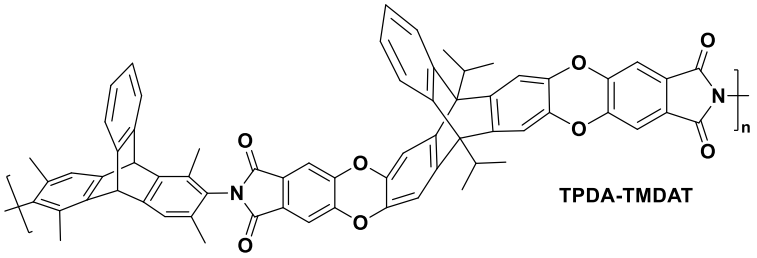


**Scheme 25** Synthesis of TPDA-TMDAT

Other PIM-PIs were prepared by the incorporation of the TB unit onto the polyimide chain by Ghanem *et al.* (2016). PIM-PI-TB-1 and -2 were prepared via the reaction between TB-based diamine and dianhydride 6FDA **Scheme 26**. Both are intrinsically microporous polymers with high surface areas of 440 $m^2/g$ and 580 $m^2/g$, respectively. Also, they showed good gas performance with high gas permeabilites coupled with good selectivites.[94]

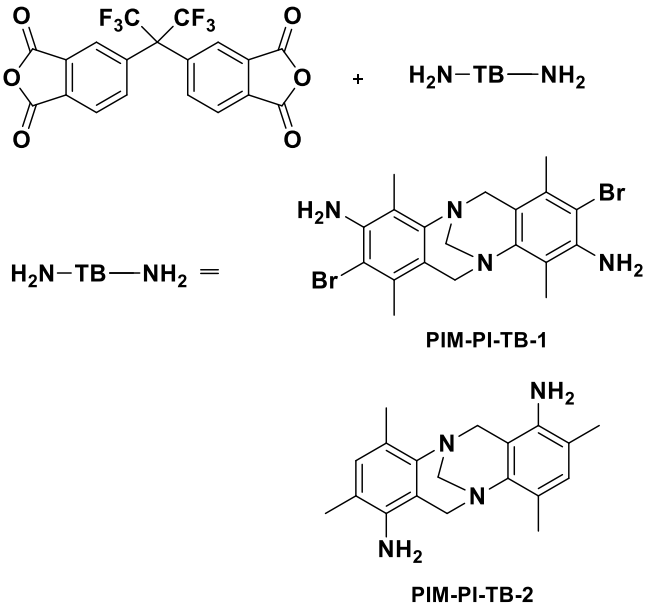


**Scheme 26** Synthesis of PIM-PI-TB-1 and PIM-PI-TB-2

In addition, 4MTBDA/PMDA a Tröger's base derived polyimide of intrinsic microporosity was reported by Lee *et al.* (2016).[95] **Scheme 27**. It was prepared via the cycloimidization reaction between 2,8-diamino-1,3,7,9-tetramethyl-6H,12H-5,11-methanodibenzo[b,f][1,5]diazocine (4MTBDA) and pyromellitic dianhydride (PMDA). It displayed an apparent BET surface area of 650 $m^2/g^{-1}$ and gas permeation data above the 2008 Robeson upper bound for $O_2/N_2$, $H_2/N_2$ and $H_2/CH_4$.

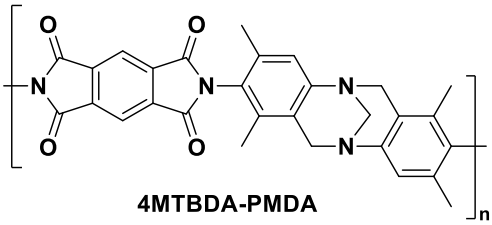


**4MTBDA-PMDA**

**Scheme 27** The chemical structure of 4MTBDA-PMDA

In recent years, Pinnau *et al*. (2017) successfully introduced a hydroxyl functional group to a series of polyimides[96,97] **Scheme 28**. All resulting hydroxyl-functionalised polyimides showed improved gas separation which make them attractive materials for natural gas sweetening **Table 1**.

**Table 1** Gas permeabilities and ideal selectivities α (Px/Py) of hydroxyl-functionalised polyimide films

| **Polymer** | **Permeability (Barrer)** | | | | | **Selectivity** | | | |
|---|---|---|---|---|---|---|---|---|---|
| | **$H_2$** | **$N_2$** | **$O_2$** | **$CH_4$** | **$CO_2$** | **$H_2/CH_4$** | **$N_2/CH_4$** | **$O_2/N_2$** | **$CO_2/CH_4$** |
| **6FDA-HTB** | 167 | 2.26 | 13.6 | 0.92 | 67 | 181 | 2.5 | 6.0 | 73 |
| **PIM-6FDA-OH**[a] | 181 | 5.5 | 23.8 | 3.4 | 119 | 53 | 1.6 | 4.3 | 35 |
| **6FDA-HSBF**[b] | 162 | 3.8 | 19.3 | 2.4 | 100 | 68 | 1.6 | 5.1 | 42 |
| **6FDA-DAT1-OH**[c] | 127 | 2.7 | 14.0 | 1.4 | 70 | 91 | 1.9 | 5.4 | 50 |

[a]Data from ref. [97] [b]Data from ref.[97] [c]Data from ref.[96]

A hydroxyl functionalized polyimide TDA1-APAF was thermally rearranged at 460 °C to produce polybenzoxazole (TR 460) **Scheme 28**. TR 460 showed BET surface area of 680 $m^2\ g^{-1}$, which was higher than that of the TDA1 polyimide (260 $m^2\ g^{-1}$). It showed an increase in $O_2$ permeability (311 Barrer) coupled with $O_2/N_2$ selectivity (5.4) with overall gas permeation located close to the 2015 upper bound for $O_2/N_2$. It, also showed an increase in the $CO_2$ permeability (1328 Barrer) with good selectivity (27). As a result, TR 460

could be useful in many applications, such as, nitrogen production from air and natural gas sweetening.[98]

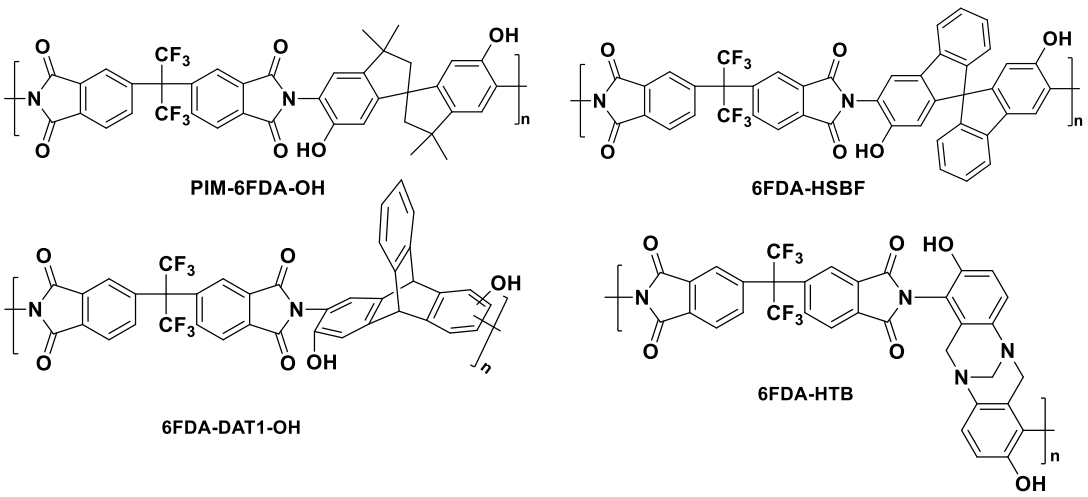


**Scheme 28** The chemical structure of 6FDA-DAT1, 6FDA-DAT1-OH, PIM-6FDA-OH and 6FDA-HSBF

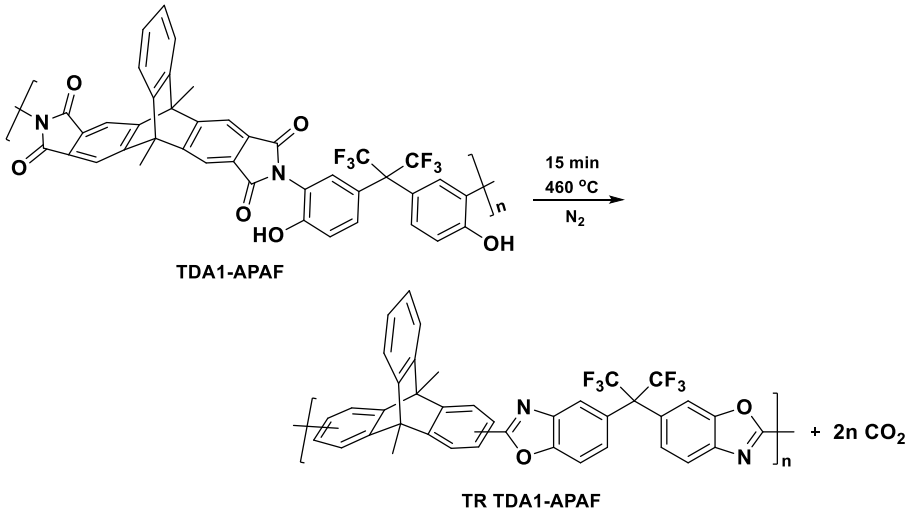


**Scheme 29** Synthesis of TDA1-APAF-derived TR membrane

## 1.4 Membranes for gas separation

### 1.4.1 Membrane properties and gas transport mechanism

A membrane has been generally defined as "*a phase or a group of phases that lies between two different phases which is physically and/or chemically distinctive from both of them and which, due to its properties and force field applied, it is able to control mass transport between these phases*".[99] Transport of permeate through the membrane is achieved as a result of a driving force created either by differences in physical and/or chemical properties between the membrane and permeate, such as, pressure,

concentration, electrical potential or temperature. Consequently, facilitating the transport of one component more readily than the other, allowing separation.[100] Clearly, this is a very general concept of membrane separation. It is more beneficial to consider membrane function in respect to the context of the work in this thesis. In 1866, Graham first reported a simple form of gas transport mechanism which depends on solution-diffusion.[101] He demonstrated the mechanism through a sequence of three steps: firstly, there is sorption, where component molecules from the upstream dissolve into the surface of the membrane. This is then followed by diffusion of the species through the bulk of the membrane. In the case of polymer membranes, molecules travel through the interstitial free volume which is the transient gap openings between polymer chains. The final step involves desorption or evaporation of the components at the downstream boundary. Separation of gas mixtures is therefore determined by both the difference in the solubility of each component in the membrane and the rate at which each component diffuses through the membrane **Figure 5**.

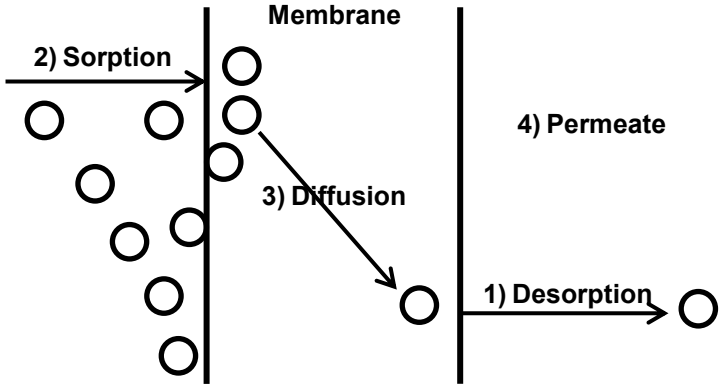


**Figure 5** Mechanism for gas transport through a membrane

According to Fick's law[102], the permeability $\mathrm{P}$ of a gas within a polymer can therefore be expressed as:

$$\mathrm{P} = \frac{\mathrm{c}_2}{\mathrm{p}_2}\,\mathrm{D}$$

Where, $\mathrm{p}_2$ = upstream pressure and $\mathrm{c}_2$ = upstream concentration.

According to Henry's law[103] of solubility, the equilibrium solubility coefficient $S$ of a gas within a polymer can be defined as the ratio of gas concentration $c$ dissolved in the polymer at equilibrium to the external partial pressure $p$:

$$S = \frac{c}{p}$$

Combining these equations gives:

$$P = SD$$

This equation establishes a relationship between the solubility $S$, diffusivity $D$ and permeability $P$ coefficients which are the fundamental transport parameters for polymer gas separation membranes. The solubility coefficient $S$ is a thermodynamic parameter which indicates the number of gas molecules sorbed by the polymer membrane. The diffusivity coefficient $D$ is a kinetic parameter which characterises the mobility of gas molecules as they diffuse through the membrane. A high degree of permeability is therefore dictated by large values of $D$ and/or large values of $S$. Another key characteristic of gas separation membranes is their selectivity or permselectivity, which effectively assesses the separating ability of the membrane. The ideal selectivity $\alpha_{xy}$ of a mixture of gases *x* and *y* is defined by the ratio of the permeability coefficients ($P_x$ and $P_y$) of the two substances:

$$\alpha = \frac{P_x}{P_y}$$

In this equation, the more permeable gas is commonly taken as gas $x$, so that $\alpha_{xy} > 1$. As already discussed, the permeability coefficient has contributions from both solubility and diffusivity coefficients. The equation may therefore be written with regards to solubility selectivity ($S_x/S_y$) and diffusivity selectivity ($D_x/D_y$):

$$\alpha_{xy} = \frac{S_x}{S_y}\frac{D_x}{D_y}$$

In 1979, Monsanto introduced the first commercial gas separation membrane system for the separation of hydrogen from the purge stream in ammonia synthesis.[104] Since then, use of polymeric membranes for gas separation has been increasing in attempts to reduce the energy costs associated with other separation techniques, such as, cryogenic, thermal, absorption and adsorption methods. Polymeric membranes can be used for a variety of useful gas separations, such as, $H_2$/hydrocarbons for hydrogen recovery from hydrogenation processes, $O_2/N_2$ for oxygen or nitrogen enriched air and $He/N_2$ for helium recovery.

## 1.4.2 The Robeson plot

The performance of a gas separation membrane is characterized by two fundamental parameters, namely, the permeability of a specific component of the gas mixture $P_x$ and the selectivity between the gases $\alpha_{xy}$. Polymers with both high permeability and selectivity are desirable. However, a general trade-off relation between permeability and selectivity has been recognized.[105] This means that as the selectivity of gas decreases the permeability of the more permeable gas increases and vice versa. In 1991, Robeson has collected the gas separation data from over 300 references and plotted *log* $\alpha$ versus *log* $P_x$. This graph yielded an upper bound performance limit **Figure 6**.[106]

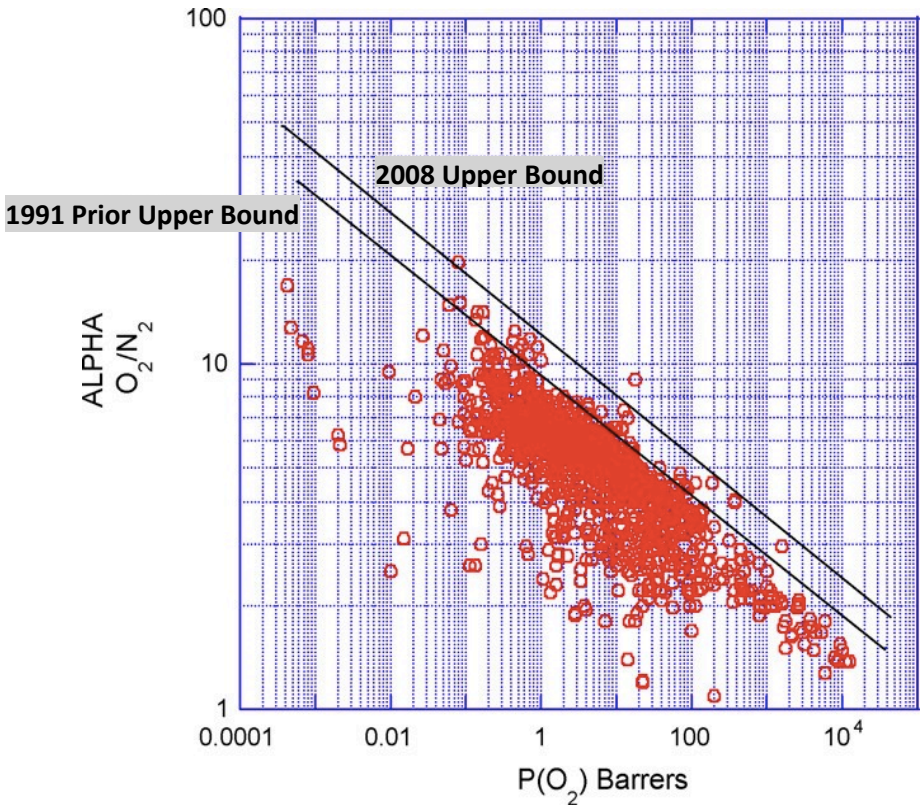


**Figure 6** The Robeson plot for $O_2/N_2$, showing the 1991 and 2008 upper bounds

The position of the data for a polymer membrane on the Robeson plot for a particular gas pair is a good indicator of how useful it may be for that gas separation. A good polymer membrane must possess both high permeability and high selectivity towards a particular gas. Consequently, good membranes with the best performance should be in the upper right-hand corner of this graph **Figure 6**. However, since 1991 many novel polymers with useful performance have been reported, such as, PIM-1[66] with data that exceed the 1991 upper bound. As a result, the 1991 upper bounds have become dated. In 2008, Robeson revised his original 1991 upper bounds to give the new 2008 upper bound limits.[107] Nevertheless, newly developed materials continue to push above the 2008 upper bounds, in 2015, a new permeability/selectivity upper bound was presented for ultramicroporous polymers (PIMs), which were reported by the groups of Mckeown *et al*. (2014) and Pinnau *et al*. (2014). Polymers:, PIM-EA-TB[79], PIM-TRIP-TB[79] **Scheme 20**, TPIM-1[69] and KAUST-PI-1[91] **Scheme 23** showed balanced combination of high gas permeability for gas separations such as $O_2/N_2$,

$H_2/N_2$ and $H_2/CH_4$ **Figure 7**, resulting from intrachain "rigidity" of bridged-bicyclic contortion centers of triptycene, ethanoanthracene and Tröger's base, with gas-sieving ultramicroporosity.

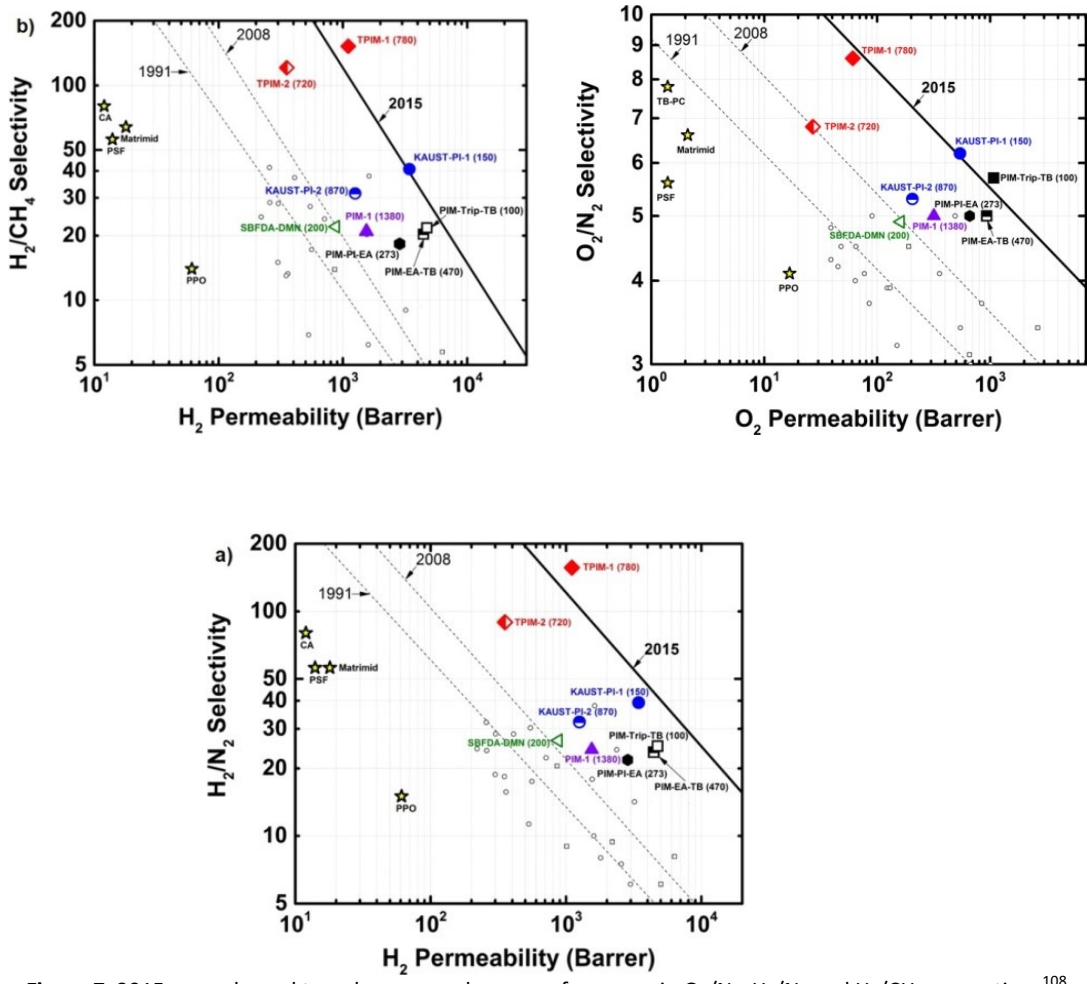


**Figure 7** 2015 upper bound to polymer membrane performance in $O_2/N_2$, $H_2/N_2$ and $H_2/CH_4$ separations[108]

The resulting PIMs overcome the trade-off relationship between permeability and selectivity, approaching practical selectivity with high permeability for important industrial gas separations.

# Chapter 2 Polystyrene derived Tröger's base (TB) polymers

## 2.1 Introduction and aims

Our aim in this work is to produce highly porous polymers by cross-linking linear polystyrene chains with inflexible Tröger's base (TB). TB was chosen due to its structural features and functionality: bicyclic ring system, central bridgehead nitrogen atoms and fused benzene rings. These structural features are expected to increase the rigidity of the resulting hypercrosslinked polymer relative to the conventional linkages introduced by Friedel-Craft chemistry. In addition, introducing basic nitrogen atoms within the polymer may provide useful functionality, for example, in heterogeneous catalysis. The plan was, firstly, the nitration of polystyrene followed by the reduction of nitropolystyrene to the aminated polystyrene which will be the suitable precursor for the TB linkage.

## 2.2 The synthesis of Polystyrene derived Tröger's base (TB) polymers

### 2.2.1 The synthesis of poly(4-nitrostyrene)

Different reaction conditions were used in order to achieve the highest nitration of polystyrene. These include trifluoroacetic nitrate method and a mixture of nitric acid and sulfuric acid in 3-nitrotoluene.

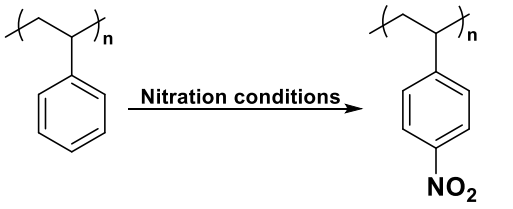


**Nitration conditions**

$NH_4NO_3$, Trifluoroacetic anhydride, $CHCl_3$

$H_2SO_4$, $HNO_3$, 3-nitrotoluene

**Scheme 30** Nitration of polystyrene

Nitration of polystyrene was performed by using ammonium nitrate ($NH_4NO_3$) according to a method available in the literature.[109] Nitrating agent, trifluoroacetyl nitrate was generated by the reaction of ammonium nitrate with trifluoroacetic anhydride (TFAA) **(eq 1)**.

$$(CF_3CO)_2O + NH_4NO_3 \longrightarrow CF_3C(O)ONO_2 + CF_3C(O)ONH_4 \quad \textbf{(1)}$$

Cleavage of the oxygen-nitrogen bond gives rise to the nitronium ion which is the true nitrating agent **(eq 2)**.

$$CF_3C(O)ONO_2 \rightleftharpoons CF_3C(O)O^- + NO_2^+ \quad \textbf{(2)}$$

Nitration was performed in chloroform due to the reasonable solubility of ammonium nitrate in this solvent. This method was chosen due to its mild conditions which are expected to prevent degradation of polymer molecular weight by oxidative cleavage of polystyrene. In order to obtain the highest % of nitration, various experiments were performed altering the reaction conditions: ratio of ammonium nitrate, temperature and duration **Table 2**.

**Table 2** Reaction conditions of the nitration reaction

| Polymer | Ratio of polystyrene repeat units to $NH_4NO_3$ | Reaction conditions | | % of nitration by $^1$H NMR |
|---|---|---|---|---|
| | | Temperature (°C) | Duration (hours) | |
| **1a** | 1:1 | Room | 18 | 51% |
| **1b** | 1:4 | Room | 120 | 56% |
| **1c** | 1:10 | 70 °C | 120 | 66% |
| **1d** | 1:20 | 70 °C | 120 | 92% |

It can be seen from the data reported in **Table 2** that the percentage nitration of polystyrene was improved when the ratio of $NH_4NO_3$, temperature and duration of reaction were all increased. It is clear that the best conditions found for the nitration of polystyrene are those for the synthesis of Polymer **1d**; when the ratio of ammonium nitrate to polystyrene is 20-fold, the temperature is 70 °C and the duration is about 120 hours.

Nitration using the conventional reagent of a mixture of nitric acid ($HNO_3$) and sulfuric acid ($H_2SO_4$) was also investigated according to a method described in literature.[110] Polystyrene was nitrated by the nitronium ion which was formed by reaction between nitric acid and sulfuric acid **(eq 3)** in a solution of 3-nitrotoluene, which proved to be an excellent solvent for the reaction.

$$HNO_3 + 2H_2SO_4 \longrightarrow NO_2^+ + 2H_2SO_4^- + H_3O^+ \quad \textbf{(3)}$$

Percentage yield of Polymer **1e** is high at 77% based on the molecular weight of the repeating unit. The excellent yield is high due to the good solubility of polystyrene in 3-nitrotoluene. Moreover, the degree of substitution, *n* is equal to 0.98, which means that the substitution is approximately quantitative. This value was calculated for the elemental analysis using:

$$n = 104\ N\%/(1400 - 45\ N\%)$$

$$N\% = 9.28$$

$$n = 0.98$$

Polymers **1a** to **1e** were characterised by $^1$H NMR to confirm the formation of *p*-nitropolystyrene and to calculate the percentage of nitration. $^1$HNMR spectra show two broad peaks in the aromatic region centred at 7.0 and 7.8 ppm from the four protons of the nitrated benzene ring in poly(*p*-nitrostyrene) in polymers **1d** and **1e Figure 8**. Therefore, the presence of these two large peaks with approximately equal integrations indicates that polystyrene was successfully nitrated in the para position. The peak centred at 7.3 ppm belongs to unnitrated polystyrene residues. Hence, the degree of nitration for polymer **1e** was calculated independently using $^1$H NMR and proved to be about 98%. Consequently, the degree of substitution, *n* calculated from elemental analysis is in good agreement with that calculated by $^1$H NMR. In addition, the nitrated polymers were characterized by IR spectroscopy with strong absorptions apparent at 3026 and 2926 $cm^{-1}$ for aliphatic C-H

stretching, 1599, 1519 $cm^{-1}$ for asymmetric ($ArNO_2$) and symmetric stretching N=O, 1345 $cm^{-1}$ for C-N stretching, which also confirm nitration.

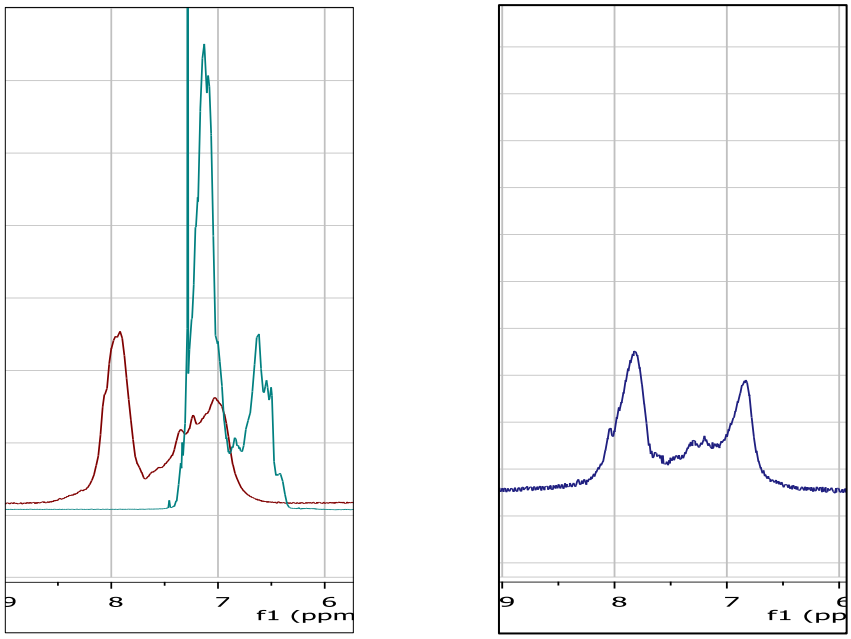


**Figure 8:** $^1$HNMR spectra of polystyrene (—), poly(*p*-nitrostyrene) **1d** (—); and poly(*p*-nitrostyrene) **1e** (—)

These polymers took on a pale yellow colour during the nitration reaction, which is characteristic of nitro compounds. Therefore, both methods had proven to be useful to nitrate polystyrene. However, conventional nitration by a mixture of nitric acid ($HNO_3$) and sulfuric acid ($H_2SO_4$) was preferred because of the better yield of recovered nitrated polystyrene, which we ascribe to the good solubility of polystyrene in the 3-nitrotoluene solvent.

## 2.2.2 The synthesis of poly(4-aminostyrene)

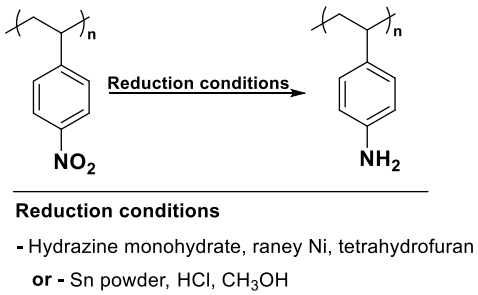


**Scheme 31** Synthesis of poly(4-aminostyrene)

Two different reducing agents were used to reduce poly(4-nitrostyrene) in order to obtain a high yield of poly(4-aminostyrene). Catalytic hydrogenation reduction by using hydrazine monohydrate/Raney Ni or metal surface/acid catalysed. Reduction of poly (4-nitrostyrene) involves a metal surface and proceeds through what is known as a single electron transfer (SET) mechanism. Such reduction proceeds through nitroso and hydroxylamine intermediates **Scheme 32**.

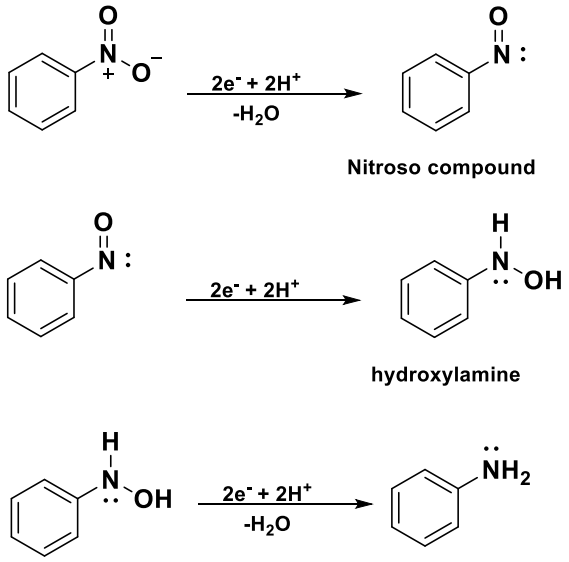


**Scheme 32** The mechanism of reduction of nitrobenzene to aniline

Nitrated polystyrenes **1a, 1b, 1c** and **1d** with different degrees of nitration were reduced with hydrazine monohydrate and Raney nickel in THF according to a method described in the literature.[111] The reaction mixture was refluxed for 17 hours under $N_2$ atmosphere. Alternatively, poly(4-nitrostyrene) **1e** was reduced with tin according to a method described in literature.[112] Sn powder was added to a mixture of HCl and ethanol before adding to a solution of polymer **1e** in ethanol. The reaction mixture was refluxed at 80 °C under $N_2$ gas for 17 hours. The resulting aminated polystyrenes **2a**, **2b**, **2c**, **2d** and **2e**, respectively, were characterized by IR, the spectra showed two bands at (3340-3213 cm-1) (unsymmetrical and symmetrical stretching of the $–NH_2$) and another absorption at (1616-1512 $cm^{-1}$) (Bending of the N-H). The C-N stretching vibration for aromatic amines is strong at 1261 $cm^{-1}$, confirming the formation of $NH_2$ group. Further indication of the formation of

aminated polystyrene is that colours of these compounds were turned to light brown. Tin/acid reduction method was preferred to the catalytic hydrogenations reduction using hydrazine monohydrate due to the better solubility of poly(4-nitrostyrene) in the mixture of (HCl + ethanol) than tetrahydrofuran, leading to a more homogenous reduction of nitro groups. The amino-substituted styrenes were used immediately due to their oxidative instability under ambient conditions.

### 2.2.3 Synthesis of TB-polystyrene polymers (TB-PS)

Attempts to prepare hypercrosslinked polymers **(TB-PS-57a, -57b, -57c, -57d** and **-75e)** were synthesised used an acid mediated reaction between poly(4-aminostyrene) **2a** to **2e** and dimethoxymethane **Scheme 33**. The mechanism of this reaction was proposed by Carlos *et al*. (2007) who used mass spectrometric experiments to devise a generally accepted mechanism for the preparation of TB analogues from derivatives of aniline and formaldehyde **Scheme 34**.[113] The mechanism proceeds by a series of *in-situ* Friedel-Crafts alkylation reactions. The reaction begins with the transformation of the aniline derivative into the unstable imine intermediate, existing in equilibrium with the iminium intermediate (A). Secondly, an electrophilic attack occurs from the ortho-position of another molecule of aniline onto the iminium intermediate, giving ortho-aminobenzylamine (B), which undergoes cyclisation with another molecule of formaldehyde, through a series of proton transfer and dehydration steps, to form tetrahydroquinazoline (C). This species picks up a third molecule of formaldehyde, by electrophilic attack, to form an iminium intermediate (D), which finally undergoes intramolecular electrophilic substitution to give the TB analogue (E).

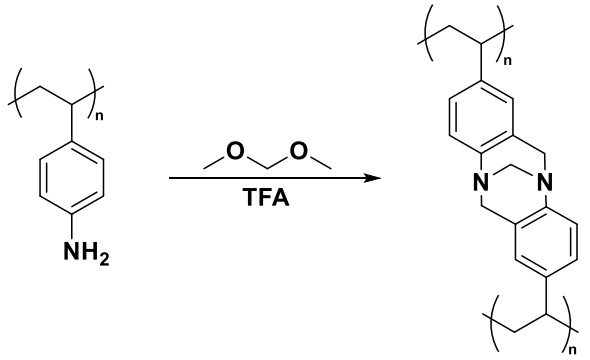


**Scheme 33** TB polystyrene synthesis

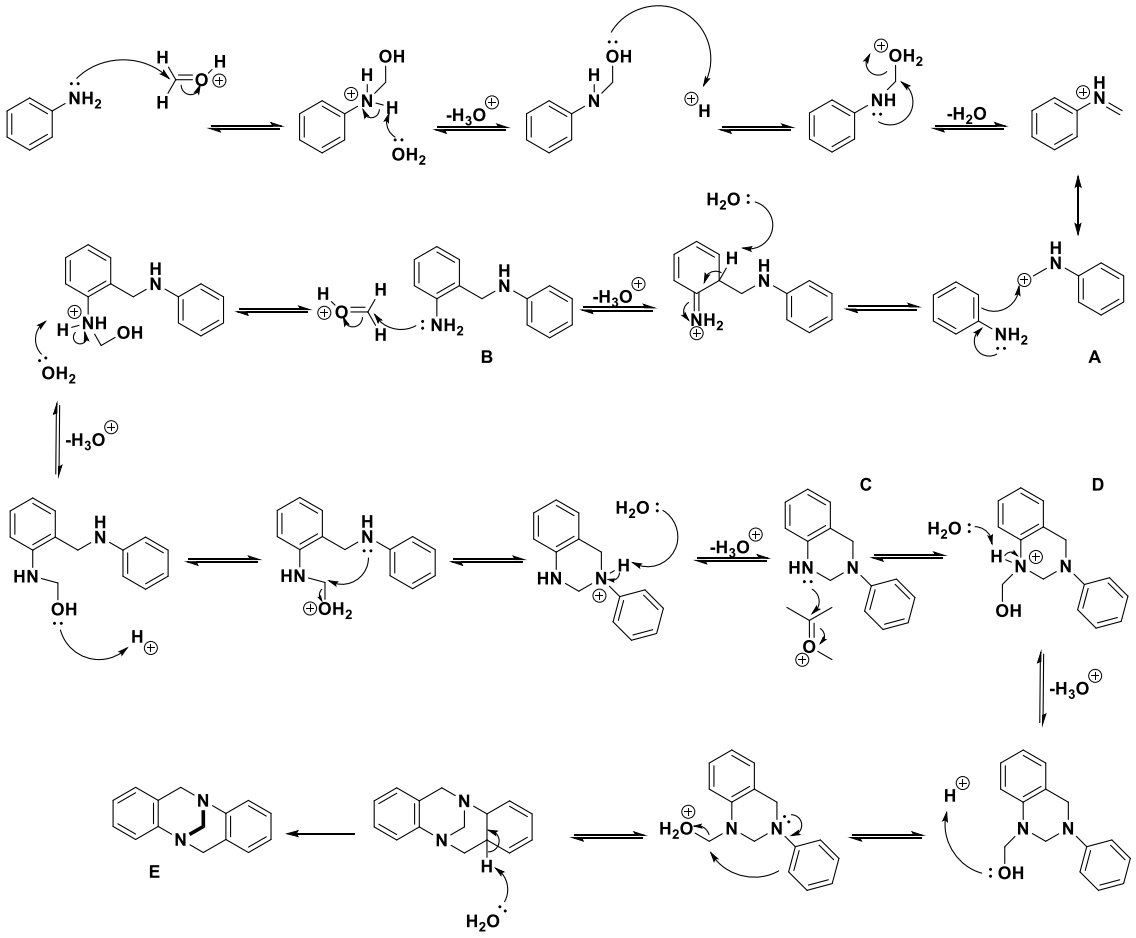


**Scheme 34** The TB condensation mechanism from an aniline derivative and formaldehyde

The Tröger's base crosslinking reaction of polymers **2a** to **2e** was performed accordingly to the reported literature procedure.[114] Aminated polystyrene was dissolved in TFA, dimethoxy methane was added dropwise and the reaction

mixture stirred under $N_2$ atmosphere. After that, the reaction mixture was quenched with water and stirred for about 2 hours before adding aqueous ammonia (35%). The product was collected and washed with water and then refluxed with THF, acetone $CHCl_3$ and methanol, each time for 2 hours. Finally, the polymer was dried in a vacuum oven at 70 °C. The polymers were precipitated as beige powders in good yields. Thermal gravimetric analysis (TGA) revealed very good thermal stabilities, with each polymer stable up to 360 °C before decomposition. The nitrogen adsorption at 77 K of compounds **TB-PS-57a, -57b, -57c, -57d** and **-75e** was measured and BET surface area calculated **Table 3**.

**Table 3** Surface area and thermal decomposition temperature (TGA) of TB-polystyrene polymers

| TB-Polystyrene polymers | Precursor Polymer | % Yield | Surface Area ($m^2\ g^{-1}$) | Decomposition Temperature |
|---|---|---|---|---|
| **TB-PS-57a** | 2a | 43 | 0.0 | 384 |
| **TB-PS-57b** | 2b | 46 | 0.3 | 383 |
| **TB-PS-57c** | 2c | 38 | 10.5 | 382 |
| **TB-PS-57d** | 2d | 44 | 14.9 | 365 |
| **TB-PS-57e** | 2e | 38 | 25.6 | 360 |

Unfortunately, none of the polymers **TB-PS-57a, -57b, -57c, -57d** and **-75e** showed significant BET surface area. This includes **TB-PS-57e**, which was obtained from polymer **2e**, obtained by an efficient reductive method from almost quantitatively nitrated polystyrene. However, this polymer does adsorb some nitrogen (~70 cc(STP)) at higher relative pressure, suggesting that porosity may have been created during the cross-linking procedure but that nitrogen accessibility is severely restricted. The high yield and insolubility of the polymers suggests that a network polymer was formed and characterisation by IR spectroscopy, showing the disappearing of characteristic bonds of the $NH_2$ group from the precursor polymers.

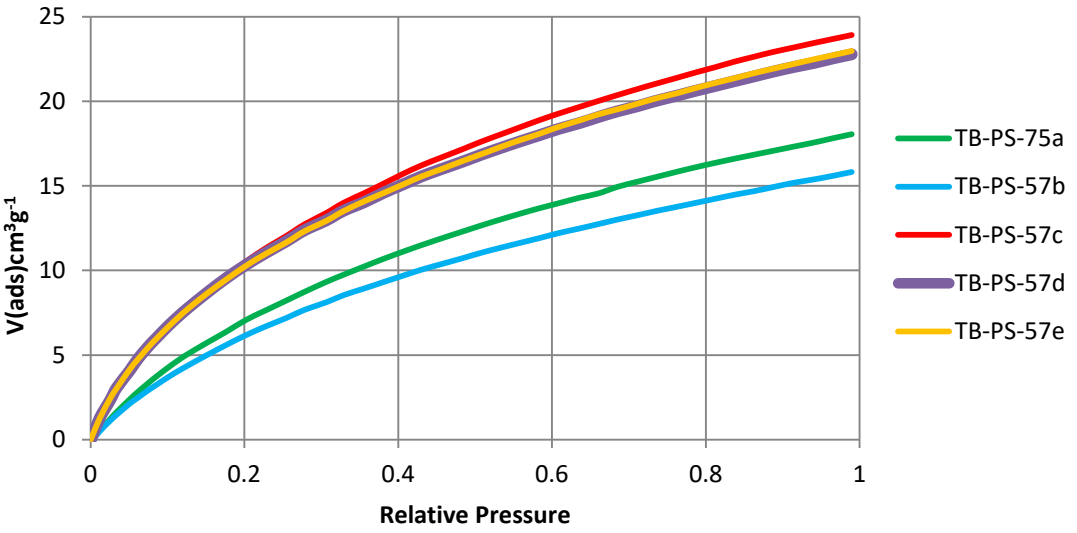


**Figure 9** $CO_2$ adsorption isotherms

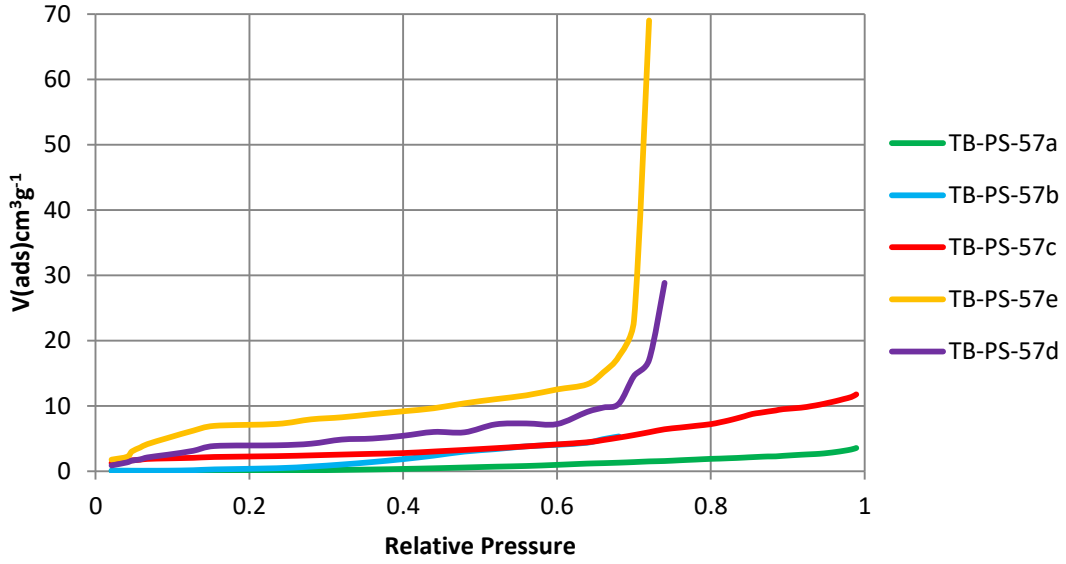


**Figure 10** $N_2$ adsorption isotherms

Characterisation by solid state $^{13}$C-NMR, showed two weak peaks for carbons of TB units. That means that the lack of porosity could be as a result of poor TB linkage formation. One possible reaction for this restriction could be the Friedel-Crafts reaction of two diamine groups with dimethoxy methane in acid medium to give methylenedianiline **Figure 11** and **Scheme 35**. However, it is difficult to conclude whether the lack of porosity arises from poor network formation (i.e. inefficient TB linkage formation) or from an

intrinsic lack of porosity in the target polymer network. Due to this disappointing result, this project was abandoned.

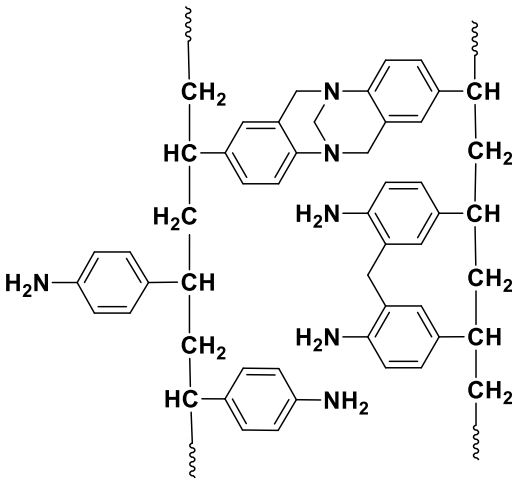


**Scheme 35** TB unit and methylenedianiline formation

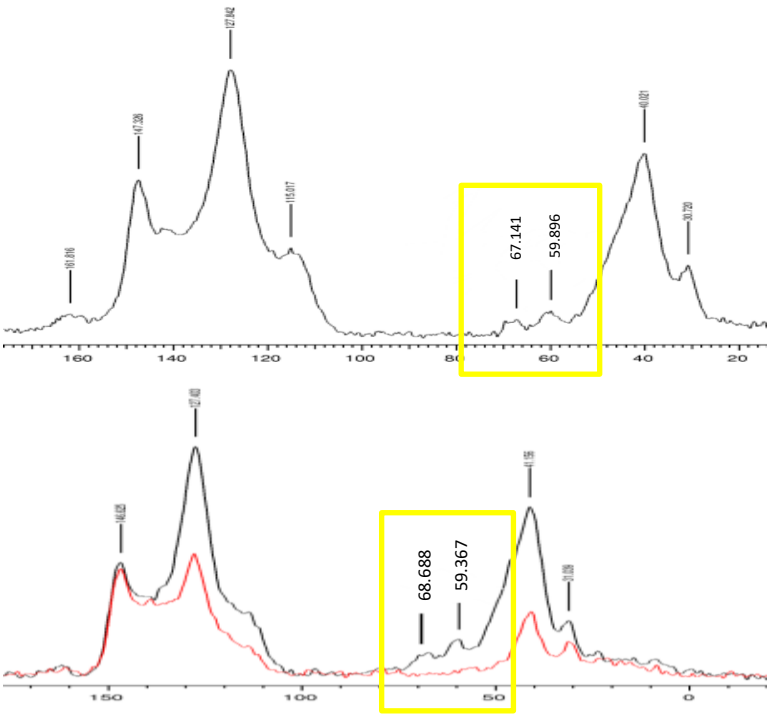


**Figure 11** Solid state $^{13}$C-NMR of TB-PS-57d and TB-PS-57d, respectively

# Chapter 3 Polybenzodioxin polymers based on tetraoxidethianthrene

## 3.1 Introduction

Novel intrinsically microporous polymers derived from different sulfone monomers were first reported in the literature as potential materials for gas separation membranes by the Guiver group working at the National Research Laboratories in Canada. Firstly, a series of copolymers were prepared via aromatic nucleophilic substitution reaction between 5,5',6,6'-tetrahydroxy-3,3,3',3'-tetramethylspirobisindane (TTSBI), 2,3,5,6-tetrafluoroterephthalonitrile (TFTPN) and the new sulfone monomer, heptafluoro-*p*-tolylphenylsulfone (HFTPS) at high temperature 160 °C for 40 minutes **Scheme 36**.[115]

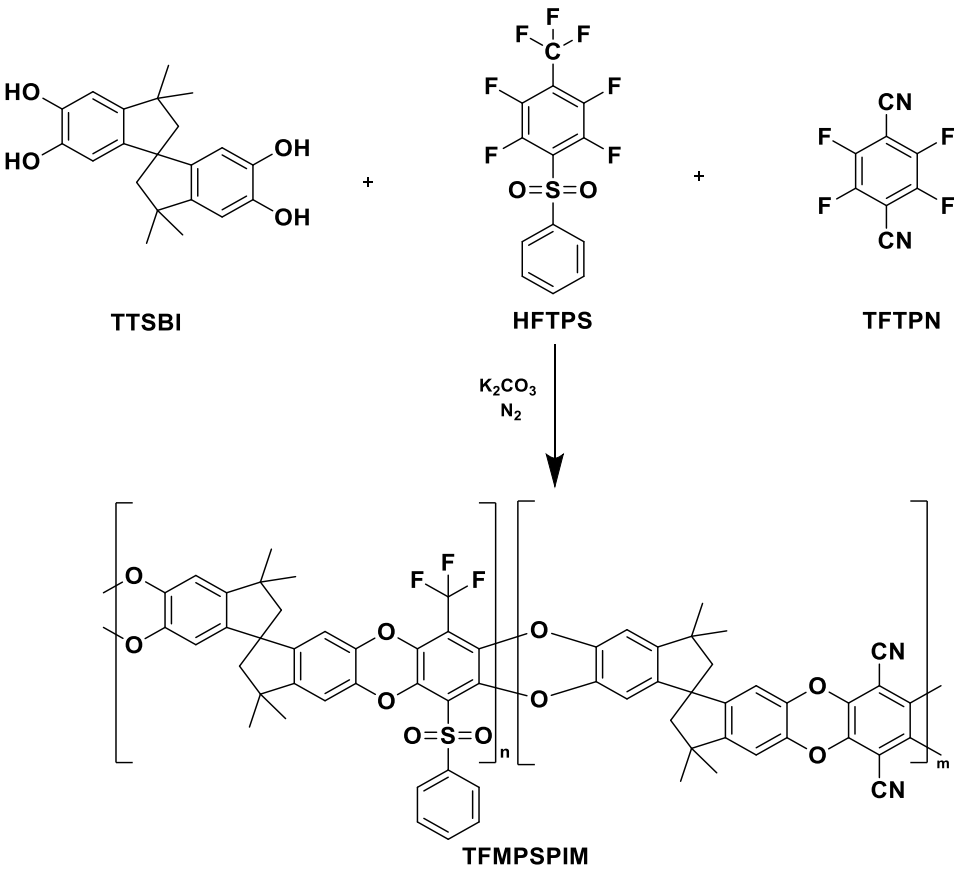


**Scheme 36** Guiver's synthesis of TFMPSPIM copolymers

The resulting ladder PIMs (TFMPS-PIM) showed intrinsic microporosity, high molecular weight ($M_n$ > 55000) and good performance towards gas separations. In particular, these PIMs exhibited high selectivities for oxygen and carbon dioxide gases versus nitrogen, while showed decreasing permeabilites for the same gases with increasing content of the trifluoromethylphenylsulfone relative to PIM-1 but with no overall loss of performance relative to the 2008 Robeson upper bound. It was suggested that the good selectivity of these ladder PIMs is due to the presence of $–CF_3$ and $–SO_2C_6H_5$ within polymer chain. A year later in 2009, the same research group published a paper describing three different PIM copolymers derived from three different disulfone monomers **Scheme 37**.[116]

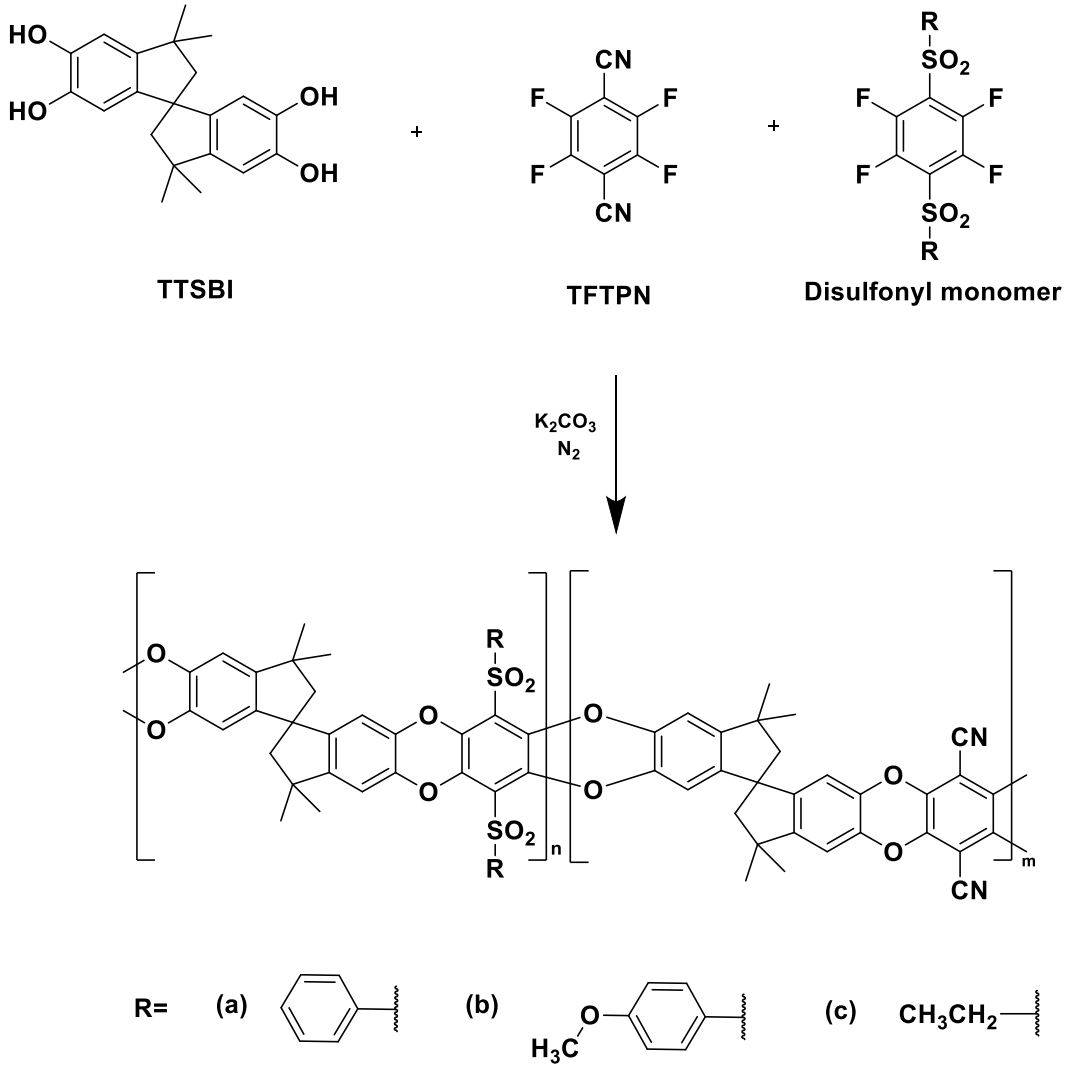


**Scheme 37** Guiver's synthesis of DS-PIMs

These copolymers showed microporosity and high molecular weight and similar performance in terms of gas separation properties as compared to the TFMPSPIM copolymers.[116] In 2010, the same group reported another series of PIMs copolymers derived from TTSBI, TFTPN and 2,3,7,8-tetrafluoro-5,5',10,10'-tetraoxidethianthrene (TFTOT), which were prepared at elevated temperature, 120 °C for 120 minutes **Scheme 38**.[117] TOTPIMS copolymers exhibited both microporosity and high molecular weight. In addition, they showed an enhancement in selectivity for oxygen, hydrogen and carbon dioxide gases versus nitrogen as compared to PIM-1, although with lower permeability for these gases following the classic permeability-selectivity trade-off. Gas permeability data of these copolymers lie above the 1991 Robeson upper bound for the separation of $O_2/N_2$ gases.

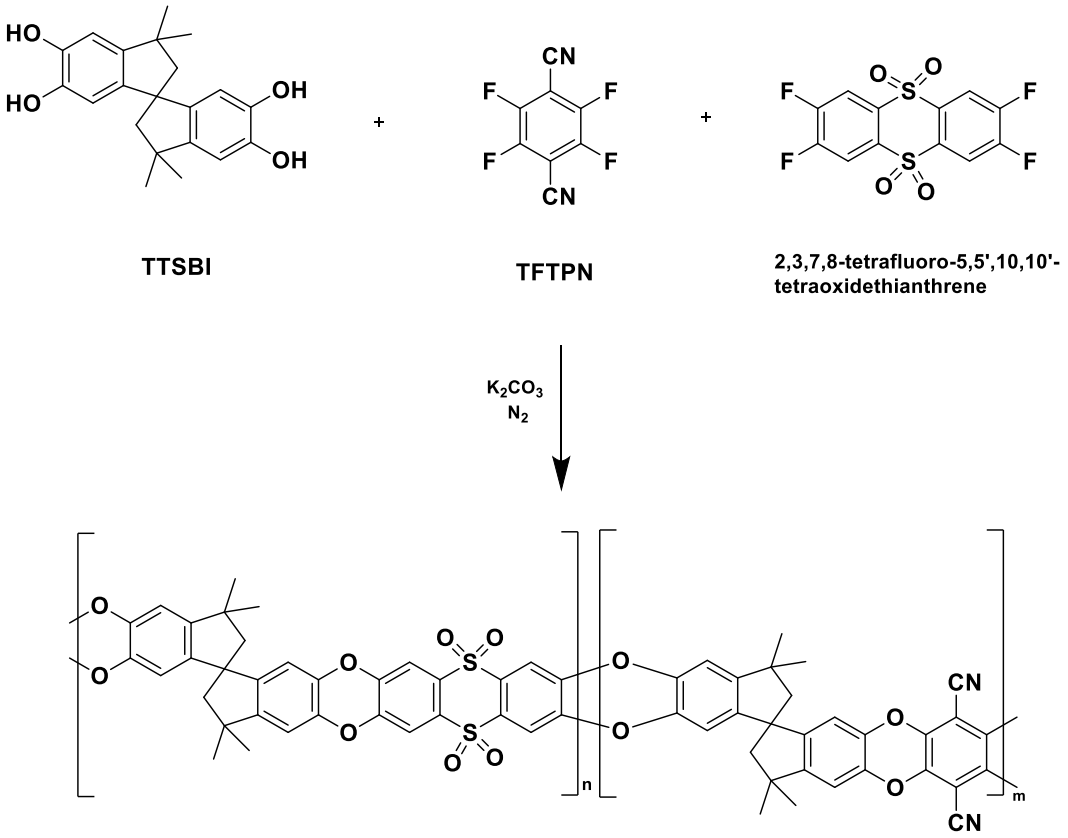


**Scheme 38** Guiver's synthesis of TOTPIMs copolymers

Inspired by the good gas separation properties of these PIMs, the objective of the present work was to expand the spectrum of PIMs containing the sulfonyl group by reacting the 2,3,7,8-tetrafluoro-5,5',10,10'-

tetraoxidethianthrene monomer with different bis- and tris-catechols which the McKeown group used to prepare PIMs with enhanced membrane properties. To approach this goal, 2,3,7,8-tetrafluoro-5,5',10,10'-tetraoxidethianthrene (TOT) was firstly prepared. Then, seven different catechol monomers, namely,9,10-dimethyl-9,10-ethano-9,10-dihydro-2,3,6,7-tetrahydroxyanthracene, 9,9-bis(3,4-dihydroxyphenyl) fluorene, 2,2',3,3'-5-tetrahydroxy-9,9'-spirobifluorene, 2,2',3,3'- tetrahydroxy -6,6'-dimethyl-9,9'-spirobifluorene, 2,2',3,3'- tetrahydroxy-6,6'-*t*-butyl-9,9'-spirobifluorene, 1,4-di(3',4'-dihydroxyphenyl)-2,3,5,6-tetraphenylbenzene, 5,8,8,11,11,14-hexamethyl-5,8,9,10,11,14-hexahydro-5,14-[1,2]benzenopentacene-2,3,18,19-tetraol and 2,3,6,7,12,13- hexahydroxytriptycene were prepared for polymer preparation using TOT.

## 3.2 The synthesis of 2,3,7,8-tetrafluoro-5,5',10,10'-tetraoxidethianthrene (TOT)(4)

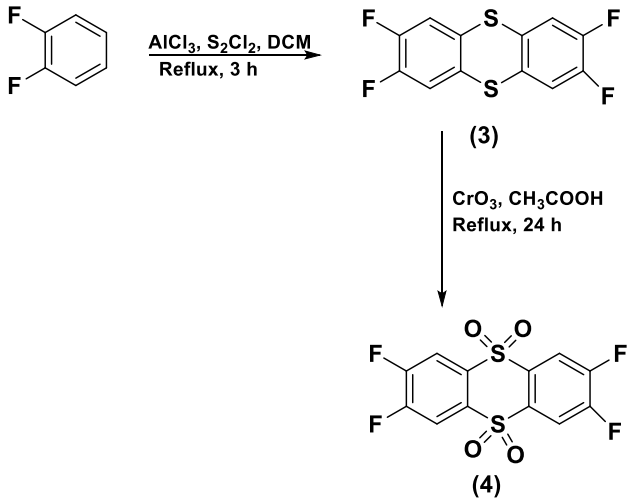


**Scheme 39** Synthesis of TOT monomer

The key monomer 2,3,7,8-tetrafluorothianthrene **(3)** was synthesised by applying some small modifications to the reported procedure by Du **Scheme 39**.[117] The original synthesis was carried out in dichloromethane below 0 °C and the product was crystallized from hexane to give colourless crystals in a reported yield of 49%. This procedure proved to be poorly reproducible leading to insufficient yields of ~3%, which did not allow further reactions to

be performed. Thus, in the present work, numerous trials were made in order to obtain a good yield of product, applying some modifications to the reported procedure. Firstly, room temperature was found to be the optimum temperature for this reaction. When performed at lower temperature the reaction led to many side products and poor yield of the desired product. In addition, nitromethane was used as a solvent instead of dichloromethane. As a result, the yield of the reaction was improved greatly. This improvement could be due to the fact that the solubility of reactants in nitromethane is better than in dichloromethane. Moreover, pure product was obtained by crystallisation in chloroform instead of hexane and with no need for further purification by column chromatography to give a yield of 30%.

## 3.3 Synthesis of catechol-based monomers

A series of bis- and tris-catechols were investigated for the co-polymerization with the disulfone monomer (TOT) to produce PIMs. Two useful biscatechols, namely, 6,6',7,7'-tetrahydroxy-4,4,4',4'-tetramethyl-2,2'-spirobischromane and the much used TTSBI are commercially available. Monomer (TTSBI) was recrystallised in ethanol before using **Scheme 40**. Other catechols were prepared according to reported procedures in literature and their synthesis are discussed in detail below.

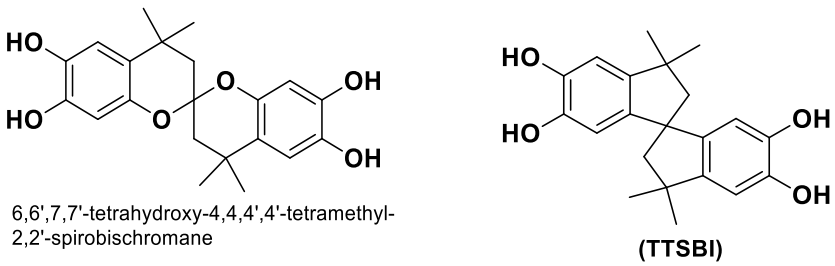


**Scheme 40** The molecular structure of commercially available monomers

### 3.3.1 Synthesis of 9,10-dimethyl-9,10-ethano-9,10-dihydro-2,3,6,7-tetrahydroxyanthracene (9)

The biscatechol monomer 9,10-dimethyl-9,10-ethano-9,10-dihydro-2,3,6,7-tetrahydroxyanthracene contains a bridged bicyclic ring system, leading to a

highly inflexible and rigid structure. This characteristic feature of this monomer makes it an attractive biscatechol to be chosen for PIMs synthesis. Previously, PIM1-CO1-100 was prepared and reported in literature[68] **Scheme 42**. This PIM, containing the ethanoanthracene unit, proved to be microporous with a BET surface area of 630 $m^2/g$. The monomer 9,10-dimethyl-9,10-ethano-9,10-dihydro-2,3,6,7-tetrahydroxyanthracene was synthesised according to Niederl and Nagel.[118] Hence, catechol and 2,5-hexanedione were left to react in sulfuric acid at room temperature for 5 days following by crystallisation from ethyl acetate to give a pure product **Scheme 41**.

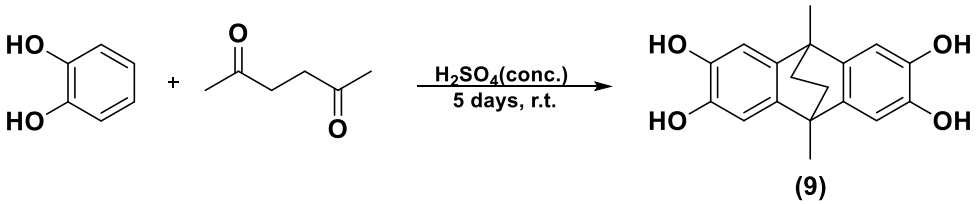


**Scheme 41** Synthesis of 9,10-dimethyl-9,10-ethano-9,10-dihydro-2,3,6,7-tetrahydroxyanthracene

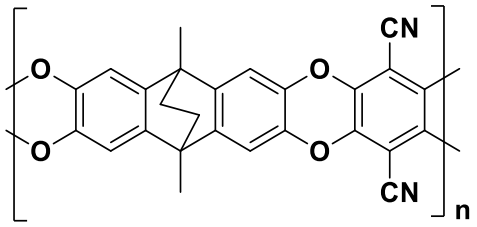


**Scheme 42** The molecular structure of 9,10-dimethyl-9,10-ethano-9,10-dihydro-2,3,6,7-tetra hydroxyanthracene monomer

## 3.3.2 Synthesis of 9,9-bis(3,4-dihydroxyphenyl)fluorene (10)

The structure of the 9,9-bis(3,4-dihydroxyphenyl)fluorene monomer contains a cyclic unit, in which one of the carbon atoms in the ring shares two catechol units, which will be incorporated into the polymer backbone and consequently forms a “cardo-polymer”. This structural feature has restricted rotation that makes it attractive for the synthesis of microporous polymers. Cardo-PIMs-1 were reported previously by the McKeown group and these were prepared by

the reaction of 9,9-bis(3,4-hydroxyphenyl)fluorene and a tetrachloride monomer **Scheme 44**.[119]

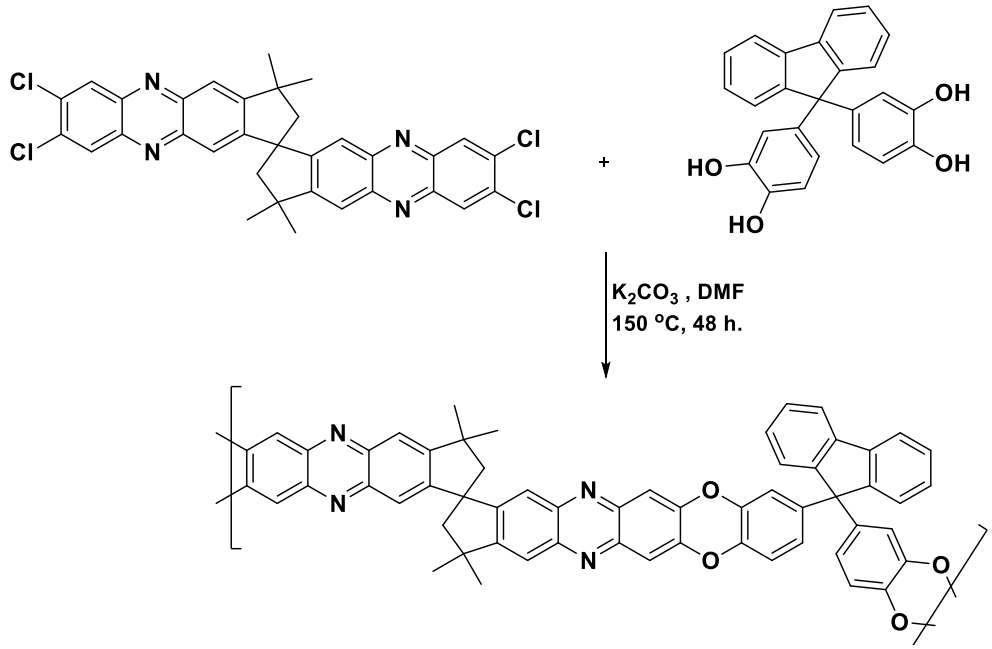


**Scheme 44** Synthesis of Cardo-PIMs-1

These resulting cardo-polymer displayed microporosity with high surface area, 621 $m^2/g$. Moreover, Cardo-PIM-1 had been cast from chloroform to obtain film which exhibited high gas permeability and good selectivity with data approximately on the 1991 Robeson upper bounds for $CO_2/CH_4$ and $O_2/N_2$. Therefore, the aim was to prepare this monomer and polymerise it with 2,3,7,8-tetrafluoro-5,5',10,10'-tetraoxidethianthrene (TOT) to obtain a novel microporous polymer. The synthesis of 9,9-bis (3,4-dihydroxyphenyl) fluorene was achieved following a patent procedure. Hence, fluorenone, catechol, toluene and phosphotungstic acid as a catalyst were refluxed under nitrogen for 8 hours while removing the generated water to give the required product in good yield and purity **Scheme 43**.[120]

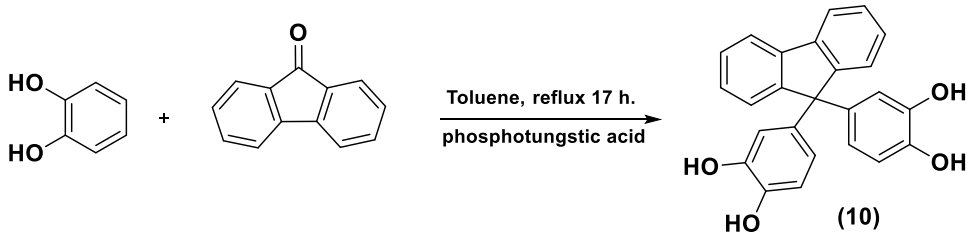


**Scheme 43** The synthesis of 9,9-bis (3,4-dihydroxyphenyl) fluoren

### 3.3.3 Synthesis of spirobifluorenes (SBFs) (16, 22, 28)

The spirobifluorene structural unit forms rigid polymers due to its fused benzene rings that restrict the movement around the spirocentre. The first PIM-SBF was prepared by the McKeown group using the reaction of 2,2',3,3'-tetrahydroxy-9,9'-spirobifluorene with 2,3,5,6-tetrafluoroterephthalonitrile[121] **Scheme 45**. The resulting PIM-SBF exhibits significant microporosity with a BET surface area of 803 $m^2$ $g^{-1}$. It could be cast from chloroform to give a robust film, which demonstrated impressive gas separation properties. For this reason, the objective was to prepare three SBF bis-catechol monomers, namely, 2,2',3,3'-tetrahydroxy-9,9'-spirobifluorene **(16)**, 2,2',3,3'-tetrahydroxy-6,6'-dimethyl-9,9'-spirobifluorene **(22)** and 2,2',3,3'- tetrahydroxy-6,6'-*t*-butyl-9,9'-spirobifluorene **(28)** and polymerise each of them with the TOT monomer. The synthetic route to the SBF monomers required six steps, starting with Suzuki coupling between the appropriate phenylboronic acid with an appropriate phenyl bromide. The resulting biphenyl was then brominated, using bromine, to give the bromobiphenyl which was then converted to the carboxylic biphenyl via reacting with butyl lithium and $CO_2$. Then the carboxylic biphenyl was reacted with methanesulfonic acid to give the fluorenone. Finally, the spirobifluorene was prepared via addition of the 2-lithio anion of appropriate bromobiphenyl to an appropriate fluorenone followed by acid mediated cyclisation. The resulting product was demethylated to give the desired spirobifluorene biscatechols **Scheme 46**.

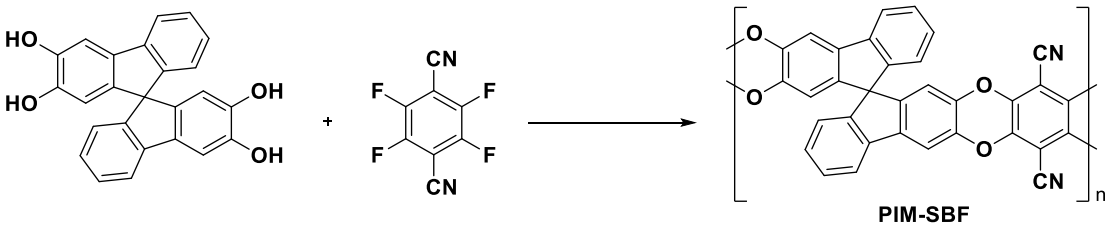


**Scheme 45** Synthesis of PIM-SBF

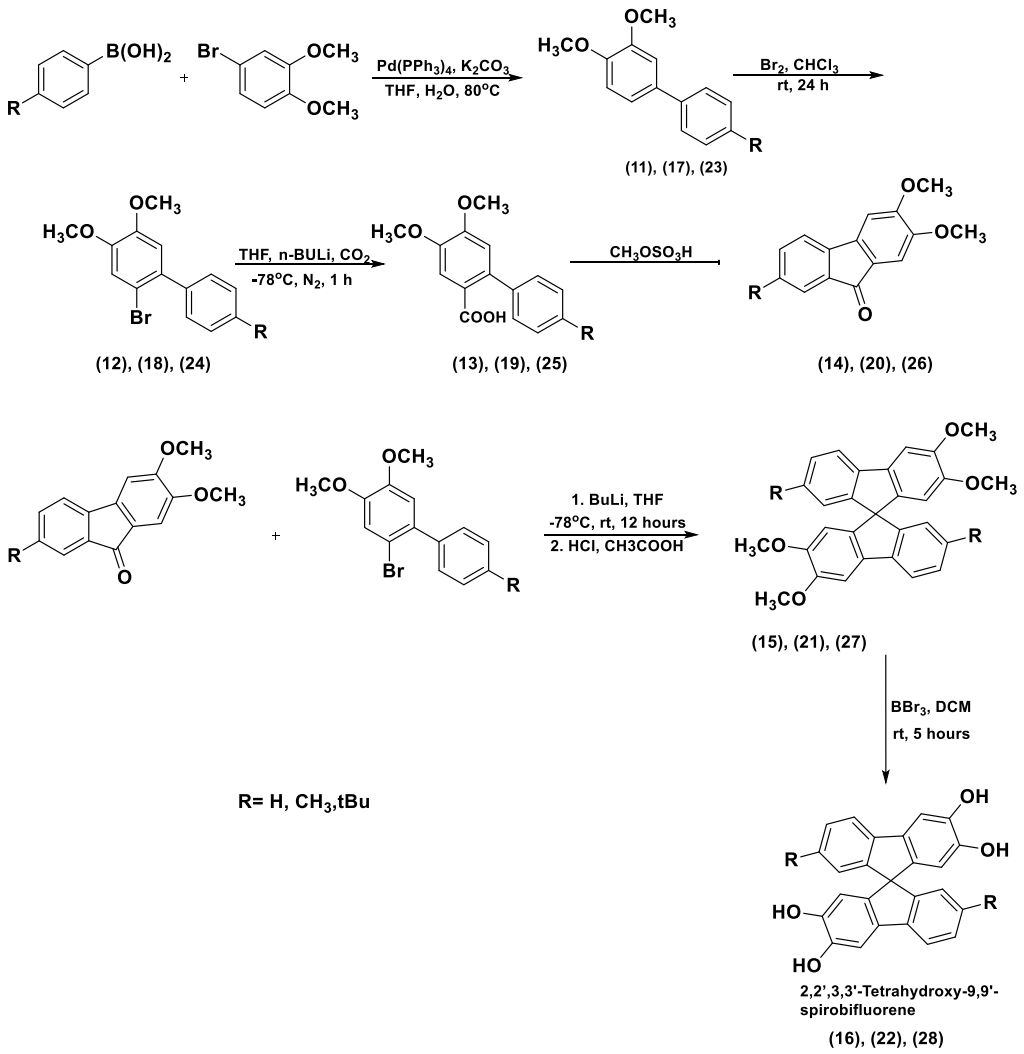


**Scheme 46** Synthesis of spirobifluorene monomers (SBFs)

## 3.3.4 Synthesis of 1,4-di(3',4'-dihydroxyphenyl)-2,3,5,6-tetraphenylbenzene (32)

Hexaphenylbenzene (HPB) is an interesting structural unit for the synthesis of microporous materials due to its shape, which consists of six benzene rings connected to single central benzene. This structure prevents the efficient packing of polymer chains, leading to high microporosity. PIM-HPB-2 was reported previously by the McKeown Group.[122] This polymer was derived from 1,4-di(3',4'-dihydroxyphenyl)-2,3,5,6-tetraphenylbenzene and 2,3,5,6-tetrafluoroterephthalonitrile **Scheme 48**. It was proven to have a significant microporosity with a BET surface area of 527 $m^2/g$ and to have a high molecular weight which was sufficient to form self-standing films by

casting from chloroform. PIM-HPB-2 film showed good gas separation properties. Due to the interesting structure of HPB and the promising gas separation properties of reported polymers containing the HPB unit, 1,4-di(3',4'-dihydroxyphenyl)-2,3,5,6-tetraphenylbenzene **(32)** was prepared for this project via the Diels-Alder reaction between 2,5-bis(3,4-dimethoxyphenyl)-3,4-diphenylcyclopenta-2,4-dien-1-one **(30)** and 2-phenylethynyl)benzene to give 1,4-di(3',4'-dimethoxyphenyl)-2,3,5,6-tetraphenylbenzene **(31)**. Then, the resulting methoxy compound was demethylated by using boron tribromide ($BBr_3$) in dichloromethane to yield the catechol **(32)** **Scheme 47**.

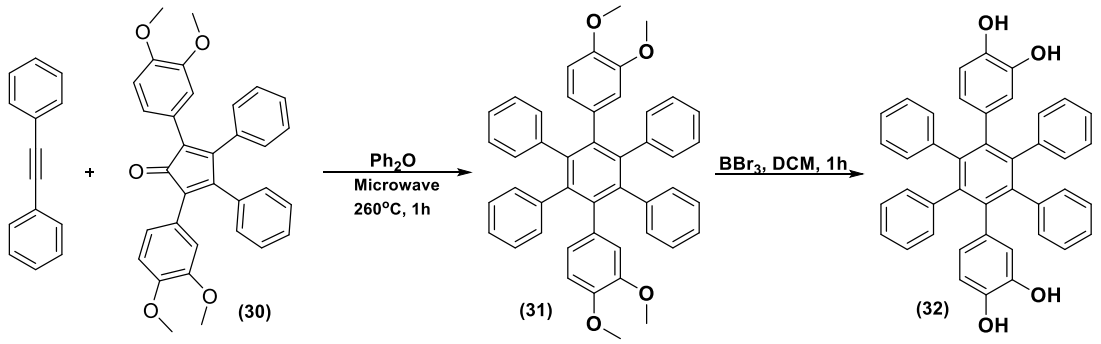


**Scheme 47** Synthesis of 1,4-di(3',4'-dihydroxyphenyl)-2,3,5,6-tetraphenylbenzene

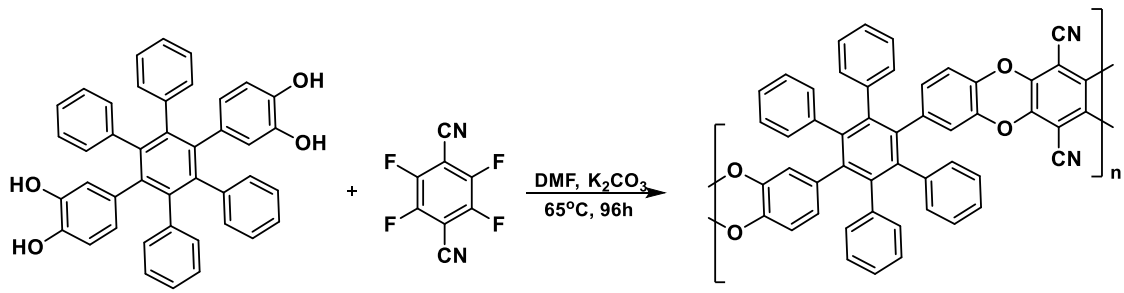


**Scheme 48** Synthesis of PIM-HPB-2

### 3.3.5 Synthesis of 2,3,6,7-tetrahydroxy-9,10-dimethyl-[12,13]-(5',5',8',8'-tetramethyl-5',6',7',8'-tetrahydronaphthyl)triptycene (39)

Benzotriptycene is a contorted and rigid structure arising from aryl units fused rings to a central bicyclic bridgehead system. The rigid structure of benzotriptycene makes them a desirable unit within a polymer backbone, producing a 2D chain structure, which leads to reduced efficiency of chain packing. This significantly improves the amount of microporosity generated. PIM-TMN-Trip polymer was prepared by Rose[123] in 2017. It is derived from 2,3,6,7-tetrahydroxy-9,10-dimethyl-[12,13]-(5',5',8',8'-tetramethyl-5',6',7',8',-tetrahydronaphthyl)triptycene and tetrafluoroterephthalonitrile. It exhibited excellent gas separation properties with high surface area of 1050 $m^2/g$ **Scheme 49**.

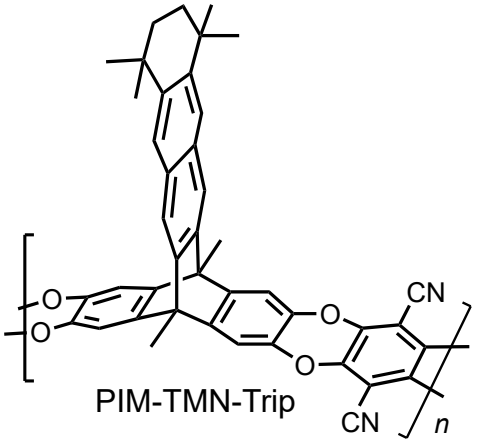


PIM-TMN-Trip

**Scheme 49** Structure of PIM-TMN-Trip

As a result, polymerisation of this unique biscatechol with the TOT monomer is highly desirable. The desired monomer 2,3,6,7-tetrahydroxy-9,10-dimethyl-[12,13]-(5',5',8',8'-tetramethyl-5',6',7',8',-tetrahydronaphthyl)triptycene was prepared *via* six steps, starting with the Friedel-Craft reaction of anhydrous benzene with 2,5-dichloro-2,5-dimethylhexane **(5)**, followed by bromination to obtain 6,7-dibromo-1,1,4,4-tetramethyl-1,2,3,4-tetrahydronaphthalene **(34)**. To form the oxygen bridge, 6,7-dibromo-1,1,4,4-tetramethyl-1,2,3,4-tetrahydronaphthalene **(34)** was subjected to a Diels-Alder reaction with anhydrous furan in the presence of *n*-BuLi at -78 °C. The resulting 5,5,8,8-

tetramethyl-1,4,5,6,7,8-hexahydro-1,4-epoxyanthracene **(35)** was reacted with 2,3,6,7-tetramethoxy-9,10-dimethylanthracene **(36)** by another Diels-Alder reaction to give (5*s*,14*s*)-2,3,18,19-tetramethoxy-5,8,8,11,11,14-hexamethyl-5,5a,6,8,9,10,11,13,13a,14-decahydro-5,14-[1,2]benzeno-6,13-epoxypentacene **(37)**. Oxygen removal from compound **(37)** was achieved by using acidic medium (TFA), following by the demethylation reaction of 2,3,18,19-tetramethoxy-5,8,8,11,11,14-hexamethyl-5,8,9,10,11,14-hexahydro-5,14-[1,2]benzenopentacene **(38)** by using $BBr_3$ in DCM to give 5,8,8,11,11,14-hexamethyl-5,8,9,10,11,14-hexahydro-5,14-[1,2]benzenopentacene-2,3,18,19-tetraol **(39) Scheme 50**.

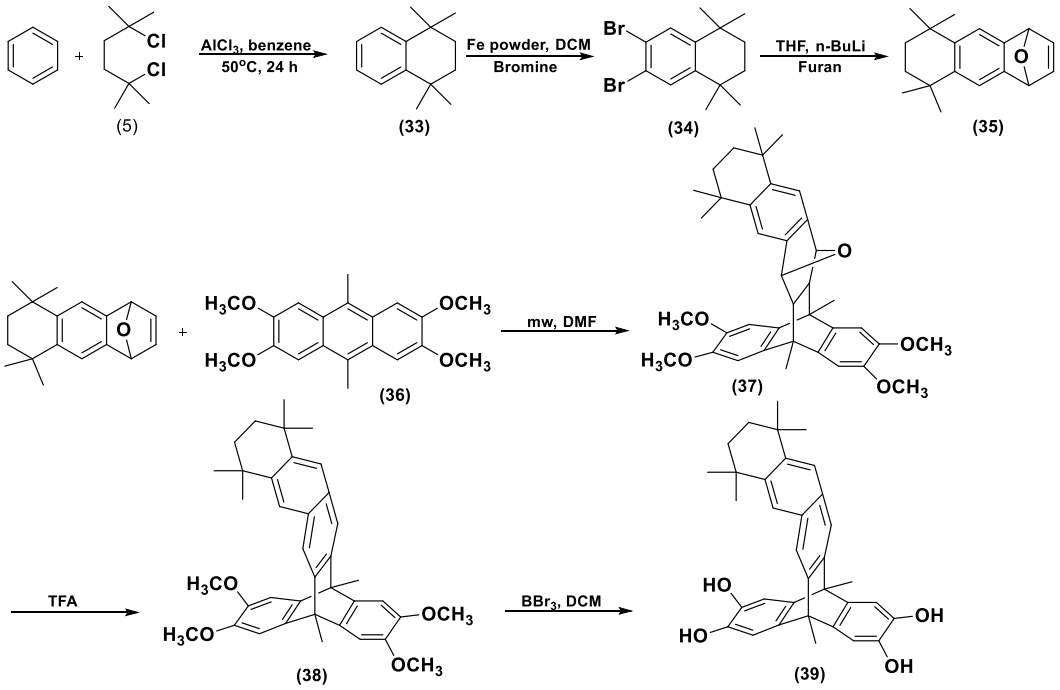


**Scheme 50** Synthesis of 5,8,8,11,11,14-hexamethyl-5,8,9,10,11,14-hexahydro-5,14-[1,2]benzenopentacene-2,3,18,19-tetraol

## 3.3.6 Synthesis of 2,3,6,7,12,13- hexahydroxytriptycene (42)

Another attractive structure for PIM synthesis is triptycene which consists of three phenyl rings which are fused to a bicyclic bridgehead leading to generate intrinsic microporosity within polymer chains. A network polymer of intrinsic microporosity (network-PIM) was prepared via the aromatic nucleophilic substitution reaction between 2,3,6,7,12,13-

hexahydroxytriptycene and tetrafluoroterephthalonitrile. It showed enhanced microporosity with a high BET surface area of 1318 $m^2/g$, which approaches that of the most porous hypercrosslinked polymers[64] **Scheme 51**.

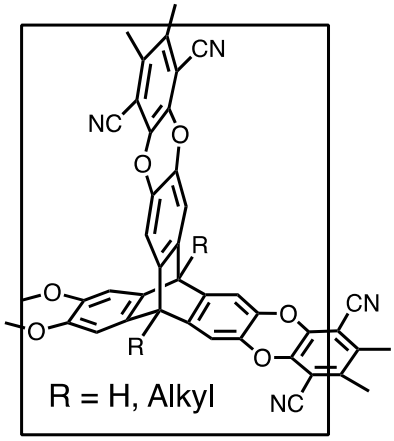


**Scheme 51** Synthesis of network-PIM

Triptycene has been used widely as components of functional molecular systems including supramolecular receptors[124], ligands[125], molecular cages[126], coordination networks[127], and polymers. However, no triptycene network polymers have been prepared using the TOT monomer and this became an objective of the project. Hence the desired monomer, 2,3,6,7,12,13-hexahydroxytriptycene, was produced by the bromination of triptycene, subsequent copper-mediated methoxylation of 2,3,6,7,12,13-hexabromotriptycene and finally demethylation of 2,3,6,7,12,13-hexamethoxytriptycene **Scheme 52**. Bromination of triptycene was performed using bromine and iron powder in dichloromethane and refluxed for 18 hours. The key precursor 2,3,6,7,12,13-hexamethoxytriptycene **(41)** could be obtained by two slightly different chemical procedures. In one the aromatic nucleophilic substitution of bromine with methoxy groups was performed with NaOMe solution (commercially available) and CuBr in toluene at 110 °C for 24 hours[128]. In the second, the reaction was performed using freshly prepared NaOMe from Na metal in anhydrous MeOH and CuBr[129]. The product yield of the former method was found to be better than that of the latter method. The second method led to a mixture of many side products from which the desired product needed to be isolated using column chromatography. In contrast, for the first method, a large excess of NaOMe

was used which seems to be essential for the methoxylation reaction to be forced to completion.

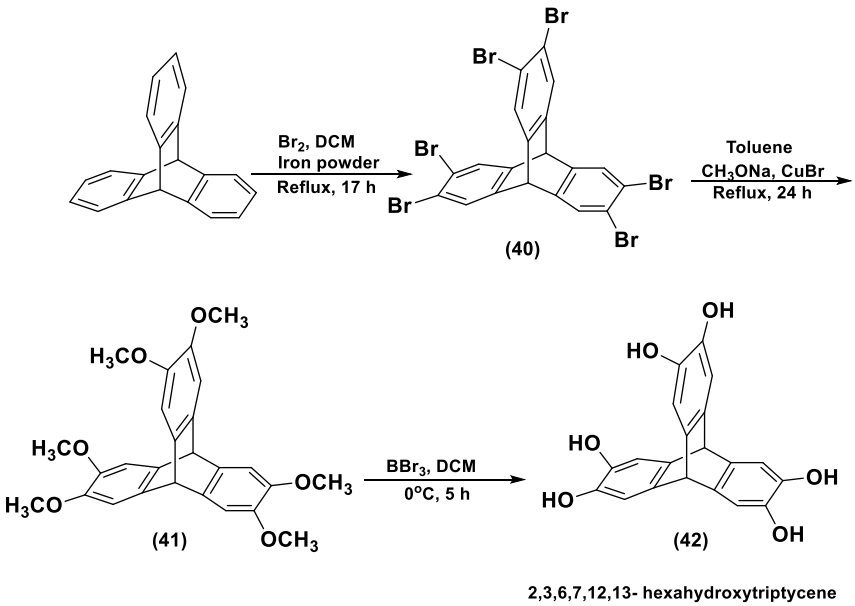


**Scheme 52** Synthesis of 2,3,6,7,12,13-hexahydroxytriptycene

## 3.4 Model compounds for the polymerization of PIMs based on the TOT disulfone monomer

Previously, 2,3,7,8-tetrafluoro-5,5',10,10'-tetraoxidethianthrene (TOT) was polymerised with 5,5',6,6'-tetrahydroxy-3,3,3',3'-tetramethylspirobisindane (TTSBI) at 160 °C for 45 minutes to prepare TOTPIM-100 as reported by Du.[117] In order to obtain the best reaction conditions for our PIMs based on the TOT monomer, optimisation of the synthesis of a model compound was achieved. The reactions studied involved aromatic nucleophilic substitution of 2,3,7,8-tetrafluoro-5,5',10,10'-tetraoxidethianthrene with 5,5,8,8-tetramethyl-5,6,7,8-tetrahydronaphthalene-2,3-diol **(7)** at 70 °C for 18 hours and also at 160 °C for 45 minutes **Scheme 54**. These two conditions were be chosen according to different chemical procedures of PIM-1 synthesis reported previously.[130,131] 5,5,8,8-tetramethyl-5,6,7,8-tetrahydronaphthalene-2,3-diol **(7)** was synthesised according to a reported procedure.[132] This involves the synthesis of 6,7-dimethoxy-1,1,4,4-tetramethyl-1,2,3,4-tetrahydronaphthalene **(6)** by the reaction of 1,2-dimethoxybenzene and 2,5-dichloro-2,5-dimethoxyhexane with aluminium chloride for 20 hours at room

temperature, following by demethylation by $BBr_3$ in DCM to give the desired catechol **Scheme 53**.

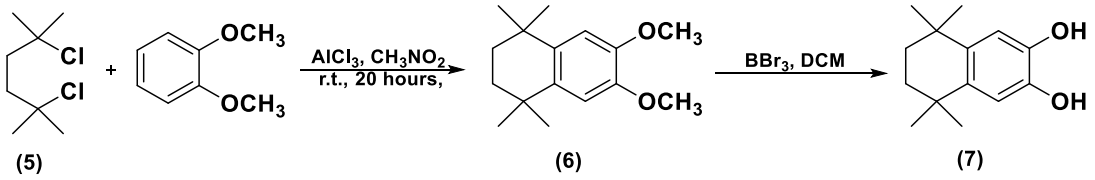


**Scheme 53** Synthesis of 6,7-dimethoxy-1,1,4,4-tetramethyl-1,2,3,4-tetrahydronaphthalene

The synthetic method performed at higher temperature and shorter reaction time was reported as an improved procedure for the PIM-1 preparation in comparison with the conventional one which is conducted at 70 °C. It was reported that the PIM-1 prepared at elevated temperature appeared to have much better mechanical properties and less crosslinked fractions than the PIM-1 that was prepared at 70 °C.

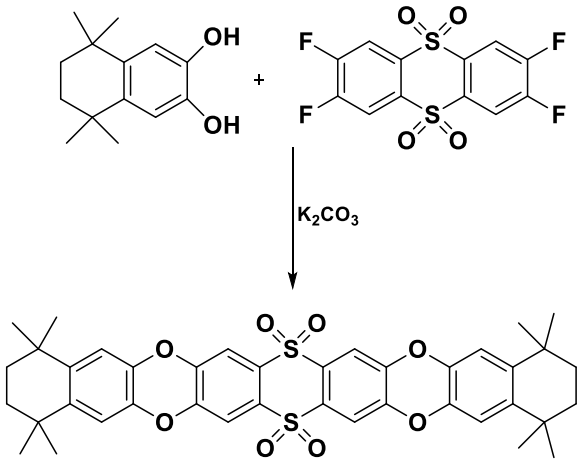


**Scheme 54** Synthesis of model compound

**Table 4** Reaction conditions for the synthesis of the model compound

| | Reaction conditions | | | % Yield |
|---|---|---|---|---|
| | Temperature (°C) | Duration | Solvent | |
| **8a** | 70 | 72 hrs. | DMF | 79 % |
| **8b** | 160 | 45 min. | NMP | 78 % |

Samples of resulting model compounds were analysed by $^{1}$HNMR and these spectra demonstrated that both different reaction conditions provided pure compound in a very good yield (~80%). As a result, both different reaction conditions were used to polymerise TOT-based PIMs from different catechols in order to obtain successful polymerisations.

## 3.5 Synthesis of tetraoxidethianthrene polybenzodioxin polymers

A series of polymers derived from combination of the TOT monomer with catechol-based monomers were synthesised using the double nucleophilic aromatic substitution that provides a fused-ring dioxin linking group **Scheme 55**. This reaction proceeds via a two-step substitution process in which a hydroxyl group displaces a fluorine atom from an activated aryl-halide system ($S_NAr$).[133] The electronegative fluorine atoms and electron-withdrawing sulfone groups both pull electron density away from the phenyl ring activating it towards nucleophilic attack by the deprotonated hydroxyl group of the catechol-based monomer. The reaction proceeds via a negatively charged species called a Meisenheimer complex, from which the fluoride leaving group is eliminated during the formation of ether-link between the two monomers. This two-step addition-elimination process then repeats until all of the tetrafluorinated monomer has been consumed by the substitution of the fluorine atoms, forming a polymer.

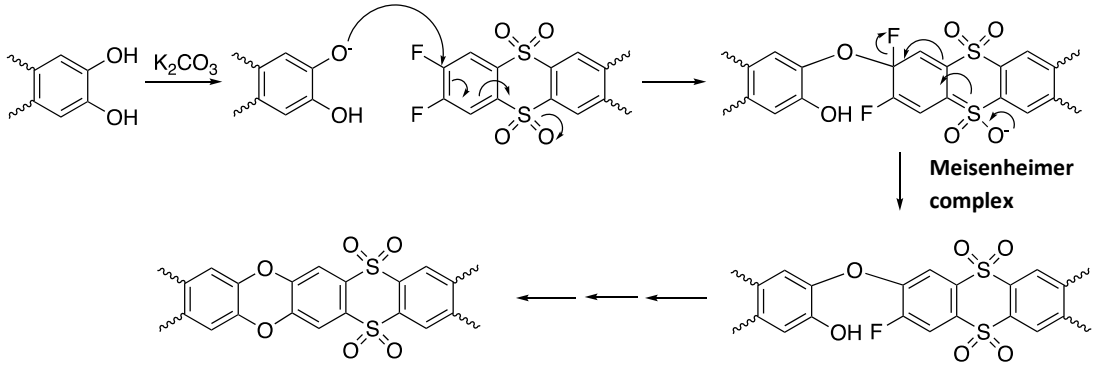


**Scheme 55** The mechanism for TOT-based PIM polymerization

All PIM-TOTs were prepared according to the conventional method at 70 °C for 72 hours but different reaction conditions were also tried in order to establish the optimum conditions. Details of the physical properties of each TOT-based polymer are provided in **Table 11** (physical data for the structurally related PIM obtained from literature is also provided for comparison). All TOT- polybenzodioxin polymers were isolated in good yield and were found to be insoluble in low boiling points solvents such as $CHCl_3$ and THF, which are commonly used for casting PIM films. However some of these polymers proved to be soluble in quinoline and could be cast successfully from quinoline solution to form films of sufficient robustness for gas separation measurements. Insolubility in chloroform prevented determination of the polymer's average molecular mass by Gel Permeation Chromatography (GPC). In each case, Thermal Gravimetric Analysis (TGA) revealed very good thermal stabilities, with each polymer being stable up to at least 350 °C before decomposition. Each polymer was prepared a number of times in order to obtain sufficiently high molecular weight to enable them to be cast into films.

## 3.5.1 Synthesis of TOT-TTSBI-based PIMs

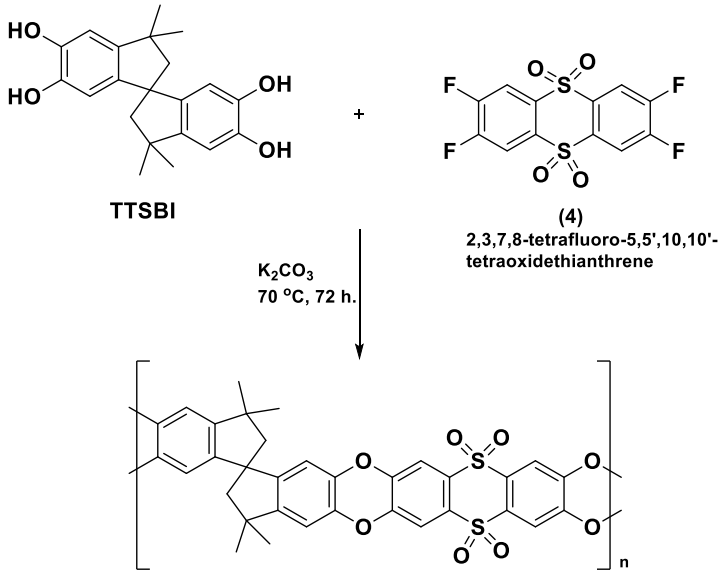


**Scheme 56** Synthesis of **TOT-TTSBI-58c**

The polymerisation reaction between monomers TTSBI and 2,3,7,8-tetrafluoro-5,5',10,10'-tetraoxidethianthrene (TOT) was reported previously in the literature[117] **Scheme 56**, but detailed information on the polymerisation procedure was lacking. It was stated that the polymerization reaction was carried out in NMP at 160 °C for 2 hours, giving a high molecular weight polymer (TOTPIM-100) which could be cast into a film from chloroform solution. In our first attempt, the polymerisation was performed using these conditions but, unfortunately, the obtained polymer did not show the same characteristics. Therefore, the polymerisation was performed numerous times in different conditions as shown in **Table 5** in an attempt to obtain a polymer of sufficiently high molecular mass for full analysis.

**Table 5 TOT-TTSBI-58a** to **-58d** polymerisation conditions and polymers properties

| | **Reaction conditions** | | | |
|---|---|---|---|---|
| | **TOT-TTSBI-58a At 160 °C for 2 h[a]** | **TOT-TTSBI-58b At 160 °C for 2 h[b]** | **TOT-TTSBI-58c At 70 °C for 72 h** | **TOT-TTSBI-58d At 160 °C for 45 m** |
| BET surface area ($m^2/g$) | 573 | 361 | 596 | 576 |
| $CO_2$ uptake (mg/g) | 46 | 48 | 45 | 27 |
| Decomposition temperature | 441 | 436 | 430 | 465 |
| Film formation | X From quinoline | X From quinoline | √ From quinoline | X brittle From chloroform |

**a** Temperature was raised gradually until 160 °C. **b** Temperature was raised directly to 160 °C.

The BET surface area of polymer batches **TOT-TTSBI-58a, 58c** and **58d** showed matching surface area results with literature, however, **TOT-TTSBI -7158a** and **-58b** proved unexpectedly insoluble in chloroform and tetrahydrofuran but were soluble in quinoline instead. **TOT-TTSBI-58c** and **-58d** polymers could be cast from quinoline and chloroform, respectively. **TOT-TTSBI-58c** film showed different gas separation performance in

comparison with reported one **TOT-PIM100** which was prepared at higher temperature for shorter time.[117] It showed higher selectivity, coupled with some increase in gas permeabilities for all gases **Table 6**. Unfortunately, film **TOT-TTSBI-58d** proved brittle which prohibits gas permeability measurements.

**Table 6** Gas permeabilities and ideal selectivities α (Px/Py) of TOT-TTSBI films

| Sample | Permeability coefficients | | | | Selectivity α(Px/Py) | | |
|---|---|---|---|---|---|---|---|
| | $O_2$ | $N_2$ | $H_2$ | $CO_2$ | $O_2/N_2$ | $CO_2/N_2$ | $H_2/N_2$ |
| **TOTPIM100**[a] | 642 | 190 | 1368 | 3056 | 3.40 | 16.1 | 7.2 |
| **TOT-TTSBI- 58c**[b] | 942 | 280 | 2382 | 5673 | 3.36 | 20.20 | 8.48 |

**a** reported PIM derived from TOT monomer[117] **b** prepared in this work.

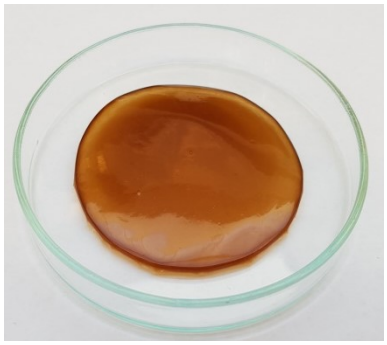

**Figure 13 TOT-TTSBI-58c**

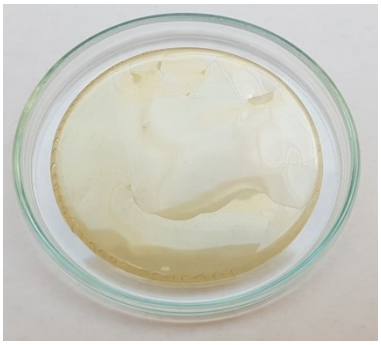

**Figure 12 TOT-TTSBI-58d**

## 3.5.2 Synthesis of TOT-SBC-based PIMs

Polymers **(TOT-SBC-59a, -59b, -59c, -59d, -59e)** were generated from the polymerisation reaction between 6,6',7,7'-tetrahydroxy-4,4,4',4'-tetramethyl-2,2'-spirobischromane (THTMSBC) and 2,3,7,8-tetrafluoro-5,5',10,10'-tetraoxidethianthrene (TOT) monomers at different temperatures and reaction times **Table 7**. Polymerisation was carried out under different reaction conditions to ensure the attainment of a high molecular weight polymer.

**Table 7** Physical characterization of **(TOT-SBC-59a, -59b, -59c, -59d, -59e)**

| | **TOT-SBC-59a at 95 °C for 24 h** | **TOT-SBC-59b at 160 °C for 17 h** | **TOT-SBC-59c at 70 °C for 72 h** | **TOT-SBC-59d at 160 °C for 2 h** | **TOT-SBC-59e at 160 °C for 45 min.** |
|---|---|---|---|---|---|
| BET surface area ($m^2/g$) | 466 | 487 | 471 | 500 | 374 |
| $CO_2$ uptake (mg/g) | 40 | 43 | 34 | 43 | 32 |
| Decomposit-ion temperature | 429 | 411 | 415 | 403 | 420 |
| Film formation | √ From quinoline | √ From quinoline | √ From quinoline | √ From quinoline | √ From quinoline |

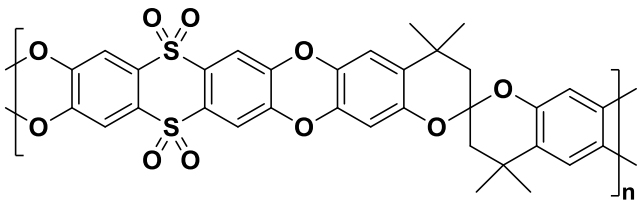

**Scheme 57** Chemical structure of **(TOT-SBC-59a, -59b, -59c, -59d, -59e)**

After purification, all **(TOT-SBC-59a, -59b, -59c, -59d, -59e)** polymers showed good and consistent surface area values with that of **TOT-SBC-59d** slightly lower. In addition, all of these polymers were successfully cast into films from quinoline solution. Films of **TOT-SBC-59c** and **-59e** were sufficiently robust to allow the measurement of their gas permeability properties Error! Reference source not found.. Both films showed the same erformance on the Robeson 1991 upper bound for $H_2/N_2$, for example **Figure 14**. In addition, the gas permeabilities and ideal selectivities α (Px/Py) for the equivalent polymer derived from 2,3,5,6-tetrafluoroterephthalonitrile is also provided in **Table 8** for comparison).

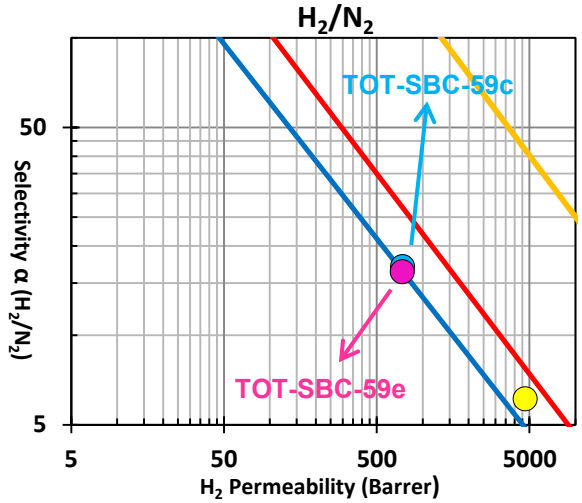


**Figure 14** Robeson plots for $H_2/N_2$ gas pair with 1991 (—), 2008 (—) and 2015 (—) upper bounds; **TOT-SBC-59c** (●),**TOT-SBC-59e** (●) and PIM-1(●)

**Table 8** Gas permeabilities and ideal selectivities α (Px/Py) for methanol treated films of **TOT-SBC-59c** and **-59e**

| Sample | Permeability coefficients | | | | | | Selectivity α(Px/Py) | | | |
|---|---|---|---|---|---|---|---|---|---|---|
| | $N_2$ | $O_2$ | $CO_2$ | $CH_4$ | $H_2$ | He | $CO_2/CH_4$ | $CO_2/N_2$ | $H_2/N_2$ | $H_2/CH_4$ |
| **TOT-SBC-59c** | 43 | 180 | 1102 | 57 | 742 | 369 | 19.07 | 25.21 | 16.98 | 12.85 |
| **TOT-SBC-59e** | 45 | 184 | 1110 | 58 | 736 | 372 | 19.06 | 24.59 | 16.31 | 12.64 |
| **PIM-CO15** | 83 | 275 | 2000 | 130 | 900 | 450 | 15.4 | 24.1 | 10.8 | 6.9 |

## 3.5.3 Synthesis of TOT-EA-based PIMs

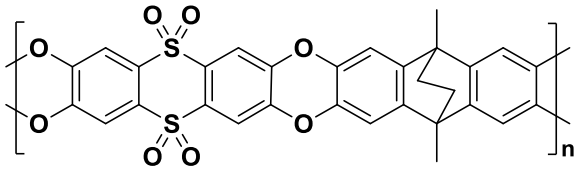


**Scheme 58** Chemical structure of **(TOT-EA-60a and -60b)**

Polymers **TOT-EA-60a** and **-60b** were generated from the polymerization reaction between 9,10-dimethyl-9,10-ethano-9,10-dihydro-2,3,6,7-tetrahydroxyanthracene (DMETHA) **(9)** and 2,3,7,8-tetrafluoro-5,5',10,10'-tetraoxidethianthrene **(4)** at different temperatures and reaction times **Table 9**.

**Table 9** Physical characterization of TOT-EA-60a and -60b

| | **TOT-EA-60a at 70 °C for 72 h** | **TOT-EA-60b at 160 °C for 45 min.** |
|---|---|---|
| BET surface area ($m^2/g$) | 713 | 527 |
| $CO_2$ uptake (mg/g) | 48 | 40 |
| Decomposition temperature | 440 | 443 |
| Film formation | X in quinoline | X in quinoline |

It can be seen from the **Table 9** that **TOT-EA-60a** and **-60b** polymers showed high surface area with a slightly increase of surface area and $CO_2$ uptake values for **TOT-EA-60a**. However, neither of these polymers could be cast into films from quinoline solution due to their insolubility. This result was not unexpected as the polymer from 2,3,5,6-tetrafluoroterephthalonitrile and DMETHA also proved insoluble in common organic solvents.[119]

## 3.5.4 Synthesis of TOT-Cardo-based PIMs

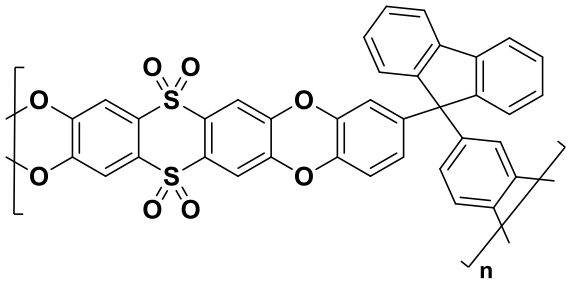


**Scheme 59** Chemical structure of **TOT-Cardo-61a** and **-61b**

Polymers **TOT-Cardo-61a** and **-61b** were prepared from the polymerization reaction between 9,9-bis(3,4-dimethoxyphenyl)fluorene **(10)** and 2,3,7,8-tetrafluoro-5,5',10,10'-tetraoxidethianthrene monomer **(4)** at different temperatures and reaction times **Table 10**. It can be seen that **TOT-Cardo-61a** has a two-fold higher surface area than **TOT-Cardo-61b**. Moreover, a film of **TOT-Cardo-61a** was cast successfully from quinoline but **TOT-Cardo-61b** polymer failed to form a film.

**Table 10** Physical characterization of **TOT-Cardo-61a** and **-61b**

| | **TOT-Cardo-61a at 70 °C for 72 h** | **TOT-Cardo-61b at 160 °C for 45 min.** |
|---|---|---|
| BET surface area ($m^2/g$) | 432 | 235 |
| $CO_2$ uptake (mg/g) | 39 | 41 |
| Decomposition temperature | 440 | 433 |
| Film formation | √ In quinoline | X in quinoline |

Based on the previous results of **TOT-TTSBI, TOT-SBC, TOT-EA** and **TOT-Cardo** which were prepared at different conditions, the optimum reaction conditions for the polymerisation using TOT not clear. Overall, performing the reaction at 70 °C for 72 hours seems to be better than at 160 °C for 45 min. for some reasons. Firstly, polymer **TOT-Cardo-61a** exhibited higher surface area than the equivalent polymer prepared at 160 °C and could be formed into a film. Moreover, it appears that a longer time of reaction at lower temperature enables the formation of a higher molecular weight of polymer. Consequently, reactions carried out at lower temperature for a longer time were used for the polymerisations between the remaining bis-catechol monomers and TOT.

## 3.5.5 Synthesis of TOT –based PIMs

A series of **TOT-SBF-62, TOT-SBF-63, TOT-SBF-64, TOT-HPB-65,** and **TOT-TMN-Trip-66** were prepared according to the general procedure at 70 °C for 72 hours, by reacting 2,3,7,8-tetrafluoro-5,5',10,10'-tetraoxidethianthrene **(4)** with 2,2',3,3'-tetrahydroxy-9,9'-spirobifluorene **(16)**, 2,2',3,3'-tetrahydroxy-6,6'-dimethyl-9,9'-spirobifluorene **(22)**, 2,2',3,3'-tetrahydroxy-6,6'-t-butyl-9,9'-spirobifluorene **(28)**, 1,4-di(3',4'-dihydroxyphenyl)-2,3,5,6-tetraphenylbenzene **(41)** and 5,8,8,11,11,14-hexamethyl-5,8,9,10,11,14-hexahydro-5,14-[1,2]benzenopentacene-2,3,18,19-tetraol **(48)**, respectively. Details of the physical properties of each

polymer are provided in Table 11. In addition, the physical data for the equivalent polymers derived from 2,3,5,6-tetrafluoroterephthalonitrile and for TOT –derived polymers **TOT-TTSBI-58c, TOT-SBC-59c, TOT-EA-60a** and **TOT-Cardo-61a** are also provided in **Table 11** for comparison.

**Table 11** Physical characterization of TOT –derived polymers

| Polymer | % Yield | $S_{BET}$ ($m^2/g$) | $T_d$ (°C) | $CO_2$ uptake mg/g | Film formation |
|---|---|---|---|---|---|
| 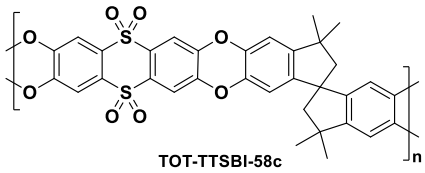 TOT-TTSBI-58c | 98% | 596 | 430 | 45 | √ From quinoline |
| 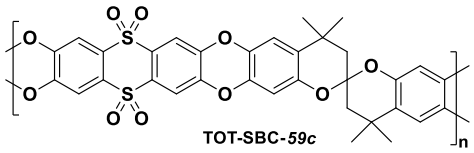 TOT-SBC-*59c* | 81% | 471 | 415 | 34 | √ From quinoline |
| 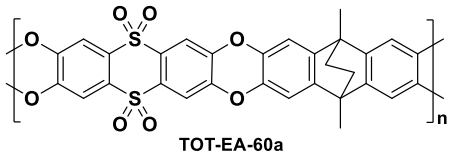 TOT-EA-60a | 92% | 713 | 440 | 48 | X |
| 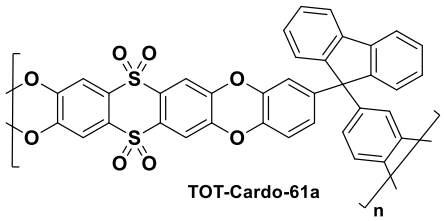 TOT-Cardo-61a | 94% | 432 | 440 | 39 | √ From quinoline |
| 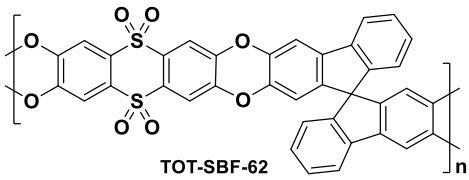 TOT-SBF-62 | 89% | 611 | 439 | 49 | √ From quinoline |

| | | | | | |
|---|---|---|---|---|---|
| 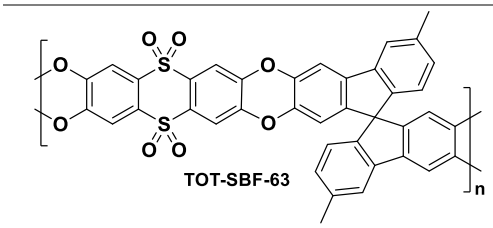 TOT-SBF-63 | 90% | 637 | 424 | 48 | √ From quinoline |
| 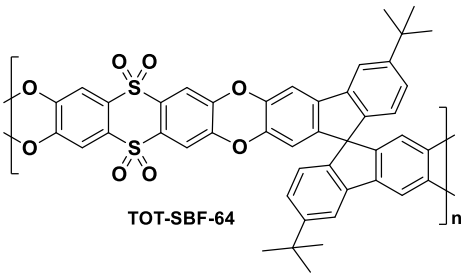 TOT-SBF-64 | 95% | 762 | 450 | 46 | √ From quinoline |
| 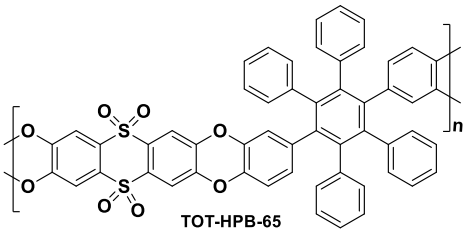 TOT-HPB-65 | 89% | 433 | 431 | 35 | X |
| 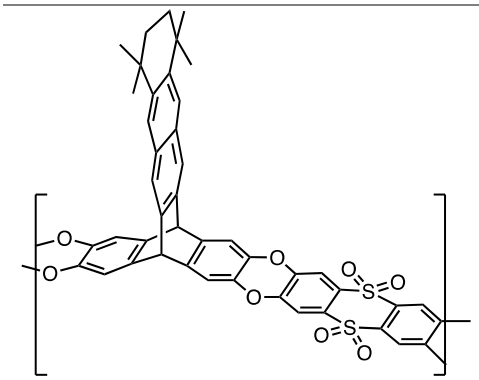 | 94% | 785 | 425 | 60 | X |
| 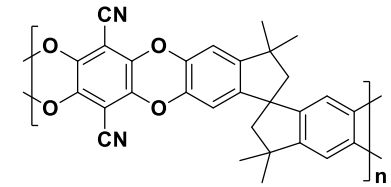 | - | 850 | - | - | √ From chloroform |
| 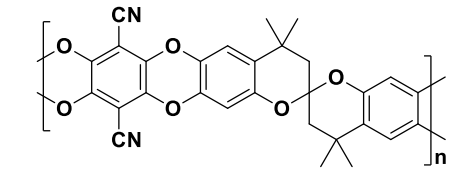 | - | 510 | - | - | √ From quinoline |

| | | | | | |
|---|---|---|---|---|---|
| 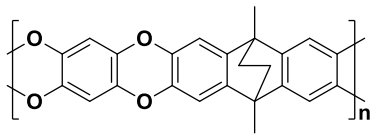 | - | 630 | - | - | x |
| 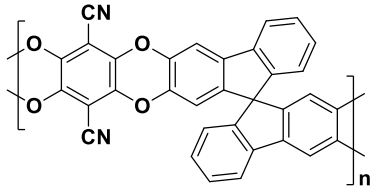 | - | 803 | - | - | √ From chloroform |
| 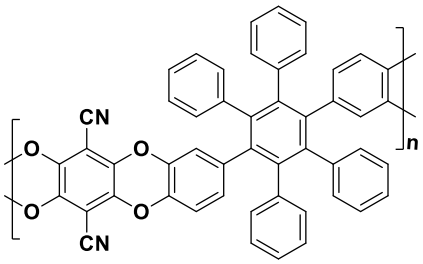 | - | 527 | - | - | √ From chloroform |
| 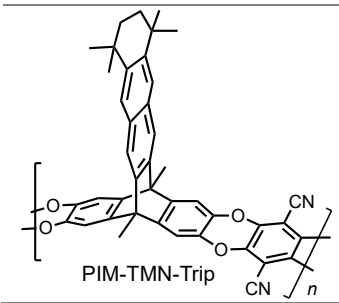 PIM-TMN-Trip | - | 1050 | - | - | √ From chloroform |

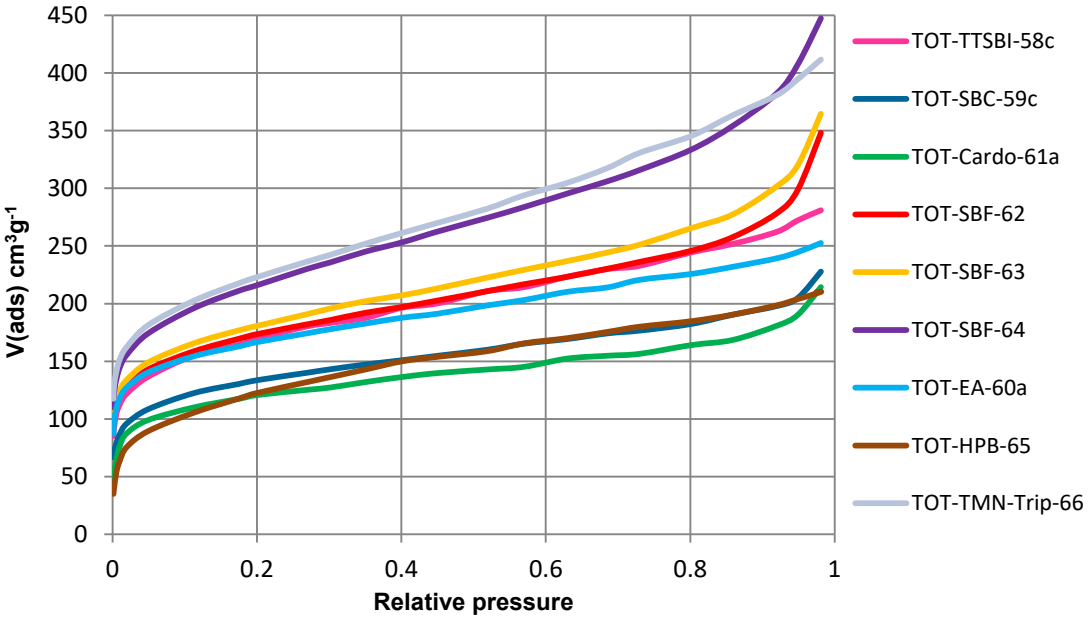


**Figure 15** $N_2$ adsorption isotherms

The infrared spectrum for each polymer sample in powder form confirmed the presence of two characteristic sulfonyl peaks in the range of (1100 – 1400) $cm^{-1}$. In addition, the absence of the (3400 - 2700 $cm^{-1}$) (OH stretch), provides a good evidence that the reaction of the bis-catechols with 2,3,7,8-tetrafluoro-5,5',10,10'-tetraoxidethianthrene **(4)** was efficient. The polymers as precipitated powders demonstrated intrinsic microporosity with large amounts of nitrogen adsorbed at low pressure, at 77 K **Figure 15**. Apparent BET surface areas were calculated from these isotherms **Table 11** with all TOT –derived polymers demonstrating high surface area values, ranging from 432 to 785 $m^2 g^{-1}$. It can be seen from the data that the surface area of substituted polymers or polymers that have a spiro-centre or bicyclic structures are higher than those of other polymers. For example, **TOT-TMN-Trip-66**, which contains a triptycene-based bicyclic structure fused with phenyl rings, showed the highest surface area of this series of polymers, whereas, the cardo-polymer **TOT-Cardo-61a** revealed the lowest surface area value. The lower porosity can be attributed to the structure of the biscatechol monomer, 9,9-bis(3,4-dimethoxyphenyl)fluorine **(10)**, which results in a polymer with two single bonds within each repeat units of the chain, about which there is relatively free rotation, resulting in more efficient packing of the polymer chains. In general, all TOT-derived polymers demonstrate lower surface areas than those of derived from the same biscatechol monomers combined with 2,3,5,6-tetrafluorophthalonitrile. This trend could be explained by the greater distance between the two sites of contortion due to the larger TOT monomer **Figure 16**.

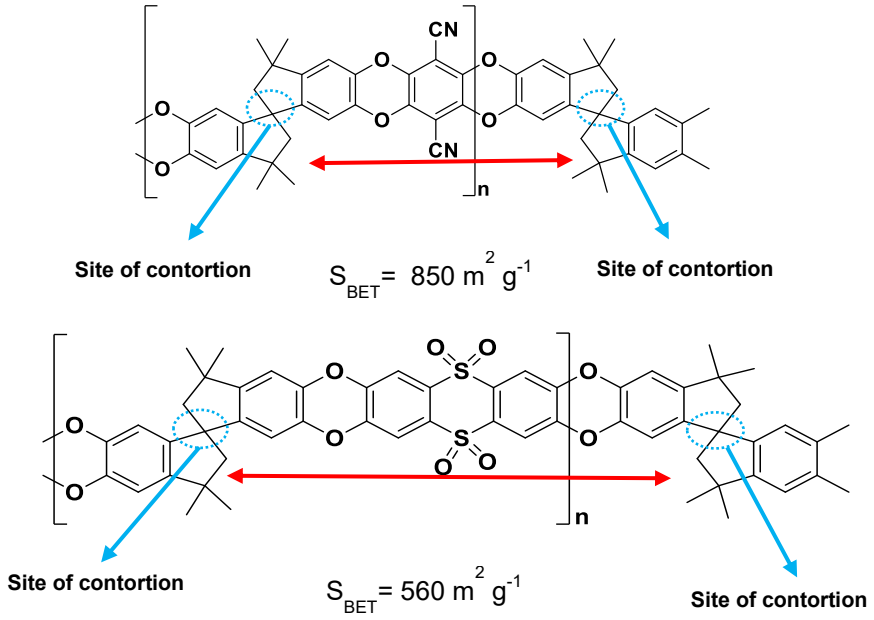


**Figure 16** The molecular structures of PIM-1 and TOTPIM-100

Therefore, the decrease in the concentration of the sites of contortion along the polymer chain may result in a more efficient packing of polymer and decrease the microporosity as compared with PIMs derived from 2,3,5,6-tetrafluorophthalonitrile. Three polymers **TOT-SBF-62**, **TOT-SBF-63** and **TOT-SBF-64**, which contain SBF structure, show the same trend as those derived from 2,3,5,6-tetrafluorophthalonitrile. Higher surface areas are demonstrated by polymers with substituted SBF units relative to the polymer with unsubstituted SBF. In addition, the surface area of the t-butyl substituted SBF polymer was higher than that of Me-substituted SBF polymer. This enhancement could be attributed to the bulky t-butyl groups which results in less efficient chain packing and consequently greater microporosity. $CO_2$ adsorption for all PIMTOT polymers showed a reasonable uptake consistent with a microporous structure **Figure 17**.

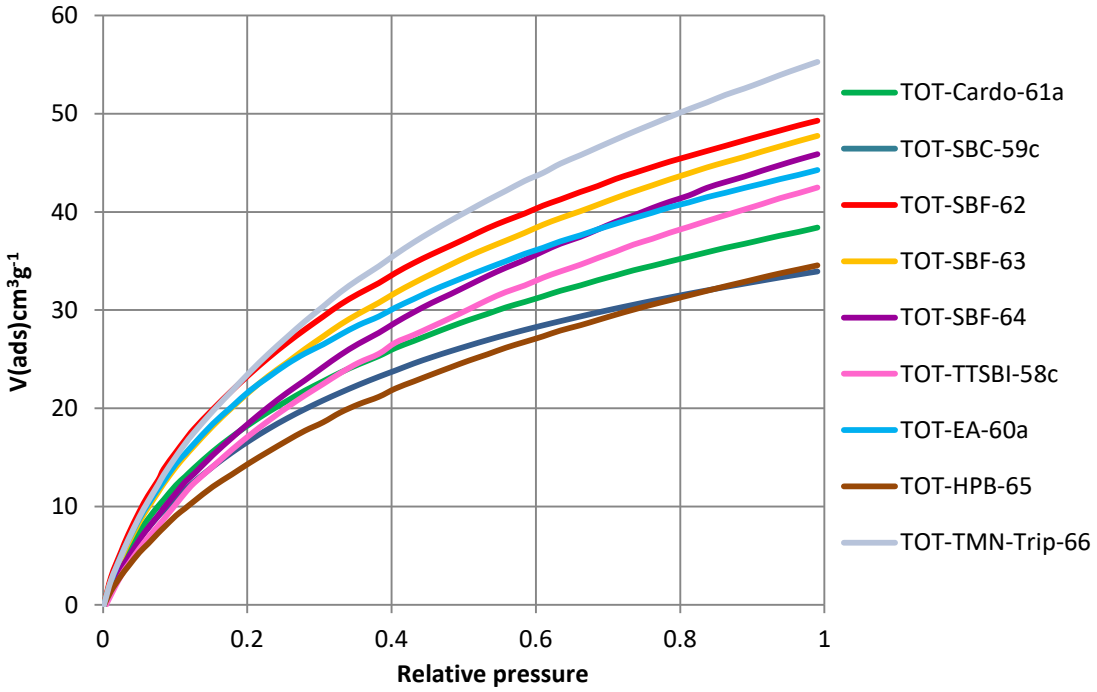


**Figure 17** $CO_2$ adsorption isotherms

Films were formed from each of **TOT-SBC-59c**, **TOT-Cardo-61a**, **TOT-SBF-62**, **TOT-SBF-63** and **TOT-SBF-64** by the slow evaporation (over two weeks) of a solution of the polymer in quinoline by using a heating system to aid evaporation of the high-boiling solvent. The formation of robust self-standing films formation confirms that molecular mass of each of these polymers is high in the absence of direct molecular mass measurement by GPC. These films proved suitable for gas separation measurements after being washed multiple times with methanol to remove any residual traces of quinoline solvent and then dried. Values for gas permeabilites and ideal selectivities of these PIMTOT films were measured by our collaborators at ITM using a single gas barometric instrument. These data are provided in **Table 12** and **Table 13**, along with the equivalents data for polymers derived from the same biscathechol monomers and 2,3,5,6-tetrafluorophthalonitrile for comparison.

**Table 12** Gas permeabilities Px, diffusivity Dx and solubility coefficient Sx, for methanol treated films of PIMTOTs

| Sample | Transport Parameters | $N_2$ | $O_2$ | $CO_2$ | $CH_4$ | $H_2$ | He |
|---|---|---|---|---|---|---|---|
| **TOT-TTSBI-58c** | $P_x$ [Barrer] | 280 | 942 | 5673 | 465 | 2382 | 963 |
| | $D_x$ [$10^{-12}$ $m^2s^{-1}$] | 66 | 216 | 84 | 27 | 3855 | 6122 |
| | $S_x$[$cm^3$ (STP) $cm^{-3}$ $bar^{-1}$] | 3.1 | 3.2 | 50.3 | 12.9 | 0.46 | 0.12 |
| **TOT-SBC-59c** | $P_x$ [Barrer] | 45 | 184 | 1110 | 58 | 736 | 372 |
| | $D_x$ [$10^{-12}$ $m^2s^{-1}$] | 12 | 46 | 17 | 4 | 1356 | 3148 |
| | $S_x$ [$cm^3$ (STP) $cm^{-3}$ $bar^{-1}$] | 2.6 | 2.9 | 47.8 | 11.0 | 0.40 | 0.09 |
| **TOT-Cardo-*61a*** | $P_x$ [Barrer] | 31 | 185 | 1025 | 52 | 729 | 328 |
| | $D_x$ [$10^{-12}$ $m^2s^{-1}$] | 9.6 | 44.6 | 14.6 | 3.2 | 1428 | 2740 |
| | $S_x$ [$cm^3$ (STP) $cm^{-3}$ $bar^{-1}$] | 2.44 | 3.12 | 52.73 | 12.27 | 0.38 | 0.09 |
| **TOT-SBF-62** | $P_x$ [Barrer] | 257 | 939 | 5434 | 392 | 2377 | 887 |
| | $D_x$ [$10^{-12}$ $m^2s^{-1}$] | 48 | 164 | 60 | 18 | 3116 | 3360 |
| | $S_x$ [$cm^3$ (STP) $cm^{-3}$ $bar^{-1}$] | 3.98 | 4.28 | 67.12 | 15.74 | 0.57 | 0.20 |
| **TOT-SBF-63** | $P_x$ [Barrer] | 326 | 1202 | 6739 | 500 | 3127 | 1114 |
| | $D_x$ [$10^{-12}$ $m^2s^{-1}$] | 54 | 203 | 75.0 | 19.4 | 3946 | 5795 |
| | $S_x$ [$cm^3$ (STP) $cm^{-3}$ $bar^{-1}$] | 4.52 | 4.44 | 67.42 | 19.40 | 0.59 | 0.14 |
| **TOT-SBF-64** | $P_x$ [Barrer] | 717 | 1964 | 11401 | 1429 | 4162 | 1517 |
| | $D_x$ [$10^{-12}$ $m^2s^{-1}$] | 165 | 443 | 183 | 74.2 | 6279 | 7924 |
| | $S_x$ [$cm^3$ (STP) $cm^{-3}$ $bar^{-1}$] | 3.24 | 3.32 | 46.52 | 14.45 | 0.50 | 0.14 |
| **PIM-1** | $P_x$ [Barrer] | 823 | 2270 | 13600 | 1360 | 5010 | 1950 |
| **PIM-SBF** | $P_x$ [Barrer] | 786 | 2640 | 13900 | 1100 | 6320 | 2200 |

**Table 13** Ideal selectivities α (Px/Py) for methanol treate d films of PIMTOTs

| Sample | Selectivity α(x/y) | | | | |
|---|---|---|---|---|---|
| | $CO_2/CH_4$ | $CO_2/N_2$ | $O_2/N_2$ | $H_2/CH_4$ | $H_2/N_2$ |
| **TOT-TTSBI-58c** | 12.2 | 20.2 | 3.3 | 5.12 | 8.4 |
| **TOT-SBC-59c** | 19 | 24.5 | 4 | 12.6 | 16.3 |
| **TOT-Cardo-61a** | 19.6 | 33 | 5.9 | 13.9 | 23.4 |
| **TOT-SBF-62** | 13.8 | 21.1 | 3.6 | 6.0 | 9.2 |
| **TOT-SBF-63** | 13.4 | 20.6 | 3.6 | 6.2 | 9.5 |
| **TOT-SBF-64** | 7.9 | 15.9 | 2.74 | 2.9 | 5.8 |
| **PIM-1** | - | 16.6 | 2.8 | - | 6.1 |
| **PIM-SBF** | - | 17.7 | 3.35 | - | 8.1 |

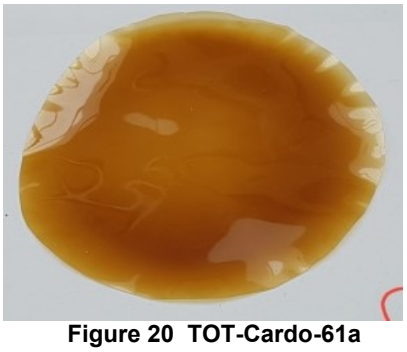

**Figure 20 TOT-Cardo-61a**

**Figure 18 TOT-SBC-59c**

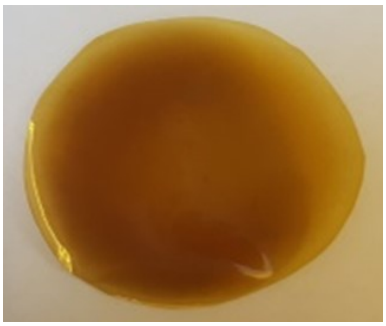

**Figure 19 TOT-SBF-62**

**TOT-TTSBI-58c, TOT-SBC-59c, TOT-Cardo-61a, TOT-SBF-62, TOT-SBF-63** and **TOT-SBF-64** films showed good separation performance which are close to or even exceed the 2008 Robeson upper bound for some common gas pairs which defines the current optimal trade-off between permeability and selectivity **Figure 21**. In more detail, three polymers of the SBF family based on TOT monomer **TOT-SBF-62, TOT-SBF-63** and **TOT-SBF-64** show the best performance for gas separation for the $CO_2/CH_4$, $CO_2/N_2$, $H_2/N_2$, and $O_2/N_2$ gas pairs. Overall, the highest gas permeability performance is demonstrated by **TOT-SBF-64**, which is close to the performance of PIM-1 with a slight decrease in permeability and the same selectivity. The permeability of the corresponding t-butyl substituted SBF polymer prepared using 2,3,5,6-tetrafluoroterephthalonitrile is also the highest in the series confirming the ability of the t-butyl group to hinder chain packing and enhance microporosity. The other two polymers in the SBF series, **TOT-SBF-63** and **TOT-SBF-62**, exhibit almost the same selectivity coupled with a slightly greater permeability for **TOT-SBF-63** over **TOT-SBF-62**. This may be attributed to the methyl group decreasing the packing efficiency of the polymer chains. The order of gas selectivities of the SBF family for the $CO_2/CH_4$, $CO_2/N_2$ and $O_2/N_2$ gas pairs is **TOT-SBF-62** >**TOT-SBF-63** >**TOT-SBF-64**. This trend of performance is attributed to the trade-off between permeability and selectivity. **TOT-Cardo-61a** exhibits surprising impressive performance which is very close to the 2008 Robeson upper bounds for $CO_2/N_2$ and $H_2/N_2$ and exceeds the upper bound for $O_2/N_2$. In comparison with PIM-1 performance, **TOT-Cardo-61a** shows the expected lower permeability consistent with its less microporous structure apparent from gas adsorption. However, it demonstrates very encouraging selectivity of up to 6 for $O_2/N_2$. It should be noted that the equivalent polymer derived from 2,3,5,6-tetrafluoroterephthalonitrile and 9,9-bis(3,4-dimethoxyphenyl)fluorene was found previously by the McKeown group to be insoluble in common organic solvents, however, quinoline was not investigated as a potential solvent.

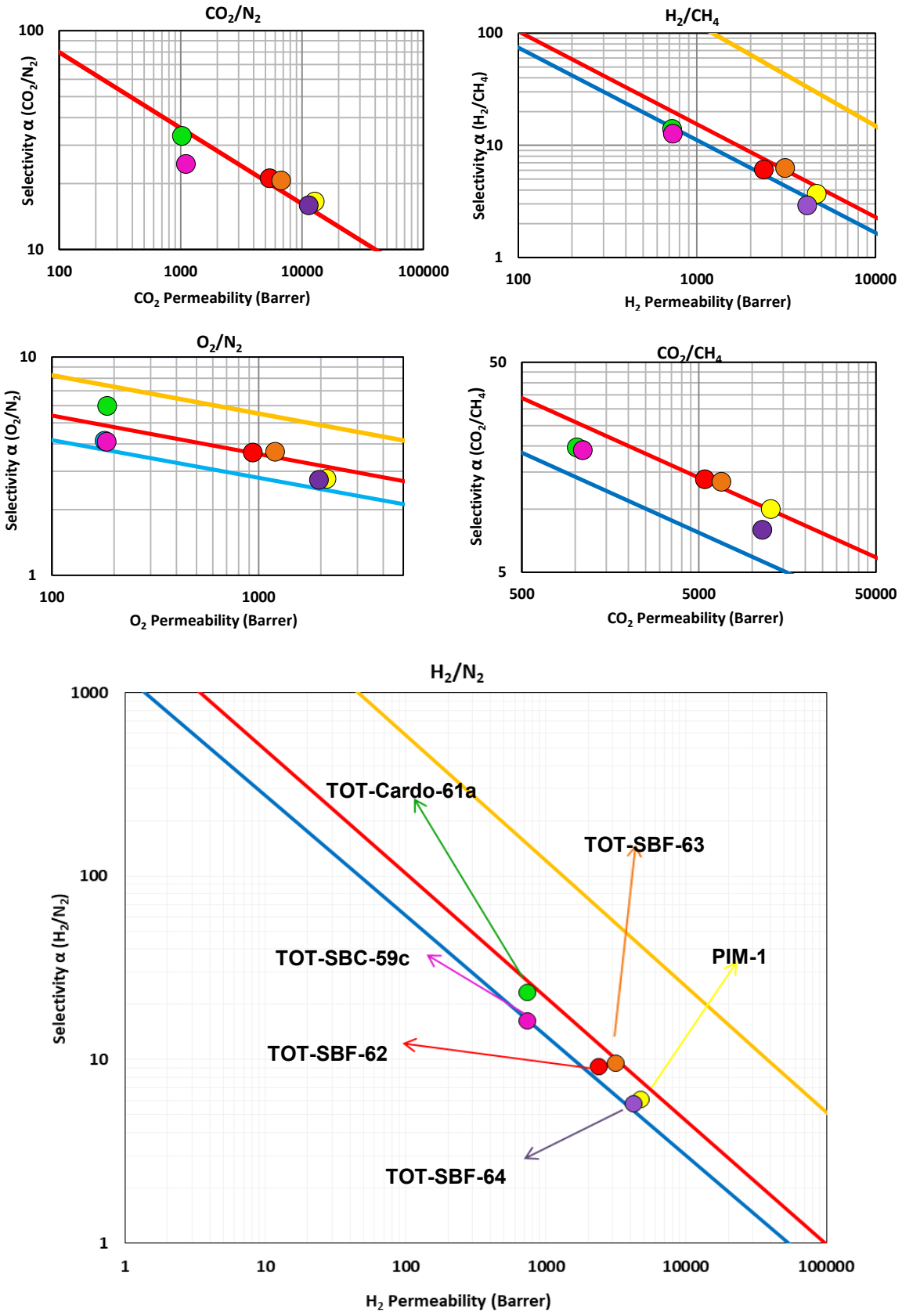


**Figure 21** Robeson plots for some gas pair with 1991 (—), 2008 (—) and 2015 (—) upper bounds; **TOT-SBF-64** (●),**TOT-SBF-62** (●),**TOT-SBC-59c** (●), **TOT-Cardo-61a** (●),**TOT-SBF-63** (●) and **PIM-1**(●)

In general, all five PIMTOT films showed encouraging performance for gas separation with higher selectivity but lower permeability as compared with PIM-1 and the equivalent polymers derived from same biscatechol monomer but combined with 2,3,5,6-tetrafluorotetraphthalonitrile. The reason of this reduction in permeability can be attributed to the longer distance between the sites of contortion due to the larger thianthrene unit resulting in more efficient packing of the polymer chains as discussed previously, **Figure 22**. Due to the associated increase in selectivity, the tetraoxidethianthrene unit can have a significant impact on the gas separation properties of PIMs.

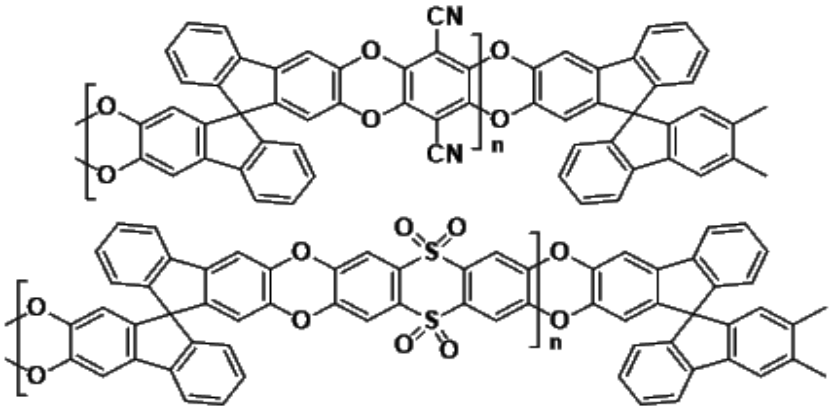


**Figure 22** The molecular structures of **TOT-SBF-62** and PIM-SBF

## 3.5.6 Synthesis of TOT-Trip-based PIMs

An insoluble network polymer of intrinsic microporosity was synthesised by the reaction between 2,3,6,7,12,13-hexahydroxytriptycene **(51)** with 2,3,7,8-tetrafluoro-5,5',10,10'-tetraoxidethianthrene **(4)** monomer using different reaction conditions **Table 14**.

**Table 14** Physical characterization of **TOT-Trip-67a** and **-67b**

| | **TOT-Trip-67a at 70 °C for 72 h** | **TOT-Trip-67b at 160 °C for 45 min** |
|---|---|---|
| BET surface area ($m^2/g$) | 699 | 629 |
| $CO_2$ uptake (mg/g) | 70 | 59 |
| Decomposition temperature | 405 | 372 |

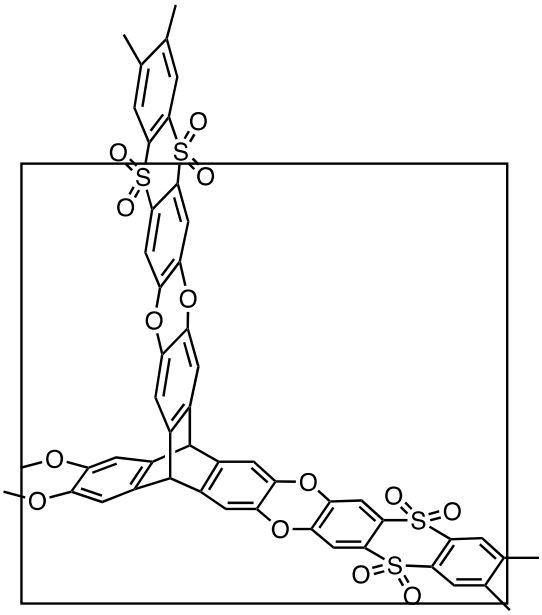

**Scheme 60** Chemical structures of **TOT-Trip-67a and -67b**

The resulting polymers **TOT-Trip-67a** and **-67b** both demonstrated lower BET surface area in comparison with (Trip-PIM-1) derived from the polycondensation between the same triptycene monomer and 2,3,5,6-tetrafluorotetraphthalonitrile (~1300 $m^2/g$). This result was consistent with those of the soluble non-network PIMs derived from TOT and biscatechol monomers, described above and follows the same trend of having lower intrinsic microporosity. Once again, the greater linear component of the polymer appears to result in enhanced chain packing. Thermal analysis of **TOT-Trip-67a** and **-67b** showed that the polymers have good thermal stability.

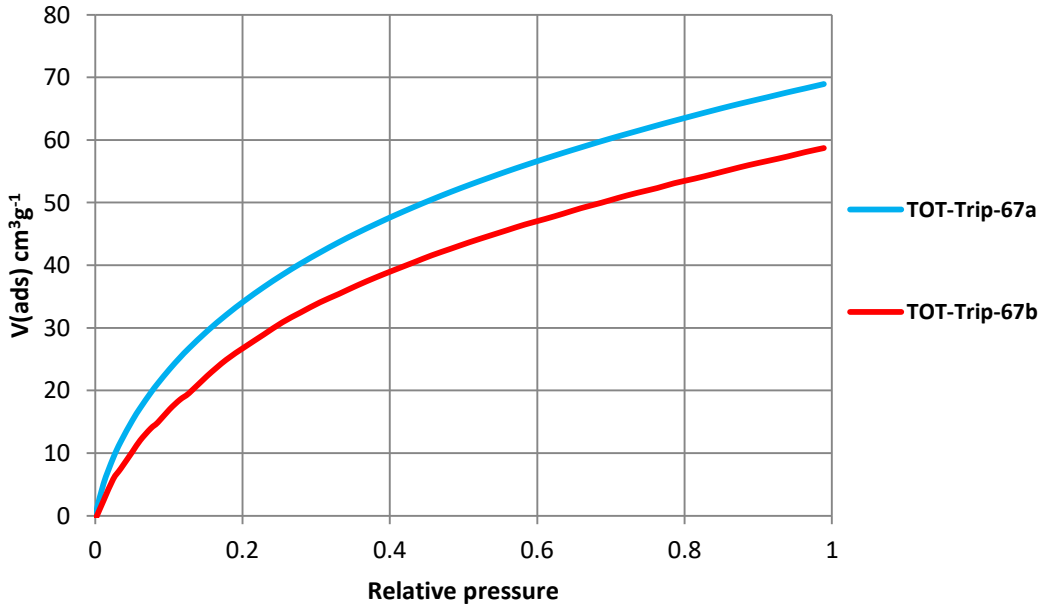


**Figure 23** $CO_2$ adsorption isotherms

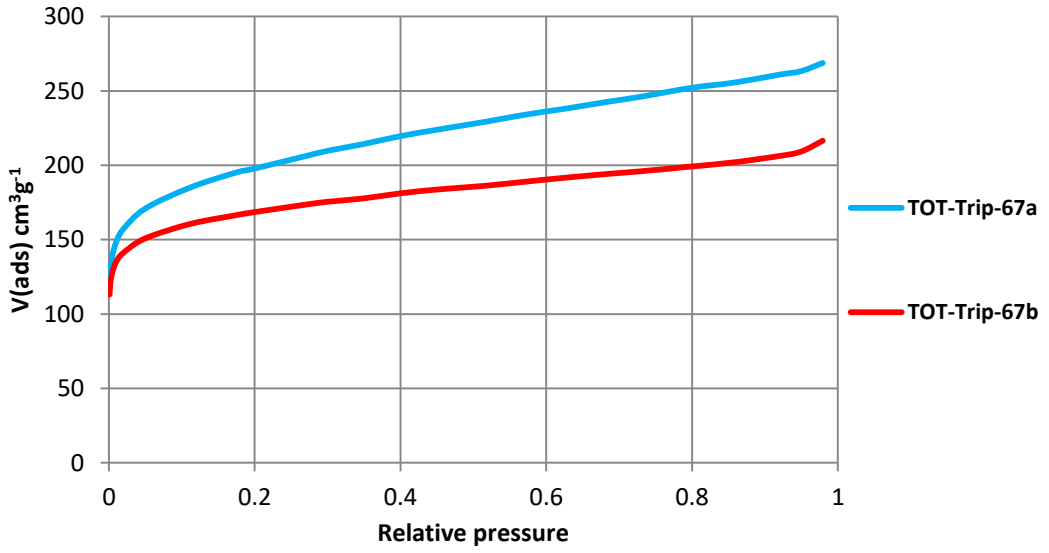


**Figure 24** $N_2$ adsorption isotherms

# Chapter 4 Poiyimides polymers based on tetraoxidethianthrene

## 4.1 Introduction

As a result of good gas separation properties for resulting **TOT-TTSBI-58c, TOT-SBC-59c, TOT-Cardo-61a, TOT-SBF-62, TOT-SBF-63 and TOT-SBF-64** polymers as described in the previous chapter of this thesis, it was desirable to prepare some polyimides based on the TOT structural unit. TADATO-ODA is a polyimide prepared by Jianqiang and co-workers[134], This polyimide was derived from 4,4'-oxydianiline and thianthrene-2,3,7,8-tetracarboxylicdianhydride-5,5,10,10-tetraoxide (TADATO). It demonstrated relatively high gas permeability for $CO_2$ and high selectivity for $CO_2/N_2$ and $CO_2/CH_4$ gas pairs relative to other non-microporous polyimides **Scheme 61**.

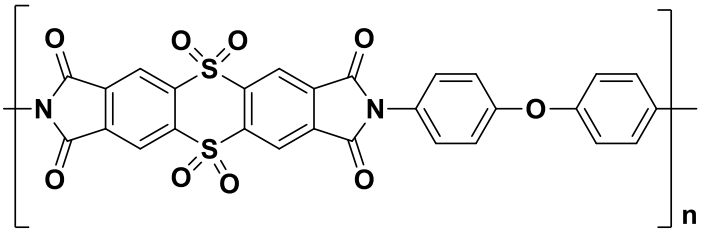


**Scheme 61** The molecular structure of TADATO-ODA

Due to the attractive properties of the TOT unit, other examples of polyimide, derived from the thianthrene-2,3,7,8-tetracarboxylicdianhydride-5,5,10,10-tetraoxide monomer were desirable targets for the current research programme. Hence, the objective was to synthesise successfully the tetraoxidethianthrene bisanhydride monomer (TADATO), then polymerise it with different diamine monomers. Commercial diamines were attractive co-monomers for two reasons. Firstly, investigation of the optimum reaction conditions for the polymerization of the TADATO monomer would be achieved without the time and effort required in monomer synthesis. Moreover, these commercial diamines had been used previously for polymerisation with different bisanhydrides and proved to be compatible with the synthesis of polyimides with good gas separation performance. Then, it was planned that several different synthetic diamines would be prepared and

then polymerised with the TADATO monomer. These synthetic diamines were being chosen due to their unique structures which provide more rigidity to the resulting polymer chain.

## 4.2 Synthesis of teraoxidethianthrene bisanhydride monomer (TADATO) (48)

A chemical procedure from literature[135] was used to prepare TADATO. The synthetic route consists of six steps. However, not all steps were performed as reported. Many modifications were required before the synthesis of TADATO was successfully achieved. The modified route also involved six steps, starting by dehydration of dichlorophthalic acid to give analogous anhydride **(43)** which was reacted with aniline to give *N*-phenyl-4,5-dichlorophthalimide **(44)**. The reaction of the latter with thiobenzamide gave *N*,*N'*-diphenyl thianthrene-2,3,7,8-tetracarboxyl bisimide **(45)**. This bisimide was refluxed with NaOH before acidification to give thianthrene-2,3,7,8-tetracarboxylic acid (TADA-4A) **(46)**. This tetra-acid was dehydrated using acetic anhydride to give thianthrene-2,3,7,8-tetracarboxylic dianhydride (TADA) **(47)**. Finally, TADATO **(48)** was produced by the oxidation of TADA with $H_2O_2$. Considerable optimisation of this synthetic route was required in order to produce sufficient quantities of TADATO for polyimide synthesis **Scheme 62**.

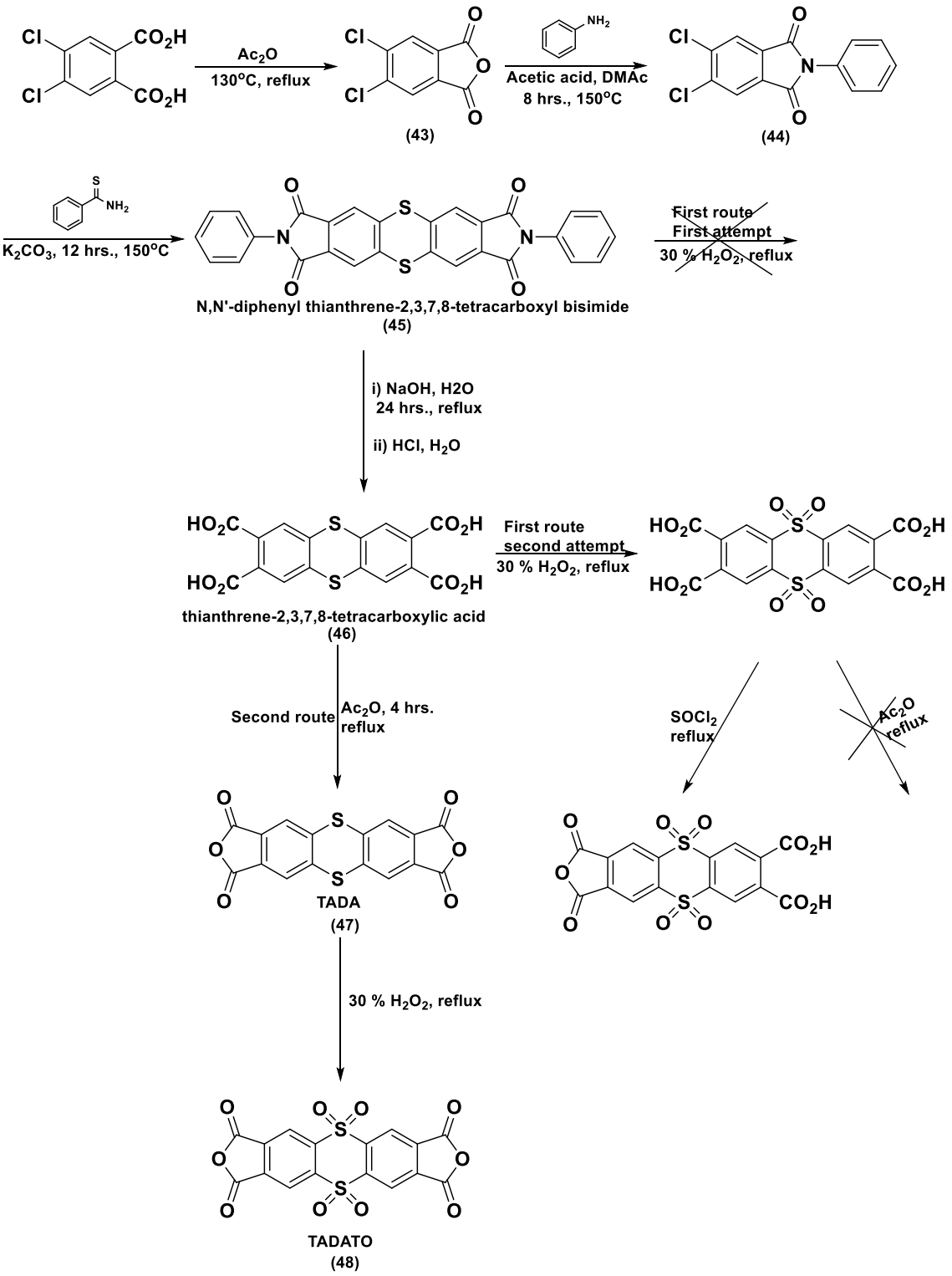


**Scheme 62** Modified synthesis of (TADATO)

Firstly, the first and second steps were done as reported and give a good yield of **(43)** and **(44)**, 92% and 83%, respectively. In the third step, the same reported procedure was followed to give a complex mixture of many products

according to $^{1}$H-NMR and $^{13}$C-NMR. Many attempted reaction were performed until the best conditions were found. The reaction mixture was refluxed for a shorter time instead of the 12 hour reflux as reported. Moreover, to obtain the TADATO monomer, several routes were attempted. The first attempt in this route was done by trying to oxidize the sulphide units within *N,N'*-diphenyl thianthrene-2,3,7,8-tetracarboxyl bisimide **(45)** by hydrogen peroxide. Unfortunately, this attempt failed and gave a complex product mixture. The second attempt involved the oxidation of sulfides within thianthrene-2,3,7,8-tetracarboxylic acid **(46)** by hydrogen peroxide, which proved successful to give the tetraoxide-tetracid. However, subsequent attempts to dehydrate this tetra-acid all failed. The third attempt aimed to dehydrate the tetracid first before oxidation. Hence, TADA-4A **(46)** was dehydrated by $Ac_2O$ to give equivalent bisanhydride which was then oxidized successfully by $H_2O_2$ to give our target. This route provided a good yield of product.

## 4.3 Commercial diamine monomers

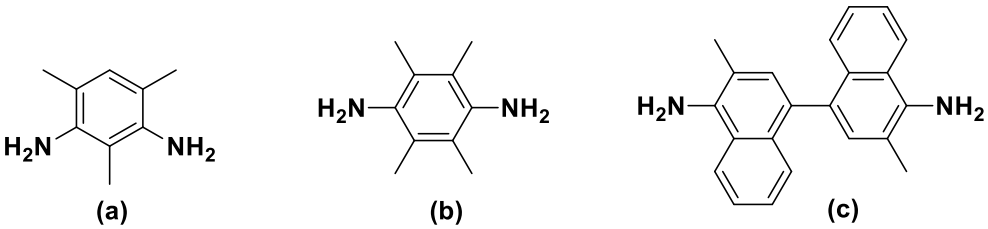


**Scheme 63** Molecular structures of (a) 3MPDA, (b) 4MPDA and (C) DMN

The commercial diamine monomers 2,4,6-trimethyl-1,3-phenylenediamine (3MPDA), 2,3,5,6-tetramethyl-1,4-phenylenediamine (4MPDA) and 3,3'-dimethylnaphthidine (DMN) were selected to be polymerised with TADATO dianhydride due to their availability and structural features **Scheme 63**. They all contain methyl groups adjacent to the amine functional group which helps to restrict the rotation about the imide bond of the resulting polymer. Such restriction of rotational mobility is proven to enhance intrinsic microporosity of polyimides and hence permeability. These monomers have been successfully used to prepare PIM-PIs. Previously PIM-PI-1 and PIM-PI-8,

were prepared by the McKeown group, and reported by Ghanem *et al.* (2009), by the reaction of commercial 2,3,5,6-tetramethyl-1,4-phenylenediamine with a spirocyclic dianhydride monomer[88] (An-1). PIM-PI-8 was also synthesised by the reaction of commercial 3,3'-dimethylnaphthidine with the same dianhydride monomer **Scheme 64**.

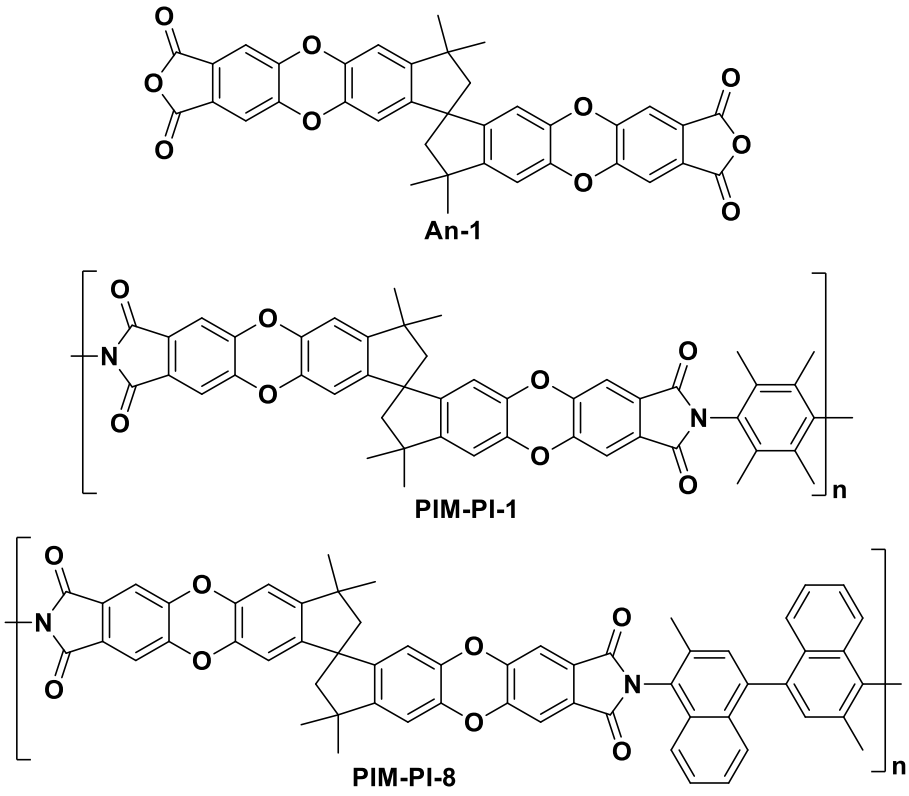


**Scheme 64** The molecular structure of An-1, PIM-PI-1 and PIM-PI-8

Both PIM-PIs were highly porous with apparent BET surface areas of 680 and 683 $m^2/g$, respectively. Moreover, PIM-PI-1 and PIM-PI-8 membranes exhibited good gas permeability with high permeability coefficients and modest selectivities for various gas pairs. For example, data for PIM-PI-1 and PIM-PI-8 are located among that of the most permeable polyimides in the Robeson plot for the $CO_2/CH_4$ pair.

## 4.4 Synthesis of diamine monomers

Three non-commercial diamines were chosen to prepare novel PIs in this work. These were 9,10-dihydro-2,6(7)-diamino-9,10-ethanoanthracene **(52)**, 9,9′-bis(4-aminophenyl) fluorene (BAPF) **(53)** and 1,3,3-trimethyl-1-

phenylindane **(56)**. Each of them has unique structure which contributes to improving gas separation properties of the resulting polymer. Moreover, all of them were used previously to synthesise different PIMs, which would allow for direct comparisons.

### 4.4.1 Synthesis of 9,10-dihydro-2,6(7)-diamino-9,10-ethanoanthracene (52)

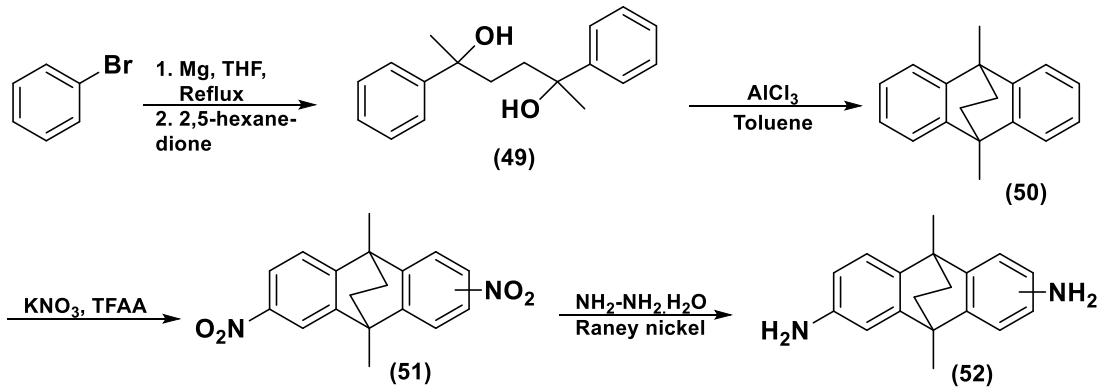


**Scheme 65** Synthesis of 9,10-dihydro-2,6(7)-diamino-9,10-ethanoanthracene

The compound 9,10-dihydro-2,6(7)-diamino-9,10-ethanoanthracene **(52)** was selected due to its rigid structure which was provided by inflexible bicyclic ethanoanthracene (EA) component and due to its utility for preparing polyimides with good gas selectivity. In 2014, The McKeown group demonstrated the incorporation of the ethanoanthracene (EA) unit into PIM-PIs by the construction of an EA bisanhydride monomer. The resulting polyimide PIM-PI-12 showed enhanced selectivity with a good overall gas performance which lies above the 2008 Robeson upper bound for the $O_2/N_2$, $H_2/N_2$, $CO_2/CH_4$ and $CO_2/N_2$ gas pairs.[136] Improved selectivity of this polyimide could be directly attributed to the highly rigid structure of the EA unit **Scheme 66**.[136]

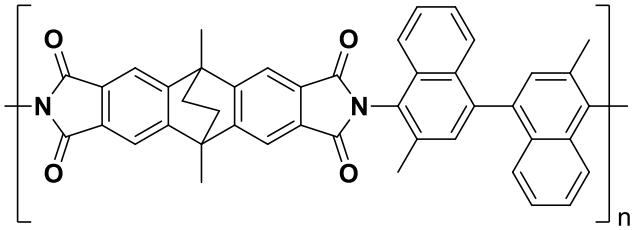

**Scheme 66** The molecular structure of PIM-PI-12

Here, the objective was the incorporation of the EA unit into PIM-PIs as a diamine component. The required EA-based diamine monomer was prepared for reaction with the TADATO dianhydride according to the reported procedure.[137] The synthetic route involves three steps, starting with synthesis of 9,10-dimethyl-9,10-dihydro-9,10-ethanoanthracene **(50)** by the reaction of 2,5-diphenylhexane-2,5-diol **(49)** with aluminium trichloride. The second step is nitration of the ethanoanthracene **(50)** by potassium nitrate, before reducing it to the diamine with Raney nickel and hydrazine monohydrate **Scheme 65**.

## 4.4.2 Synthesis of 9,9′-bis(4-aminophenyl) fluorene (BAPF) (53)

The monomer 9,9′-bis(4-aminophenyl) fluorene (BAPF) **(53)** is another attractive diamine for preparing a novel polyimide with the TADATO dianhydride. The biphenylfluorene unit involves four aryl substituents connected to a single quaternary carbon atom. A biphenylfluorene (BAPF) based polyimide was reported[138] in 2002. This PI showed large gas permeabilities and good selectivity for the important $CO_2/N_2$ gas pair. PI-4 showed a high glass transition temperature (Tg) which was as a result of the rigidity of the BAPF unit within polyimide chain **Scheme 68**. 9,9′-Bis(4-aminophenyl) fluorene **(53)** can be produced in one step by using cheap starting materials. Hence, 9-fluorenone was reacted with aniline in the presence of aniline hydrochloride[139] **Scheme 67**.

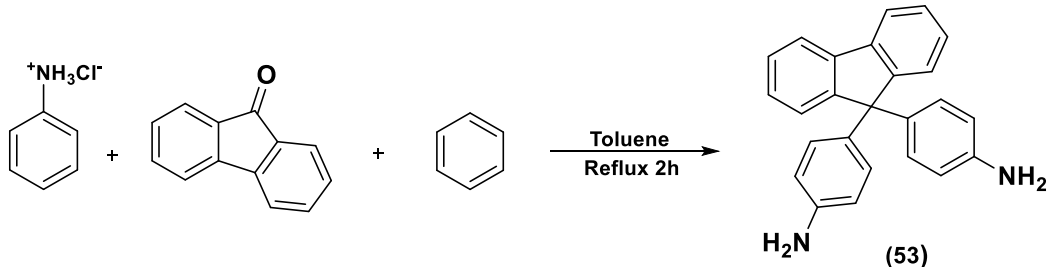


**Scheme 67** Synthesis of BAPF

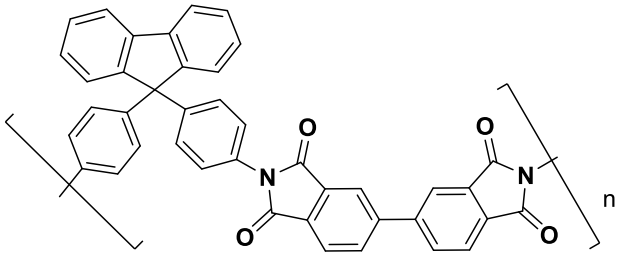


**Scheme 68** The molecular structure of PI-BAFL-BPDA (PI-4)

## 4.4.3 Synthesis of 6,(7)-amino-1,3,3-trimethyl-1-(4-aminophenyl)indane (56)

Another diamine selected for investigation as a co-monomer with the TADATO dianhydride was 6,(7)-amino-1,3,3-trimethyl-1-(4-aminophenyl)indane **(56)** which is the diamine used in the commercial available PI Matrimid that forms the basis for industrial gas separation membranes. The phenylindane skeleton contains a single carbon-carbon bond between the phenyl and indane unit allowing free rotation, which helps efficient chain packing. Such single carbon-carbons are not desirable feature for PIMs, however, the reaction of this diamine with the TADATO dianhydride will allow for a direct comparison with Matrimid®, which is prepared by the reaction of diaminophenylindane (DAPI) diamine with 3,3',4,4'-benzophenone tetracarboxylic dianhdride.[140] Matrimid has been scaled-up into a hollow fibre membrane exhibited a $CO_2$ permeability of 12.7 Barrers with a $CO_2/CH_4$ selectivity of 40 at the feed pressure of 20 bars. **Scheme 69**.

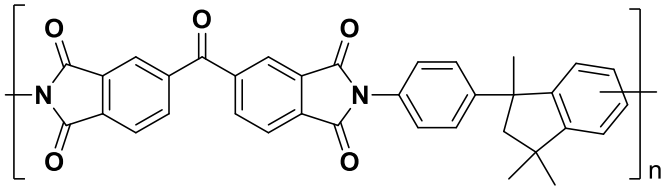

**Scheme 69** The molecular structure of Matrimid

The desired diamine was obtained by dimerisation of α-methylstyrene in the presence of trifluoroacetic acid (TFA) followed by nitration with trifluoroacetyl nitrate ($CF_3CO_2NO_2$). The last step is the reduction by hydrazine monohydrate in the presence of Raney nickel **Scheme 70**.

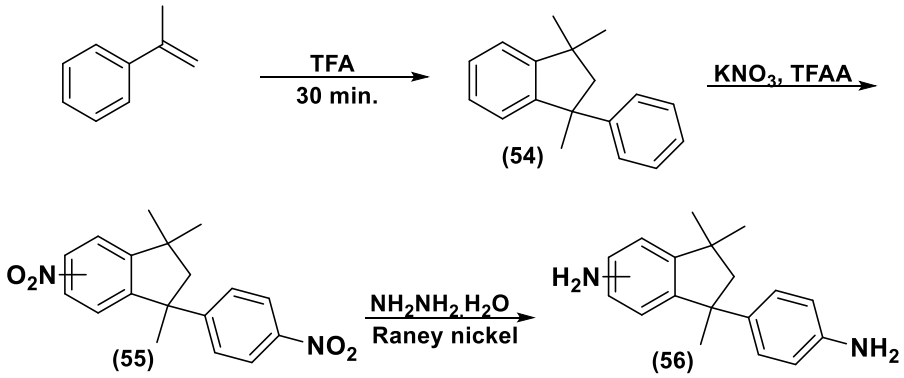


**Scheme 70** Synthesis of 6,(7)-amino-1,3,3-trimethyl-1-(4-aminophenyl)indane

## 4.5 Synthesis of polyimide polymers based on tetraoxidethianthrene

There are a number of different synthetic methods used in the formation of polyimides.[141] The classic two-step method of polyimide synthesis was used in this work. This consists of first forming the polyamic acid (PAA) precursor and then subsequently forming the imide linkage. The polyamic acid is generally formed via the reaction of a particular dianhydride with an appropriate diamine monomer in the presence of a polar aprotic solvent. This reaction is a reversible nucleophilic substitution in which the amine attacks one of the carbonyl carbons in the anhydride moiety to form an amide linkage **Scheme 71**.

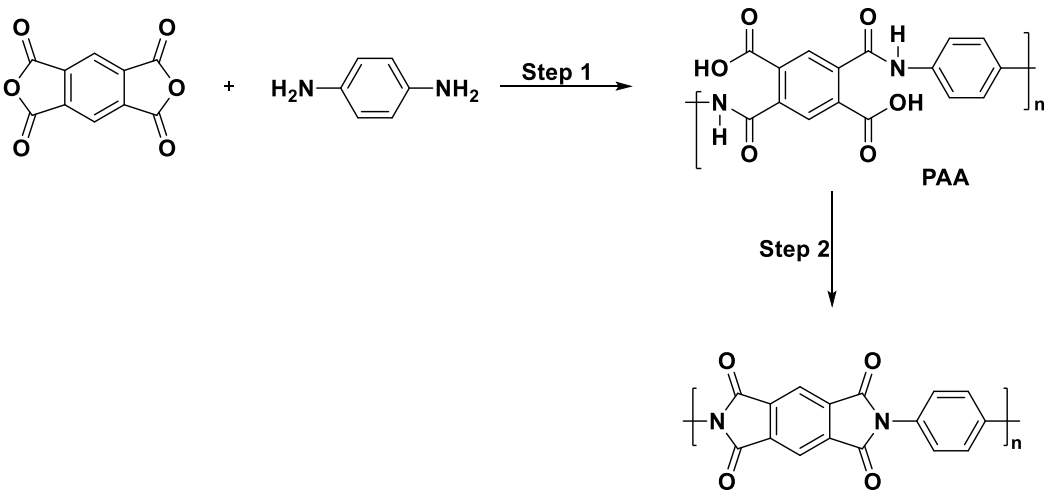


**Scheme 71** The classic two-step method of polyimide formation

Cyclisation of the PAA is then achieved through thermal imidization in solution at elevated temperatures. A reaction mechanism for the imidization of homogeneous systems in solution was proposed by Kim *et al*. (1993)[142] **Scheme 72**. A series of polyimide polymers were synthesised according to reported procedures.[83] All polymerisations were carried out under a nitrogen atmosphere in a two-necked flask equipped with Dean-Stark apparatus and reflux condenser **Figure 25**.

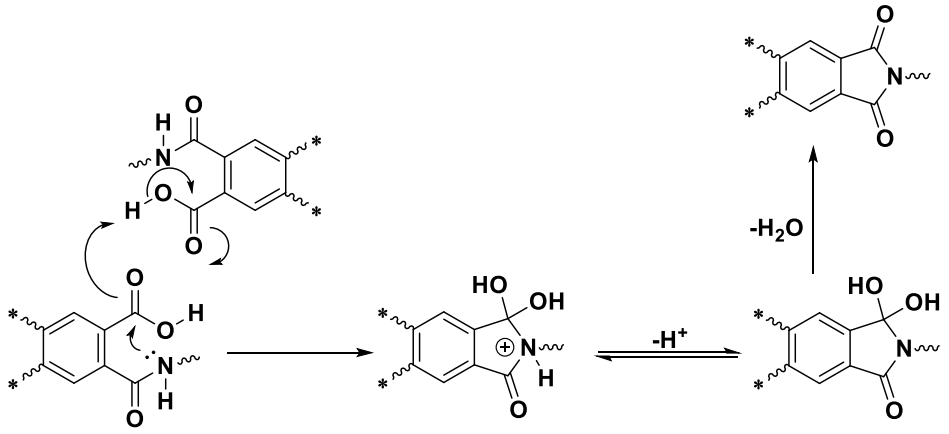


**Scheme 72** Proposed reaction mechanism for the solution imidization process

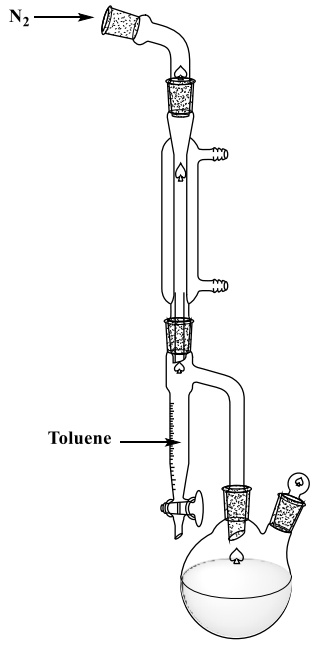


**Figure 25** Typical polyimide apparatus set-up

A mixture of TADATO dianhydride, selected diamine, m-cresol, isoquinoline and anhydrous toluene was added and heated at 80 °C for 1 h before gradually heating to 200 °C in 20 °C increments. This temperature was then maintained until a viscous solution was obtained. During this time water was removed via azeotropic distillation of the toluene. On cooling at room temperature, the mixture was poured dropwise into vigorously stirred methanol (MeOH) to produce a precipitate, which was collected by vacuum filtration. The polymer was purified by refluxing in MeOH. The off-white polymer powder was finally collected by filtration, and dried in vacuum oven at 100 °C for 17 h to give the required polyimide. **TOT-PDA-68**, **TOT-PDA-69**, **TOT-DMN-70**, **TOT-EA-71**, **TOT-BAPF-72** and **TOT-TMPI-73** were synthesised using the TADATO **(48)** dianhydride monomer with different diamines, namely, 2,4,6-trimethyl-1,3-phenylenediamine (3MPDA) and 2,3,5,6-tetramethyl1,4-phenylenediamine (4MPDA), 3,3'-dimethylnaphthidine (DMN), 9,10-dihydro-2,6(7)-diamino-9,10-ethanoanthracene **(52)**, 9,9′-bis(4-aminophenyl) fluorene (BAPF) **(53)** and 6,(7)-amino-1,3,3-trimethyl-1-(4-aminophenyl)indane **(56)**, respectively. In addition, **TOT-PDA-74** and **-75** were synthesised from the thianthrene-2,3,7,8-tetracarboxylic dianhydride

**(TADA) (47)** with 2,4,6-trimethyl-1,3-phenylenediamine (3MPDA) and 2,3,4,5-tetramethyl1,4-phenylenediamine (4MPDA). Properties of resulting polymers **TOT-PDA-74** and **TOT-PDA-75** were compared with those of the equivalent polyimides which were prepared from the equivalent diamines with **TADATO (48)**. This comparison was done in order to have an idea of the influence of sulfonyl groups (-$SO_2$) on the properties of the polyimide. Details of the physical properties of each polymer are provided in **Table 15**.

**Table 15** Physical characterization of **TADATO–** and **TADA-** derived polymers

| Polymer | % Yield | $M_w$ g $mol^{-1}$ | $S_{BET}$ ($m^2$/g) | $T_d$ (°C) | $CO_2$ uptake mg/g | Film form-ation |
|---|---|---|---|---|---|---|
| 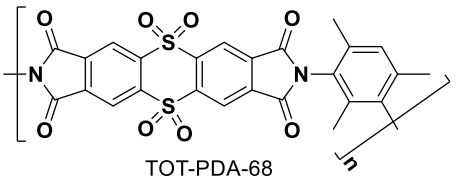 TOT-PDA-68 | 53% | - | 103 | 420 °C | 26 | X |
| 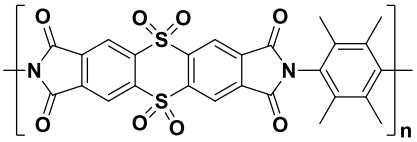 TOT-PDA-69 | 63% | 10700 | 42 | 375 °C | 24 | X |
| 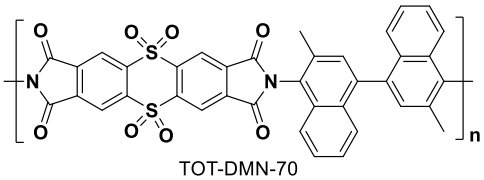 TOT-DMN-70 | 79% | 10600 | 39 | 439 °C | 19 | X |
| 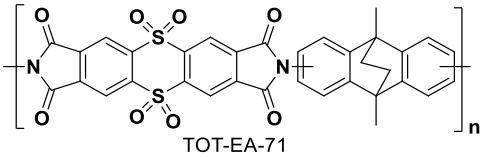 TOT-EA-71 | 93% | - | 60 | 401 °C | 25 | X |

| | | | | | | |
|---|---|---|---|---|---|---|
| 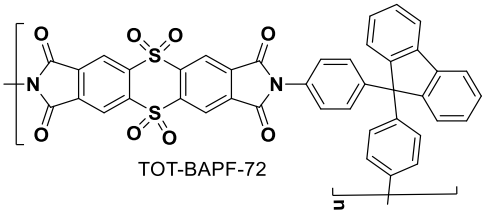 TOT-BAPF-72 | 64% | 6100 | 32 | 402 °C | 15 | X |
| 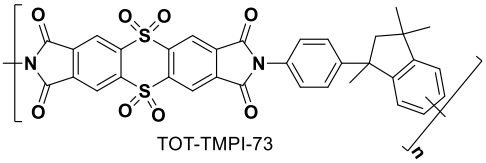 TOT-TMPI-73 | 24% | - | 1 | 362 °C | 9.50 | X |
| 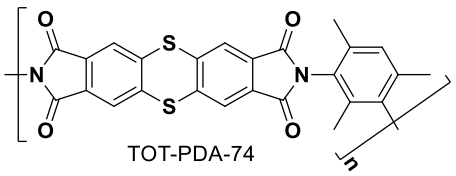 TOT-PDA-74 | 83% | - | 329 | 379 °C | 28 | X |
| 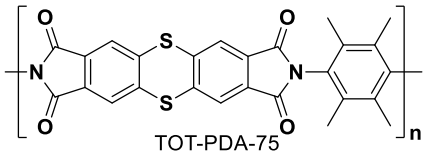 TOT-PDA-75 | 74% | - | 334 | 532 °C | 22 | X |

(-)The molecular weight of polyimide was not measured by GPC, since the polymer was not soluble in chloroform

It can be seen from the data **Table 15** that all resulting polyimides were isolated in good yield except **TOT-TMPI-73**. The infrared spectra for all polymer powder samples confirmed the presence of a characteristic peaks in the range of 1700-1800 $cm^{-1}$ for the symmetric and asymmetric stretch of the carbonyl group in the five-membered imide ring and another peak in the range of (1377-1400 $cm^{-1}$) (C-N stretch) confirmed the formation of imide linkages. Apparent BET surface areas were calculated from the nitrogen adsorption isotherms at 77 K **Figure 27.** All PI-TADATOs polymers showed poor microporosity with low surface area values. The polymers with a more rigid and contorted structure, such as **TOT-PDA-68**, with the 3MPDA diamine contributing a meta linkage and methyl groups to restrict rotation

about the imide bond demonstrates significant nitrogen uptake at higher pressures and largest uptake of carbon dioxide at 273 K. **TOT-TMPI-73** was found to be non-porous, which was expected considering that it possesses considerable flexibility and rotational freedom since it has a single carbon-carbon bond connecting the phenyl and indane ring in the diamine structure, so the polymer chains can pack space efficiently. Unexpectedly, **TOT-PDA-74** and **-75** showed better microporosity than the equivalent polyimides based on TADATO. It is possible that the dipole moments associated with the sulfone groups enhance cohesion between polymer chains encouraging greater efficiency in chain packing. $CO_2$ adsorption data for all **TADATO–** and **TADA-** derived polymers show low uptake ranging from 10 to 25 $cm^3\ g^{-1}$ at 1 bar and 273 K **Figure 26**.

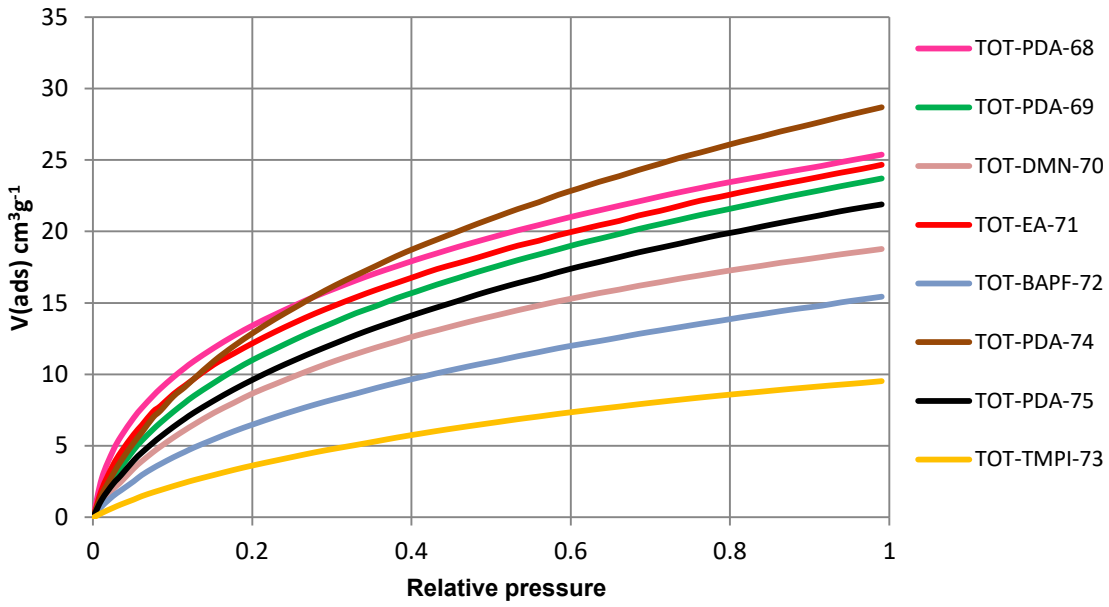


**Figure 26** $CO_2$ adsorption isotherms

**TOT-PDA-69**, **TOT-DMN-70** and **TOT-BAPF-72** were found to be soluble in low boiling point solvents (e.g. $CHCl_3$). **TOT-PDA-68**, **- TOT-EA-71** and **TOT-TMPI-73** were soluble in high boiling point solvent (i.e. quinoline). Unfortunately, all polymers failed to form more than small fragments of polymer membrane on solvent casting, indicating that their molecular weights were insufficient for membrane formation. This is in good agreement with the

low molecular weight of polyimides estimated from GPC measurements for those soluble in $CHCl_3$ **Table 15**. However, **TOT-PDA-74** and **-75** were insoluble in $CHCl_3$, THF and quinoline. For all polyimides, multiple attempts to improving molecular mass were carried out, for example, extending the reaction times but no improvement was achieved. Thermal gravimetric analysis (TGA) revealed very good thermal stabilities, with each polymer is stable up to at least 350 °C before decomposition.

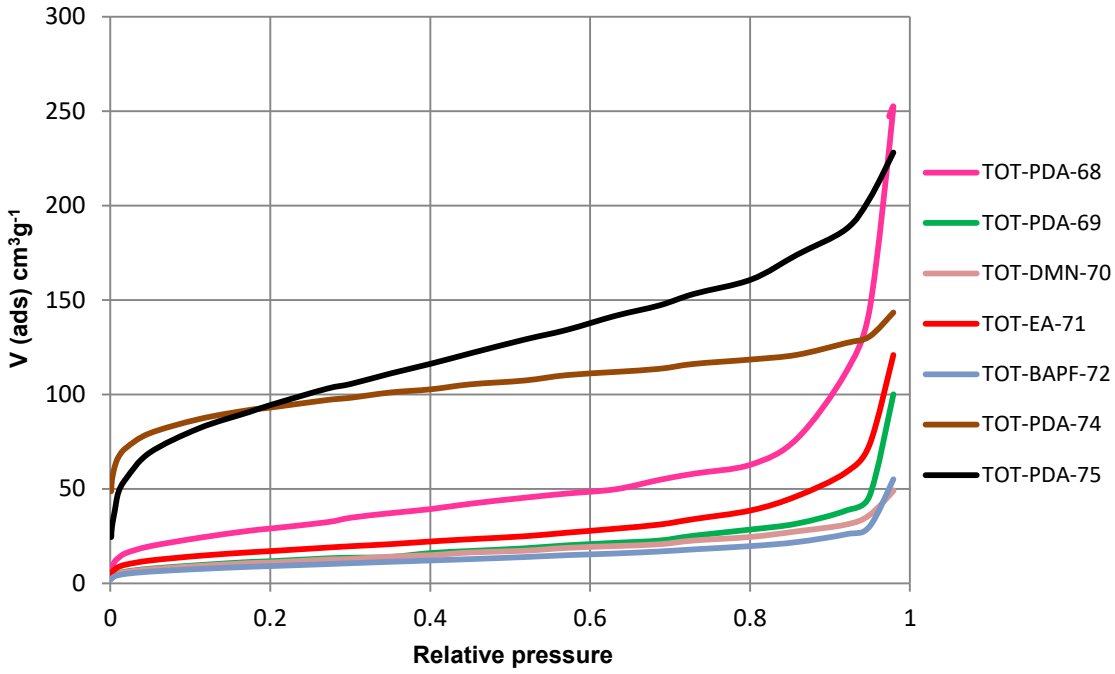


**Figure 27** $N_2$ adsorption isotherms

# Conclusions

The work reported in this thesis involves the successful synthesis of novel polymers of intrinsic microporosity. Two series of PIMs based on the thianthrene unit were prepared. The first, consists of new ladder and network dibenzodioxin-based PIMs derived from different catechol-containing monomers in combination with the 2,3,7,8-tetrafluoro-5,5',10,10'-tetraoxidethianthrene monomer (TOT). The second consists of new polyimides derived from different diamines monomers with thianthrene-2,3,7,8-tetracarboxylic acid anhydride-5,5,10,10-tetraoxide. The first series of dibenzodioxin-based PIMs exhibited high porosity and good thermal stability. Five examples were cast into self-standing films from which gas permeability data could be measured. These polymers showed promising performance for gas separations involving the following gas pairs: $CO_2/CH_4$, $CO_2/N_2$, $H_2/N_2$, $O_2/N_2$ and $H_2/CH_4$. All of these polymers showed improved selectivities for some gas pairs as compared with the equivalent polymers derived from the same biscatechol monomers and 2,3,5,6-tetrafluorophthalonitrile. Although these properties are promising for gas separation applications, the required use of quinoline as casting solvent will likely preclude the use of these polymers for use in commercial membranes.

The second series of polymers derived from thianthrene-2,3,7,8-tetracarboxylic acid anhydride-5,5,10,10-tetraoxide, **TOT-PDA-68, TOT-PDA-69, TOT-DMN-70, TOT-EA-71, TOT-BAPF-72** and **TOT-TMPI-73**, showed poor microporosity, whereas PIMs in the same series derived from thianthrene-2,3,7,8-tetracarboxylic dianhydride, **TOT-PDA-74 and -75**, exhibited modest microporosity. Unfortunately, only low molecular mass polymers were obtained, and therefore did not form films, which prevented the determination of their potential as gas separation membranes.

# Future Work

1- Due to the poor microporosity of polyimides derived from thianthrene-2,3,7,8-tetracarboxylic acid anhydride-5.5.10.10-tetraoxide as reported in this thesis, greater rigidity of polymer chains are suggested to improve the microporosity and prevent the efficient packing of the polymer chain. One possible idea to achieve this goal is to combine Tröger's base unit with thianthrene unit by introducing Tröger's base unit into diamine monomers or by using Tröger's base reaction **Scheme 73**. Similarly bisamines derived from triptycene or benzotriptycenes might be used to introduce greater intrinsic microporosity.

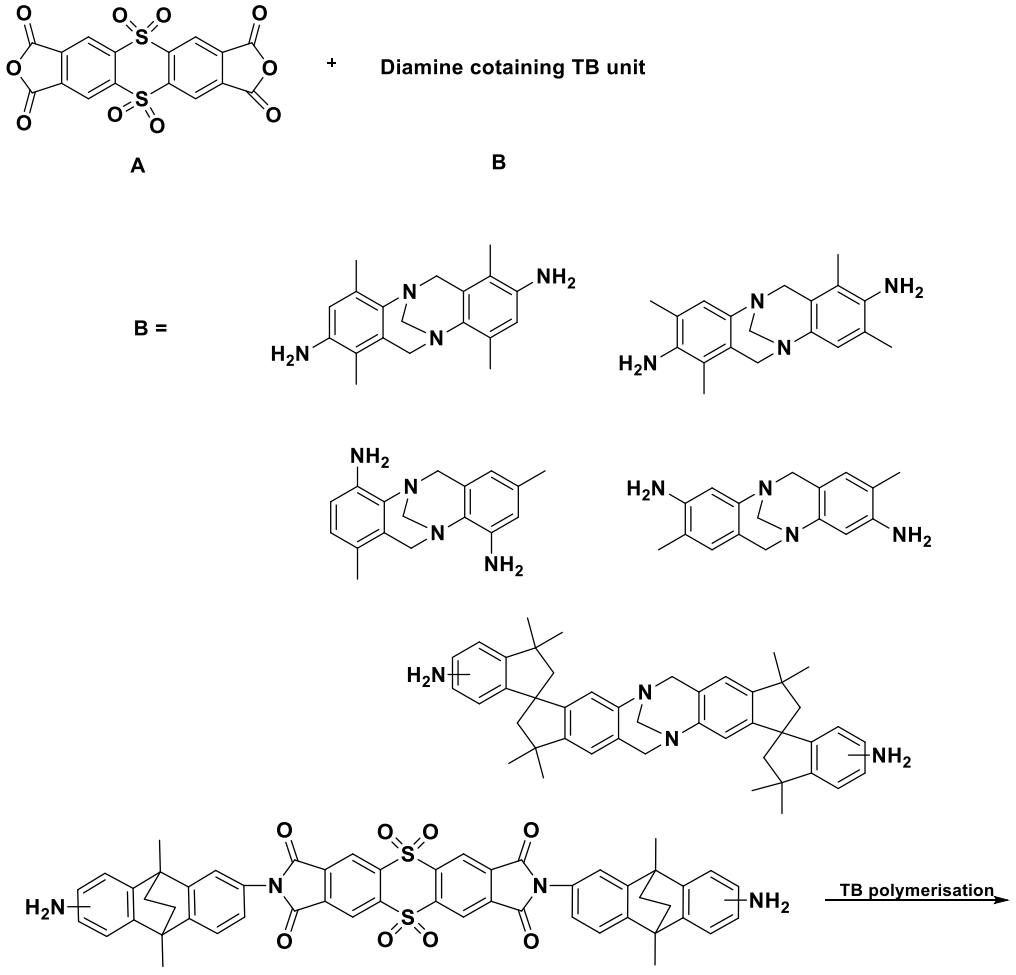


**Scheme 73** Chemical structures of proposed monomers

2- Due to the disappointing porosity obtained for the TB-polystyrene polymers reported in this thesis, more investigation is required. In particular, the influence of the molecular weight of the polystryrene could be studied using a range of commercially available polystyrenes with different molecular weights as precursors. In addition, TB can be prepared using a range of different acid conditions and, therefore, a systematic investigation to optimise porosity by reaction conditions should be performed.

3- One potential advantage of the tetraoxide-based PIMs reported in the thesis is their likely stability towards hydrolysis as compared to nitrile-containing PIMs derived from 2,3,5,6-tetrafluoroterephthalonitrile. This may be advantageous for application where the membrane is used in highly acidic or highly basic conditions such as for redox-flow batteries or fuel cells. Therefore the relative hydrolytic stability of the polymers described in Chapter 3 should be investigated.

# Chapter 5 Experimental

## 5.1 Techniques

Chemical reagents were purchased from commercial sources and used without further purification unless stated otherwise. Air/moisture sensitive reactions were carried out under a nitrogen atmosphere using glassware dried in an oven prior to use. Anhydrous solvents were obtained following passage through a column of activated molecular sieves (hexane) or through activated alumina (diethyl ether, THF, toluene). TLC analysis refers to analytical thin layer chromatography, using aluminium-backed plates coated with Merck TLC silica gel 60 $F_{254}$. Column chromatography was performed over a silica gel (pore size 60 Å, particle size 40 – 63 μm) stationary phase.

**Melting points (mp)**

Melting points were recorded using a Stuart SMP10 melting point apparatus and are uncorrected; (dec.) refers to a decomposition temperature.

**Infrared spectra (IR)**

Infrared spectra were recorded in the 400-4000 $cm^{-1}$ range by using PerkinElmer FTIR spectrometer, as KBr disk or as film on NaCl plate or using a Shimadzu IR Affinity-1S FTIR spectrophotometer, as powder.

**Nuclear Magnetic Resonance (NMR)**

$^{1}H$ NMR, $^{13}C$ NMR and $^{19}F$ NMR were recorded in an Avance Bruker AVA 400, AVA 500, PRO 500 or AVA 600 instrument. Chemical shifts δ were recorded in parts per million (ppm) and corrected according to solvent peaks listed in **Table 16**. Solid state $^{13}C$ NMR spectra were recorded by the solid-state NMR service at St. Andrews University.

**Table 16** Corrected $^{1}H$ and $^{13}C$ chemical shifts for deuterated solvents

| Solvent | Formula | $^{1}H$ corrected δ | $^{13}C$ corrected δ |
|---|---|---|---|
| Chloroform-d | $CDCl_3$ | 7.26 | 77.23 |
| Acetone-$d_6$ | $(CD_3)_2CO$ | 2.05 | 29.90, 206.68 |
| DMSO-$d_6$ | $(CD_3)_2SO$ | 2.50 | 39.51 |
| Methanol-$d_4$ | $CD_3OD$ | 3.31 | 49.15 |

### Mass spectrometry

Small molecule (MW<1000 g $mol^{-1}$) low-resolution mass spectrometric (LRMS) and high-resolution mass spectrometric (HRMS) data were obtained using a Fisons VG Platform II quadrupole instrument plus Thermo finnigan MAT 900 XP, Electron Ionisation Sector MS.

### BET surface areas

Low-temperature (77 K) nitrogen and $CO_2$ (273 K) adsorption/desorption isotherms were obtained using either a Coulter SA3100 surface area analyser or a Quantachrome Quadrasorbevo automated surface area analyser. Accurately weighed powdered samples of roughly 100 mg were degassed for 16 h at 100 °C under high vacuum prior to analysis.

### Thermo-Gravimetric Analysis (TGA)

Thermo-gravimetric analysis was performed on a Thermal Analysis SDT Q600 system, heating samples at a rate of 10 °C/min up to 1000 °C.

### Film Fabrication for Membrane Gas Permeation Studies

Film formation was achieved by preparing a solution of polymer (e.g. 0.60 g in quinoline, 20 ml). Quinoline was added to polymer and left stirring at room temperature until polymer was dissolved followed by full dissolution of any remaining solid using sonication. Then, the solution was filtered through cotton and poured into 8 cm circular glass dish. The film was allowed to form by slow solvent evaporation at 50 °C for at least two weeks. The resulting film was treated by soaking in methanol for 17 hours to remove residual casting solvent.

## 5.2 Experimental procedures

### Poly(4-nitrostyrene) (1a-1e)

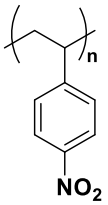


**Ammonium nitrate method**

**General procedure (1) Nitration of polystyrene with ammonium nitrate**

According to a literature procedure[109], polystyrene, ammonium nitrate, chloroform and trifluoroacetic anhydride were stirred under nitrogen atmosphere at the required temperature for an appropriate time. The solution was precipitated into methanol, the resulting solid was washed several times with water and dried in vacuum oven.

General procedure **(1)** was followed to synthesise poly(4-nitrostyrene) **(1a)** by using polystyrene (5.17 g, 49.64 mmol, per repeating unit), ammonium nitrate (3.97 g, 49.64 mmol), chloroform (70 ml) and trifluoroacetic anhydride (10 ml). The reaction mixture was stirred at room temperature for 18 hours to give the product as a yellow powder (6.00 g, 40.23 mmol, 81% based on the molecular weight of the repeating unit, considering 100% nitration; percentage of nitration calculated to be 51%); $^{1}$H NMR (601 MHz, $CDCl_3$) δ 8.05 (br. m, 0.79H), 6.93 (br. m, 1.86H), 1.86 (br. m, 3H); $^{13}$CNMR (500 MHz, $CDCl_3$) δ 128.9, 128.0, 127.4, 123.6, 41.0, 29.5.

General procedure **(1)** was followed to synthesise poly(4-nitrostyrene) **(1b)** by using polystyrene (5.03 g, 48.29 mmol per repeating unit), ammonium nitrate (15.45 g, 193.2 mmol), chloroform (70 ml) and trifluoroacetic anhydride (10 ml). The reaction mixture was stirred at room temperature for 120 hours to give the product as a yellow powder (5.08 g, 38.88 mmol, 71% based on the molecular weight of the repeating unit, considering 100% nitration; percentage of nitration calculated to be 56%); $^{1}$H NMR (500 MHz,

$CDCl_3$) $\delta$ 7.94 (br. m, 1.17H), 6.91 (br. m, 3.01H), 1.67 (br. m, 3H); $^{13}C$ NMR (126 MHz, DMSO) $\delta$ 128.63, 127.28, 125.81, 123.03, 40.11, 39.61.

General procedure **(1)** was followed to synthesise poly(4-nitrostyrene) **(1c)** by using polystyrene (5g, 48 mmol per repeating unit), ammonium nitrate (38.40 g, 480 mmol), chloroform (70ml) and trifluoroacetic anhydride (12.50 ml). The reaction mixture was stirred at 70 °C for 120 hours to give the product as a yellow powder (5.99 g, 40.16 mmol, 84% based on the molecular weight of the repeating unit, considering 100% nitration; percentage of nitration calculated to be 66%); $\nu_{max}$ ($cm^{-1}$) 3583, 3077, 2920, 1596, 1518, 1493, 1452, 1346, 910, 855, 732, 701; $^1H$ NMR (500 MHz, $CDCl_3$) $\delta$ 8.01(br. m, 1.24H), 7.11 (br. m, 2.68), 1.76 (br. m, 3H); $^{13}C$ NMR (500 MHz, $CDCl_3$) $\delta$128.2, 127.1, 124.5, 123.8, 41.9, 41.0.

General procedure **(1)** was followed to synthesise 4-poly(nitrostyrene) **(1d)** by using polystyrene (8 g, 76.81mmol per repeating unit), ammonium nitrate (61.44 g, 767 mmol), chloroform (150 ml) and trifluoroacetic anhydride (15 ml). The reaction mixture was stirred at 70 °C for 120 hours to give a yellow powder. The level of nitration of poly(nitrostyrene) is low; about 54% of nitropolystyrene. Due to the low level of nitration of product, further nitration was done on the resulting product with the same pervious procedure. Poly(4-nitrostyrene) (4g, 38.41 mmol per repeating unit), ammonium nitrate (30.73g, 384.1 mmol), chloroform (100 ml) and trifluoroacetic anhydride (12 ml) were stirred at 70 $^oC$ for 120 hours to give the product as a yellow powder. (3 g, 20.11 mmol, 25.36 % based on the molecular weight of the repeating unit, considering 100% nitration; percentage of nitration calculated to be 92%); $^1H$ NMR (500 MHz, Acetone) δ 8.37 (br. s, 1.42), 7.56 (br. m, 1.57), 2.35 (br. s, 3H); $^{13}C$ NMR (500 MHz, $CDCl_3$) δ 146.6, 128.1, 123.7, 40.9, 29.7.

**Nitric acid/sulfuric acid mixture in 3-nitrotoluene method**

A literature procedure[110] was followed to synthesise poly(4-nitrostyrene) **(1e)**. Under a nitrogen atmosphere, nitric acid (80 ml) was added to a solution of polystyrene (5 g, 48 mmol) in 3-nitrotoluene (100 ml). The solution was cooled to 10 °C before slowly adding sulfuric acid (20 ml). The reaction solution was stirred for 17 hours at room temperature then poured into 2-propanol, the resulting solid was washed with water, 2-propanol and dried in a vacuum oven to give a yellow powder (5.50 g, 36.88 mmol, 76.82% based on the molecular weight of the repeating unit, considering 100% nitration; percentage of nitration was calculated to be 98%); $^{1}$H NMR (500 MHz, DMSO) *δ* 7.86 (br. m, 1.32H), 6.83 (br. m, 1.24H), 1.67 (br. m, 3H); $^{13}$C NMR (126 MHz, DMSO) *δ* 129.29, 128.31, 123.47, 120.44, 40.11, 20.45.

**Poly(4-aminostyrene) (2a-2e)**

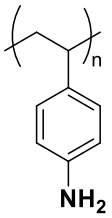


**Reduction with hydrazine monohydrate**

**General procedure (2)**

According to a literature procedure[111], the appropriate nitrated polystyrene (1 equivalent) was dissolved in THF, then hydrazine monohydrate (~ 35 equivalent) and Raney nickel (2 medium spatula) were added. The reaction mixture was refluxed for 18 hours under a nitrogen atmosphere. Then, the reaction mixture was cooled in ice and filtered; the filtrate was extracted with chloroform. Solvent was removed under reduced pressure and the product dried under stream of $N_2$ gas.

General procedure **(2)** was followed to synthesise poly(4-aminostyrene) **(2a)** by using poly(4-nitrostyrene) **(1a)** (2 g, 13.41 mmol per repeating unit) in tetrahydrofuran (40 ml), hydrazine monohydrate (23.47 g, 469.35 mmol) and

Raney nickel (2 medium spatula) to give the product as a pale brown powder (0.5 g, 3.35 mmol, 32%, based on repeating unit); $v_{max}$ ($cm^{-1}$) 3584, 3475, 3351, 3023, 2919, 1620, 1514, 1452, 1179, 826, 753; $^{1}H$ NMR (600 MHz, $CDCl_3$) $\delta$ 7.36 - 6.06 (br., m, 3H) 3.42 (br. s, 1.04H), 2.54-0.94 (br. m, 3H).

General procedure **(2)** was followed to synthesise poly(4-aminostyrene) **(2b)** by using poly(4-nitrostyrene) **(1b)** (3 g, 20.11 mmol per repeating unit) in tetrahydrofuran (40 ml), hydrazine monohydrate (35.16g, 0.70 mmol) and Raney nickel (2 medium spatula) to give the product as a pale brown powder (1.20g, 10.07 mmol, 50%, based on repeating unit); $v_{max}$ ($cm^{-1}$) 3400, 3367, 2919, 1621, 1525, 1493, 1263, 825, 755, 701, 672; $^{1}H$ NMR (500 MHz, $CDCl_3$) $\delta$ 7.53-6.00 (br. m, 3.94 H), 3.38 (br. s, 1.27 H), 2.65-0.86 (br. m, 3H); $^{13}C$ NMR (126 MHz, $CDCl_3$) $\delta$ 143.93, 128.29, 125.55, 115.26, 40.72, 39.62.

General procedure **(2)** was followed to synthesise poly(4-aminostyrene) **(2c)** by using poly(4-nitrostyrene) **(1c)** (1.89 g, 12.67 mmol per repeating unit) in tetrahydrofuran (40 ml), hydrazine monohydrate (23.44g, 468.79mmol) and Raney nickel (2 medium spatula) to give the product as a pale brown powder (1.08 g, 15.10 mmol, 72%, based on repeating unit); $^{1}H$ NMR (500 MHz, $CDCl_3$) $\delta$ 7.31-6.09 (br. m, 2.38 H), 3.43 (br. s, 1.06 H), 2.65-0.94 (br. m, 3 H); $^{13}C$ NMR (126 MHz, $CDCl_3$) $\delta$ 128.75, 128.42, 115.81, 115.61, 32.44, 30.10.

General procedure **(2)** was followed to synthesise poly(4-aminostyrene) **(2d)** by using poly(4-nitrostyrene) **(1d)** (3 g, 20.11 mmol per repeating unit) in tetrahydrofuran (40 ml), hydrazine monohydrate (35.16g, 0.70 mmol) and Raney nickel (2 medium spatula) to give the product as a pale brown powder (1.30g, 10.91 mmol, 54%, based on repeating unit); $^{1}H$ NMR (500 MHz, $CDCl_3$) $\delta$ 8.30-6.16 (br. m, 3.85H), 2.74-1.01 (br. m, 3H); $^{13}C$ NMR (126 MHz, DMSO) $\delta$ 146.00, 127.57, 126.25, 113.96, 39.94, 39.78.

**Reduction of amino compounds with tin(II) chloride**

A literature procedure[143] was followed to synthesise poly(4-aminostyrene) **(2e)**. Sn powder (19.90 g, 167.60 mmol) was added to a mixture of hydrochloric acid (60 ml) and ethanol (60 ml), the reaction solution was stirred for 17 hours at 80 °C until the solution became clear. To this, a solution of poly(4-nitrostyrene) **(1e)** (5 g, 33.52 mmol) in methanol (30 ml) was added and the reaction was refluxed at 80 °C for 17 hours under nitrogen. The resulting solid polystyrene amine hydrochloride was collected, dissolved in water and neutralized by adding NaOH 30%. The solid was collected and dried under vacuum to give a brown powder (1.40 g, 11.70 mmol, 35%, based on repeating unit); $\nu_{max}$ ($cm^{-1}$) ; 3429, 3344, 3016, 2916, 1618, 1525, 1448, 1265, 1178, 823, 750, 684; $^{1}H$ NMR (500 MHz, $CD_3OD$) $\delta$ 7.42-5.77 (br. m, 3.47 H), 2.43-0.83 (br. m, 3H). $^{13}C$ NMR (126 MHz, DMSO) $\delta$ 146.99, 128.89, 127.89, 115.25, 41.42, 41.09.

**2,3,7,8-tetrafluorothianthrene (3)**

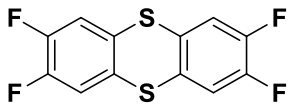


According to a modified literature procedure[117], a mixture of 1,2-difluorobenzene (10 g, 87.65 mmol), aluminium chloride (11.69 g, 87.65 mmol), and nitromethane (130 ml) was added dropwise to disulfur dichloride (11.83 g, 87.65 mmol). The reaction mixture was refluxed under a nitrogen atmosphere for three hours, and then poured into water, washed with 8N hydrochloric acid and extracted with dichloromethane. Solvents were evaporated and the crude product was crystallized from chloroform to give a colourless powder (3.82 g, 11.79 mmol, 30 %); mp 200-201 °C; $\nu_{max}$($cm^{-1}$) 3039, 1602, 1589, 1560, 1487, 1465, 1444, 1373 852, 835, 810, 790, 756, 744, 696, 678, 665, 617; $^{1}H$ NMR (500 MHz, $CDCl_3$) $\delta$ 7.32 (t, $J$ = 8.5 Hz, 4H); $^{13}C$ NMR (126 MHz, DMSO) $\delta$ 150.26, 150.67, 148.30, 130.85, 118.01,;

$^{19}$F NMR (471 MHz, DMSO) $\delta$ -137.69 (s, 4F); HRMS (EI, *m/z*) calculated 287.96851 found 287.96858 [$M^+$].

**2,3,7,8-tetrafluoro-5,5',10,10'-tetraoxidethianthrene (4)**

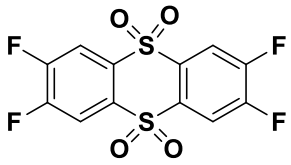

According to a literature procedure[117], a mixture of 2,3,7,8-tetrafluorothianthrene **(3)** (3 g, 10.41 mmol), acetic acid (40 ml) and chromium trioxide (6.25 g, 62.46 mmol) were reacted at 100 °C for 24 hours. The solid was collected by filtration, washed with water and dried in oven to give a white powder (3.30 g, 9.37 mmol, 90 %); mp > 300 °C; $v_{max}$(cm$^{-1}$) 3103, 3072, 3049, 1595, 1585, 1500, 1479, 1392, 1352, 1338, 1305, 1226, 1211, 1176, 1145, 1107, 802, 715, 673, 636, 621; $^1$H NMR (500 MHz, DMSO) δ 8.59 (t, J = 8.0 Hz, 4H); $^{13}$C NMR (126 MHz, DMSO) $\delta$ 153.40, 151.46, 136.04, 117.71; $^{19}$F NMR (471 MHz, DMSO) $\delta$ -124.75 (t, J = 8.0 Hz, 4F); HRMS (EI, *m/z*) calculated 351.94817, found 351.94813 [$M^+$].

**Synthesis of 2,5-dichloro-2,5-dimethylhexane (5)**

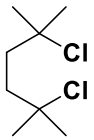

According to a literature procedure[144], concentrated hydrochloric acid (600 ml) was added to 2,5-dimethyl-2,5-hexanediol (40 g, 273.54 mmol) and the reaction mixture was left stirred at room temperature for 17 hours, the mixture was then filtered and the precipitate washed with water to give a white powder (37 g, 445.14 mmol, 74%); mp = 55-56 °C; $v_{max}$(cm$^{-1}$) 2995, 2981, 2966, 2922, 1467, 1450, 1438, 1381, 1371, 819, 781, 763, 742; $^1$H NMR (500 MHz, $CDCl_3$) $\delta$ 1.93(s, 4H), 1.60(s, 12H); $^{13}$C NMR (126 MHz,

$CDCl_3$) $\delta$ 70.29, 40.96, 32.42; LRMS (EI, *m/z*) calculated 182.06 found 147.1 [$M^+$- Cl].

**Synthesis of 6,7-dimethoxy-1,1,4,4-tetramethyl-1,2,3,4-tetrahydronaphthalene (6)**

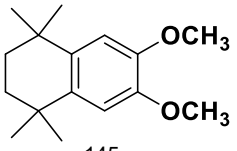


According to a literature procedure[145], a solution of aluminium chloride (4.19 g, 31.41 mmol) in nitromethane (30 ml) was added drop wise to a solution of 1,2-dimethoxybenzene (1 ml, 7.82 mmol) and 2,5-dichloro-2,5-dimethoxyhexane **(5)** (2.87 g, 15.70 mmol) in of nitromethane (30 ml). The reaction mixture was left stirring at room temperature for 20 hours. Then, the reaction mixture was poured into ice-water, the precipitate was collected by filtration, refluxed in ethanol and filtered to give a white powder (1.26 g, 5.07 mmol, 65%); mp 60-62 °C; $\nu_{max}$($cm^{-1}$) 2989, 2970, 2947, 2922, 1608, 1451, 1392, 1361, 1342, 812, 785, 742, 686; $^1$H NMR (500 MHz, $CDCl_3$) $\delta$ 6.77(s, 2H), 3.86(s, 6H), 1.67(s, 4H), 1.27(s, 12H); $^{13}$C NMR (126 MHz, $CDCl_3$) $\delta$ 146.77, 136.86, 109.21, 55.94, 35.14, 33.76, 31.75.

**General procedure (3) Demethylation**

According to a literature procedure[146], the methoxybenzene (1 equivalent) was dissolved in anhydrous dichloromethane and cooled to 0 ºC. To this, boron tribromide (1.5 equivalents) was added drop-wise and the mixture was left stirring at 0 ºC for 30 mins before warming to room temperature. The reaction mixture was poured into ice/water and dichloromethane was allowed to evaporate. The resulting solid product was filtered off, washed with water and dried under $N_2$ to give a desired catechol.

**5,5,8,8-tetramethyl-5,6,7,8-tetrahydronaphthalene-2,3-diol (7)**

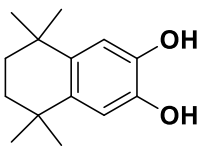

General procedure **(3)** was followed by using 6,7-dimethoxy-1,1,4,4-tetramethyl-1,2,3,4-tetrahydronaphthalene **(6)** (0.8 g, 3.22 mmol), anhydrous dichloromethane (25 mL) and boron tribromide (0.61 g, 6.44 mmol) to give a white powder (0.41 g, 1.86 mmol, 58%); mp 182-184 $^{o}$C; $v_{max}$(cm$^{-1}$) 3200, 3400, 2924, 2856, 1600, 1512, 1452, 1431, 1384, 1361, 877, 867, 852, 7796, 777, 742; $^{1}$H NMR (500 MHz, Acetone) $\delta$ 7.40 (s, 2H), 6.73 (s, 2H), 1.63 (s, 4H), 1.19 (s, 12H); $^{13}$C NMR (126 MHz, Acetone) $\delta$ 143.72, 136.90, 113.55, 36.03, 34.23, 32.32.

**Model compound (8a-8b)**

**General procedure (4) Synthesis of model compound**

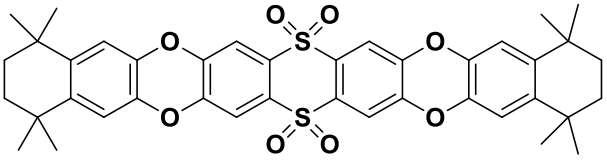

Under a nitrogen atmosphere, 2,3,7,8-tetrafluoro-5,5',10,10'-tetraoxidethianthrene (1 equivalent) and 5,5,8,8-tetramethyl-5,6,7,8-tetrahydronaphthalene-2,3-diol (2 equivalent) were dissolved in *N*-methyl-2-pyrrolidone (10 ml) then potassium carbonate was added. The reaction was stirred at the desired temperature for an appropriate time then poured into water, washed with 10% hydrochloric acid, extracted with dichloromethane. The solvent was evaporated under vacuum to give the product.

General procedure **(4)** was followed to synthesise model compound **(8a)** by reacting 2,3,7,8-tetrafluoro-5,5',10,10'-tetraoxidethianthrene **(4)** (0.2 g, 0.57 mmol), 5,5,8,8-tetramethyl-5,6,7,8-tetrahydronaphthalene-2,3-diol **(7)** (0.25g, 1.14 mmol), *N,N*-dimethylformamide (12 ml) and potassium carbonate (0.63 g, 4.56 mmol) at 70 °C for 72 h to give a product as a pale yellow powder (0.319 g, 0.45 mmol, 79 %); $^{1}$H NMR (500 MHz, $CDCl_3$) $\delta$ 7.58 (s, 4H), 6.80 (s, 4H), 1.65 (s, 8H), 1.24 (s, 24H); $^{13}$C NMR (126 MHz, $CDCl_3$) $\delta$ 146.37, 143.25, 138.43, 135.51, 115.20, 114.72, 35.09, 34.57, 32.06.

General procedure **(4)** was followed to synthesise model compound **(8b)** by reacting 2,3,7,8-tetrafluorothianthrene **(4)** (0.2 g, 0.57 mmol), 5,5,8,8-tetramethyl-5,6,7,8-tetrahydronaphthalene-2,3-diol **(7)** (0.25g, 1.14 mmol), *N*-methyl-2-pyrrolidone (12 ml) and potassium carbonate (0.63 g, 4.56 mmol) at 160 °C for 45 min. to give a product as a pale yellow powder (0.317 g, 0.44 mmol, 78%); $^{1}$H NMR (500 MHz, $CDCl_3$) $\delta$ 7.59 (s, 4H), 6.81 (s, 4H), 1.67 (s, 8H), 1.25 (s, 24H); $^{13}$C NMR (126 MHz, $CDCl_3$) $\delta$ 145.83, 142.72, 137.90, 134.98, 114.67, 114.20, 34.56, 34.04, 31.53.

**9,10-dimethyl-9,10-ethano-9,10-dihydro-2,3,6,7-tetrahydroxyanthracene (9)**

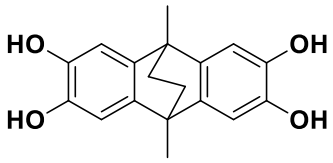


According to a literature procedure[147], 1,2-dihydroxybenzene (5 g, 45.41 mmol) was added to ice-cooled sulfuric acid (100 ml, 70%). To this, 2,5-hexanedione (2.84 ml, 22.71 mmol) was added dropwise. Then, the reaction mixture was stirred at room temperature for 5 days. By this time, crystalline product started to precipitated. The resulting solid was collected by filtration, washed with water and crystallized from ethyl acetate to give grey crystalline powder (3.2 g, 10.73 mmol, 47%); mp 265 °C; $\nu_{max}$(cm$^{-1}$) 3468, 3250, 2962, 2947, 2860, 1624, 1598, 1508, 1446, 1382, 1373, 991, 881, 812, 796, 711; $^{1}$H NMR (500 MHz, DMSO) $\delta$ 8.37 (s, 4H), 6.60 (s, 4H), 1.67 (s, 6H), 1.40 (s, 4H); $^{13}$C NMR (126 MHz, DMSO) $\delta$ 142.08, 137.99, 108.91, 36.37, 18.66; HRMS (EI, *m/z*) calculated 298.11996 found, 298.11924 [M$^{+}$].

**9,9-bis (3,4-dihydroxyphenyl) fluorene (10)**

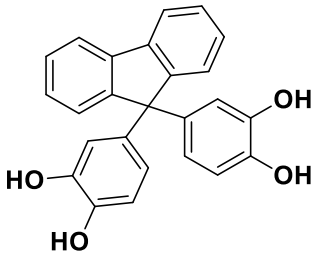

According to a literature procedure[148,149], fluorenone (2.66g, 14.76 mmol), catechol (6.50 g, 59.03 mol), toluene 50 ml and phosphotungstic acid (0.5 g) were refluxed under a nitrogen atmosphere for 8 hours whilst removing the generated water out of the reaction system by azeotropic distillation with toluene. Then to this reaction solution, acetone (10 ml) and toluene (10 ml) were added and the solution was slowly cooled to 10 °C. Precipitated crystals were collected and dried to give a white product (3.62 g, 9.47 mmol, 64%); mp 238 °C; $\nu_{max}$ ($cm^{-1}$) 3350, 1700, 1606, 1514, 1446, 1435, 1373, 1359, 1350, 808, 781, 727, 684; $^1$H NMR (500 MHz, acetone-$d_6$) $\delta$ 7.85 (dt, $J$ = 7.2 Hz, 2H), 7.77(dd,2H), 7.42 (dt, $J$ = 7.6 Hz , 2H), 7.36 (td, $J$ = 7.4, 1.2 Hz, 2H), 7.29 (td, $J$ = 7.5, 1.2 Hz, 2H), 6.68 (dd, $J$ = 5.3, 3.0 Hz, 4H), 6.53(dd, $J$ = 8.3, 2.3 Hz, 2H); $^{13}$C NMR (126 MHz, acetone-$d_6$) $\delta$ 152.95, 145.18, 144.58, 140.61, 138.49, 128.12, 127.92, 126.95, 120.70, 120.32, 116.35, 115.48, 65.15; HRMS (EI, *m/z*) calculated 382.11996 found, 382.11873 [$M^+$].

**General procedure (5) Synthesis of biphenyls via Suzuki coupling**

According to a literature procedure[150], the appropriate phenylboronic acid (1 equivalent), the appropriate phenyl bromide (1 equivalent), and $K_2CO_3$ (2 equivalents) were added to a degassed solution of $H_2O$ (10 ml per g of reagent) and THF (10 ml per g of reagent). The solution was heated to 80 °C and $Pd(PPh_3)_4$ (0.7% eq) added. After 36 h, the reaction mixture was allowed to reach r.t., the THF was removed under vacuum and the product extracted with dichloromethane (DCM). Then the solvent was evaporated under reduced pressure. The resulting solid was filtered through a pad of silica gel eluting firstly with hexane and then with DCM. Further purification by recrystallization by slow evaporation of methanol afforded the product as colourless crystals.

**3,3-dimethoxybiphenyl (11)**

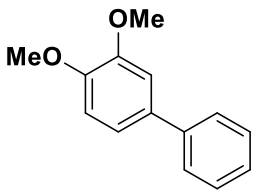

General procedure **(5)** was followed by reacting phenylboronic acid (4.35 g, 35.7 mmol), 4-bromoveratrole (9.30 g, 42.8 mmol), and $K_2CO_3$ (9.80 g, 71.4 mmol) to give colourless crystals (7.17 g, 93%); mp 68-70 °C; $\nu_{max}$ ($cm^{-1}$) 3059, 3028, 2962, 2935, 2834, 1606, 1590, 1521, 1488, 1466, 1441, 1407, 1253, 1217, 1173, 1144, 1026, 855, 761, 703; $^1$H NMR (400 MHz, $CDCl_3$, $\delta$): 7.57 (d, $J$ = 7.3 Hz, 2 H), 7.43 (t, $J$ = 7.6 Hz, 2 H), 7.32 (t, $J$ = 7.3 Hz, 1 H), 7.16 (dd, $J$ = 8.2, 1.9 Hz, 1 H), 7.12 (d, $J$ = 1.9 Hz, 1 H), 6.96 (d, $J$ = 8.2 Hz, 1 H), 3.96 (s, 3H), 3.93 (s, 3H); $^{13}$C NMR (100 MHz, $CDCl_3$, $\delta$): 149 .3, 148.7, 141.1, 134.3, 128.8, 126.9, 119.4, 111.5, 110.5, 56.0; LRMS, (APCI, *m/z*) found 215.11 [$MH^+$].

**General procedure (6) Bromination of biphenyls**

According to a literature procedure[151], the appropriate 3,4-dimethoxybiphenyl precursor (1 equivalent) was dissolved in $CHCl_3$ (20 ml per g of reagent). Neat bromine (1.1 equivalents) was added drop-wise with stirring at 0 ºC. The reaction was stirred for 24 h at room temperature then poured into water. The organic layer was separated then washed with an aqueous solution of sodium thiosulfate to eliminate excess of bromine, filtered and the solvent evaporated under vacuum. The crude compound was recrystallised by slow evaporation of methanol affording white crystals.

**2-bromo-4,5-dimethoxy-biphenyl (12)**

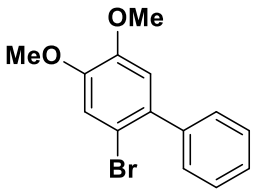


General procedure **(6)** was followed by reacting 3,4-dimethoxy-4'-methyl-1,1'-biphenyl **(11)** (4.90 g, 21.46 mmol) and bromine (3.77 g, 23.61 mmol) to give white crystals (6.22 g, 95%); mp 100-102 °C; $\nu_{max}$ ($cm^{-1}$) 3059, 2964, 2938, 2910, 2838, 1603, 1519, 1505, 1489, 1441, 1379, 1208, 1020, 860, 770, 704; $^1$H NMR (400 MHz, $CDCl_3$, $\delta$): 7.31 (d, $J$ = 8.1 Hz, 2H), 7.24 (d, $J$ = 7.9 Hz, 2H), 7.12 (s, 1H), 6.83 (s, 1H), 3.91 (s, 3H), 3.86 (s, 3H); $^{13}$C NMR (100 MHz,

$CDCl_3$, *δ*): 148.7, 148.3, 138.3, 137.2, 129.4, 128.7, 115.9, 114.1, 112.6, 56.3, 56.1, 21.2; LRMS (EI, *m/z*) found 292.01[$M^+$].

**General procedure (7) Synthesis of carboxylic biphenyl precursor**

According to a literature procedure[152], the appropriate bromo-biphenyl precursor (1 equivalent) was dissolved in anhydrous THF (20 ml per g of precursor) under inert atmosphere. A solution of *n*-butyl lithium (1.25 equivalents, 2.5 M in hexanes) was added at -78 °C and left under stirring for 1 hour. Dry gaseous $CO_2$ was bubbled through the solution for 2 hours. The reaction was quenched with ice water and the THF evaporated under vacuum. To the resulting product, water was added and the solution carefully acidified until *pH* 5 and the resulting white precipitate collected to afford the acid precursor as a white solid.

**4,5-dimethoxy-2-phenylbenzoic acid (13)**

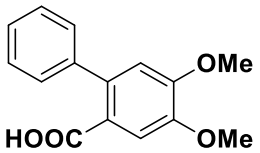


General procedure **(7)** was followed by reacting 2-bromo-4,5-dimethoxy-biphenyl **(12)** (4.50 g, 15.41 mmol) and *n*-butyl lithium (7.7 ml of a solution 2.5 M in hexanes, 19.26 mmol) to give a yellow oil (2.98 g, 75%); $^1$H NMR (400 MHz, $CDCl_3$, *δ*): 7.53 (s, 1H), 7.36 (m, 5H), 6.78 (s, 1H), 3.95 (s, 3H), 3.92 (s, 3H); $^{13}$C NMR (100 MHz, $CDCl_3$, *δ*): 172.2, 152.0, 147.8, 141.5, 138.75, 128.8, 128.1, 127.3, 120.4, 114.1, 113.6, 56.3, 56.2; HRMS (EI, *m/z*) calculated 258.0892 found 258.0898 [$M^+$] .

**General procedure (8) Synthesis of fluorenones**

According to a literature procedure[153], the appropriate carboxylic biphenyl precursor was dissolved into methanesulfonic acid (10 g per g of precursor) and left under stirring for 3 hours. The reaction was quenched with iced water

and the resulting precipitate collected and recrystallised from methanol to give a yellow/orange solid.

**2,3-dimethoxy-9H-fluoren-9-one (14)**

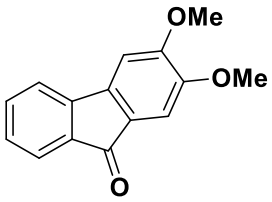


General procedure **(8)** was followed by reacting 4,5-dimethoxy-2-phenylbenzoic acid **(13)** (2.00g, 7.74 mmol) and methanesulfonic acid (20 ml) to give a white solid (1.45 g, 78%); m.p. 159-161 °C; $^{1}$H NMR (400 MHz, $CDCl_3$, *δ*): 7.55 (dd, *J* = 7.3, 0.7 Hz, 1H), 7.40 (td, *J* = 7.4, 1.1 Hz, $^{1}$H), 7.37 – 7.33 (m, 1H), 7.23 – 7.16 (m, 2H), 7.00 (s, 1H), 4.01 (s, 3H), 3.93 (s, 3H); $^{13}$C NMR (100 MHz, $CDCl_3$, *δ*): 193.4, 154.8, 149.9, 144.1, 139.7, 134.9, 134.4, 128.4, 127.1, 123.9, 119.3, 107.4, 103.6, 56.5, 56.4; HRMS (EI, *m/z*) calculated 240.0786 found 240.0786 [$M^+$].

**General procedure (9) Synthesis of spirobifluorenes (SBFs)**

According to a literature procedure[121], *n*-Butyl lithium solution in hexanes (2.5 M 1.2 equivalents) was added drop-wise to a solution of the appropriate bromo-biphenyl (1.1 equivalents) in anhydrous THF (20 ml per g of bromo-biphenyl) at -78 °C. After 1.5 hour, the appropriate fluorenone (1 equivalent) was added to the reaction mixture, which was allowed to slowly reach r.t. and stirred for 12 hours then quenched with water. The THF was evaporated under vacuum, and the aqueous layer extracted with DCM. The organic extracts were washed with water, filtered and the solvent evaporated under reduced pressure. The crude pale yellow carbinol precursor was triturated in methanol then filtered to give a white solid. The obtained solid was dissolved in cold glacial acetic acid and conc. hydrochloric acid was added drop-wise to the solution, which was then refluxed for 3h. After cooling, the mixture was poured into water and the precipitate was filtered off then triturated in

methanol to give white solid.

**2,2',3,3''-tetramethoxy-9,9'-spirobifluorene (15)**

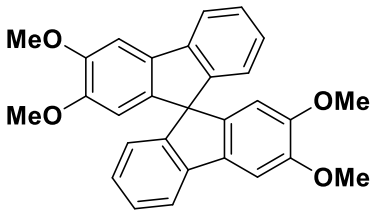


General procedure **(9)** was followed by reacting *n*-butyl lithium solution in hexanes (2.5 M; 5.2 ml, 13 mmol), 2-bromo-4,5-dimethoxybiphenyl **(12)** (2.92 g, 10 mmol) and 2,3-dimethoxy-9H-fluoren-9-one **(14)** (2.00 g, 8.3 mmol) in anhydrous THF (60 ml) to give a white solid (2.70 g, 75%); mp 221- 223 ºC; $^{1}$H NMR (400 MHz, $CDCl_3$, *δ*): 7.72 (d, *J* = 7.5 Hz, 2H), 7.35 (s, 2H), 7.32 (dd, *J* = 7.5, 1.0 Hz, 2H), 7.03 (td, *J* = 7.5, 1.0 Hz, 2H), 6.66 (d, *J* = 7.5 Hz, 2H), 6.24 (s, 2H), 4.03 (s, 6H), 3.64 (s, 6H); $^{13}$C NMR (100 MHz, $CDCl_3$, *δ*): 149.6, 149.4, 149.2, 142.0, 140.9, 134.4, 127.6, 126.7, 123.7, 118.9,106.9, 103.0, 65.9, 56.3, 56.1; HRMS (EI, *m/z*) calculated 436.1675 found 436.1682 [$M^+$].

**2,2',3,3'-tetrahydroxy-9,9'-spirobifluorene (16)**

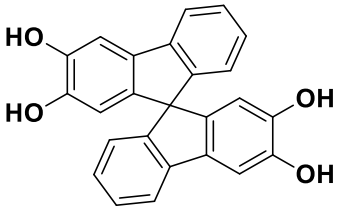


General procedure **(3)** was followed by reacting $BBr_3$ (1.74 g, 6.9 mmol) and 2,2',3,3'-tetramethoxy-9,9'- spirobifluorene **(15)** (1.00 g, 2.3 mmol) in anhydrous DCM (20 ml) to give a white powder (0.80 g, 92%); mp decomposes before melting; $^{1}$H NMR (400 MHz, acetone-$d_6$) δ 8.03 (br s, 2H), 7.97 (br s, 2H), 7.73 (d, *J* = 7.6 Hz, 2H), 7.40 (s, 2H), 7.29 (s, 2H), 7.00 (s, 2H), 6.59 (d, *J* = 7.5 Hz, 2H), 6.17 (s, 2H); $^{13}$C NMR (100 MHz, acetone $d_6$) *δ* 150.0, 146.1, 146.0, 142.9, 141.4, 134.2, 128.0, 126.7, 123.9, 119.5,

111.0, 107.4, 65.7; HRMS (ESI-, *m/z*) calculated 379.0970 found 379.0975 [M-H$^+$].

**3,4-dimethoxy-4'-methyl-1,1'-biphenyl (17)**

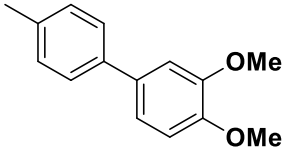


General procedure **(5)** was followed by reacting 3,4-dimethoxyphenylboronic acid (5.00 g, 29.0 mmol), 4-bromotoulene and $K_2CO_3$ (8.00 g, 58.0 mmol) to give colourless crystals (6.00 g, 91%); mp 63-65 °C; $^1$H NMR (400 MHz, $CDCl_3$, *δ*): 7.37 (d, *J* = 8.1 Hz, 2H), 7.15 (d, *J* = 8.1 Hz, 2H), 7.02 (m, 2H), 6.85 (d, *J* = 8.2 Hz, 1H), 3.86 (s, 3H), 3.83 (s, 3H), 2.30 (s, 3H); $^{13}$C NMR (100 MHz, $CDCl_3$, *δ*): 149.2, 148.5, 138.2, 136.6, 134.3, 129.4, 126.7, 119.2, 111.6, 110.5, 56.0, 55.9, 21.0; HRMS (EI, *m/z*) calculated 228.1150 found 228.1145 [M$^+$].

**1-bromo-3,4-dimethoxy-4'-methyl-1,1'-biphenyl (18)**

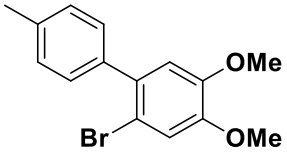


General procedure **(6)** was followed by reacting 3,4-dimethoxy-4'-methyl-1,1'-biphenyl **(17)** (4.90 g, 21.46 mmol) and bromine (3.77 g, 23.61 mmol) to give white crystals (6.22 g, 95%); mp 100-102 °C; $^1$H NMR (400 MHz, $CDCl_3$, *δ*): 7.31 (d, J = 8.1 Hz, 2H), 7.24 (d, *J* = 7.9 Hz, 2H), 7.12 (s, 1H), 6.83 (s, 1H), 3.91 (s, 3H), 3.86 (s, 3H), 2.41 (s, 3H); $^{13}$C NMR (100 MHz, $CDCl_3$, *δ*): 148.7, 148.3, 138.3, 137.2, 129.4, 128.7, 115.9, 114.1, 112.6, 56.3, 56.1, 21.2; HRMS (EI, *m/z*) calculated 306.0255 found 306.0252 [M$^+$].

**4,5-dimethoxy-2-(4-methylphenyl)benzoic acid (19)**

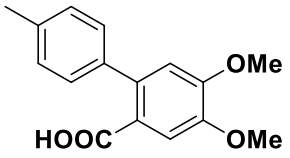


General procedure **(7)** was followed by reacting 1-bromo-3,4-dimethoxy-4'-methyl-1,1'-biphenyl **(18)** (3.00 g, 9.76 mmol) and *n*-butyl lithium (4.9 ml of a solution 2.5 M in hexanes, 12.2 mmol) to give a yellow oil (2.98 g, 75%); m.p. 208-210 °C; $^{1}$H NMR (400 MHz, $CDCl_3$, *δ*): 7.53 (s, 1H), 7.22 (d, *J* = 8.2 Hz, 2H), 7.19 (d, *J* = 8.2 Hz, 2H), 6.77 (s, 1H), 3.95 (s, 3H), 3.92 (s, 3H), 2.40 (s, 3H); $^{13}$C NMR (100 MHz, $CDCl_3$, *δ*): 171.5, 152.1, 147.8, 138.7, 138.6, 137.1, 128.9, 128.7, 120.5, 114.3, 113.9, 56.3, 56.2, 21.3; HRMS (EI, *m/z*) calculated 272.1049 found 272.1046 [$M^+$].

**2,3-dimethoxy-7-methyl-9H-fluoren-9-one (20)**

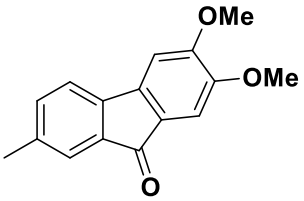


General procedure **(8)** was followed by reacting 4,5-dimethoxy-2-(4-methylphenyl)benzoic acid **(19)** (1.90 g, 6.95 mmol) and methanesulfonic acid (20 ml) to give a white solid (1.41 g, 80%); mp 190-192 °C; $^{1}$H NMR (400 MHz, $CDCl_3$, *δ*): 7.36 (s, 1H), 7.23 (d, *J* = 7.5 Hz, 1H), 7.19 (d, *J* = 7.5 Hz, 1H), 6.95 (s, 1H), 4.00 (s, 3H), 3.91 (s, 3H), 2.34 (s, 3H); $^{13}$C NMR (100 MHz, $CDCl_3$, δ): 193.5, 154.8, 149.6, 141.4, 139.9, 138.4, 135.2, 134.6, 127.1, 124.8, 119.1, 107.4, 103.5, 77.2, 56.5, 56.4, 21.4; HRMS (EI, m/z) calculated 254.0943 found 254.0944 [$M^+$].

## 2,2',3,3'-tetramethoxy-6,6'-dimethyl-9,9'-spirobifluorene (21)

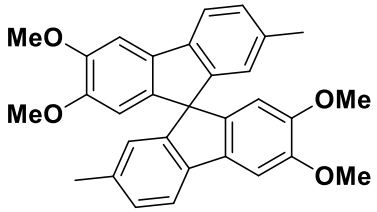


General procedure **(9)** was followed by reacting *n*-butyl lithium solution in hexanes (2.5 M; 2.9 ml, 7.20 mmol), 1-bromo-3,4-dimethoxy-4'-methyl-1,1'-biphenyl **(9)** (2.04 g, 6.65 mmol) and 2,3-dimethoxy-7-methyl-9H-fluoren-9-one **(20)** (1.41 g, 5.54 mmol) in anhydrous THF (60 ml) to give white solid (1.93 g, 75%); mp 155-157 ºC; $^{1}$H NMR (400 MHz, $CDCl_3$, δ): 7.53 (d, *J* = 7.0 Hz, 2H), 7.27 (m, 2H), 7.07 (d, *J* = 7.0 Hz, 2H), 6.40 (s, 2H), 6.14 (s, 2H), 3.95 (s, 6H), 3.57 (s, 6H), 2.12 (s, 6H); $^{13}$C NMR (100 MHz, $CDCl_3$, *δ*): 149.6, 149.3, 140.9, 139.2, 136.4, 134.4, 128.3, 124.4, 118.4, 107.2, 102.8, 67.5, 56.2, 56.1, 21.4; HRMS (EI, *m/z*) calculated 464.1988 found 464.1984 [$M^+$].

## 2,2',3,3'- tetrahydroxy -6,6'-dimethyl-9,9'-spirobifluorene (22)

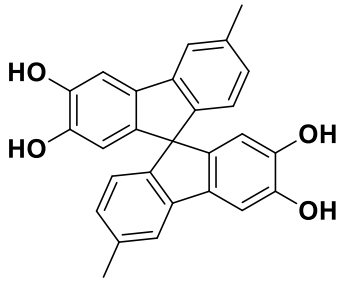


General procedure **(3)** was followed by reacting tribromoboron (2.34 g, 9.68 mmol) and 2,2',3,3'-tetramethoxy -6,6'-dimethyl-9,9'-spirobifluorene **(21)** (1.50 g, 3.22 mmol) in anhydrous DCM (30 ml) to give a white powder (1.20 g, 92%); mp decomposes before melting; $^{1}$H NMR (400 MHz, acetone-$d_6$, *δ*): 8.01 (s, 2H), 7.93 (s, 2H), 7.59 (d, *J* = 7.7 Hz, 2H), 7.32 (s, 2H), 7.10 (d, *J* = 7.7 Hz, 2H), 6.39 (s, 2H), 6.13 (s, 2H), 2.15 (s, 6H); $^{13}$C NMR (100 MHz, Acetone-$d_6$, *δ*): 150.8, 146.2, 145.9, 141.7, 140.5, 136.5, 134.6, 129.0, 124.8, 119.5, 111.3, 107.3, 21.3; HRMS ($ESI^+$, *m/z*): calculated 408.1362 found 408.1367 [M-$H^+$] .

**3,4-dimethoxy-4'-*t*-butyl-1,1'-biphenyl (23)**

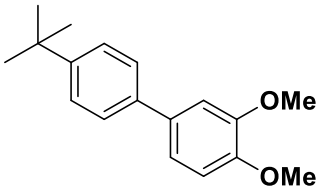


General procedure **(5)** was followed by reacting 3,4-dimethoxyphenylboronic acid (4.25 g, 23.4 mmol), 4-*t*-butyl-bromotoluene (5.00 g, 23.4 mmol) and $K_2CO_3$ (6.45 g, 46.8 mmol) to give colourless crystals (6.00 g, 95%); mp 60-62 °C; $^1$H NMR (400 MHz, $CDCl_3$, *δ*): 7.48 (dd, *J* = 20.8, 8.5 Hz, 4H), 7.13 (m, 2H), 6.94 (d, *J* = 8.5 Hz, 1H), 3.94 (s, 3H), 3.92 (s, 3H), 1.36 (s, 9H); $^{13}$C NMR (100 MHz, $CDCl_3$, *δ*): 150.0, 149.2, 148.5, 138.4, 134.3, 126.7, 125.9, 119.4, 111.6, 110.5, 56.2, 56.1, 34.7, 31.6; HRMS (EI, *m/z*) calculated 270.1620 found 270.1625 [$M^+$].

**1-bromo-3,4-dimethoxy-4'-*t*-butyl-1,1'-biphenyl (24)**

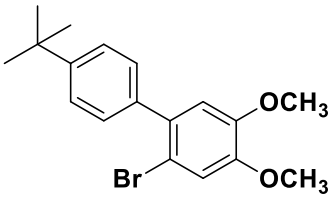


General procedure **(6)** was followed by reacting 3,4-dimethoxy-4'-*t*-butyl-1,1'-biphenyl **(23)** (5.50 g, 20.41 mmol) and bromine (3.59 g, 22.45 mmol) to give colourless crystals (6.97 g, 98%); mp 70-72 °C; $^1$H NMR (400 MHz, $CDCl_3$, *δ*): 7.44 (d, *J* = 8.5 Hz, 2H), 7.35 (d, *J* = 8.5 Hz, 2H), 7.12 (s, 1H), 6.85 (s, 1H), 3.91 (s, 3H), 3.86 (s, 1H), 1.37 (s, 3H); $^{13}$C NMR (100 MHz, $CDCl_3$, *δ*): 150.3, 148.3, 138.1, 129.1, 124.9, 115.9, 114.2, 112.5, 56.3, 56.1, 34.6, 31.4; HRMS (EI, *m/z*) calculated 348.0725 found 348.0732 [$M^+$].

**2-(4-*t*-butylphenyl)-4,5-dimethoxybenzoic acid (25)**

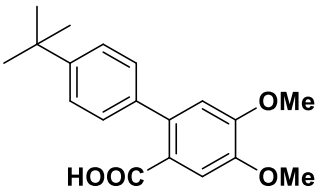


General procedure **(7)** was followed by reacting 1-bromo-3,4-dimethoxy-4'-*t*-butyl-1,1'-biphenyl (4.50 g, 12.88 mmol) **(24)** and *n*-butyl lithium (6.45 ml of a solution 2.5 M in hexanes, 16.1 mmol) to give a white solid (3.46 g, 85%); mp 120-122 °C; $^{1}$H NMR (400 MHz, $CDCl_3$, $\delta$): 7.53 (s, 1H), 7.39 (d, $J$ = 8.5 Hz, 2H), 7.25 (d, $J$ = 8.5 Hz, 2H), 6.79 (s, 1H), 3.95 (s, 3H), 3.92 (s, 3H), 1.36 (s, 9H); $^{13}$C NMR (100 MHz, $CDCl_3$, $\delta$): 172.1, 152.0, 150.2, 147.7, 138.6, 138.4, 128.5, 125.0, 120.5, 114.3, 113.8, 56.3, 56.2, 34.7, 31.5; HRMS (EI, *m/z*) calculated 314.1518 found 314.1512 [$M^+$].

**2,3-dimethoxy-7-t-butyl-9H-fluoren-9-one (26)**

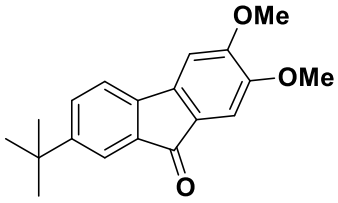


General procedure **(8)** was followed by reacting 2-(4-*t*-butylphenyl)-4,5-dimethoxybenzoic acid **(25)** (3.20 g, 10.17 mmol) and methanesulfonic acid (30 ml) to give a white solid (2.56 g, 85%); mp 160-162 °C; $^{1}$H NMR (400 MHz, $CDCl_3$, $\delta$): 7.62 (d, $J$ = 1.8 Hz, 1H), 7.42 (dd, $J$ = 7.8, 1.8 Hz, 1H), 7.27 (d, $J$ = 7.8 Hz, 2H), 7.18 (s, 1H), 6.97 (s, 1H), 4.01 (s, 3H), 3.92 (s, 3H), 1.33 (s, 9H); $^{13}$C NMR (100 MHz, $CDCl_3$, $\delta$): 193.8, 154.8, 152.1, 149.7, 141.4, 139.9, 135.1, 130.9, 127.4, 121.4, 118.9, 107.5, 103.5, 56.5, 56.4, 35.1, 31.3; HRMS (EI, *m/z*) calculated 296.1412 found 296.1418 [$M^+$].

**2,2',3,3'-tetramethoxy-6,6'-*t*-butyl-9,9'-spirobifluorene (27)**

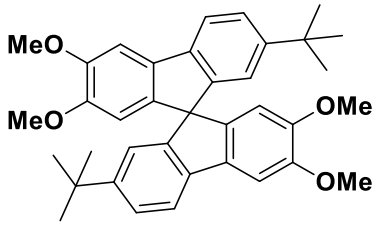


General procedure **(9)** was followed by reacting *n*-butyl lithium solution in hexane (2.5 M; 4.05 ml, 7.75 mmol), 1-bromo-3,4-dimethoxy-4'-*t*-butyl-1,1'-biphenyl **(24)** (3.25 g, 9.30 mmol) and 2,3-dimethoxy-7-*t*-butyl-9H-fluoren-9-one **(26)** (2.29 g, 7.75 mmol) in anhydrous THF (60 ml) to give a white solid (2.38 g, 75%); mp 120-122 ºC; $^{1}$H NMR (400 MHz, $CDCl_3$) $\delta$ 7.64 (d, $J$ = 8.0 Hz, 2H), 7.38 (dd, $J$ = 8.0, 1.6 Hz, 2H), 6.64 (d, $J$ = 1.6 Hz, 2H), 6.19 (s, 2H), 4.03 (s, 6H), 3.63 (s, 6H), 1.15 (s, 18H); $^{13}$C NMR (100 MHz, $CDCl_3$) $\delta$ 150.1, 149.6, 149.3, 149.3, 141.8, 139.6, 134.6, 124.5, 120.9, 118.2, 107.2, 102.9, 66.2, 56.3, 56.2, 34.9, 31.6; HRMS (EI, *m/z*) calculated 548.2927 found 548.2931 [$M^+$].

**2,2',3,3'- tetrahydroxy-6,6'-*t*-butyl-9,9'-spirobifluorene (28)**

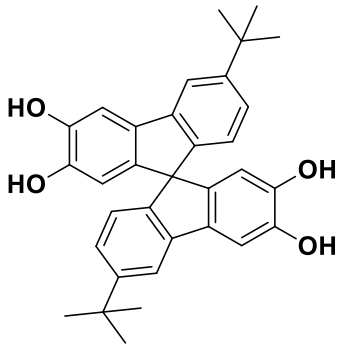


General procedure **(3)** was followed by reacting $BBr_3$ (1.61 g, 6.45 mmol) and 2,2',3,3'- tetramethoxy-6,6'-*t*-butyl-9,9'-spirobifluorene **(27)** (1.18 g, 2.15 mmol) in anhydrous DCM (20 ml) to give a white powder (1.20 g, 92%); mp decomposes before melting; $^{1}$H NMR (400 MHz, acetone-$d_6$) δ 7.96 (s, 2H), 7.86 (s, 2H), 7.64 (d, $J$ = 8.0 Hz, 2H), 7.36 (d, $J$ = 8.0 Hz, 2H), 7.33 (s, 2H), 6.65 (s, 2H), 6.11 (s, 2H), 1.13 (s, 18H); $^{13}$C NMR (100 MHz, Acetone) δ 150.6, 150.1, 146.1, 145.9, 142.5, 140.8, 134.4, 125.3, 121.0, 119.2, 111.3,

107.5, 66.4, 35.3, 31.8; HRMS (ESI-, *m/z*) calculated 491.2222 found 491.2220 [M-H$^+$].

**1,3-bis(3,4-dimethoxyphenyl)propan-2-one (29)**

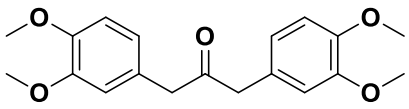

According to a literature procedure[154], a solution of 2-(3,4-dimethoxyphenyl)acetic acid (10 g, 51 mmol) in DCM (80 mL) was added dropwise to a solution of dicyclohexylcarbodiimide (11 g, 53.5 mmol) and 4-(dimethylamino)pyridine (1.55 g, 12.75 mmol) in DCM (120 ml) and the resulting mixture stirred at 25 °C for 72 hours under nitrogen atmosphere. Then the precipitated solid was filtered off and the organic solution was purified by flash chromatography (hexane:ethyl acetate 70:30) before crystallisation from EtOH to give a yellow powder (5.34 g, 63%); mp 150 – 152 °C; $^1$H NMR (400 MHz, $CDCl_3$) $\delta$ 6.81 (d, $J$ = 8.2 Hz, 2H), 6.69 (dd, $J$ = 8.2, 1.9 Hz, 2H), 6.62 (d, $J$ = 1.9 Hz, 2H), 3.86 (s, 6H), 3.82 (s, 6H), 3.65 (s, 4H); $^{13}$C NMR (101 MHz, $CDCl_3$) $\delta$ 206.5, 149.2, 148.3, 126.7, 121.8, 112.7, 111.6, 56.0, 56.0, 48.6; LRMS (EI$^+$) *m/z* = 330.16.

**2,5-bis(3,4-dimethoxyphenyl)-3,4-diphenylcyclopenta-2,4-dien-1-one (30)**

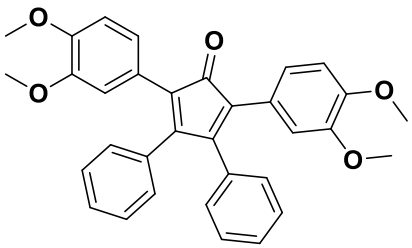

According to a literature procedure[154], KOH (1.51 mmol) in EtOH was added to a mixture of 1,3-bis(3,4-dimethoxyphenyl)propan-2-one **(29)**(1 g, 3.02 mmol), benzil (0.64 mg, 3.02 mmol) and EtOH (10 ml), which was heated at 85 °C. The reaction mixture was heated for one hour. The precipitated solid

was filtered off, washed with water and EtOH to give a black powder (1.10 g, 72%); mp 170 – 172 $^{o}$C; $^{1}$H NMR (500 MHz, $CDCl_3$) $\delta$ 7.22 (m, 6H), 6.97 (m, 6H), 6.78 (d, $J$ = 8.5 Hz, 2H), 6.70 (d, $J$ = 1.9 Hz, 2H), 3.85 (s, 6H), 3.54 (s, 6H); $^{13}$C NMR (126 MHz, $CDCl_3$) $\delta$ 201.4, 153.5, 148.8, 148.5, 133.8, 129.4, 128.4, 128.2, 124.5, 123.7, 123.2, 113.3, 111.1, 55.8, 55.5; HRMS (EI, *m/z*) calculated 504.1937 found 504.1935.

**1,4-di(3',4'-dimethoxyphenyl)-2,3,5,6-tetraphenylbenzene (31)**

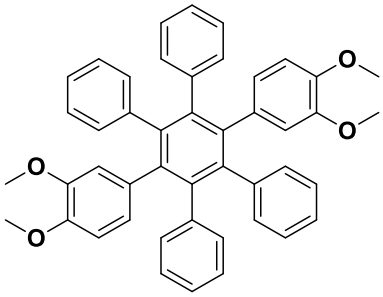

According to a literature procedure[154], a mixture of 2,5-bis(3,4-dimethoxyphenyl)-3,4-diphenylcyclopenta-2,4-dien-1-one **(30)** (1.15 g, 2.28 mmol), 2-phenylethynyl)benzene (447 mg, 2.50 mmol) and $Ph_2O$ (3 ml) was heated at 260 °C for 1 h in a microwave reactor. Then, the mixture was cooled to room temperature, poured into cold MeOH and the resulting precipitate collected by filtration. The solid was washed with warm hexane to dissolve residual $Ph_2O$ and the solid was collected by filtration to give a white powder (0.9g, 60%); mp 284 – 286 °C; $^{1}$H NMR (400 MHz; $CDCl_3$) $\delta$ 6.86 (m, 20H) 6.32 (m, 6H) 3.68 (s, 6H) 3.40 (s, 6H); $^{13}$C NMR (101 MHz; $CDCl_3$) $\delta$147.2, 146.4, 140.9, 140.5, 139.7, 132.9, 131.5, 131.4, 131.3, 131.2, 126.8, 126.7, 126.7, 126.6, 126.5, 125.1, 124.2, 115.4, 109.3, 55.5, 55.4; HRMS (EI, *m/z*) calculated 654.2770; found 654.2784 [$M^+$].

## 1,4-di(3',4'-dihydroxyphenyl)-2,3,5,6-tetraphenylbenzene (32)

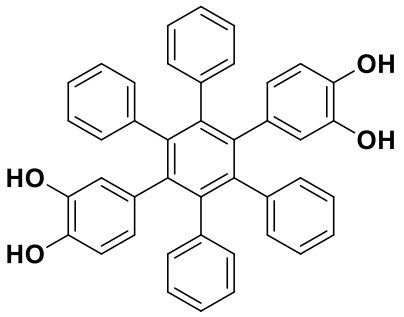


General procedure **(3)** was followed by reacting $BBr_3$ (0.92 g, 3.66 mmol) and 1,4-di-(3',4'-dimethoxyphenyl)-2,3,5,6-tetraphenylbenzene **(31)** (0.8 g, 1.22 mmol) in anhydrous DCM (40 ml) to give a white powder (0.78 g, 95%); mp > 300 °C; $^1$H NMR (500 MHz, acetone-$d_6$) $\delta$ 6.99-6.79 (br. m, 20H), 6.37 (dd, $J$ = 4.5, 1.9 Hz, 2H), 6.30 (d, $J$ = 8.1 Hz, 2H), 6.23-6.19 (m, 2H); $^{13}$C NMR (126 MHz, acetone-$d_6$) $\delta$ 144.58, 143.50, 142.23, 141.54, 140.99, 133.63, 132.35, 127.43, 126.01, 124.31, 119.66, 119.58, 114.76, 114.60; HRMS (EI, *m/z*) calculated 598.2144 found 598.2136.

## 1,1,4,4-tetramethyl-1,2,3,4-tetrahydronaphthalene (33)

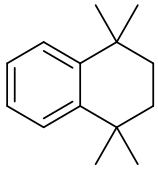

According to a literature procedure[155], anhydrous benzene (250ml, 2.75 mol) was added to 2,5-dichloro-2,5-dimethylhexane **(13)** (20 g, 106 mmol) and heated to 50 °C. To this, aluminium chloride (5.87 g, 40 mmol) was added portion-wise. The reaction solution was left stirring at 50 °C for 24 h. Then, the solution was cooled to room temperature, poured into dilute hydrochloric acid and extracted with dichloromethane. The solvent was removed under vacuum and the resulting orange oil was purified by vacuum distillation to give a colourless oil (14 g, mmol, 66 %); $^1$H NMR (500 MHz, $CDCl_3$) $\delta$ 7.36

(dd, *J* = 5.9, 3.4 Hz, 2H), 7.18 (dd, *J* = 5.9, 3.4 Hz, 2H), 1.75 (s, 4H), 1.35 (s, 12H); $^{13}$C NMR (126 MHz, $CDCl_3$) *δ* 145.01, 126.74, 125.83, 35.45, 34.48, 32.09; LRMS (EI, *m/z*) calculated 188.16 found 188.1 [$M^+$].

**6,7-dibromo-1,1,4,4-tetramethyl-1,2,3,4-tetrahydronaphthalene (34)**

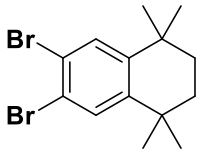


General procedure **(6)** was followed by adding Fe powder (catalytic amount) to a solution of 1,1,4,4-tetramethyl-1,2,3,4-tetrahydronaphthalene **(33)** (20.70 g, 109.93 mmol) in anhydrous dichloromethane (200 mL). To this, bromine (52.70 g, 329.79 mmol) was added drop-wise and the reaction was left stirring at room temperature for 3 h. Then the reaction mixture was poured into water, organic layer separated, washed with sodium carbonate solution (3 x 100 mL). The solvent was removed under vacuum and the crude was purified by column chromatography (hexane) to give white solid (16 g, 2.89 mmol, 42%); mp 111-112 °C; $v_{max}$ ($cm^{-1}$) 2951, 2937, 2862, 1494, 1431, 1386, 1377, 1361, 1348, 1090, 1047, 1020, 935, 887, 860, 837, 756, 682; $^1$H NMR (500 MHz, $CDCl_3$) *δ* 7.48 (s, 2H), 1.67 (s, 4H), 1.25 (s, 12H); $^{13}$C NMR (126 MHz, $CDCl_3$) *δ* 146.28, 131.69, 121.34, 34.81, 34.14, 31.38; LRMS (EI, *m/z*) calculated 345.9 found 345.9 [$M^+$].

**5,5,8,8-tetramethyl-1,4,5,6,7,8-hexahydro-1,4-epoxyanthracene (35)**

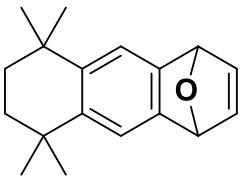


According to a reported procedure[156], the mixture of 6,7-dibromo-1,1,4,4-tetramethyl-1,2,3,4-tetrahydronaphthalene **(34)** (15 g, 43.34 mmol) and anhydrous furan (26.56 g, 390.06 mmol) was dissolved in anhydrous THF

(50 mL). To this, *n*-BuLi (15.33 g, 56.34 mmol) in anhydrous THF (10 mL) was added drop wise and left to stir at -78 ºC for 1.5 h. The reaction solution was allowed to warm to room temperature before water adding. The organic layer was extracted with dichloromethane and the solvent was removed under vacuum. The solid product washed with hexane, filtered off and dried to give white powder (6.5 g, 25.55 mmol, 59% ); mp 124-126$^{o}$C; $\nu_{max}$ (cm$^{-1}$) 3018, 2972, 2947, 2906, 2854, 2560, 1473, 1465, 1396, 1282, 1222, 1195, 1161, 1049, 1001, 916, 898, 877, 867, 833, 694; $^{1}$H NMR (500 MHz, $CDCl_3$) $\delta$ 7.20 (s, 2H), 6.98 (t, $J$ = 1.0 Hz, 2H), 5.65 (s, 2H), 1.64 (s, 4H0, 1.23 (s, 12H); $^{13}$C NMR (126 MHz, $CDCl_3$) $\delta$ 145.23, 142.43, 140.77, 118.44, 82.16, 35.07, 34.28, 31.67, 31.58; HRMS (EI, *m/z*) calculated 254.17 found 254.1678 [M$^{+}$].

**2,3,6,7-tetramethoxy-9,10-dimethylanthracene (36)**

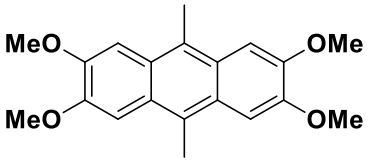


According to a reported procedure[157], a solution of veratrole (21.69 g, 157 mmol), acetaldehyde (6.92 g, 157 mmol) and acetonitrile (6.44 g, 157 mmol) was cooled to 0 ºC. To this, concentrated sulfuric acid (75.0 mL) was added drop-wise and left stirring at 0 ºC for 2 h. Then, the reaction solution was poured into ice, neutralised with aqueous ammonium hydroxide solution and filtered. The solid product washed with water and methanol and crystallised from acetone to give a white solid (9.8 g, 29.98 mmol, 19%); mp > 300 °C; $^{1}$H NMR (500 MHz, $CDCl_3$) $\delta$ 7.41 (s, 4H), 4.08 (s, 12H), 2.95 (s, 6H); $^{13}$C NMR (126 MHz, $CDCl_3$) $\delta$ 149.13, 126.21, 124.26, 103.04, 56.09, 15.17. LRMS (EI, *m/z*) calculated 326.15 found 326.1 [M$^{+}$].

**(5*s*,14*s*)-2,3,18,19-tetramethoxy-5,8,8,11,11,14-hexamethyl-5,5a,6,8,9,10,11,13,13a,14-decahydro-5,14-[1,2]benzeno-6,13-epoxypentacene (37)**

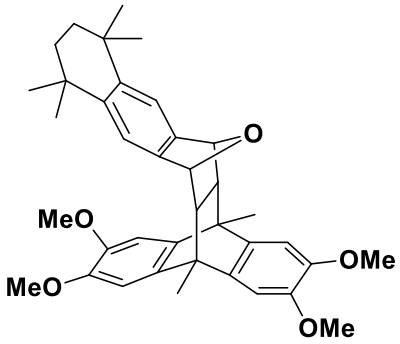


According to a reported procedure[158], 2,3,6,7-tetramethoxy-9,10-dimethylanthracene **(36)** (2 g, 6.13 mmol) and 5,5,8,8-tetramethyl-1,4,5,6,7,8-hexahydro-1,4-epoxyanthracene **(35)** (1.56 g, 6.13 mmol) were dissolved in DMF (15 mL) and heated in a microwave reactor at 250 ºC for 2.5 h. Solvent was removed under vacuum and the crude product was purified by column chromatography to give a brown product (2.29 g, 3.49 mmol, 64%); mp 288-289 °C; $\nu_{max}$ ($cm^{-1}$) 2950, 1585, 1512, 1454, 1436, 1404, 1359, 1280, 1244, 1226, 1195, 1163, 1097, 1049, 906, 854, 835, 819, 785, 748; $^{1}H$ NMR (500 MHz, $CDCl_3$) δ 7.02 (s, 2H), 6.86 (s, 2H), 6.83 (s, 2H), 4.92 (s, 2H), 3.88 (s, 6H), 3.82 (s, 6H), 2.07 (s, 6H), 1.99 (s, 2H), 1.59 (s, 4H), 1.19 (s, 12H); $^{13}C$ NMR (126 MHz, $CDCl_3$) δ 147.21, 146.77, 144.50, 142.90, 140.90, 137.18, 116.82, 106.99, 106.38, 80.02, 57.23, 56.80, 56.73, 43.49, 35.54, 34.83, 32.49, 32.24, 17.53; HRMS (EI, m/z) calculated 580.32 found 580.3181 [$M^+$].

## 2,3,18,19-tetramethoxy-5,8,8,11,11,14-hexamethyl-5,8,9,10,11,14-hexahydro-5,14-[1,2]benzenopentacene (38)

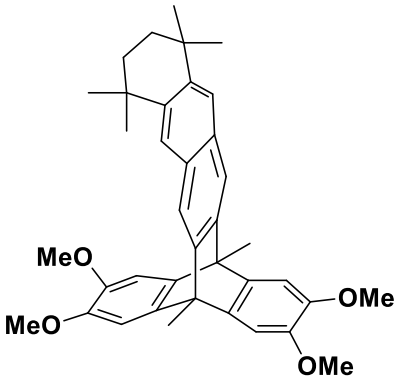


According to a reported procedure[18], (5*s*,14*s*)-2,3,18,19-tetramethoxy-5,8,8,11,11,14-hexamethyl-5,5a,6,8,9,10,11,13,13a,14-decahydro-5,14-[1,2]benzeno-6,13-epoxy-pentacene **(37)** (2 g, 3.44mmol) was dissolved in TFA (40 ml) and left at room temperature for 24 h. The reaction mixture was poured into water, neutralised with ammonium hydroxide solution, and extracted with DCM. Solvent was removed under vacuum and crude product was purified by column chromatography to give a brown product (1.60 g, 2.84 mmol, 83 %); mp > 300 °C; $\nu_{max}$ ($cm^{-1}$) 2953, 1602, 1516, 1462, 1440, 1433, 1404, 1377, 1236, 1193, 1182, 1163, 1109, 1039, 1029, 904, 867, 854, 835,802, 763, 752, 702; $^{1}H$ NMR (500 MHz, $CDCl_3$) $\delta$ 7.63 (s, 2H), 7.56(s, 2H), 6.96 (s, 4H), 3.84 (s, 12H), 2.47 (s, 6H), 1.70 (s, 4H), 1.31(s, 12H); $^{13}C$ NMR (126 MHz, $CDCl_3$) $\delta$ 146.05, 144.94, 143.83, 140.72, 129.41, 124.43, 117.27, 105.89, 56.32, 47.31, 35.03, 34.32, 32.37, 14.08; HRMS (EI, *m/z*) calculated 562.32 found 562.3069 [$M^+$].

## 5,8,8,11,11,14-hexamethyl-5,8,9,10,11,14-hexahydro-5,14-[1,2]benzenopentacene-2,3,18,19-tetraol (39)

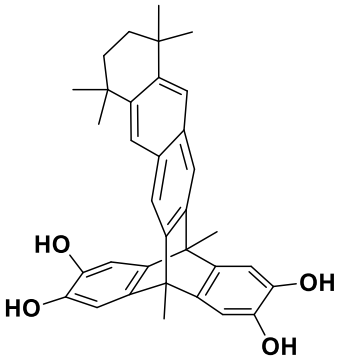


General procedure **(3)** was followed by using 2,3,18,19-tetramethoxy-5,8,8,11,11,14-hexamethyl-5,8,9,10,11,14-hexahydro-5,14[1,2]benzenopentacene **(38)** (1.5 g, 2.67 mmol), anhydrous DCM (40 mL) and $BBr_3$ (2 g, 8.01 mmol) to give a white powder (1g, 1.97 mmol, 67%); mp > 300 °C; $\nu_{max}$ ($cm^{-1}$) 3250, 1622, 1462, 1444, 1375, 1361, 902, 875, 860, 839, 812, 771, 761; $^{1}H$ NMR (500 MHz, acetone-$d_6$) δ 7.73 (s, 2H), 7.57 (s, 2H), 6.89 (s, 4H), 2.32 (s, 6H), 1.74 (s, 4H), 1.33 (s, 12H); $^{13}C$ NMR (126 MHz, acetone-$d_6$) δ 146.95, 144.12, 142.23, 141.08, 130.70, 125.40, 117.77, 109.79, 47.48, 35.88, 35.01, 32.76, 14.59; HRMS (EI, *m/z*) calculated 506.25 found 506.2456 [$M^+$].

## 2,3,6,7,12,13-hexabromotriptycene (40)

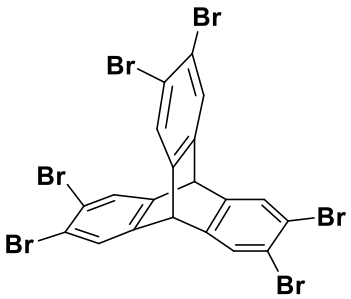


Bromine (11.86 g, 74 mmol) was added dropwise to a solution of iron powder (20 mg), triptycene (3 g, 11.8 mmol) and anhydrous dichloromethane (45 ml) and the reaction mixture was refluxed for 18 hours. The reaction mixture was allowed to reach room temperature, then poured into water, extracted with dichloromethane, dried over $MgSO_4$ and the solvent was evaporated under

reduced pressure. The crude product was triturated in hexane and filtered to give a white powder (6 g, 8.2 mmol, 71 %); mp > 300 °C; $v_{max}$ ($cm^{-1}$) 3030, 2972, 1440, 1357, 1097, 891, 883, 839, 802, 717; $^{1}H$ NMR (500 MHz, $CDCl_3$) $\delta$ 7.61 (s, 6H), 5.22 (s, 2H); $^{13}C$ NMR (126 MHz, $CDCl_3$) $\delta$ 144.34, 129.47, 122.17, 51.49.

**2,3,6,7,12,13-hexamethoxytriptycene (41)**

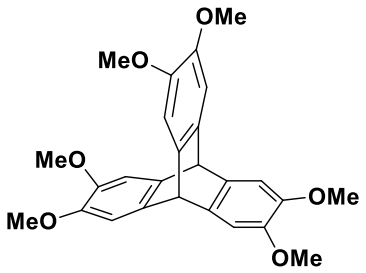


A solution of sodium methoxide (66.6 g, 370 mmol) was added to a solution of 2,3,6,7,12,13-hexabromotriptycene (3 g, 4.1 mmol) **(40)** in anhydrous toluene (150 ml). The temperature was raised to 110 °C then copper(I)bromide (0.2 g, 1.4 mmol) was added. The reaction mixture was refluxed for 24 hours under nitrogen. Then, the mixture was allowed to reach room temperature, poured into water, washed with *aq* HCl (1M), extracted with dichloromethane, dried over $MgSO_4$ and the solvent evaporated under reduced pressure. The crude product was purified by column chromatography on silica (ethyl acetate:petroleum ether, 0.1:1) to give a white powder (1.55 g, 3.6 mmol, 86 %); mp > 300 $^{o}C$; $v_{max}$ ($cm^{-1}$) 3008, 2949, 2829, 1614, 1585, 1485, 1462, 1402, 1280, 1220, 1184, 1159, 1143, 1100, 1016, 981, 877, 798, 773, 742, 607; $^{1}H$ NMR (500 MHz, $CDCl_3$) $\delta$ 7.00 (s, 6H), 5.18 (s, 2H), 3.84 (s, 18H); $^{13}C$ NMR (126 MHz, $CDCl_3$) $\delta$ 146.21, 139.37, 108.85, 56.68, 53.60; HRMS (EI, *m/z*) calculated 434.17239 found 434.17056 [$M^{+}$].

## 2,3,6,7,12,13-hexahydroxytriptycene (42)

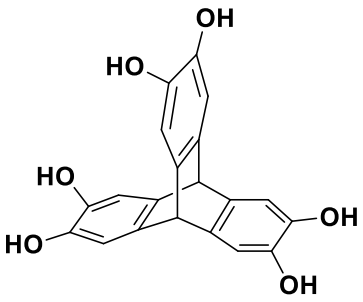


General procedure **(3)** was followed by using 2,3,6,7,12,13-hexamethoxytriptycene **(41)** (1 g, 2.3 mmol), anhydrous DCM (25 mL) and $BBr_3$ (5.3 g, 21.1 mmol) to give a white powder (0.7 g, 2 mmol, 87.5 %); mp > 300 °C; $\nu_{max}$ ($cm^{-1}$) 3466, 3348, 2962, 1693, 1608, 1485, 1452, 1342, 1234, 1176, 1138, 1093, 1053, 947, 842, 808, 790, 752, 721; $^1H$ NMR (500 MHz, DMSO) $\delta$ 6.25 (s, 6H), 4.42 (s, 2H); $^{13}C$ NMR (126 MHz, acetone-$d_6$) $\delta$ 141.94, 139.88, 112.35, 53.07; HRMS (EI, *m/z*) calculated 350.07849 found 350.07745 [$M^+$].

## 4,5-dichlorophthalic acid anhydride (43)

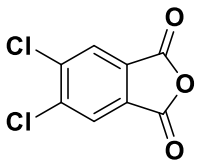


Following a literature procedure[ref], acetic anhydride (100 mL) was added to 4,5-dichlorophthalic acid (25 g, 106.3 mmol) and the solution was refluxed for 5 h. The reaction mixture was cooled to room temperature and white solid was precipitated. The precipitate was collected by filtration, washed with petroleum ether and dried to give a colourless solid (20 g, 92.17 mmol, 92%); mp 195 °C; $\nu_{max}$ ($cm^{-1}$) 3095, 3025, 1825, 1775, 1625, 1475, 912, 902, 731, 713; $^1H$ NMR (500 MHz, $CDCl_3$) $\delta$ 8.11 (s, 2H); $^{13}C$ NMR (126 MHz, $CDCl_3$) $\delta$ 160.56, 141.63, 130.18, 127.32; HRMS (EI, *m/z*) calculated 215.93755, found 215.93736 [$M^+$].

**N-phenyl-4,5-dichlorophthalimide (44)**

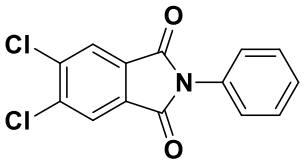

According to a reported procedure[159], a mixture of 4,5-dichlorophthalic acid anhydride **(43)** (18 g, 82.95 mmol), glacial acetic acid (120 mL), and *N,N*-dimethylacetamide (100 mL) were cooled to 10 °C. To this, a solution of aniline (7.73 g, 82.95 mmol) in *N,N*-dimethylacetamide (20 mL) was added dropwise. Then, the reaction solution was stirred under a nitrogen atmosphere at 150 °C for 8 hours. Then, the reaction solution was cooled to room temperature and a white solid was precipitated. The precipitate was collected by filtration, washed with water and dried under reduced pressure to give colourless crystals (21 g, 71.89 mmol, 86.67%); mp 215 °C; $\nu_{max}$ ($cm^{-1}$) 3062, 3045, 1786, 1703, 1600, 1535, 910, 898, 860, 842, 785, 736, 727, 682; $^{1}H$ NMR (500 MHz, DMSO) $\delta$ 8.29 (s, 2H), 7.56-7.53 (m, 2H), 7.47-7.43 (m, 3H); $^{13}C$ NMR (126 MHz, DMSO) $\delta$ 165.23, 137.46, 131.59, 128.91, 128.30, 127.24, 125.53; HRMS (EI, *m/z*) calculated 290.98484 found 290.98440 [$M^{+}$].

***N,N'*-diphenyl thianthrene-2,3,7,8-tetracarboxyl bisimide (45)**

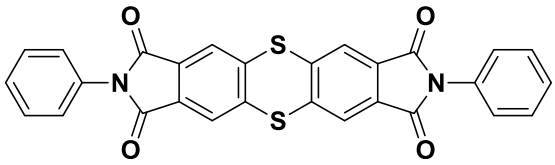

According to a reported procedure[19], a mixture of *N,N*-dimethylacetamide (140 mL), *N*-phenyl-4,5-dichloro-phthalimide **(44)** (10 g, 34.23 mmol), thiobenzamide (6.04g, 44.02 mmol) and anhydrous potassium carbonate (6.08 g, 44.02 mol) was refluxed under a nitrogen atmosphere at 150 °C for 4 hours. Then, the reaction solution was cooled to room temperature, poured into distilled water. The precipitate was collected by filtration, washed with

water, refluxed in methanol and dried to give a yellow solid (8 g, 15.79 mmol, 46%); mp > 300 °C; $v_{max}$ ($cm^{-1}$) 3487, 3059, 1701, 1598, 1500, 1303, 1290, 1226, 1116, 889, 862, 738, 727, 682, 615, 599; $^{1}H$ NMR (500 MHz, DMSO) $\delta$ 8.19 (s, 4H), 7.55-7.43 (m, 10H); $^{13}C$ NMR (126 MHz, DMSO) $\delta$ 165.74, 140.36, 131.93, 131.65, 128.89, 128.20, 127.23, 123.53; HRMS (EI, *m/z*) calculated 506.03895 found 506.03949 [$M^{+}$].

**Thianthrene-2,3,7,8-tetracarboxylic acid (46)**

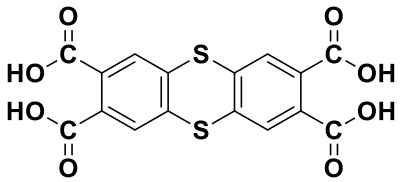

According to a reported procedure[19], sodium hydroxide solution (2 M, 150 ml) was added to *N,N'*-diphenyl thianthrene-2,3,7,8-tetracarboxyl bisimide **(45)** (13 g, 25.66 mmol) and the reaction solution was refluxed under a nitrogen atmosphere for 24 hours. After cooling to room temperature, insoluble matter was filtered off, 10% aqueous hydrochloric acid was added and solid was precipitated. The precipitate was collected by filtration, washed with water and dried in oven at 100 °C to give colourless solid (9.5 g, 24.21 mmol, 94%); mp > 300 °C; $v_{max}$ ($cm^{-1}$) 2500-3400 (br), 3100, 1714, 1269, 1224, 904, 887, 821, 806, 792, 771, 603; $^{1}H$ NMR (500 MHz, DMSO) $\delta$ 7.87 (s, 4H); $^{13}C$ NMR (126 MHz, DMSO) δ 166.81, 135.81, 132.47, 128.10; HRMS (EI, *m/z*): calculated 392.97334 found 392.97360 [$M^{+}$].

**Thianthrene-2,3,7,8-tetracarboxylic acid anhydride (47)**

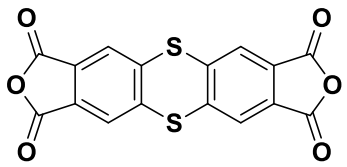

According to a reported procedure[19], acetic anhydride (40 mL) was added to thianthrene-2,3,7,8-tetracarboxylic acid **(46)** (2 g, 5.10 mmol) and the mixture

was refluxed under a nitrogen atmosphere for 6 hours at 100 °C. The reaction solution was cooled to room temperature and the solid was collected by filtration, washed with hexane and dried in oven at 100 °C to give a yellow solid (1.62 g, 4.55mmol, 89%); mp > 300 °C; $\nu_{max}$ ($cm^{-1}$) 3084, 3010, 1797, 1770, 1598, 1581, 1097, 1076, 950, 894, 877, 704; $^{1}H$ NMR (400 MHz, DMSO-$d_6$) $\delta$ 8.49 (s, 4H); $^{13}C$ NMR (126 MHz, DMSO-$d_6$) $\delta$ 161.94, 141.74, 131.71, 125.21; HRMS (EI, *m/z*) calculated 355.94438 found 355.94505 [$M^+$].

**Thianthrene-2,3,7,8-tetracarboxylic acid anhydride-5,5,10,10-tetraoxide (48)**

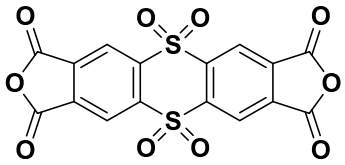

According to a reported procedure[160], thianthrene-2,3,7,8-tetracarboxylic acid anhydride (1 g, 2.81 mmol) **(47)** was heated to reflux in 30% $H_2O_2$ solution (10ml) for 5 hours. Then, the reaction solution was cooled to room temperature and a solid was precipitated. The precipitate was collected by filtration, washed with dichloromethane and dried at 100 °C to give colourless solid (0.99 g, 2.36 mmol, 84%); mp > 300 °C; $\nu_{max}$ ($cm^{-1}$) 3481, 3315, 1766, 1716, 1668, 1327, 1159, 1136, 1087, 914, 875, 800, 786, 754, 707; $^{1}H$ NMR (500 MHz, DMSO-$d_6$) $\delta$ 8.58 (s, 4H); $^{13}C$ NMR (126 MHz, DMSO-$d_6$) $\delta$ 166.04, 139.92, 138.17, 126.45; HRMS (EI, *m/z*) calculated 419.92404 found 419.92566 [$M^+$].

**2,5-diphenylhexane-2,5-diol (49)**

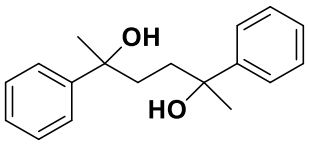

According to a reported procedure[161], bromobenzene (44 ml, 411 mmol) was added dropwise to a mixture of magnesium turnings (10 g, 411 mmol) and an

iodine crystal (~5 mg) in anhydrous tetrahydrofuran (200 ml) and the reaction mixture was refluxed under a nitrogen atmosphere until all magnesium had been consumed. A solution of 2,5-hexanedione (24 ml, 206 mmol) was then slowly added and the mixture was refluxed for a further 1 h before cooling to room temperature. The mixture was poured over crushed ice, extracted with diethyl ether and the solvent was removed under vacuum to give yellow oil. The resulting yellow oil was dissolved in boiling acetone, precipitated with hexane and filtered to give a colourless powder (36.10 g, 133 mmol, 65%); mp 121-122 ºC; $\nu_{max}$ ($cm^{-1}$): 3398 (br), 2939, 2864; $^{1}H$ NMR (400 MHz, $CDCl_3$) $\delta$ 7.35 (m, 6H), 7.24 (m, 2H), 2.43 (s, br, 2H), 1.88 (m, 2H), 1.73 (m, 2H), 1.54 (s, 3H), 1.49 (s, 3H); $^{13}C$ NMR (101 MHz, $CDCl_3$) $\delta$ 147.85, 147.60, 128.18, 126.52, 126.50, 124.86, 124.80, 74.53, 74.41, 38.10, 37.95, 31.32, 30.48.

**9,10-dimethyl-9,10-dihydro-9,10-ethanoanthracene (50)**

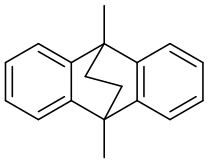

According to a reported procedure[137], under a nitrogen atmosphere, aluminium trichloride (10.80 g, 81 mmol) was added slowly to the cold mixture (0 – 10 °C) of 2,5-diphenylhexane-2,5-diol **(49)** (22 g, 81 mmol) and toluene (70 ml). Then the mixture was stirred for 1 h, followed by warming the reaction to room temperature and stirring for a further 1 hour. Then, the mixture was refluxed for 24 hours before cooling to room temperature. The reaction was poured over crushed ice, extracted with chloroform and the solvent removed under vacuum. The crude product was subjected to column chromatography (hexane) and the resulting oil was crystallised from hexane to give colourless crystals (6.77 g, 29 mmol, 36%); mp 129-130 ºC; $\nu_{max}$ ($cm^{-1}$) 2924, 2857; $^{1}H$ NMR (400 MHz, $CDCl_3$) $\delta$ 7.51 (m, 4H), 7.36 (m, 4H), 2.17 (s, 6H), 1.83 (s, 4H); $^{13}C$ NMR (101 MHz, $CDCl_3$) $\delta$ 146.56, 125.42, 120.51, 41.93, 36.05, 18.57.

**General procedure (10) for dinitro compounds**

According to a literature procedure[1], trifluoroacetic anhydride was added dropwise to a mixture of potassium nitrate and the corresponding substrate in acetonitrile and the reaction mixture was stirried for 24 hours. Then, the solvent was removed under vacuum and the residue stirred was in water. The product was extracted with chloroform and subjected to column chromatography (chloroform) to obtain the nitro product.

**9,10-dimethyl-9,10-dihydro-2,6(7)-dinitro-9,10-ethanoanthracene (51)**

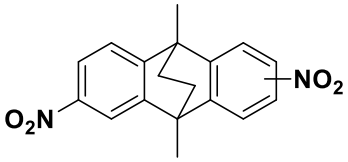


General procedure **(10)** was followed by using trifluoroacetic anhydride (37.5 ml, 270 mmol), potassium nitrate (8.15 g, 81 mmol) and 9,10-dimethyl-9,10-dihydro-9,10-ethanoanthracene **(50)** (9 g, 38.5 mmol) in acetonitrile (350 ml) to give a powder (11.46 g, 35.30 mmol, 92%); mp 185-186 ºC; $\nu_{max}$ ($cm^{-1}$): 2965, 2922, 2851, 1522, 1343; $^1H$ NMR (500 MHz, $CDCl_3$) $\delta$ 8.14 (m, 2H, Ar H), 8.06 (d, $J$ = 8.30 Hz, 1H, Ar H), 8.05 (d, $J$ = 8.30 Hz, 1H, Ar H), 7.48 (d, $J$ = 4.83 Hz, 1H, Ar H), 7.46 (d, $J$ = 4.83 Hz, 1H), 2.10 (m, 6H) 1.73 (s, 4H); $^{13}C$ NMR (125 MHz, $CDCl_3$) $\delta$ 152.40, 151.97, 146.96, 146.53, 146.48, 121.67, 121.63, 121.56, 116.15, 116.01, 43.18, 42.90, 42.63, 34.99, 34.91, 34.83, 18.18, 18.05, 17.92.

**9,10-dihydro-2,6(7)-diamino-9,10-ethanoanthracene (52)**

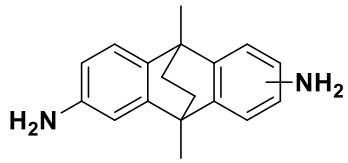


General procedure **(2)** was followed by using 9,10-dimethyl-9,10-dihydro-2,6(7)-dinitro-9,10-ethanoanthracene **(51)** (4.10 g, 13 mmol) in diethyl ether (200 ml), Raney nickel (~35 mg) and hydrazine monohydrate (12.3 ml, 253 mmol) to give a colourless powder; mp 62-64 ºC; $\nu_{max}$ ($cm^{-1}$): 3456, 3342,

3261, 2958, 2933, 2857, 1619, 1476; $^{1}$H NMR (500 MHz, $CDCl_3$) $\delta$ 7.03 (d, $J$ = 7.9 Hz, 2H), 6.66 (d, $J$ = 3.30 Hz, 1H), 6.65 (d, $J$ = 3.30 Hz, 1H), 6.45 (m, 2H), 3.39 (s, br, 4H), 1.88 (m, 6H), 1.61 (s, 4H); $^{13}$C NMR (125 MHz, $CDCl_3$) $\delta$ 148.33, 147.53, 143.83, 143.66, 137.80, 136.93, 120.99, 120.67, 111.40, 111.19, 108.77, 108.45, 65.85, 41.72, 41.04, 40.37, 36.43, 36.20, 36.00, 18.42, 15.29.

**9,9′-bis(4-aminophenyl) fluorene (BAPF) (53)**

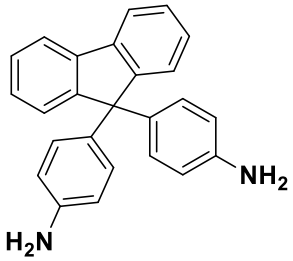


According to a reported procedure[139], a mixture of 9-fluorenone (1.89 g, 10.49 mmol), aniline hydrochloride (1.94 g, 15 mmol), aniline (12 mL), and toluene (5 mL) were refluxed for 2 hours while removing the generated water out of the reaction system by azeotropic distillation with toluene. Then the resulting reaction mixture was cooled to room temperature, followed by adding 35 mL 10 % NaOH aqueous solution and stirring for 0.5 h. The crude product was extracted with chloroform, recrystallised from toluene and dried under vacuum at room temperature for 24 h to give a white powder (1.1g, 3.16 mmol, 30%); $\nu_{max}$ ($cm^{-1}$) 3429, 3350, 3250, 3025, 1614, 1508, 835, 821, 812, 729; $^{1}$H NMR (400 MHz, $CDCl_3$) $\delta$ 7.72 (d, 2H), 7.38-7.22 (m, 10H), 6.99 (d, 4H), 6.53 (d, 4H); $^{13}$C NMR (126 MHz, $CDCl_3$) δ 152.12, 144.69, 139.81, 136.01, 128.94, 127.41, 126.92, 125.88, 119.85, 114.72, 64.02. HRMS (EI, *m/z*): calculated 348.16210 found 348.16387 [$M^+$].

**1,3,3-trimethyl-1-phenylindane (54)**

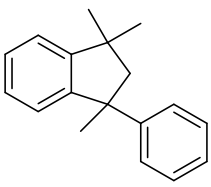

According to a reported procedure[162], a solution of α-methyl styrene (20.0 g, 22.0 ml) in *n*-hexane (300 ml) was filtered through basic alumina to remove 4-tert-butylcatechol (an free radical inhibitor) and the solvent was removed under vacuum. Purified α-methyl styrene (10.0 g, 11.0 ml, 85 mmol) was added drop-wise to trifluoroacetic acid (20.0 ml) with vigorous stirring for 30 min. Then, the mixture was quenched in water (200 ml), extracted with chloroform and washed with saturated sodium hydrogen carbonate solution. The crude product was distilled under reduced pressure (1.2 mbar) and the fraction boiling at 112-113 ºC was collected to give a colourless liquid (2.35g, 9.94 mmol, 11.69 %); mp 50 °C; $^{1}$H NMR (400 MHz, $CDCl_3$) δ 7.44- 7.25 (m, 9H), 2.56 (d, 1H), 2.36 (d, 1H), 1.84 (s, 3H), 1.50 (s, 3H), 1.19 (s, 3H); $^{13}$C NMR (126 MHz, $CDCl_3$) *δ* 152.49, 151.33, 149.03, 128.40, 127.65, 127.05, 125.85, 125.15, 122.80, 58.75,51.10, 43.20, 31.30, 30.50; HRMS (EI, *m/z*) calculated 236.15595 found 236.15402 [$M^+$].

**6,(7)-nitro-1,3,3-trimethyl-1-(4-nitrophenyl)indane (55)**

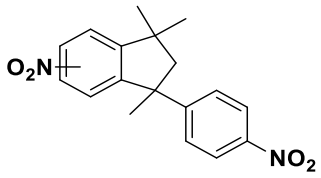


General procedure **(10)** was followed by using trifluoroacetic anhydride (14.31 g, 68.13mmol), potassium nitrate (1.97 g, 19.48 mmol) and 1,3,3-trimethyl-1-phenylindane **(54)** (2.3 g, 9.73 mmol) in acetonitrile (50 ml) to give a yellow solid (1.5 g, 4.59 mmol, 47.17%); $\nu_{max}$ ($cm^{-1}$) 2960, 1602, 1591, 1510, 1473, 1456, 1442, 1325, 904, 893, 854, 835, 808, 796, 754, 748, 738, 725, 700; $^{1}$H NMR (500 MHz, $CDCl_3$) *δ* 8.15 (m, 4H), 7.31 (m, 3H), 2.52 (d, 1H), 2.37 (d, 1H), 1.78 ( d, 3H), 1.41 ( d, 3H), 1.10 (d, 3H); $^{13}$C NMR (126 MHz, $CDCl_3$) *δ* 160.00, 157.30, 155.15, 154.44, 149.56, 148.86, 148.27, 146.71, 127.75, 125.92, 124.17, 124.05, 123.33, 120.62, 118.96, 59.34, 59.24, 51.78, 51.48, 43.82, 43.60, 30.88, 30.62, 30.44; HRMS (EI, *m/z*) calculated 326.12611 found 326.12593 [$M^+$].

**6,(7)-amino-1,3,3-trimethyl-1-(4-aminophenyl)indane (56)**

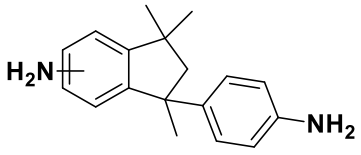


General procedure **(2)** was followed by using 6,(7)-nitro-1,3,3-trimethyl-1-(4-nitrophenyl)indane **(55)** (2.00 g, 6.13 mmol) in ethanol (100 ml ), Raney nickel (~35 mg) and hydrazine monohydrate (5.00 g, 99.88 mmol). The organic phase was extracted with diethyl ether to give the desired product (1.6 g, 6.00 mmol, 92%); mp 45 °C; $\nu_{max}$ ($cm^{-1}$) 3434, 3349, 3215, 3006, 2955, 2861, 1618, 1511; $^{1}H$ NMR (500 MHz, $CDCl_3$) $\delta$ 7.02 (m, 3H), 6.53 (m, 4H), 2.32 (m, 1H) , 2.11 (m, 1H), 1.65 (m, 3H), 1.26 (m, 3H), 1.05 (m, 3H); $^{13}C$ NMR (126 MHz, $CDCl_3$) $\delta$ 153.70, 151.00, 148.33, 147.97, 146.42, 146.35, 141.95, 140.94, 140.45, 138.78, 127.89, 127.84, 125.82, 123.24, 112.68, 112.61, 112.09, 109.44, 106.75, 60.25, 60.14, 60.03, 50.35, 49.60, 43.02, 42.36, 31.61, 31.42, 31.27, 31.06, 30.89, 30.63; LRMS (EI, *m/z*) calculated 266.18 found 266.18 [$M^+$].

**TB-polystyrene polymers (TB-PS-57)**

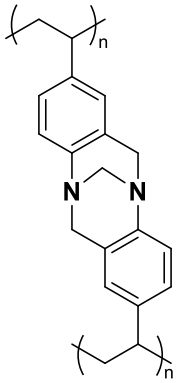


**General procedure (11) of TB-polystyrene polymers**

According to a literature procedure[114], poly(4-aminostyrene) was dissolved in dimethoxymethane and the solution was cooled in an ice bath. To this, trifluoroacetic acid was added dropwise and the reaction was stirred under a

nitrogen atmosphere for 72 hours at room temperature. The reaction solution was poured into ammonium hydroxide solution and stirred for 3 hours. The resulting solid was collected by filtration, washed with water, refluxed in acetone, chloroform and methanol, and dried in a vacuum oven.

General procedure **(11)** was followed to synthesise **TB-PS-57a** by using poly(4-aminostyrene) **(2a)** (0.40 g, 3.36 mmol), dimethoxymethane (0.86 g, 11. mmol) and trifluoroacetic acid (10 ml) to give the product as a brown powder (0.4g, 1.46 mmol, 43%, based on repeating unit) which was insoluble in all common solvents; $\nu_{max}$ ($cm^{-1}$) 3022, 2917, 1613, 1516, 1492, 1450, 1314, 1260, 1205, 900, 821, 699; BET surface area = 0.1 $m^2$ $g^{-1}$; TGA (nitrogen): weight loss due to thermal degradation started at 384 °C.

General procedure **(11)** was followed to synthesise **TB-PS-57b** by using poly(4-aminostyrene) **(2b)** (1.02 g, 8.56 mmol), dimethoxymethane (2.58 g, 33.88 mmol) and trifluoroacetic acid (25 ml) to give the product as a brown powder (1.08g, 3.49 mmol, 46%, based on repeating unit) which was insoluble in all common solvents; BET surface area = 0.3 $m^2$ $g^{-1}$; TGA (nitrogen): weight loss due to thermal degradation started at 383 °C.

General procedure **(11)** was followed to synthesise **TB-PS-57c** by using poly(4-aminostyrene) **(2c)** (1.08 g, 9.06 mmol), dimethoxymethane (2.58 g, 33.88 mmol) and trifluoroacetic acid (25 ml) to give the product as a brown powder (0.95g, 3.46 mmol, 38%, based on repeating unit) which was insoluble in all common solvents; BET surface area = 10.5 $m^2$ $g^{-1}$; TGA (nitrogen): weight loss due to thermal degradation started at 382 °C.

General procedure **(11)** was followed to synthesise **TB-PS-d** by using poly(4-aminostyrene) **(2d)** (1.30 g, 10.91mmol), dimethoxymethane (4.12 g, 54.20 mmol) and trifluoroacetic acid (30 ml) to give the product as a brown powder (1.30 g, 4.74 mmol, 44%, based on repeating unit) which was insoluble in all

common solvents; BET surface area = 14.9 $m^2$ $g^{-1}$; TGA (nitrogen): weight loss due to thermal degradation started at 365 °C.

General procedure **(11)** was followed to synthesise **TB-PS-57e** by using poly(4-aminostyrene) **(2e)** (1.14 g, 9.57 mmol), dimethoxymethane (3.61 g, 47.44 mmol) and trifluoroacetic acid (15 ml) to give the product as a brown powder (1g, 3.64 mmol, 38%, based on repeating unit) which was insoluble in all common solvents; BET surface area = 25.5 $m^2$ $g^{-1}$; TGA (nitrogen): weight loss due to thermal degradation started at 396 °C.

**General procedure (12) polybenzodioxin polymers synthesis**

According to a reported procedure[130], 2,3,7,8-tetrafluoro-5,5',10,10'-tetraoxide-thianthrene thianthrene (1 equivalent) and bis catechol monomer (1 equivalent) were dissolved in N-methyl-2-pyrrolidone. To this, excess of potassium carbonate was added and the reaction mixture was stirred under a nitrogen atmosphere at the desired temperature for required time. Then, the reaction mixture was poured into water. The precipitate was collected by filtration, refluxed in water, acetone and methanol, and dried in the vacuum oven at 100 °C.

**TOT-TTSBI-58**

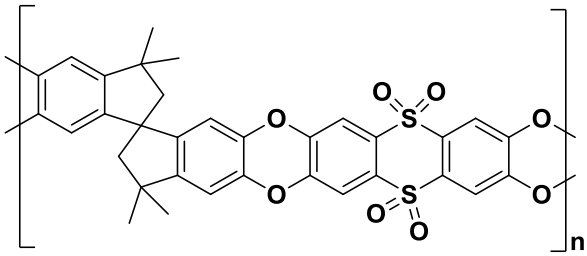


The general procedure **(12)** was followed to prepare **TOT-TTSBI-58a** by reacting 2,3,7,8- tetrafluoro-5,5',10,10'-tetraoxidethianthrene **(4)** (0.500 g, 1.419 mmol), 5,5',6,6'-tetrahydroxy-3,3,3',3'-tetramethylspirobisindane (TTSBI), (0.483 g, 1.419 mmol), *N*-methyl-2-pyrrolidone (20 ml) and potassium carbonate (3.1 g, 22.70 mmol) at 160 °C for 2 hours to give a

polymer (0.85 g, 1.39 mmol, 98%), which was soluble in quinoline; $v_{max}$ ($cm^{-1}$) 2953, 1566, 1475, 1325, 1275, 1170, 1138, 1107, 889, 719, 704; BET surface area = 573 $m^2$ $g^{-1}$; TGA (nitrogen): weight loss due to thermal degradation started at 441 °C.

The general procedure **(12)** was followed to synthesise **TOT-TTSBI-58b** by reacting 2,3,7,8- tetrafluoro-5,5',10,10'-tetraoxidethianthrene **(4)** (1 g, 2.60 mmol), 5,5',6,6'-tetrahydroxy-3,3,3',3'-tetramethylspirobisindane (TTSBI), (0.886 g, 2.60 mmol), *N*-methyl-2-pyrrolidone (20 ml) and potassium carbonate (5.7 g, 41.6 mmol) 160 °C for 2 hours to give a polymer (1.44 g, 2.35 mmol, 91 %) which was soluble in quinoline; $v_{max}$ ($cm^{-1}$) 2954, 1566, 1469, 1315, 1269, 1170, 1136, 1107, 889, 742, 717, 702; BET surface area = 361 $m^2$ $g^{-1}$; TGA (nitrogen): weight loss due to thermal degradation started at 436 °C.

The general procedure **(12)** was followed to synthesise **TOT-TTSBI-58c** by reacting 2,3,7,8- tetrafluoro-5,5',10,10'-tetraoxidethianthrene **(4)** (1 g, 2.79 mmol), 5,5',6,6'-tetrahydroxy-3,3,3',3'-tetramethylspirobisindane (TTSBI), (0.949 g, 2.79 mmol), *N*-methyl-2-pyrrolidone (25ml) and potassium carbonate (6.16 g, 44.64 mmol) at 70 °C for 72 hours to give a polymer (1.68 g, 2.74 mmol, 98%) which was soluble in quinoline; $v_{max}$ ($cm^{-1}$) 2975, 1566, 1469, 1315, 1269, 1172, 1138, 1107, 889, 744, 719, 704; solid state $^{13}C$ NMR (101 MHz, $CDCl_3$) δ 145.97, 140.42, 136.91, 112.84, 57.62, 43.26, 30.08; BET surface area = 597 $m^2$ $g^{-1}$.

The general procedure **(12)** was followed to synthesise **TOT-TTSBI-58d** by reacting 2,3,7,8-tetrafluoro-5,5',10,10'-tetraoxidethianthrene **(4)** (0.5g, 1.419 mmol), 5,5',6,6'-tetrahydroxy-3,3,3',3'-tetramethylspirobisindane (TTSBI), (0.483 g, 1.419 mmol), *N*-methyl-2-pyrrolidone (25ml) and potassium carbonate (1.56 g, 11.35 mmol) were reacted at 160 °C for 45 minutes to give a polymer (0.69 g, 1.13 mmol, 78 %) which was soluble chloroform; BET

surface area = 576 $m^2$/g; TGA (nitrogen): weight loss due to thermal degradation started at 465 °C.

**TOT-SBC-59**

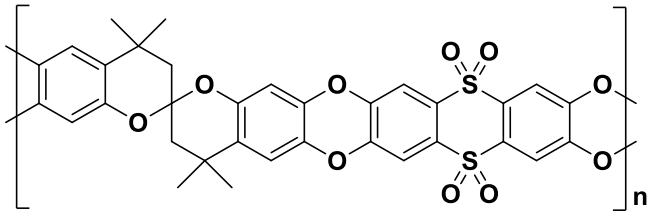

The general procedure **(12)** was followed to synthesise **TOT-SBC-59a** by reacting 2,3,7,8-tetrafluoro-5,5',10,10'-tetraoxidethianthrene **(4)** (0.5 g, 1.419 mmol), 6,6',7,7'-tetrahydroxy-4,4,4',4'-tetramethyl-2,2'-spirobischromane (0.528 g, 1.419 mmol), *N*-methyl-2-pyrrolidone (20 ml) and potassium carbonate (3.14 g, 22.7 mmol) at 95 °C for 24 hours to give a pale yellow powder (0.55 g, 0.85 mmol, 60%) which was soluble in quinoline; $\nu_{max}$ ($cm^{-1}$) 3975, 1568, 1327, 1292, 1242, 1111, 1150, 1475, 908, 875, 725, 704; solid state $^{13}C$ NMR (101 MHz) $\delta$ 147.06, 136.11, 128.90, 113.79, 106.27, 98.22, 47.49, 31.28; BET surface area = 466 $m^2$ $g^{-1}$; TGA (nitrogen): weight loss due to thermal degradation started at 429°C.

The general procedure **(12)** was followed to synthesise **TOT-SBC-59b** by reacting 2,3,7,8-tetrafluoro-5,5',10,10'-tetraoxidethianthrene **(4)** (0.5 g, 1.419 mmol), 6,6',7,7'-tetrahydroxy-4,4,4',4'-tetramethyl-2,2'-spirobischromane (0.528 g, 1.419 mmol), N-methyl-2-pyrrolidone (20 ml) and potassium carbonate (3.14 g, 22.7 mmol) at 160 °C for 17 hours to give a pale yellow powder (0.75 g, 1.16 mmol, 82%) which was soluble in quinoline; $\nu_{max}$ ($cm^{-1}$) 2975, 1568, 1471, 1427, 1327, 1292, 1242, 1132, 908, 875, 719; BET surface area = 487 $m^2$ $g^{-1}$; TGA (nitrogen): weight loss due to thermal degradation started at 411 °C.

The general procedure **(12)** was followed to synthesise **TOT-SBC-59c** by reacting 2,3,7,8-tetrafluoro-5,5',10,10'-tetraoxidethianthrene **(4)** (0.5 g, 1.419 mmol), 6,6',7,7'-tetrahydroxy-4,4,4',4'-tetramethyl-2,2'-spirobischromane (0.528 g,

1.419 mmol), *N*-methyl-2-pyrrolidone (20 ml) and potassium carbonate (3.14 g, 22.7 mmol) at 70 °C for 72 hours to give a pale yellow powder (0.74 g, 1.15 mmol, 81%) which was soluble in quinoline; $\nu_{max}$ ($cm^{-1}$) 2925, 1590, 1471, 1427, 1328, 1292, 1242, 1132, 908, 875, 719; solid state $^{13}C$ NMR (101 MHz) δ 146.66, 136.24, 129.30, 113.74, 105.84, 98.51, 46.53, 31.38; BET surface area = 471 $m^2$ $g^{-1}$; TGA (nitrogen): weight loss due to thermal degradation started at 415 °C.

The general procedure **(12)** was followed to synthesise **TOT-SBC-59d** by reacting 2,3,7,8-tetrafluoro-5,5',10,10'-tetraoxidethianthrene **(4)** (0.5 g, 1.419 mmol), 6,6',7,7'-tetrahydroxy-4,4,4',4'-tetramethyl-2,2'-spirobischromane (0.528 g, 1.419 mmol), *N*-methyl-2-pyrrolidone (20 ml) and potassium carbonate (3.14 g, 22.7 mmol) were reacted at 160 °C for 2 hours to give a pale yellow powder (0.82 g, 1.27 mmol, 90%) which was soluble in quinoline; $\nu_{max}$ ($cm^{-1}$) 2975, 1568, 1471, 1427, 1327, 1292, 1242, 1132, 1111, 908, 875, 719; BET surface area = 500 $m^2$ $g^{-1}$; TGA (nitrogen): weight loss due to thermal degradation started at 403 °C.

The general procedure **(12)** was followed to synthesise **TOT-SBC-59e** by reacting 2,3,7,8-tetrafluoro-5,5',10,10'-tetraoxidethianthrene **(4)** (1 g, 2.747 mmol), 6,6',7,7'-tetrahydroxy-4,4,4',4'-tetramethyl-2,2'-spirobischromane (1.023 g, 2.747 mmol), *N*-methyl-2-pyrrolidone (20 ml) and potassium carbonate (3.04 g, 21.9 mmol) were reacted at 160 °C for 45 minutes to give a pale yellow powder (1.64 g, 2.54 mmol, 93%) which was soluble in quinoline; Solid state $^{13}C$ NMR (101 MHz) δ 147.09, 136.04, 128.86, 113.83, 105.77, 98.60, 46.59, 31.40; BET surface area = 374 $m^2$/g; TGA (nitrogen): weight loss due to thermal degradation started at 420 °C.

**TOT-EA-60**

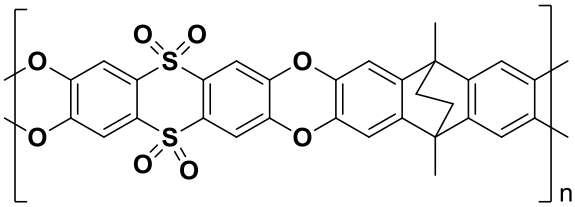

The general procedure **(12)** was followed to synthesise **TOT-EA-60a** by reacting 2,3,7,8-tetrafluoro-5,5',10,10'-tetraoxidethianthrene **(4)** (1 g, 2.754 mmol), 9,10-dimethyl-9,10-ethano-9,10-dihydro-2,3,6,7-tetrahydroxyanthracene **(9)** (0.851 g, 2.754 mmol), *N*-methyl-2-pyrrolidone (35 ml) and potassium carbonate (3.04 g, 22.03 mmol) at 70 °C for 72 hours to give a beige powder (1.45 g, 2.53 mmol, 92%) which was insoluble in all common solvents; $v_{max}$ ($cm^{-1}$) 2975, 1562, 1454, 1311, 1269, 1170, 1136, 1109, 889, 719, 702; BET surface area = 713 $m^2$ $g^{-1}$; TGA (nitrogen): weight loss due to thermal degradation started at 405 °C.

The general procedure **(12)** was followed to synthesise **TOT-EA-60b** by reacting 2,3,7,8-tetrafluoro-5,5',10,10'-tetraoxidethianthrene **(4)** (1 g, 2.838 mmol), 9,10-dimethyl-9,10-ethano-9,10-dihydro-2,3,6,7-tetrahydroxyanthracene **(9)** (0.874g, 2.838mmol), *N*-methyl-2-pyrrolidone (20 ml) and potassium carbonate (3.14 g, 22.70 mmol) at 190 °C for 45 minutes to give a beige powder (1.45 g, 2.54 mmol, 90%) which was insoluble in all common solvents; $v_{max}$ ($cm^{-1}$) 2975, 1564, 1456, 1311, 1271, 1172, 1138, 1109, 891, 719, 704; Solid state $^{13}C$ NMR (101 MHz) $\delta$ 144.45, 138.04, 113.44, 109.05, 41.47, 35.62, 17.19; BET surface area = 527 $m^2$ $g^{-1}$; TGA (nitrogen): weight loss due to thermal degradation started at 443 °C.

**TOT-Cardo-61**

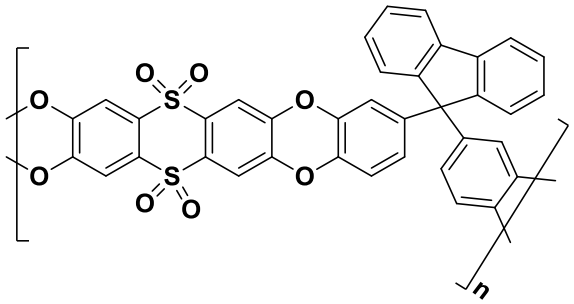


The general procedure **(12)** was followed to synthesise **(TOT-Cardo-61a)** by reacting 2,3,7,8-tetrafluoro-5,5',10,10'-tetraoxidethianthrene **(4)** (0.837 g, 2.348 mmol), 9,9-bis(3,4-dimethoxyphenyl)fluorene **(10)** (1 g, 2.348 mmol), *N*-methyl-2-pyrrolidone (25 ml) and potassium carbonate (2.59 g, 18.8 mmol)

at 70 °C for 72 hours to give a beige powder (1.45 g, 2.21 mmol, 94%), which was insoluble in all common solvents; $\nu_{max}$ ($cm^{-1}$) 3050, 1564, 1500, 1342, 1280, 1172, 1138, 1109, 742, 719, 615; solid state $^{13}C$ NMR (101 MHz) $\delta$ 145.40, 140.04, 126.96, 115.43, 64.00; BET surface area = 433 $m^2\ g^{-1}$; TGA (nitrogen): weight loss due to thermal degradation started at 440 °C.

The general procedure **(12)** was followed to synthesise **(TOT-Cardo-61b)** by reacting 2,3,7,8-tetrafluoro-5,5',10,10'-tetraoxidethianthrene **(4)** (1 g, 2.839 mmol), 9,9-bis (3,4-dihydroxyphenyl) fluorene **(10)** (1.121 g, 2.839mmol), *N*-methyl-2-pyrrolidone (25 ml) and potassium carbonate (3.14 g, 22.71 mmol) at 160 °C for 45 minutes to give a beige powder (1.76 g, 2.69 mmol, 95%), which was insoluble in all common solvents; $\nu_{max}$ ($cm^{-1}$): 3075, 2350, 1564, 1500, 1469, 1280, 1172, 1138, 1109, 891, 742, 719; solid state $^{13}C$ NMR (101 MHz) $\delta$ 145.42, 140.05, 127.18, 115.56, 63.99; BET surface area = 235 $m^2\ g^{-1}$; TGA (nitrogen): weight loss due to thermal degradation started at 433 °C.

**TOT-SBF-62**

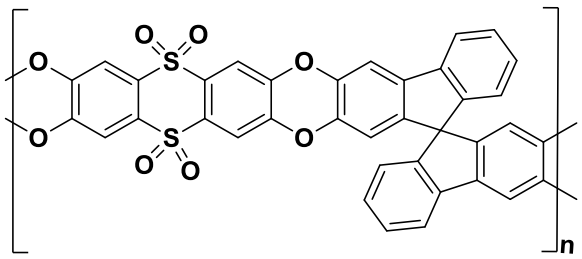


The general procedure **(12)** was followed by reacting 2,3,7,8-tetrafluoro-5,5',10,10'-tetraoxidethianthrene **(4)** (0.721 g, 2.005 mmol), 2,2',3,3'-tetrahydroxy-9,9'-spirobifluorene (0.8 g, 2.005 mmol) **(16)**, *N*-methyl-2-pyrrolidone (25ml) and potassium carbonate (2.22 g, 16.04 mmol) at 70 °C for 72 hours to give a beige powder (1.17 g, 1.79 mmol, 89%) which was insoluble in all common solvents; $\nu_{max}$ ($cm^{-1}$): 3050, 1564, 1469, 1448, 1348, 1290, 1269, 1172, 1138, 1109, 891, 719; solid state $^{13}C$ NMR (101 MHz) $\delta$

145.43, 140.41, 127.61, 123.89, 119.28, 113.13, 65.88; BET surface area = 611 $m^2$/g; TGA (nitrogen): weight loss due to thermal degradation started at 439 °C.

**TOT-SBF-63**

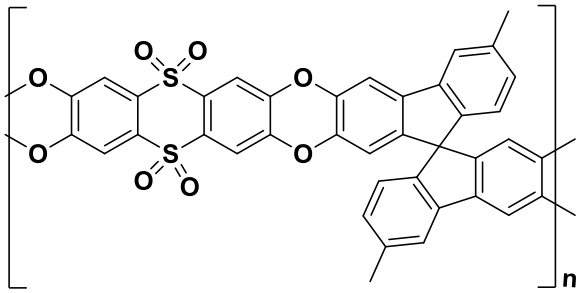

The general procedure **(12)** was followed by reacting 2,3,7,8-tetrafluoro-5,5',10,10'-tetraoxidethianthrene **(4)** (0.645 g, 1.832 mmol), 2,2',3,3'-tetrahydroxy -6,6'-dimethyl-9,9'-spirobifluorene **(22)** (0.785 g, 1.832 mmol), *N*-methyl-2-pyrrolidone (25- ml) and potassium carbonate (2.03 g, 1.83 mmol) at 70 $^{o}$C for 72 hours to give a beige powder (1.13 g, 1.66 mmol, 90 %) which was insoluble in all common solvents; $\nu_{max}$ ($cm^{-1}$): 3075, 1564, 1465, 1348, 1288, 1269, 1172, 1139, 1109, 850, 810,719; solid state $^{13}$C NMR (101 MHz) $\delta$ 145.44, 138.06, 128.53, 123.69, 118.83, 113.30, 65.71, 19.97; BET surface area = 637 $m^2$ $g^{-1}$; TGA (nitrogen): weight loss due to thermal degradation started at 424 °C.

**TOT-SBF-64**

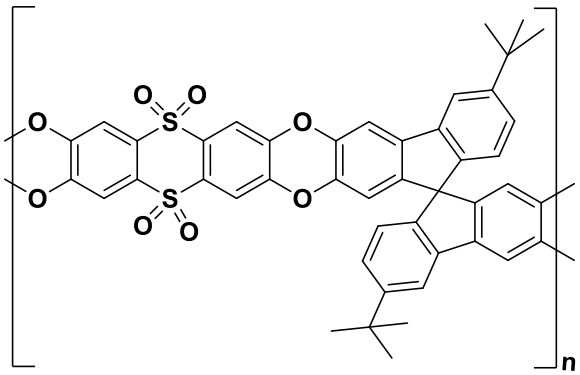

The general procedure **(12)** was followed by reacting 2,3,7,8-tetrafluoro-5,5',10,10'-tetraoxidethianthrene **(4)** (0.715 g, 2.03 mmol), 2,2',3,3'-tetrahydroxy -6,6'-*t*-butyl-9,9'-spirobifluorene **(28)** (1 g, 2.03 mmol), *N*-methyl-2-pyrrolidone (25 ml) and potassium carbonate (2.24 g, 16.24 mmol) at 70 °C for 72 hours to give a beige powder (1.47 g, 1.92 mmol, 95%) which was insoluble in all common solvents; $\nu_{max}$ ($cm^{-1}$) 2975, 1564, 1463, 1348, 1286, 1296,1172, 1139, 1107, 825, 875, 719; solid state $^{13}C$ NMR (101 MHz) $\delta$ 151.40, 145.54, 138.47, 124.30, 119.77, 113.49, 107.89, 66.15, 34.52, 30.57; BET surface area = 762 $m^2/g$; TGA (nitrogen): weight loss due to thermal degradation started at 450 °C.

**TOT-HPB-65**

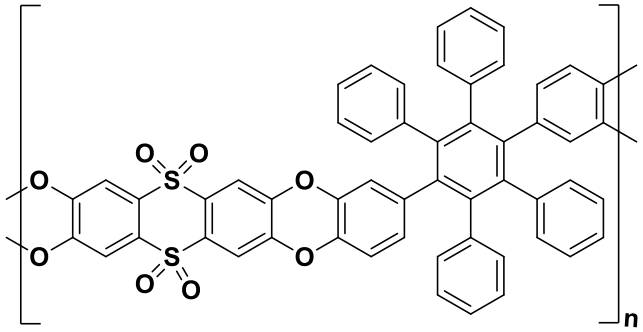


The general procedure **(12)** was followed by reacting 2,3,7,8-tetrafluoro-5,5',10,10'-tetraoxidethianthrene **(4)** (0.446 g, 1.266 mmol), 1,4-di(3',4'-dihydroxyphenyl)-2,3,5,6-tetraphenylbenzene **(32)** (0.758 g, 1.266 mmol), *N*-methyl-2-pyrrolidone (25 ml) and potassium carbonate (1.40 g, 10.13 mmol) at 70 °C for 72 hours to give a beige powder (0.98 g, 1.13 mmol, 89%) which was insoluble in all common solvents; $\nu_{max}$ ($cm^{-1}$) 3050, 1600, 1500, 1473, 1278, 1138, 875, 719,696; solid state $^{13}C$ NMR (101 MHz) $\delta$ 145.40, 139.75, 131.45, 126.81, 119.82, 114.53; BET surface area = 433 $m^2/g$; TGA (nitrogen): weight loss due to thermal degradation started at 431 °C.

**TOT-TMN-Trip-66**

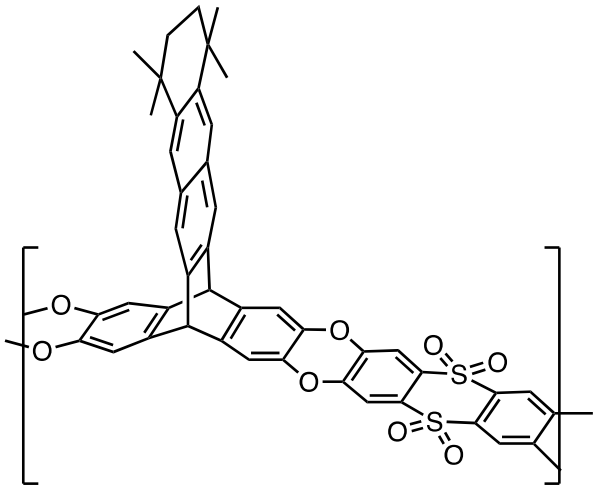

A general procedure **(12)** was followed by reacting 2,3,7,8-tetrafluoro-5,5',10,10'-tetraoxidethianthrene **(4)** (0.673 g, 1.91 mmol), 5,8,8,11,11,14-hexamethyl-5,8,9,10,11,14-hexahydro-5,14-[1,2]benzenopentacene-2,3,18,19-tetraol **(39)** (1 g, 1.91 mmol), *N*-methyl-2-pyrrolidone (25 ml) and potassium carbonate (2.11 g, 15.28 mmol) at 70 °C for 72 hours to give a beige powder (1.40 g, 2.41 mmol, 94%) which was insoluble in all common solvents; $\nu_{max}$ ($cm^{-1}$) 2975, 1564, 1465, 1452, 1307, 1269, 1172, 1138, 1109, 887, 721; solid state $^{13}C$ NMR (101 MHz) $\delta$ 145.04, 137.67, 130.42, 124.24, 117.48, 113.74, 109.36, 47.49, 34.13, 12.83; BET surface area = 785 $m^2$ $g^{-1}$; TGA (nitrogen): weight loss due to thermal degradation started at 425 °C.

**TOT-Trip-67**

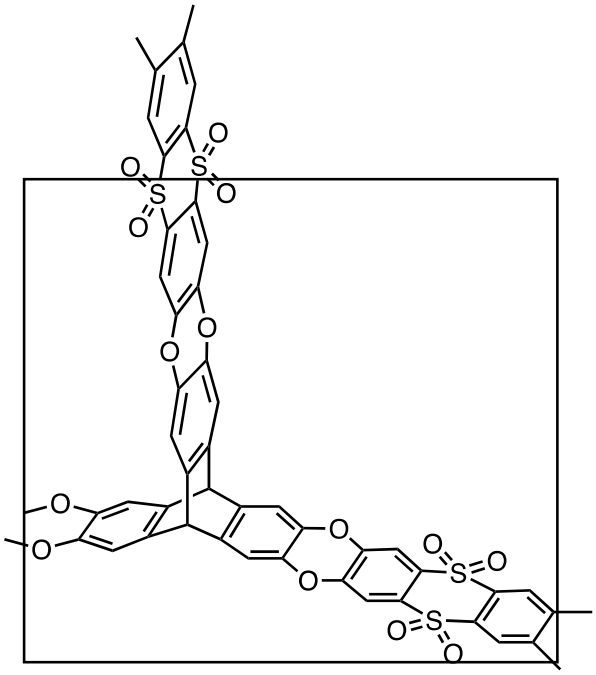

The general procedure **(12)** was followed to synthesise **(TOT-Trip-67a)** by reacting 2,3,7,8-tetrafluoro-5,5',10,10'-tetraoxidethianthrene **(4)** (1.042 g, 2.95 mmol), 2,3,6,7,12,13-hexahydroxytriptycene **(42)** (0.691 g, 1.97 mmol), *N,N*-dimethylformamide (120 ml) and potassium carbonate (4.9 g, 35.51 mmol) at 70 °C for 72 hours to give a beige powder (1.28 g, 1.68 mmol, 86%) which was insoluble in all common solvents; BET surface area = 699 $m^2$ $g^{-1}$; TGA (nitrogen): weight loss due to thermal degradation started at 405 °C.

The general procedure **(12)** was followed to synthesise (**TOT-Trip-67b**) by reacting 2,3,7,8-tetrafluoro-5,5',10,10'-tetraoxidethianthrene **(4)** (1.249 g, 3.42 mmol), 2,3,6,7,12,13-hexahydroxytriptycene **(42)** (1 g, 2.28 mmol), *N*-methyl-2-pyrrolidone (120 ml) and potassium carbonate (5.67 g, 41.054mmol) at 160 °C for 72 hours to give a beige powder (1.5 g, 1.98 mmol, 87%) which was insoluble in all common solvents; $\nu_{max}$ ($cm^{-1}$) 3075, 1566, 1460, 1313, 1276, 1170, 1134, 1111, 891, 719; solid state $^{13}C$ NMR (101 MHz) $\delta$ 142.20, 138.06, 113.17, 53.14; BET surface area = 629 $m^2/g$; TGA (nitrogen): weight loss due to thermal degradation started at 372 °C.

**General procedure (13) Polyimide polymers synthesis**

The polyimides were synthesised according to a reported procedure.[146] Under a nitrogen atmosphere, the appropriate bisanhydride, the appropriate diamine, *m*-cresol, isoquinoline and anhydrous toluene were added to a flask equipped with Dean-Stark apparatus and reflux condenser. After stirring the mixture at room temperature for 15 minutes, the temperature was raised gradually to 200 °C in 20 °C increments. This temperature was then maintained until a viscous solution was obtained. During this time water was removed from the reaction mixture by azeotropic distillation. The mixture was cooled to room temperature and then added dropwise to vigorously stirred methanol. The resulting solid precipitate was collected by filtration, washed with methanol and dried to obtain the desired polymer.

**TOT-PDA-68**

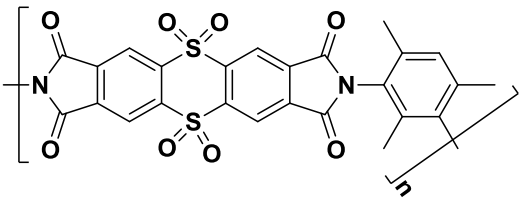

The general procedure **(13)** was followed by reacting thianthrene-2,3,7,8-tetracarboxylic acid anhydride-5,5,10,10-tetraoxide **(48)** (1.350 g, 3.21 mmol), 2,4,6-trimethyl-1,3-phenylenediamine (0.480 g, 3.21 mmol), isoquinoline (0.1 ml) and anhydrous toluene (3 ml) to give a beige powder (0.9 g, 1.68 mmol, 53%) which was insoluble in all common solvents; $\nu_{max}$ ($cm^{-1}$) 3095, 1780, 1716, 1610, 1587, 1487, 1419, 1355, 1130, 1001, 927, 867, 777; BET surface area = 103 $m^2/g$; TGA (nitrogen): weight loss due to thermal degradation started at 420 °C.

**TOT-PDA-69**

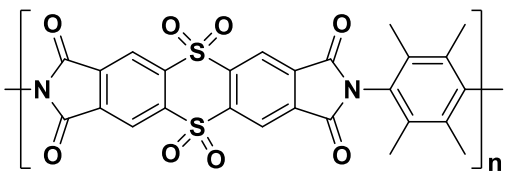

The general procedure **(13)** was followed by reacting thianthrene-2,3,7,8-tetracarboxylic acid anhydride-5,5,10,10-tetraoxide **(48)** (1.35 g, 3.21 mmol), 1,4-phenylenediamine (0.527 g, 3.21 mmol), isoquinoline (0.1) and anhydrous toluene (3 ml) to give a beige powder (1.10 g, 2.00 mmol, 63%) which was soluble in chloroform; $\nu_{max}$ ($cm^{-1}$) 3093, 3032, 1784, 1614, 1587, 1462, 1346, 1282, 1165, 1124, 1725, 858, 721; BET surface area = 42 $m^2$ $g^{-1}$; TGA (nitrogen): weight loss due to thermal degradation started at 375 °C.

**TOT-DMN-70**

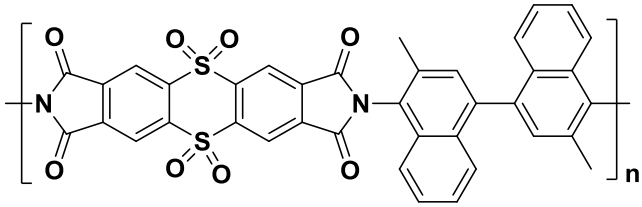

The general procedure **(13)** was followed by reacting thianthrene-2,3,7,8-tetracarboxylic acid anhydride-5,5,10,10-tetraoxide **(48)** (1 g, 2.38 mmol), 3,3'-dimethylnaphthidine (0.743 g, 2.38 mmol), isoquinoline (0.1) and anhydrous toluene 3 ml) to give a beige powder (1.3 g, 1.86 mmol, 79%), which was soluble in chloroform; $\nu_{max}$ ($cm^{-1}$) 3050, 1784, 1722, 1614, 1388, 1352, 1251, 1155, 1101, 873, 742; BET surface area = 39 $m^2$ $g^{-1}$; TGA (nitrogen): weight loss due to thermal degradation started at 439 °C.

**TOT-EA-71**

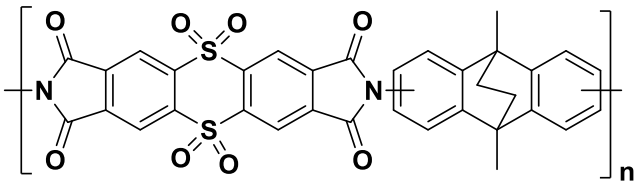

The general procedure **(13)** was followed by reacting thianthrene-2,3,7,8-tetracarboxylic acid anhydride-5,5,10,10-tetraoxide **(48)** (1 g, 2.38 mmol), 9,10-dihydro-2,6(7)-diamino-9,10-ethanoanthracene **(52)** (0.629 g, 2.38 mmol), isoquinoline (0.1 ml) and anhydrous toluene (3 ml) to give a beige

powder (1.44 g, 2.22 mmol, 93%) which was insoluble in all common solvents; $v_{max}$ ($cm^{-1}$) 3025, 2975, 1778, 1725, 1587, 1489, 1475, 1458, 1375, 1282, 1151, 879, 775, 740; BET surface area = 60 $m^2$ $g^{-1}$; TGA (nitrogen): weight loss due to thermal degradation started at 401 °C.

**TOT-BAPF-72**

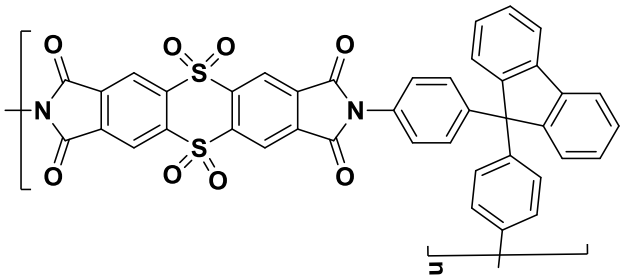

The general procedure **(13)** was followed by reacting thianthrene-2,3,7,8-tetracarboxylic acid anhydride-5,5,10,10-tetraoxide **(48)** (1 g, 2.38 mmol), 9,9′-bis(4-aminophenyl) fluorene (BAPF) **(53)** (0.829 g, 2.38 mmol), isoquinoline (0.1 ml) and anhydrous toluene (3 ml) to give a beige powder (1.100 g, 1.50 mmol, 64%) which was soluble in chloroform; $v_{max}$ ($cm^{-1}$) 3047, 1778, 1714, 1587, 1508, 1417, 1373, 1325, 1265, 927, 852, 823, 777; BET surface area = 32 $m^2$ $g^{-1}$; TGA (nitrogen): weight loss due to thermal degradation started at 402 °C.

**TOT-TMPI-73**

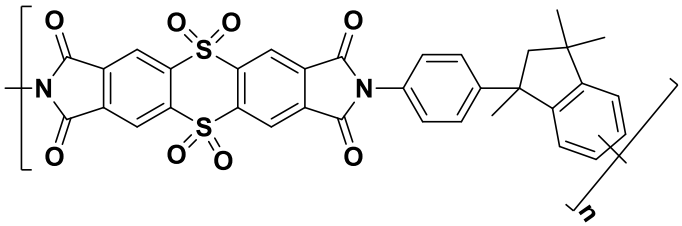

A general procedure **(13)** was followed by reacting thianthrene-2,3,7,8-tetracarboxylic acid anhydride-5.5.10.10-tetraoxide **(48)** (2.436 g, 5.79 mmol), 6,(7)-amino-1,3,3-trimethyl-1-(4-aminophenyl)indane **(56)** (1.544 g, 5.79 mmol), isoquinoline (0.1 ml) and anhydrous toluene (3 ml) to give a beige powder (0.9 g, 1.38 mmol, 24%) which was insoluble in all common solvents; $v_{max}$ ($cm^{-1}$) 3047, 1778, 1714, 1587, 1508, 1417, 1373, 1325, 1265,

927, 852, 823, 777; BET surface area = 1.1 $m^2$/g; TGA (nitrogen): weight loss due to thermal degradation started at 362 °C.

**TOT-PDA-74**

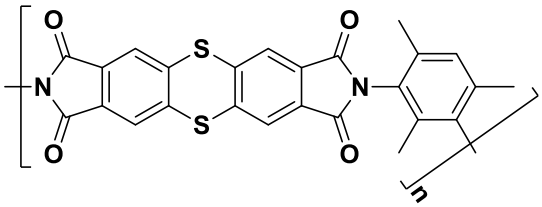

The general procedure **(13)** was followed by reacting thianthrene-2,3,7,8-tetracarboxylic acid anhydride **(47)** (0.5 g, 1.40 mmol), 2,4,6-trimethyl-1,3-phenylenediamine (0.21g, 1.40 mmol), isoquinoline (0.2 ml) and anhydrous toluene (3 ml) to give a yellow powder (0.59 g, 1.25 mmol, 83 %) which was insoluble in all common solvents; $\nu_{max}$ ($cm^{-1}$) 3075, 1774, 1708, 1604, 1485, 1346, 1311, 1226, 1188, 1111, 1029, 867, 783, 744, 702; BET surface area = 329 $m^2$ $g^{-1}$.

**TOT-PDA-75**

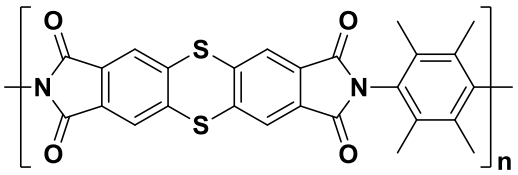

The general procedure **(13)** was followed by reacting thianthrene-2,3,7,8-tetracarboxylic acid anhydride **(47)** (0.5 g, 1.40 mmol), 2,4,6-trimethyl-1,3-phenylenediamine (0.231 g, 1.40 mmol), isoquinoline (0.2) and anhydrous toluene (3 ml) to give a yellow powder (0.5 g, 1.03 mmol, 74%) which was insoluble in all common solvents. $\nu_{max}$ ($cm^{-1}$) 3075, 1774, 1710, 1625, 1485, 1352, 1311, 1228, 1114, 867, 785, 746, 624; BET surface area = 334 $m^2$ $g^{-1}$; TGA (nitrogen): weight loss due to thermal degradation started at 532 °C.

# Bibliography


1 X. S. Zhao, *J. Mater. Chem.*, 2006, **16**, 623–625.
2 J. Rouquerol, D. Avnir, C. W. Fairbridge, D. H. Everett, J. M. Haynes, N. Pernicone, J. D. F. Ramsay, K. S. W. Sing and K. K. Unger, *Pure Appl. Chem.*, 1994, **66**, 1739–1758.
3 F. Dullien, *Porous Media: Fluid Transport and Pore Structure. Porous Media: Fluid Transport and Pore Structure*, 1992.
4 K. Rouquerol, Jean; Baron, Gino; Denoyel, Renaud; Giesche, Herbert; Groen, Johan; Klobes, Peter; Levitz, Pierre; Neimark, Alexander V.; Rigby, Sean; Skudas, Romas; Sing, Kenneth; Thommes, Matthias; Unger, *Pure Appl. Chem.*, 2012, **84**, 107–136.
5 G. S. Larsen, P. Lin, K. E. Hart and C. M. Colina, *Macromolecules*, 2011, **44**, 6944–6951.
6 I. Langmuir, *J. Am. Chem. Soc.*, 1917, **39**, 1848–1906.
7 S. Brunauer, P. H. Emmett and E. Teller, *J. Am. Chem. Soc.*, 1938, **60**, 309–319.
8 M. D. Donohue and G. L. Aranovich, *Adv. Colloid Interface Sci.*, 1998, **76**, 137–152.
9 M. Ismail, *Carbon*, 1990, **28**, 423–34.
10 N. B. McKeown and P. M. Budd, *Chem. Soc. Rev.,* 2006, **35**, 675–683.
11 A. Corma, H. Gracia and F. X. Liabres i Xamena, *Chem. Rev.*, 2006, **110**, 4606–4655.
12 S. Sircar, W. E. Waldron, M. B. Rao and M. Anand, *Sep. Purif. Technol.*, 1999, **17**, 11–20.
13 P. M. Budd, N. B. McKeown, B. S. Ghanem, K. J. Msayib, D. Fritsch, L. Starannikova, N. Belov, O. Sanfirova, Y. Yampolskii and V. Shantarovich, *J. Memb. Sci.*, 2008, **325**, 851–860.
14 D. Zhao, D. Yuan and H.-C. Zhou, *Energy Environ. Sci.*, 2008, **1**, 222.
15 N. B. McKeown, B. Gahnem, K. J. Msayib, P. M. Budd, C. E. Tattershall, K. Mahmood, S. Tan, D. Book, H. W. Langmi and A. Walton, *Angew. Chem. Int. Ed.*, 2006, **45**, 1804–1807.
16 T. Maesen, *Stud. Surf. Sci. Catal.*, 2007, **168**, 1–12.
17 J. Yu, *Synthesis of zeolites*, Elsevier B.V., 2007, vol. 168.
18 R. M. Barrer, *J. Chem. Soc.*, 1948, 127–132.
19 G. T. Kerr, *Inorg. Chem.*, 1966, **5**, 1539–1541.
20 A. F. Masters and T. Maschmeyer, *Microporous Mesoporous Mater.*, 2011, **142**, 423–438.
21 US 2882243, 1959.
22 S. T. Wilson, *Stud. Surf. Sci. Catal.*, 2007, **168**, 105–135.
23 S. Cinar and B. Beler-Baykal, *Water Sci. Technol.*, 2005, **51**, 71–77.
24 B. S. Sekhon and M. K. Sangha, *Resonance*, 2004, **9**, 35–45.
25 A. S. Čejka, Jiří van Bekkum, Herman Corma, *Introduction to Zeolite science and practice*, 3rd edn., 2007.
26 D. C. Baerlocher, C.; McCusker, L.; and Olson, *Atlas of zeolite framework types*, 2007.
27 M. Sobiesiak, B. Gawdzik, A. M. Puziy and O. I. Poddubnaya, *Appl.*

*Surf. Sci.*, 2010, **256**, 5355–5360.
28 E. Sawa, *Fuller. Sci. Technol.*, 1999, 637.
29 S. M. Manocha, *Sadhana*, 2003, **28**, 335–348.
30 Y. Zhao, L. Zhao, K. X. Yao, Y. Yang, Q. Zhang and Y. Han, *J. Mater. Chem.*, 2012, **22**, 19726.
31 H. Li, M. Eddaoudi, M. O'Keeffe and O. M. Yaghi, *Nature*, 1999, **402**, 276–279.
32 O. M. Yaghi, C. E. Davis, G. Li and H. Li, *J. Am. Chem. Soc.*, 1997, **119**, 2861–2868.
33 S. S. Y. Chui, S. M. F. Lo, J. P. H. Charmant, A. G. Orpen and I. D. Williams, *Science*, 1999, **283**, 1148–1150.
34 H. Furukawa, N. Ko, Y. B. Go, N. Aratani, S. B. Choi, J. Kim and O. M. Yaghi, *Science*, 2010, 424–429.
35 M. Michael, *Angew. Chem., Int. Ed.*, 2008, **47**, 445–447.
36 K. Severin, *Dalton Trans.*, 2009, **9226**, 5254.
37 L. Wang, L. Wang, J. Zhao and T. Yan, *J. Appl. Phys.*, 2012, **111**.
38 H. M. El-Kaderi, J. R. Hunt, J. L. Mendoza-Cortes, A. P. Cote, R. E. Taylor, M. O'Keeffe, O. M. Yaghi, J. L. Mendoza-Cortés, A. P. Côté, R. E. Taylor, M. O'Keeffe and O. M. Yaghi, *Science*, 2007, **316**, 268–272.
39 C. D. Wood, B. Tan, A. Trewin, H. Niu, D. Bradshaw, M. J. Rosseinsky, Y. Z. Khimyak, N. L. Campbell, R. Kirk, E. Stckel and A. I. Cooper, *Chem. Mater.*, 2007, **19**, 2034–2048.
40 M. P. Tsyurupa, M. M. Ilyin, a. I. Andreeva and V. a. Davankov, *Fresenius J Anal Chem*, 1995, **352**, 672–675.
41 V. Davankov and M. Tsyurupa, *J. Chromatogr. A*, 2005, **1087**, 3–12.
42 B. C. Pan, Y. Xiong, a. M. Li, J. L. Chen, Q. X. Zhang and X. Y. Jin, *React. Funct. Polym.*, 2002, **53**, 63–72.
43 Z. Xu, Q. Zhang, J. Chen, L. Wang and G. K. Anderson, *Chemosphere*, 2011, **38**, 2003–2011.
44 M. Rose, W. Böhlmann, M. Sabo and S. Kaskel, *Chem. Commun.*, 2008, **1**, 2462.
45 J. Germain, F. Svec and J. M. J. Frechet, *Chem. Mater.*, 2008, 7069–7076.
46 F. Svec, J. Germain and J. M. J. Fre, *Chem. Commun.*, 2009, 1526–1528.
47 S. M. Aharoni, V. A. Davankov and M. P. Tsyurupa, *Synthesis, Characterisation and Theory of Polymeric Networks and Gels*, 1992.
48 V. A. Davankov and M. P. Tsyurupa, *Reactive Polymers*, 1990, **13**, 27–42.
49 J. A. Patterson, *Biochemical Aspects of Reaction on solid Supports*, Academic Press, New York, 1971.
50 A. Li, Q. Zhang, J. Chen, Z. Fei, C. Long and W. Li, *React. Funct. Polym.*, 2001, **49**, 225–233.
51 R. Dawson, A. I. Cooper and D. J. Adams, *Prog. Polym. Sci.*, 2012, **37**, 530–563.
52 L. D. Belyakova, T. I. Schevchenko, V. A. Davankov and P. Tsyurupam, *Adv. Colloid Interface Sci.*, 1986, **25**, 249–266.
53 V. A. Davankov and M. P. Tsyurupa, *Pure & Appl. Chern.*, 1989, **61**,

1881–1888.
54 V. A. Rosenberg, G.I., Shabaeva, A.S., Moryakov, V.S., Musin, T.G., Tsyurupa, M.P., Davankov, *Reactive polymers.*, 1983, **1**, 175.
55 M. P. Tsyurupa, L. A. Maslova, A. I. Andreeva, T. A. Mrachkovskaya and V. A. Davankov, *Reactive Polymers*, 1995, **25**, 69–78.
56 N. E. Oro and C. A. Lucy, *J. Chromatogr. A*, 2010, **1217**, 6178–6185.
57 V. A. Tsyurupa, M. P.; Cjurupa, M P; Lalaev, V V; Davankov, *Acta Polym.*, 1984, **35**, 451–455.
58 S. V. Davankov, V. A.; Tsyurupa, M. P.; Rogozhin, *Angew. Makromol. Chem.*, 1976, **53**, 19–27.
59 M. P. Davankov, V. A.; Rogozhin, S. V.; Tsyurupa, *J. polym. sci., Polym. symp.*, 1974, **47**, 95–101.
60 N. B. McKeown and P. M. Budd, *Encyclopedia of Polymer Science and Technology*, John Wiley & Sons, Inc., 2009.
61 N. B. McKeown, *Phthalocyanine Materials: Synthesis, Structure and Function*, CUP, Cambridge, UK, 1998.
62 S. Makhseed, F. Al-Kharafi, J. Samuel and B. Ateya, *Catal. Commun.*, 2009, **10**, 1284–1287.
63 H. J. MacKintosh, P. M. Budd and N. B. McKeown, *J. Mater. Chem.*, 2008, **18**, 573–578.
64 B. S. Ghanem, M. Hashem, K. D. M. Harris, K. J. Msayib, M. Xu, P. M. Budd, N. Chaukura, D. Book, S. Tedds, A. Walton and N. B. McKeown, *Macromolecules*, 2010, **43**, 5287–5294.
65 B. S. Ghanem, K. J. Msayib, N. B. McKeown, K. D. M. Harris, Z. Pan, P. M. Budd, A. Butler, J. Selbie, D. Book and A. Walton, *Chem. Commun.*, 2007, 67–69.
66 N. B. McKeown, P. M. Budd, K. J. Msayib, B. S. Ghanem, H. J. Kingston, C. E. Tattershall, S. Makhseed, K. J. Reynolds and D. Fritsch, *Chem. Eur. J.*, 2005, **11**, 2610–2620.
67 P. M. Budd, B. S. Ghanem, S. Makhseed, N. B. McKeown, K. J. Msayib and C. E. Tattershall, *Chem. Commun. (Cambridge, U. K.)*, 2004, 230–231.
68 T. Emmler, K. Heinrich, D. Fritsch, P. M. Budd, N. Chaukura, D. Ehlers, K. Rätzke and F. Faupel, *Macromolecules*, 2010, **43**, 6075–6084.
69 B. S. Ghanem, R. Swaidan, X. Ma, E. Litwiller and I. Pinnau, *Adv. Mater.*, 2014, 6696–6700.
70 K. Yuan, C. Liu, S. Zhang, L. Jiang and C. Liu, *J. Membr. Sci.*, 2017, **541**, 403–412.
71 J. W. Jeon, D. Kim, E. Sohn, Y. Yoo, Y. S. Kim, B. G. Kim and J. Lee, *Macromolecules*, 2017, 8019–8027.
72 B. Shrimant, S. V Shaligram, U. K. Kharul and P. P. Wadgaonkar, *J. Polym. Sci., Part A: Polym. Chem.*, 2018, 16–24.
73 J. Tröger, *J. Prakt. Chem.*, 1887, **36**, 225–245.
74 M. Spielman, *J. Am. Chem. Soc.*, 1935, 583–585.
75 P. W. V. Prelog, *Helv. Chim. Acta*, 1944, **27**, 1127–34.
76 E. Poli, E. Merino, U. Díaz, D. Brunel and A. Corma, *J. Phys. Chem. C*, 2011, **115**, 7573–7585.
77 J. Byun, S.-H. Je, H. a Patel, A. Coskun and C. T. Yavuz, *J. Mater.*

*Chem. A,* 2014, **2**, 12507–12512.
78 Z. G. Wang, X. Liu, D. Wang and J. Jin, *Polym. Chem.*, 2014, **5**, 2793.
79 M. Carta, M. Croad, R. Malpass-Evans, J. C. Jansen, P. Bernardo, G. Clarizia, K. Friess, M. Lanč and N. B. McKeown, *Adv. Mater.*, 2014, **26**, 3526–3531.
80 I. Rose, M. Carta, R. Malpass-evans, M. Ferrari, P. Bernardo, G. Clarizia, J. C. Jansen and N. B. Mckeown, *ACS Macro Lett.*, 2015, 4–7.
81 R. Williams, E. Esposito, J. C. Jansen, E. Tocci, C. Rizzuto and M. Carta, *J. Mater. Chem. A.*, 2018, **24**, 5661–5667.
82 C. E. Sroog, *Prog. Polym. Sci.*, 1991, **16**, 561–694.
83 B. S. Ghanem, N. B. McKeown, P. M. Budd, J. D. Selbie and D. Fritsch, *Adv. Mater.*, 2008, **20**, 2766–2771.
84 M. Calle, A. E. Lozano, J. de Abajo, J. G. de la Campa and C. Álvarez, *J. Membr. Sci.*, 2010, **365**, 145–153.
85 K. L. Ghosh, M. K.; Mittal, *Polyimides: Fundamentals And Applications*, Marcel Dekker, New York, 1996.
86 D. J. Liaw, K. L. Wang, Y. C. Huang, K. R. Lee, J. Y. Lai and C. S. Ha, *Prog. Polym. Sci.*, 2012, **37**, 907–974.
87 S. Sridhar, R. S. Veerapur, M. B. Patil, K. B. Gudasi and T. M. Aminabhavi, *J. Appl. Polym. Sci.*, 2007, **106**, 1585–1594.
88 B. S. Ghanem, N. B. McKeown, P. M. Budd, N. M. Al-Harbi, D. Fritsch, K. Heinrich, L. Starannikova, A. Tokarev and Y. Yampolskii, *Macromolecules*, 2009, **42**, 7881–7888.
89 X. Ma, B. Ghanem, O. Salines, E. Litwiller and I. Pinnau, *ACS Macro Lett.*, 2015, **4**, 231–235.
90 R. Swaidan, M. Al-Saeedi, B. Ghanem, E. Litwiller and I. Pinnau, *Macromolecules*, 2014, **47**, 5104–5114.
91 B. S. Ghanem, R. Swaidan, E. Litwiller and I. Pinnau, *Adv. Mater.*, 2014, **26**, 3688–3692.
92 B. Ghanem, F. Alghunaimi, X. Ma, N. Alaslai and I. Pinnau, *Polymer*, 2016, **101**, 225–232.
93 B. S. Ghanem, F. Alghunaimi, Y. Wang, G. Genduso and I. Pinnau, *ACS Omega*, 2018, **3**, 11874–11882.
94 B. Ghanem, N. Alaslai, X. Miao and I. Pinnau, *Polymer*, 2016, **96**, 13–19.
95 M. Lee, C. G. Bezzu, M. Carta, P. Bernardo, G. Clarizia, J. C. Jansen and N. B. Mckeown, *Macromolecules*, 2016.
96 N. Alaslai, X. Ma, B. Ghanem, Y. Wang and F. Alghunaimi, *Macromol. Rapid Commun.*, 2017, **1700303**, 1–5.
97 M. Abdulhamid, X. Miao and I. Pinnau, *Macromolecules*, 2017, **50**, 9569−9576.
98 F. Alghunaimi, B. Ghanem, Y. Wang, O. Salinas, N. Alaslai and I. Pinnau, *Polymer*, 2017, **121**, 9–16.
99 Y. P. Yampolskii and D. R. Paul, *Polymeric Gas Separation Membranes*, CRC Press, 1993.
100 M. Mulder, *Basic Principles of Membrane Technology, Second Edition.*, 996.
101 T. Graham, *Philos. Mag.*, 1866, 401–420.

102 M. Mulder, *Basic Principles of Membrane Technology Second Edition*, 1996.
103 W. R. Vieth, J. M. Howell and J. H. Hsieh, *J. Membr. Sci.*, 1976, **1**, 177–220.
104 W. Koros, *Gas Separation in: Membrane Separation System- Recent Developments and Future Directions*, William Andrew Puplishing, 1991.
105 B. D. Freeman, *Macromolecules*, 1999, **32**, 375–380.
106 L. M. Robeson, *J. Membr. Sci.*, 1991, **62**, 165–185.
107 L. M. Robeson, *J. Membr. Sci.*, 2008, **320**, 390–400.
108 R. Swaidan, B. Ghanem and I. Pinnau, *ACS Macro Lett.*, 2015, **4**, 947–951.
109 J. V. Crivello, *J. Org. Chem.*, 1981, **46**, 3056–3060.
110 A. Philippides, P. M. Budd, C. Price and A. V. Cuncliffe, *Polymer*, 1993, **34**, 3509–3513.
111 A. Furst and R. E. Moore, *J. Am. Chem. Soc.*, 1957, **79**, 5492–5493.
112 A. Kausar, W. Wajid-Ullah, B. Muhammad and M. Siddiq, *Mater. Manuf. Processes*, 2015, **30**, 346–355.
113 C. A. M. Abella, M. Benassi, L. S. Santos, M. N. Eberlin and F. Coelho, *J. Org. Chem.*, 2007, **72**, 4048–4054.
114 M. Carta, R. Malpass-Evans, M. Croad, Y. Rogan, C. J. Johannes, P. Bernardo, F. Bazzarelli and N. McKeown, *Science*, 2013, **339**, 303–308.
115 N. Du, G. P. Robertson, J. Song, I. Pinnau, S. Thomas and M. D. Guiver, *Macromolecules*, 2008, **41**, 9656–9662.
116 N. Du, G. P. Robertson, I. Pinnau and M. D. Guiver, *Macromolecules*, 2009, **42**, 6023–6030.
117 N. Du, G. P. Robertson, I. Pinnau and M. D. Guiver, *Macromolecules*, 2010, **43**, 8580–8587.
118 B. Niederl and H. Nagel, *J. Am. Chem. Soc.*, 1940, **62**, 3070–3072.
119 B. S. Ghanem, N. B. McKeown, P. M. Budd and D. Fritsch, *Macromolecules*, 2008, **41**, 1640–1646.
120 JP 2007197367, 2007.
121 C. G. Bezzu, M. Carta, A. Tonkins, J. C. Jansen, P. Bernardo, F. Bazzarelli and N. B. Mckeown, *Adv. Mater.*, 2012, **24**, 5930–5933.
122 R. Short, M. Carta, C. G. Bezzu, D. Fritsch, B. M. Kariuki and N. B. McKeown, *Chem. Commun.*, 2011, **47**, 6822.
123 I. Rose, C. G. Bezzu, M. Carta, B. Comesanã-Gándara, E. Lasseuguette, M. C. Ferrari, P. Bernardo, G. Clarizia, A. Fuoco, J. C. Jansen, K. E. Hart, T. P. Liyana-Arachchi, C. M. Colina and N. B. McKeown, *Nat. Mater.*, 2017, **16**, 932–937.
124 O. W. , Webster Owen W., & Webster, *Macromol. Symp.*, 1994, **77**, 177–182.
125 C. Azerraf, O. Grossman and D. Gelman, *J. Organomet. Chem.*, 2007, **692**, 761–767.
126 C. Zhang and C. F. Chen, *J. Org. Chem.*, 2007, **72**, 9339–9341.
127 M. Munakata, L. P. Wu, K. Sugimoto, T. Kuroda-Sowa, M. Maekawa, Y. Suenaga, N. Maeno and M. Fujita, *Inorg. Chem.*, 1999, **38**, 5674–

5680.
128 H. L. Aalten, G. van Koten, D. M. Grove, T. Kuilman, O. G. Piekstra, L. A. Hulshof and R. A. Sheldon, *Tetrahedron*, 1989, **45**, 5565–5578.
129 T. S. Navale and R. Rathore, *Synthesis*, 2012, **44**, 805–809.
130 P. M. Budd, E. S. Elabas, B. S. Ghanem, S. Makhseed, N. B. McKeown, K. J. Msayib, C. E. Tattershall and D. Wang, *Adv. Mater.*, 2004, **16**, 456–459.
131 D. Naiying, S. Jingshe, G. P. Robertson, I. Pinnau and M. D. Guiver, *Macromol. Rapid Commun.*, 2008, **29**, 783–788.
132 R. G. D. Taylor, C. G. Bezzu, M. Carta, K. J. Msayib, J. Walker, R. Short, B. M. Kariuki and N. B. McKeown, *Chem. Eur. J.*, 2016, **22**, 2466–2472.
133 K. R. Carter, *Macromolecules*, 1995, **28**, 6462–6470.
134 J. Hao, K. Tanaka, H. Kita and K. Okamoto, *J. Polym. Sci., Part A: Polym. Chem.*, 1997, 485–494.
135 JP 2009067937, 2009.
136 Y. Rogan, R. Malpass-Evans, M. Carta, M. Lee, J. C. Jansen, P. Bernardo, G. Clarizia, E. Tocci, K. Friess, M. Lanč and N. B. McKeown, *J. Mater. Chem. A.*, 2014, **2**, 4874–4877.
137 L. R. C. Barclay and R. A. Chapan, *Can. J. Chem.*, 1984, **84**, 265–283.
138 S. Kazama, T. Teramoto and K. Haraya, *J. Membr. Sci.*, 2002, **207**, 91–104.
139 D. Chao, S. Wang, R. Yang, E. B. Berda and C. Wang, *Colloid Polym. Sci.*, 2013, **291**, 2631–2637.
140 C. Guo, L. Zhou and J. Lv, *J. Appl. Polym. Sci.*, 2013, **21**, 449–456.
141 D. Wilson, H. Stenzenberger and P. Hergenrother, *Polyimides*, 1990.
142 Y. J. Kim, T. E. Glass, G. D. Lyle and J. E. McGrath, *Macromolecules*, 1993, **26**, 1344–1358.
143 A. Kausar, Wajid-Ullah, B. Muhammad and M. Siddiq, *Mater. Manuf. Processes*, 2015, **30**, 346–355.
144 L. J. Irwin, J. H. Reibenspies and S. A. Miller, *J. Am. Chem. Soc.*, 2004, **126**, 16716–16717.
145 V. J. Chebny, T. S. Navale, R. Shukla, S. V. Lindeman and R. Rathore, *Org. Lett.*, 2009, **11**, 2253–2256.
146 B. S. Ghanem, M. Hashem, K. D. M. Harris, K. J. Msayib, M. Xu, P. M. Budd, N. Chaukura, D. Book, S. Tedds, A. Walton and N. B. McKeown, *Macromolecules*, 2010, **43**, 5287–5294.
147 D. Fritsch, G. Bengtson, M. Carta and N. B. McKeown, *Macromol. Chem. Phys.*, 2011, **212**, 1137–1146.
148 CN 105001027, 2015, 19.
149 M. Moritsugu, R. Seto, K. Matsumoto and T. Endo, *J. Polym. Sci., Part A: Polym. Chem.*, 2016, **54**, 1409–1416.
150 H. Hart, K. Harada and C. J. F. Du, *J. Org. Chem.*, 1985, **50**, 3104–3110.
151 C. L. Hilton, C. R. Jamison, H. K. Zane and B. T. King, *J. Org. Chem.*, 2009, **74**, 405–407.
152 J. Ke, D. D. Laskar, D. Singh and S. Chen, *Biotechnol Biofuels*, 2011, **4**, 17.

153 C. F. Koelsch and R. N. Flesch, *J. Org. Chem.*, 1955, **20**, 1270–1276.
154 M. Carta, P. Bernardo, G. Clarizia, J. C. Jansen and N. B. McKeown, *Macromolecules*, 2014, **47**, 8320–8327.
155 H. Toyama, M. Nakamura, M. Nakamura, Y. Matsumoto, M. Nakagomi and Y. Hashimoto, *Bioorg. Med. Chem.*, 2014, **22**, 1948–1959.
156 R. Luo, J. Liao, L. Xie, W. Tang and A. S. C. Chan, *Chem. Commun.*, 2013, **49**, 9959.
157 K. Hagiwara, M. Otsuki, M. Akita and M. Yoshizawa, *Chem. Commun.*, 2015, **51**, 10451–10454.
158 S. A. Sydlik, Z. Chen and T. M. Swager, *Macromolecules*, 2011, **44**, 976–980.
159 JP 2009067937, 2009, 14.
160 P. Karrer, N. J. Antia and R. Schwyzer, *Helv. Chimi. Acta*, 1950, **51**, 1392–1399.
161 S. Achyutha Rao and M. Periasamy, *Tetrahedron*, 1988, **29**, 1583–1586.
162 M. Hojo, T. Ichi and K. Shibato, *J. Org. Chem.*, 1985, **50**, 1478–1482.